HER receptor-mediated dynamic signalling in breast cancer cells

Doctor of Philosophy

Huizhong Hu

University of Edinburgh

2011

Contents

Declaration i
Acknowledgement ii
Abstract iv
Abbreviations vi
Chapter One: Introduction 1
1 Introduction 2
1.1 The anatomy and physiology of the normal breast 2
1.2 Biology of breast cancer 4
1.3 Metastasis of breast cancer 4
1.4 Grading and staging of breast cancer 6
1.5 Histopathological classification of breast cancer 9
1.6 Molecular classification of breast cancer 13
1.7 Risk factors for breast cancer 19
1.8 Treatments for breast cancer 23
1.9 Cell signalling pathways in breast cancer 26
1.9.1 HER receptor tyrosine kinase family and therapy of breast cancer 26
1.9.2 Raf/ MEK 1&2/ERK 1&2 and PI3K/Akt pathways and feedback loops in breast cancers 34
1.9.3 Oscillatory dynamics in Raf/MEK 1&2 /ERK 1&2 pathway 42
1.10 Aims 44
Chapter Two: Materials and Methods 47
2 Materials and Methods 48
2.1 Materials 48
2.1.1 Tissue culture reagents and inhibitors 48
2.1.2 Reagents used for the preparation of double charcoal stripped serum 48
2.1.3 Reagents used in the Sulphorhodamine B (SRB) assay 48
2.1.4 Reagents and other materials used in protein detection in cell lines 49
2.1.5 Reagents and other materials used in protein detection in tumours 50
2.1.6 Primary Antibodies used in Western Blot 51
2.1.7 List of primary antibodies used in RPPA 52

2.1.8 Near-infrared fluorophore conjugated secondary antibodies used in this study purchased from LI-COR Biosciences 52
2.1.9 Kits used in the gene expression analysis 53
2.1.10 Reagents and other materials used in the cell cycle analysis 53
2.2 Methods 53
2.2.1 Cell Culture 53
2.2.2 Double charcoal stripped serum preparation 55
2.2.3 SRB assay for growth studies 55
2.2.4 Protein detection in cell lines 56
2.2.5 Protein detection in tumours 64
2.2.6 Gene expression analysis 67
2.2.7 Flow cytometric analysis for cell cycle 69
2.2.8 Statistics 70
Chapter Three: Methodology Development 72
3 Methodology development 73
3.1 RPPA development 73
3.1.1 Sample preparation 74
3.1.2 Application of automated robotic microarrayer 75
3.1.3 Application of different blocking buffers 76
3.1.4 The application of LI-COR imaging system in RPPA 78
3.2 In-cell Western development 78
Chapter Four: Results 82
4 Results 83
4.1 The oscillatory dynamics of phospho-ERK1/2(T^{202}/Y^{204}) and phospho-Akt (S^{473})… 83
4.1.1 Characteristics of the cell line models used 83
4.1.2 Observation of signalling oscillation and experimental confirmation ... 88
4.1.3 Transcriptional feedback further modulated the oscillation 92
4.1.4 HER-2 over-expression induces oscillation in a cell line dependent manner……..…….103
4.1.5 Role of crosstalk with the PI3K/Akt pathway in the modulation of oscillation of p-ERK1/2 103

4.1.6 Effects of EGF concentration on the oscillation 106
4.1.7 Serum deprivation affected the generation of oscillation 108
4.1.8 Discussion on the oscillatory dynamics of p-Akt and p-ERK1/2 110
4.2 Effects of trastuzumab, pertuzumab and their combination in breast cancer cell lines 117
4.2.1 Growth inhibitory effects of trastuzumab, pertuzumab and their combination 117
4.2.2 Trastuzumab regulates gene expression 128
4.2.3 Effects of trastuzumab, pertuzumab and their combination on signalling dynamics 131
4.2.4 Discussion 144
4.3 Tumour suppressor PTPN13 in breast cancer 151
4.3.1 PTPN13 as a candidate transcriptional regulator of the oscillation 151
4.3.2 The expression level of PTPN13 was correlated with PIK3CA mutation… 153
4.3.3 Discussion 156
Conclusion 158
References 165
Supplement 195

Declaration

I declare that all the work presented in this thesis is my own, unless otherwise stated. No part of this work has been, or will be submitted, for any other degree or qualification.

Huizhong Hu
2011
Breakthrough Breast Cancer Research Unit
Edinburgh Cancer Research Centre
University of Edinburgh
Western General Hospital
Crewe Road South
Edinburgh
EH4 2XU

Acknowledgement

The completion of this thesis project would not have been possible without the efforts of my primary supervisor, Dr. Simon Langdon who is knowledgeable and patient. I would like to appreciate the efforts he has made on my phD supervision. I would also like to express my gratefulness to him for helping me overcome the hardship after the scholarship terminates. From him not only do I learn how to do a scientific research but also how to write an informative and structured paper as well as the oral presentation. Stronger confidence has been established under his supervision. He always encourages me when I am depressed by the failure of the experiments and takes long time to analyse what may cause the failure even he is very busy with his own massive work. I would also like to appreciate Dr. Dana Faratian who is intelligent and perceptive. He gave me the ideas without which I would have struggled in the dark for a while. I am also grateful for all Professor David Harrison has done for the supervision of my study as well as the offer of stipend to help me bridge over difficulties. From him I have a better understand of non-parametric statistical tests. I would like to thank him for supporting me to carry out my ideas. Apart from sciences, he also creates relaxing environments for the whole group with which I have had a very happy life. I would like to thank Mr. Peter Mullen for the help in daily lab work and the early development of RPPA. Dr. Andy Sims and Liang Liang's help for the gene expression analysis is also highly appreciated. I would like to thank Kate Briton and Helen Caldwell for the daily management of the lab including order of consumables, arrangement of SOP writing and maintenance of instruments. Without their routine work, the project is hard to finish on time. I appreciate Rui Huang, Colette Meyer and Charlene Kay for doing me a favour of extracting and amplifying mRNA. I appreciate Danielle Wilson and In hwa Um for helping immunofluorescence analysis. I would like to thank the other lovely colleague for their supports. I am grateful that Dr. Alexey Goltsov helps me to establish a model for my oscillation work. I would also like to thank China Scholarship Council and University of Edinburgh for financially supporting my phD study and Dr. Dorothy Watson in University of Edinburgh to help the phD application. I would like to thank *Susan G. Komen for the Cure*® for supporting me

to present some findings within this thesis in the 33rd San Antonio Breast Cancer Symposium (AACR Translational Research Scholars scholarship supported by Susan G. Komen for the Cure® in the 33rd Annual CTRC-AACR San Antonio Breast Cancer Symposium, December 8-12, 2010.)

Particularly, I would like to appreciate all my family has done for me. My wife Jianing Bai understands and supports me and looks after the family very well which makes me be able to concentrate on the study. I thank my sister and brother-in-law who take my responsibility to look after my parents when I am not around them. I thank my parents and grandparents for supporting my study. Particularly, I would like to thank my late grandfather who kept telling me to work hard. I would like to thank my uncle in Japan who is always supporting my study financially since I was eight.

Abstract

The dynamics of cell signalling are critical to cell fate decisions. Human Epidermal growth factor Receptors (HERs)-mediated Ras/Raf/MEK/ERK and PI3K/Akt signalling cascades relay extracellular signals from the plasma membrane to targets in the nucleus and cytoplasm and play pivotal roles in cell fate determination including proliferation, differentiation and cell survival. Both pathways, once activated, are further regulated by complex feedback loops which may exert either positive or negative effects on cascade components and can result in signalling oscillation. In this study, heregulin (HRG) - and epidermal growth factor (EGF)-stimulated oscillation of both p-ERK1/2 and p-Akt expression in breast cancer cell lines was demonstrated. The oscillation was cell line dependent and was observed in MCF-7 and MCF-7/HER2-18 cells but not in BT474 cells. The oscillation was augmented by cycloheximide implicating transcriptional involvement. Gene expression analysis identified 29 genes as possible candidates involved in the transcriptional feedback regulation. Apart from the feedback regulation, feed-forward regulation was also observed. To expedite the analyses In-cell Western and Reverse Phase Protein Array (RPPA) assays were developed. A scheme of transcriptional feedback loops regulating the oscillation in the ERK1/2 pathway is proposed, including negative feedback loops to ERK1/2 from DUSPs, early positive and late negative feedback loops to MEK1/2 and positive feedback loops to HER-3 from AREG, HB-EGF, CYR61 and CTGF. Two HER-2-targeted inhibitory monoclonal antibodies were investigated – trastuzumab and pertuzumab. Trastuzumab not only inhibited the growth of HER-2 over-expressing MCF-7/HER2-18 cells and BT474 cells but also that of EGF-driven MCF-7 cells which expressed low/moderate HER-2 levels. Pertuzumab blocked the growth of both MCF-7 and MCF-7/HER2-18 driven by either EGF or HRG. When used in combination with trastuzumab, pertuzumab had much more potent activity in inhibiting cell growth and signalling than either single drug. Trastuzumab and pertuzumab had opposing effects on immediate p-ERK1/2 signalling and trastuzumab's effects on signalling could be mimicked by the PI3K inhibitor LY294002. PTPN13, a non-receptor type tyrosine protein phosphatase, is a proposed tumour suppressor in breast cancer. This was investigated as a candidate regulator of the signalling oscillation and although not

observed as a transcriptional modulator of the oscillation, its high expression level was observed to be associated with cell growth inhibition in MCF-7/HER2-18 cells by trastuzumab. Moreover, immunohistochemical analysis of 121 clinical tumours which had received trastuzumab treatment revealed the correlation between the expression level of PTPN13 and the mutation status of PIK3CA. In conclusion, the observed oscillation may contribute to the elucidation of the complex regulation of signalling pathways, which is vital to the different cell fate decision made through the same core pathway. The synergy between trastuzumab and pertuzumab supports the clinical use of the combination treatment and suggested PI3K/Akt pathway as the major pathway in controlling tumour growth.

Abbreviations

Ab: antibody

AD: actinomycin D

ADCC: antibody dependent cellular cytotoxicity

AF-1: activation function-1

AIBI: amplified in breast cancer I

Akt: AKT8 virus oncogene cellular homolog

AR: amphiregulin

Bad: BCL-2 associated death promoter protein

BCA: bicinchoninic acid

BRCA1: breast cancer gene 1

BRCA2: breast cancer gene 2

BTC: betacellulin

CHX: cycloheximide

c-Myc: myelocytomatosis oncogene cellular homolog

CST: Cell Signalling Technology

DAB: 3, 3'-diaminobenzidine

DAPI: 4', 6-diamidino-2-phenylindole

DCIS: ductal carcinoma in situ

DCSS: double charcoal stripped serum

DMEM: Dulbecco's Modified Eagle's medium

DMSO: dimethyl sulphoxide

DUSPs: dual specificity phosphatases

ECD: extracellular domain

ECL: enhanced chemiluminescence

EDTA: ethylenediaminetetraacetic acid

EGTA: ethylene glycol tetraacetic acid

EGF: epidermal growth factor

Elk: Ets-like transcription factor

ELISA: enzyme-linked immunosorbent assay

EMT: epithelial-to-mesenchymal transition

EPR: epiregulin

ER: oestrogen receptor

ERK: extracellular signal regulated kinase

ErbB: erythroblastosis oncogene B

E2: 17β-oestradiol

FBS: foetal bovine serum

FCS: foetal calf serum

FISH: fluorescence in situ hybridization

FPPA: forward phase protein array

g: gram(s); mg: milli gram(s); µg: micro gram(s)

GAPDH: glyceraldehyde 3-phosphate dehydrogenase

Grb2: growth factor receptor-bound 2

GDP: guanosine 5'-diphosphate

GTP: guanosine 5'-triphosphate

HB-EGF: heparin-binding EGF

HRG: heregulin-β1

HRP: horseradish peroxidase

HRT: hormone replacement therapy

HER: human epidermal growth factor receptor

IDC: infiltrating ductal carcinoma

IGF- I: insulin like growth factor- I

IgG: immunoglobulin G

IHC: immunohistochemistry

ILC: infiltrating lobular carcinoma

JNK: c-Jun N-terminal kinase

KSR: kinase suppressor of Ras

LCIS: lobular carcinoma in situ

M: mole(s) per liter; nM: nano mole(s) per liter; µM: micro mole(s) per liter; mM: milli mole(s) per liter

mAb: monoclonal antibody

MAPK: mitogen activated protein kinase

ml: milli liter(s)

mTOR: mammalian target of rapamycin

mTORC2: mammalian target of rapamycin complex 2

2-ME: β-mercaptoethanol

MEK: MAPK or ERK Kinase

NF-κB: nuclear factor-κB

NRG: neuregulin

NSCLC: non-small cell lung cancer

OD: optical density

OD540: optical density at 540nm

p-: phospho-

PAK1: p21-activated kinase 1

PARP: poly ADP ribose polymerase

PBS: phosphate buffered saline

PDK1: phosphoinositide dependent kinase 1

Pert: pertuzumab

PH: pleckstrin homology

PI3K: phosphoinositide 3-kinase

PIK3CA: PI3K catalytic domain

PIP3: phosphoinositol-3, 4, 5-triphosphate

PIP2: phosphatidylinositol 4, 5-bisphosphate

PR: progesterone receptor

PTEN: phosphatase and tensin homolog

PTPN13: protein tyrosine phosphatase, non-receptor type 13

PVDF: polyvinylidene fluoride

Ref: reference

RKIP: Raf kinase inhibitor protein

RNA: ribonucleic acid

rpm: revolutions per minute

RPPA: reverse phase protein array

RT: room temperature

SAP-1: switch-activating protein 1

SCB: Santa Cruz Biotechnology

SD: standard deviation

SDS-PAGE: sodium dodecyl sulphate-polyacrylamide gel electrophoresis

Ser, S: serine

SERMs: selective oestrogen receptor modulators

SOS: son of sevenless

SRB: sulphorhodamine B

Tam: tamoxifen

TBS: Tris buffered saline

TCA: trichloracetic acid

TGF: transforming growth factor

Thr, T: threonine

TKI: tyrosine kinase inhibitor

Tras: trastuzumab

Tris: tris (hydroxymethyl) aminomethane

Tyr,Y: tyrosine

Chapter One: Introduction

1 Introduction

Breast cancer is a malignant heterogeneous disease which originates in normal breast cells. It arises mostly in women, but men can get breast cancers too. Breast cancer is the most commonly diagnosed cancer among women in the UK. Nearly 46,000 new cases arise each year and nearly 1,000 women die of breast cancer every month in the UK (from www.breakthrough.org.uk). To better understand breast cancers, it is necessary and helpful to have some basic knowledge about the anatomy and physiology of the normal breast.

1.1 The anatomy and physiology of the normal breast

The female breast, which is located over the pectoral muscles of the chest wall and attached to the chest wall by fibrous strands called Cooper's ligaments, is basically composed of glandular tissues and stroma including fatty and fibrous tissues as well as blood and lymphatic vessels. A layer of fatty tissue surrounds the breast glands and extends throughout the breast providing a soft consistency for the breast. The anatomy is illustrated in Figure 1. The glandular tissues consist of lobules and lactiferous ducts. During lactation, milk is produced by the bulbs at the end of the lobules and transferred to the nipple through the lactiferous ducts. The arteries transport oxygen-rich blood from the heart to the breast and the veins bring the oxygen-depleted blood back to the heart. The breast is also made up of lymphatic tissues which offer the breast immunity to foreign invaders. An understanding of the lymphatic system (shown in Figure 2) is important since it is the major route for breast cancer cells to spread. The lymph nodes which are small bean-shaped collections of immune cells are connected by the lymphatic vessels. In the lymphatic vessels is clear fluid called lymph. The breast tissue fluid and waste products are carried away from the breasts in the lymph through the lymphatic vessels. Sometimes breast cancer cells can spread to the lymph nodes (initially to the axillary lymph nodes). The more lymph nodes in which cancer cells are found, the higher is the possibility of metastases to other organs. However, not all women with breast cancer

cells in lymph nodes will have metastasis and women developing metastases may not have breast cancer cells in lymph nodes.

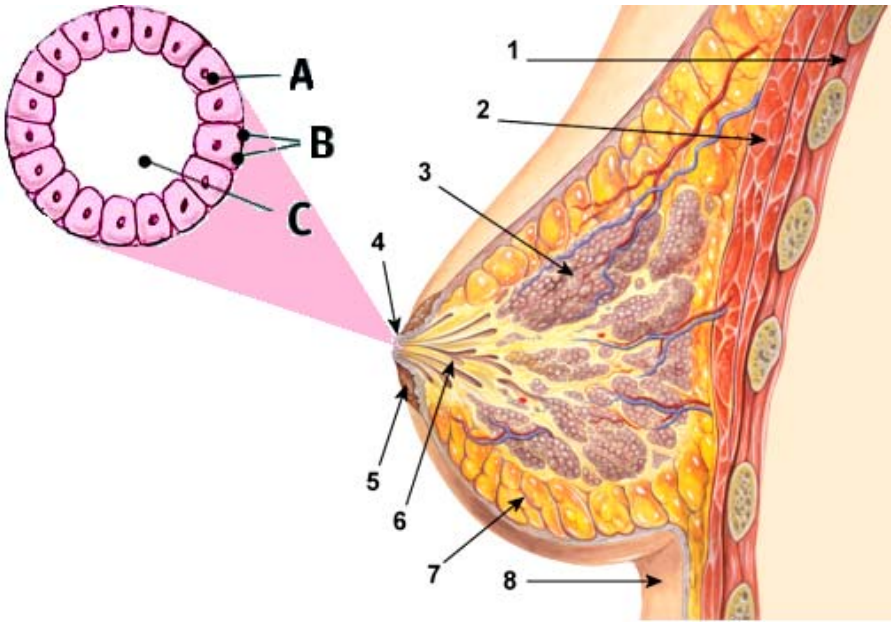

Figure 1 The anatomy of normal breast. 1. Chest wall, 2. Pectoral muscles, 3. Lobules, 4. Nipple, 5. Areola, 6. Lactiferous duct, 7. Fat, 8. skin. The top left of the picture shows the enlargement of cross section of the duct**: A** normal duct cells, **B** basement membrane, **C** lumen (this picture is reproduced from Wikipedia).

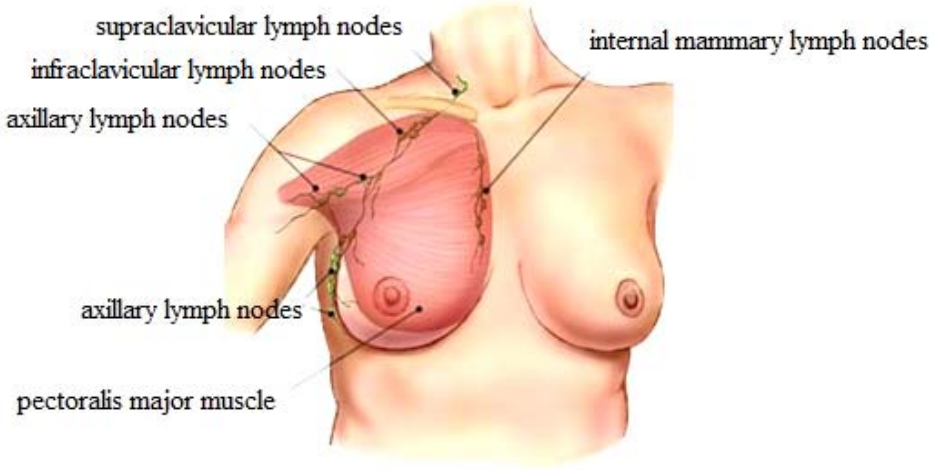

Figure 2 The lymphatic system of female breasts. Most of the lymph vessels in the breast are connected to the under-arm nodes which are called axillary lymph nodes while some are connected to the nodes inside the chest called internal mammary lymph nodes and to the nodes above the collarbone (supraclavicular lymph nodes) or below (infraclavicular lymph nodes).
(Reproduced from the online resources of BC Cancer Agency, http://www.bccancer.bc.ca/HPI/Nursing/Education/breastcancer/breasthealthbasics.htm).

1.2 Biology of breast cancer

Cancer is a class of diseases characterized by uncontrolled cell growth, invasion and sometimes metastasis. These three malignant properties differentiate cancers from benign tumours which are abnormal tissue masses with limited growth, no invasion or metastasis. Among the three properties, metastasis accounts for more than 90% of cancer-related deaths (1). Cancers can be classified into the following five groups by the types of cells that form the tumours.

1) **Carcinoma**: malignant tumours derived from epithelial cells.
2) **Sarcoma**: malignant tumours derived from connective tissue, or mesenchymal cells.
3) **Lymphoma** and **leukemia:** malignancies derived from hematopoietic cells.
4) **Germ cell tumour:** tumours derived from totipotent cells.
5) **Blastic tumour or blastoma:** A tumour (usually malignant) which resembles an immature or embryonic tissue.

Breast cancer refers to cancers originating in breast tissues. The majority of breast cancers are carcinomas. The most common types of breast cancer develop initially from abnormalities in epithelial cells of the ducts. These cells are shown in the enlargement of Figure 1.

1.3 Metastasis of breast cancer

The process of breast cancer spreading to other parts of the body is called metastasis. The major sites of metastasis are the bone, lungs, liver and the brain (2). Among these sites bones are the most common sites of metastasis (3). Primary tumours need to undergo several steps before becoming metastatic. Tumour cells proliferate and then invade across basement membrane into local healthy tissues. The invading tumour cells then invade the circulatory system through spreading to lymph nodes. Some cells survive in the circulatory system and then spread to distant target sites where cancer cells proliferate and form a micrometastasis. Finally, the micrometastasis becomes a metastasis through progressive colonisation.

As mentioned at the beginning of Section 1.2, metastasis accounts for more than 90% cancer-related death. So it is critically important to understand metastasis mechanisms to propose efficacious therapy strategies. Several models of cancer metastasis have been primarily described by Talmadge (4). The most prevailing model is the clonal selection of metastasis. Primary tumours from the same cells undergo multiple biochemical and molecular changes and then lead to clonal evolutions with phenotypic and behavioural diversities including enhanced migration capability, invasiveness and metastasis. In this model, tumour metastasis is believed to be the outcome of a clonally selective process during tumour progression, which has been supported by experimental data (5-8).

Based on the observations that genetic alteration of breast cancer cells disseminated in bone marrow was generally different from that of primary tumour cells (9), another model called parallel evolution was proposed. This model interprets that dissemination of cancer cells in bone marrow occurs at an early stage and then cancer cells in bone marrow become metastatic in a primary tumour-independent way, which means that metastasis occurs at the beginning of progression and then primary tumours and metastatic tumours undergo parallel evolutions (10).

The third model is the dynamic heterogeneity model of metastasis. This model suggests that the metastatic efficiency is determined by the generation rate of metastatic variants within tumours (4). The metastatic variants may be unstable, leading to a dynamic equilibrium of generation and loss of metastatic variants (11). This model also incorporates epithelial-to-mesenchymal transition (EMT) (4). EMT is a complex molecular and cellular programme that allows the transition of basement membrane-attaching epithelial cells to a motile and unpolarised mesenchymal cell phenotype including enhanced motility, invasiveness, increased production of extracellular matrix components and elevated resistance to apoptosis (12). In EMT epithelial cells lose the well-differentiated features such as cell-cell adhesion, polarity and immotility (13). EMT plays a critical role in embryonic development (14), however, its role in tumour metastasis has been increasingly recognised (15, 16). It was demonstrated that EMT could result in the generation of

breast cancer cells with stem cell-like characteristics (17, 18). The existence of EMT in human tumours provides the basis to explain the characteristics of cancer progression and metastasis.

1.4 Grading and staging of breast cancer

The grading and staging of breast cancers can help doctors to assess prognosis and make a decision around the most appropriate treatment options to obtain the best outcome.

Within pathological assessment, grading is a measure of the differentiation of tumours. For grading breast cancer, the Bloom-Richardson system (19) is used and has a scoring scale of 1 to 3. This grading system determines how aggressive breast cancers are by examining breast cancer cells and tissue structure under the microscope. The following three features are taken into account in this system and each feature is scored from 1 to 3.

1) Percentage of tubular structures in tumours. If there is extensive tubule formation, score 1 is given. If there is a moderate attempt at tubule formation, score 2 is awarded. If there is a slight or no tubule formation and cells grow in sheets and strands, score 3 is assigned.
2) Degree of hyperchromatic and mitotic activity which is indicated by the number of hyperchromatic or mitotic figures in a microscopic high power field (400x magnification level). If only occasional hyperchromatic or mitotic figures are present per field, score 1 is assigned. Score 2 is given if there are two or three such figures present in most fields. Score 3 is awarded if more than three such figures are present in most fields.
3) Nuclear grade which is indicated by nucleus size and uniformity. Score 1 is given if nuclei are fairly uniform in size, shape and staining. Score 2 is given if variation in uniformity is moderate. If a marked nuclear irregularity is observed, score 3 is given.

Scores for the three features are all summed to a total ranging from 3 to 9. In terms of the total, breast cancers can be categorized into three grades as shown by Table 1.

Table 1 Tumour grade of breast cancers

Total feature score	*Tumour grade*	*Appearance of cells*
3-5	Grade 1 (low malignancy)	well-differentiated
6-7	Grade 2 (moderate malignancy)	moderately-differentiated
8-9	Grade 3 (high malignancy)	poorly-differentiated

Grade 1 (low grade) tumours look very like normal breast tissues, grow slowly and are not aggressive. They have the best prognosis. Grade 3 (high grade) tumours look very abnormal, grow more quickly and are aggressive. They have the worst prognosis. Grade 2 (moderate grade) tumours fall between the above two grades and have medium prognosis.

Staging of breast cancer can tell doctors whether cancer is limited to one area in the breast, or if it has spread to healthy tissues inside the breast or to other parts of the body. The most commonly used staging system for breast cancers is the American Joint Committee on Cancer (AJCC) TNM system. 'T' describes the size of a tumour and whether it has invaded local tissues. 'N' describes whether a cancer has spread to regional lymph nodes. 'M' describes whether a cancer has spread to other parts of the body (distant metastasis). According to the fifth edition of '*AJCC cancer staging manual*'(20) , this system classifies breast cancers based on the following criteria.

Primary tumour (T) categories:

TX: Primary tumour cannot be assessed*.

T0: No evidence of primary tumour.

Tis: Carcinoma in situ or Paget disease of the nipple with no associated tumour mass.

T1: Tumour is 2 cm or less across in diameter.

T2: Tumour is more than 2 cm but not more than 5 cm across.

T3: Tumour is more than 5 cm across.

T4: Tumour of any size extending into the chest wall or skin. This includes inflammatory breast cancer.

*Use of an "X" rather than a number or other suffix means that the parameter can not be assessed.

Regional lymph nodes (N) categories:

NX: Regional lymph nodes cannot be assessed.

N0: Cancer cells have not spread to regional lymph nodes.

N1: Cancer cells have spread to movable ipsilateral axillary lymph node(s)

N2: Cancer cells have spread to ipsilateral axillary lymph node(s) fixed to one another or to other structures

N3: Cancer cells have spread to ipsilateral infraclavicular lymph node(s) or internal mammary lymph node(s) with axillary lymph nodes or supraclavicular lymph node(s).

Distant Metastasis (M) categories:

MX: Presence of distant metastasis cannot be assessed.

M0: No distant metastasis is present.

M1: Distant metastasis to other parts of the body is present.

Once the characteristics of T, N, and M are determined, information is combined to define a breast cancer stage.

Stage 0: Tis, N0, M0

Stage I: T1, N0, M0

Stage IIA: T0 or T1, N1, M0; T2, N0, M0

Stage IIB: T2, N1, M0; T3, N0, M0

Stage IIIA: T0 to T2, N2, M0; T3, N1 or N2, M0

Stage IIIB: T4, any N, M0**;** any T, N3, M0

Stage IV: any T, any N, M1

Based on the determined stages of breast cancer, mean survival rate for patients with the same stages can be statistically predicted (Table 2). A 5-year survival rate refers to the percentage of patients who are still alive 5 years after diagnosis with a specific stage of breast caner. Deaths from other causes are not taken into account. Survival

rate is calculated based on previous outcomes of large number of patients who are diagnosed with breast cancer, but for individual patients doctors can not predict with certainty what will happen to them 5 years after prognosis.

Table 2 Breast cancer stages and 5-year survival rate (adapted from American Cancer Society)

Stage	5-year Mean Survival Rate
0	93%
I	88%
IIA	81%
IIB	74%
IIIA	67%
IIIB	41%
IV	15%

1.5 Histopathological classification of breast cancer

Pathologists categorise breast cancers according to their microscopic anatomy and other criteria including pathological grade of tumours. For example, the most common pathological types of breast cancer are invasive ductal carcinoma and invasive lobular carcinoma. There are four common forms of breast cancer.

Lobular carcinoma in situ (LCIS): LCIS describes primary tumours initially developing in lobules which spread no further. It accounted for approximately 12% of in situ breast cancer diagnosed from 2002-2006 in the USA (21). Traditionally many pathologists believe that LCIS is an indicator of increased risk for developing invasive breast cancer in the future rather than a real cancer. It is also called lobular neoplasia. Women who are diagnosed with LCIS have a 25% chance of developing invasive breast cancers within 25 years of the initial diagnosis. Nowadays the majority of women who are diagnosed with LCIS on biopsy don't receive therapy. Instead, their disease will be closely monitored after diagnostic biopsy including regular screening mammograms, annual clinical breast examinations and monthly breast self-examinations. For the prevention of invasive breast cancer with high risks or reduction of the risks, some women who have major concerns about developing cancer choose prophylactic mastectomy (no requirement of the removal of axillary lymph nodes) generally followed by breast reconstruction. Many breast surgeons

regard this approach as too aggressive. The alternative option to reduce the risk of developing invasive breast cancer is via administration of tamoxifen. Tamoxifen can reduce the risk of developing invasive breast cancer by 49% according to the clinical trial results of the American National Surgical Adjuvant Breast and Bowel Project P-1 Study (22). The application of tamoxifen for women at high risk of breast cancer for prevention has been approved by the U.S. Food and Drug Administration (FDA) in 1998.

Ductal carcinoma in situ (DCIS): DCIS is the most common non-invasive breast cancer and accounts for 80% cases of in situ breast cancers diagnosed from 2002-2006 in America (21). DCIS develops in ducts of the breast but doesn't break the internal wall of the ducts and invade the surrounding tissues. DCIS is typically classified according to the architectural pattern (solid, cribriform, papillary and micropapillary), the tumour grade (low, intermediate and high) and the presence or absence of comedo necrosis (23). The presence of comedo necrosis suggests the likelihood of the DCIS becoming more aggressive. The incidence of DCIS has increased profoundly since the early 1970s which may be due to the widespread use of screening mammography (21). For example, the estimated incidence in 1975 was 5.8 per 100,000 women while the estimated incidence was 32.5 per 100,000 women in 2004 (23). DCIS is often detected by mammogram and then confirmed by biopsy. Nearly all women who are diagnosed with DCIS can be cured. The treatment of DCIS includes simple mastectomy and lumpectomy usually followed by radiation treatment. Simple mastectomy is the surgical removal of the entire breast not including the axillary lymph nodes. Lumpectomy is the removal of the cancerous mass including the margin of normal breast tissues. Lumpectomy is a breast conserving surgery. However, not all women are suitable for lumpectomy. According to the American Cancer Society online resources (Treatment of stage 0 (non-invasive) breast cancers; http://www.cancer.org/Cancer/BreastCancer/DetailedGuide/breast-cancer-treating-stage0) women who have the following conditions are not ideal candidates for lumpectomy.

1) The area of DCIS is very large.
2) More than one area of cancer was detected in the same breast.

3) Lumpectomy can not completely remove the cancer.
4) Women are pregnant at the time of radiation.
5) Women have connective diseases.

If the DCIS is ER-positive, tamoxifen can be administered after surgery to reduce the risk of recurrence and of developing invasive breast cancer.

Infiltrating lobular carcinoma (ILC): ILC is also known as invasive lobular carcinoma, which develops in the lobules initially and then breaks the wall of the lobules and invades to connective tissue of the breasts. It is the second most common type of breast cancer after IDC and accounts for 8%-14% of breast cancers (24-26), but for unknown reasons the incidence of ILC is increasing from 1977 among women of age 50 and above according to an epidemiological study (27). ILC's features include hyperchromatic small round cells forming single infiltrating files. Patients with ILC often show no palpable mass or vague thickening in the breasts without distinct border (28).

Infiltrating ductal carcinoma (IDC): IDC is also known as invasive ductal carcinoma, which develops in the ducts initially and then penetrates the wall of the ducts and invade other tissues within the breast or other regions of the body. It is the most common type of breast cancers and accounts for 80% of breast cancer diagnoses (from Cancer Research UK online resources).

Additionally, there are also some less common types of breast cancer.

Medullary carcinoma: medullary carcinoma is a type of IDC and takes the name from its colour, close to the colour of medulla of the brain. Tumour cells have large vesicular nuclei and prominent nucleoli. This type of tumour tends to form clear boundary between the tumour and the normal tissues. Prominent lymphocytic infiltrate both at the periphery and within the tumour is present. A tumour with less lymphocytic infiltration or an infiltrating margin in parts of the tumour is regarded as an atypical medullary carcinoma (29).

Mucinous carcinoma: A wide range of breast cancers produce mucin which is the major component of mucus. Among them is mucinous carcinoma which is characterized by the proliferation of clusters of generally small and uniform cells. These cells float in large amount of the extracellular mucus. The mucus is often visible to the naked eye (29). In mucinous carcinoma, mucin is the major component and surrounds the breast cancer cells.

Tubular carcinoma: Tubular carcinoma is a rare subtype of infiltrating ductal carcinoma, accounting for less than 2% of all breast cancer cases (29, 30). Compared with IDC Not Otherwise Specified (NOS IDC), it occurs often among older patients with small size and dramatically less nodal involvement. It is characterized by well-differentiated, tube-shaped breast cancer cells which grow slowly and metastasize infrequently. The size of tubular carcinoma is very small usually ranging from 0.2 to 2 cm in diameter. The majority of the cases are 1cm or less (29). It is nearly always oestrogen and progesterone positive and mostly HER-2 negative (31, 32).

Inflammatory breast cancer: Inflammatory breast cancer (IBC) is a rare type of highly aggressive breast cancers. It is so called because of the symptoms being similar to those found in inflammation. It is defined in the clinic by the rapid development of diffuse erythema and edema (peau d'orange) over more than 1/3 of the breast surface often without palpable mass (29, 33). Invasion of cancer cells to local dermal lymph vessels may form tumour emboli which may impair the drainage and inflame and cause breast swell. IBC is characterized by the early age at diagnosis, poor prognosis and negative oestrogen/progesterone status. Approximately 60% of IBC have HER-2 over-expression. The treatments of IBC involve multimodality therapy including chemotherapy, radiotherapy, surgery, endocrine therapy and trastuzumab therapy.

Paget's disease of the nipple: Paget's disease of the nipple was described by Sir James Paget in 1874 as a syndrome in which the ulceration of the nipple was associated with underlying cancer (29). It is characterized in the clinic by nipple or areola erythema, eczema, ulceration, bleeding and itching. The diagnosis is often

delayed for months due to these clinical characteristics. The diagnosis is confirmed with the full thickness biopsy of the areola and nipple (34). There is an underlying cancer in 80% of the cases and the cancers are not necessarily adjacent to the nipple-areola area (35).

Phyllodes tumour: Phyllodes tumours of breast are unusual fibroepithelial tumours which are categorized as benign, borderline and malignant subtypes. The prognosis of Phyllodes tumours is usually favourable. Regardless of the histological subtype, wide local excision with tumour-free margins of 1 cm or above is the primary therapy (29, 36).

1.6 Molecular classification of breast cancer

Breast cancer is a heterogeneous disease. Individual cancers have different prognoses and different responses to therapies. According to the prognostic and predictive value of the receptor status of cancer cells, breast cancers can be primarily grouped into hormone receptor-positive (ER^+/PR^+), HER-2-positive ($HER\text{-}2^+$) and triple receptor negative (ER^-, PR^- and $HER\text{-}2^-$) categories based on immunohistochemistry (IHC) and fluorescence in situ hybridization (FISH). Classification of breast cancers into the former two categories is particularly useful since the targeted therapies available are only effective in these subsets of patients. For example, determination of hormone receptor status is useful to determine whether patients are candidates for endocrine therapy. Patients with hormone receptor negative status don't benefit from endocrine therapy. However, even within the same hormone receptor-positive group, breast cancers can have a large variation in response to tamoxifen and 25% of ER^+/PR^+ fail to respond (37). A similar situation applies to HER-2 positive tumours and response to trastuzumab (38). Investigations are underway to understand the causes of differences in response to the same therapeutic regime and to define further the molecular classification of breast cancer, in particular whether further sub-grouping of the molecular signatures might help differentiate which breast cancers respond to a particular therapy. Moreover, the techniques used to test the receptor status (IHC and FISH) can produce intra- and inter-laboratory variations since the interpretation of staining is to some degree subjective to individual pathologists and

thereby can result in false positives or false negatives which interfere with the use of appropriate therapies.

The advent of high throughput gene expression profiling provides us with an opportunity to answer the above questions and to classify breast cancers based on gene expression patterns. Gene expression profiling revealed four broad subsets of breast cancers with distinct differences in prognosis and responsiveness to therapy according to gene expression patterns: luminal-like, basal-like, normal-like and HER-2 positive (39). As shown in Figure 3, these four subtypes of breast cancers have their own distinct gene expression patterns and their distinct different prognoses are shown in Figure 4. These four subtypes are defined by the expression of particular clusters of genes which are characteristically expressed under specific circumstances such as in luminal epithelial cells, basal epithelial cells and normal breast cells and when *HER-2* oncogene is over-expressed.

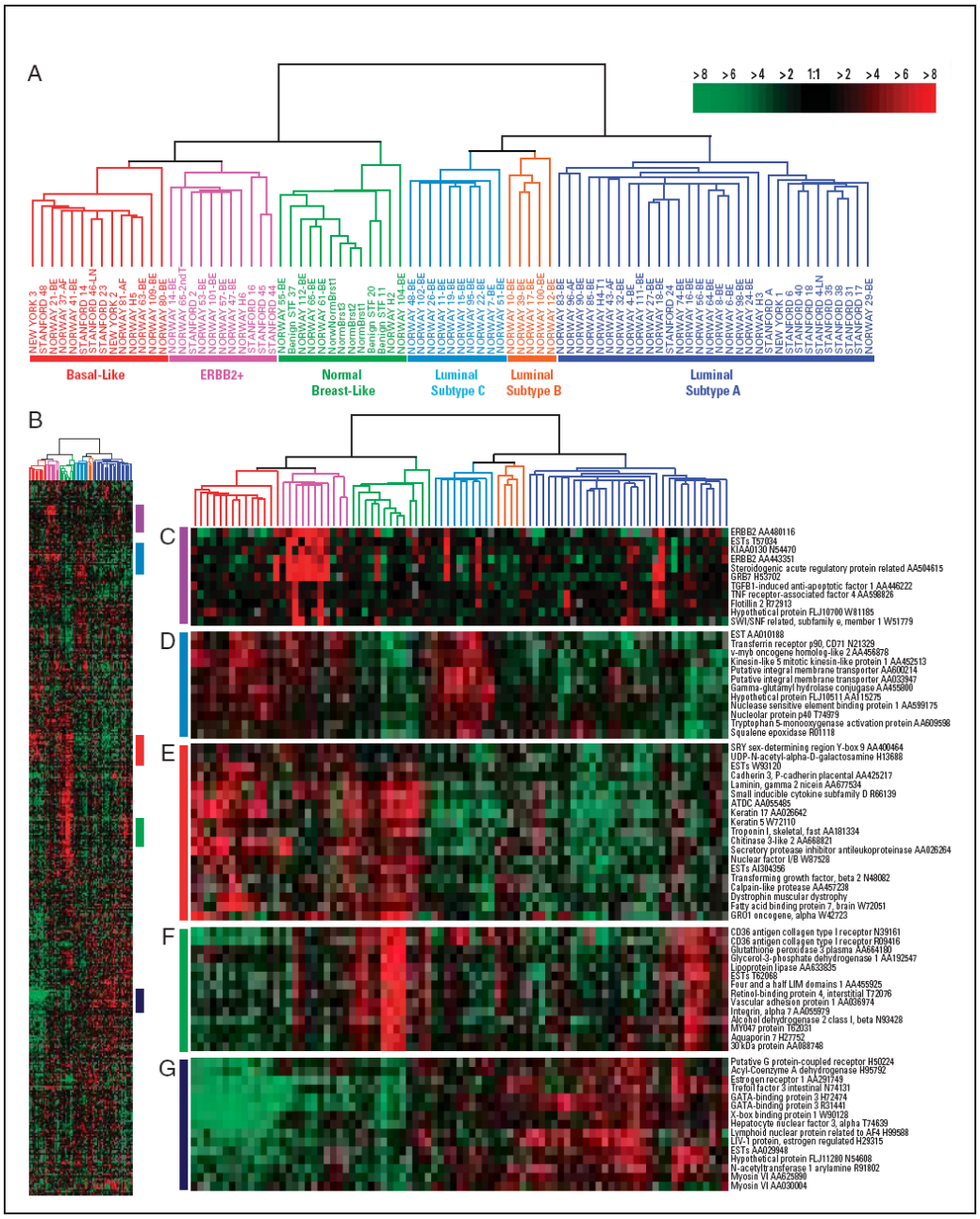

Figure 3 Gene expression patterns of 85 experimental samples representing 78 carcinomas, 3 benign tumours, and 4 normal tissues, analyzed by hierarchical clustering using the 476 cDNA intrinsic clone set. (A) The tumour specimens were divided into five (or six) subtypes based on differences in gene expression. The cluster dendrogram showing the five (six) subtypes of tumours are coloured as: luminal subtype A, dark blue; luminal subtype B, yellow; luminal subtype C, light blue; normal breast-like, green; basal-like, red; and ERBB2+, pink. (B) The full cluster diagram scaled down. The coloured bars on the right represent the inserts presented in C–G. (C) ERBB2 amplicon cluster. (D) Novel unknown cluster. (E) Basal epithelial cell-enriched cluster. (F) Normal breast-like cluster. (G) Luminal epithelial gene cluster containing ER. **Reprinted from ref (40)**.

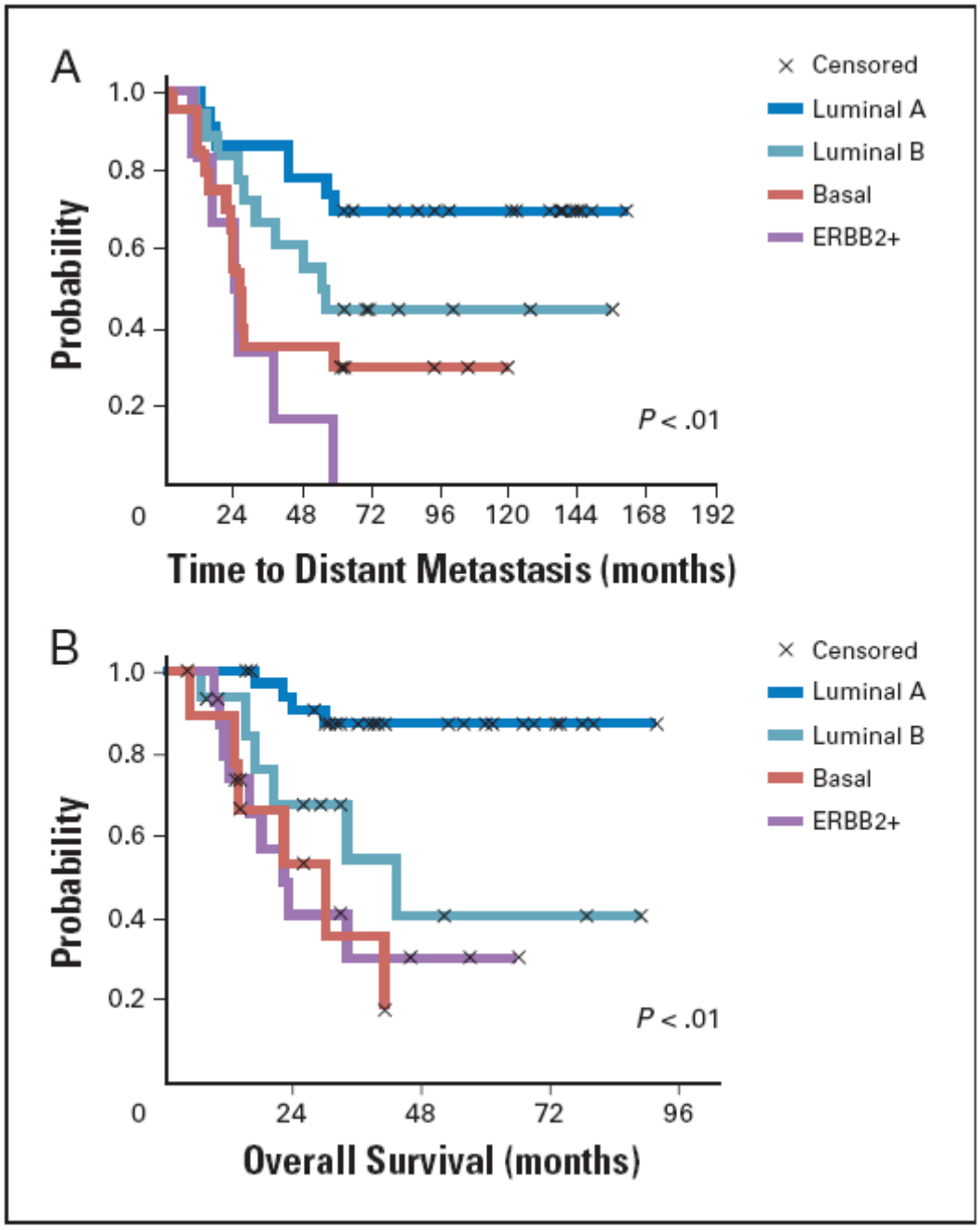

Figure 4 Disease outcomes in two patient cohorts. (A) Time to development of distant metastasis in the 97 sporadic cases. (B) Overall survival for 72 patients with locally advanced breast cancer in the Norway cohort. The normal-like tumour subgroups were omitted from both data sets in this analysis. **Reprinted from ref (41)**.

In the luminal cluster, cytokeratins 8 and 18, transcriptional factors including GATA-binding protein 3, X-box binding protein 1 and hepatocyte nuclear factor 3, ER and ER-activating genes such as *LIV1* and *CCND1* are expressed (Figure 3G) (39, 42). All luminal-like subtypes are ER-positive, fewer than 20% of luminal-like breast

cancers have TP53 (tumour protein 53 whose mutation was suggested to be an early event in breast cancer development and associated with poor prognosis (43)) mutations (42) and 63% of these tumours are low or intermediate grade (44), therefore these subtypes are generally sensitive to endocrine therapy. Within the luminal-like cluster, at least two subtypes have been differentiated: luminal A and luminal B (40, 42). Although in the same cluster, luminal A and luminal B have distinct characteristics. In general, luminal A cancers have higher ER-related gene expression and lower expression of proliferation-related genes than luminal B tumours (40, 41). Generally, luminal-like breast cancers have a good prognosis. However, there is a clear difference in the outcome between luminal A and luminal B with luminal B cancers having a significantly worse prognosis in multiple data sets (41, 45).

Brenton et al in a review paper (45) emphasized that the array designation of HER-2 positive tumours should not be confused with the clinical HER-2 over-expression tumours identified by IHC or FISH since not all clinical HER-2 over-expression tumours have mRNA expression changes that define the cluster. The HER-2-array subtype refers to a large group of tumours which are hormone receptor negative (low ER or related genes expression in array) but have a HER-2 associated gene expression pattern in the array. Clinical HER-2 over-expression tumours refer to those tumours identified by IHC for protein expression or by FISH for the excess number of gene copies. Most clinical HER-2 over-expression tumours will however fall into the HER-2-array positive subtype. However, others will over-express hormone receptors and most of these tumours are grouped into the luminal-like subtype (40-42). HER-2-array positive tumours carry a poor prognosis and are more than two-fold more likely to involve axillary lymph nodes than luminal A subtype besides having poor differentiation and higher grade (46). HER-2 array positive tumours are characterized by over-expression of other genes in the HER-2 amplicon such as GRB7 (Figure 3C). In spite of their poor prognosis, HER-2 array positive tumours demonstrated sensitivity to anthracycline and taxane-based neoadjuvant therapy (47). They also respond to molecularly targeted therapies such as trastuzumab.

The expression pattern of the basal-like subtype mimics that of basal epithelial cells in other parts of the body and normal myoepithelial cells in breasts. In this subtype the expression of *ER* and *ER*-related genes as well as *HER-2* and related genes are deficient, but basal cytokeratins 5, 6, 14 and 17, integrin-β4 and laminin genes are strongly expressed (Figure 3E) (39). Proliferation-related genes are also expressed (39, 42). Basal-like breast tumours are more likely to have aggressive features such as *TP53* mutation and a higher likelihood of being grade 3 than luminal A tumours (40, 46). Multiple independent data sets have also shown a poorer prognosis for basal-like tumours (40-42). Given their triple-negative receptor status, basal-like tumours are refractory to conventional targeted therapies such as endocrine therapy and trastuzumab therapy, leaving only chemotherapy as a systemic therapy. Despite the poor prognosis, basal-like tumours are sensitive to chemotherapy (45). Rouzier et al (47) and Carey et al (46) observed the higher response of basal-like tumours to anthracycline-based or combination of anthracycline and taxane-based neoadjuvant chemotherapies than non-basal-like tumours. This sensitivity however may not apply to all chemotherapeutic agents. As demonstrated by Sorlie et al (41) and Turner et al (48), most women carrying *BRCA1* mutations generally develop basal-like breast cancers. BRCA1 functions in DNA repair and cell cycle checkpoint and loss of its functions may result in sensitivity to DNA damaging agents and resistance to mitotic spindle poisons (49).

In the first study to examine the comprehensive gene expression pattern of breast cancers (39), several tumours samples were clustered with three normal breast specimens (Figure 3 A, light green branches). Gene expression pattern of normal-like breast tumours are typified by the high expression of genes characteristic of basal epithelial cells and adipose cells and low expression of genes characteristic of luminal epithelial cells (39).

This molecular classification has its inherent limitations, since up to 30% of breast cancers do not fall into any of the four categories (50). Evolution of the molecular classification may require new technological platform, availability of larger datasets as well as more understanding of breast cancer biology.

1.7 Risk factors for breast cancer

Every woman is at risk of developing breast cancer, but some are at higher probability of developing the disease. It is very important to understand the risk factors since they influence the medical decision making. Risk factors have been identified through epidemiologic studies and new ones continue to be identified. Joy et al in their book '*Saving women's lives: strategies for improving breast cancer detection and diagnosis'* (51) listed a number of risk factors. Here I summarize and describe these factors briefly.

Germ-line and somatic mutations

Before a cell becomes malignant, molecular changes which alter the protein's function must accumulate. For example, the loss of function of tumour suppressor genes or gain of function of oncogenic genes may cause the occurrence of breast cancers. Some changes (mutations) may be inherited. Approximately 5-10% of breast cancer cases result from these types of change (52). Among the genes involved in breast cancer susceptibility, BRCA1 (breast cancer gene 1) and BRCA2 (breast cancer gene 2) are two human tumour suppressor genes which account for a 60% risk of being diagnosed with breast cancer during a woman's lifetime when they become abnormal according to the online resources of National Cancer Institute, USA (BRCA1 and BRCA2: Cancer Risk and Genetic Testing, http://www.cancer.gov/cancertopics/factsheet/Risk/BRCA#r4). They help to repair DNA damage and kill cells in which the DNA damage can't be repaired. When these two genes are damaged, cells harbouring the DNA damage may duplicate without control and develop into cancers. Women inheriting the deleterious mutations of BRCA1 or BRCA2 have increasingly higher risks for breast cancer than those women whose BRCA1 or BRCA2 functions normally, although these mutations are present in far less than 1% of the general population (53). Despite the risk for breast cancer being very substantial for the individual women who carry the inherited mutations, less than 10% of breast cancer cases result from germ-line mutations. The majority of breast cancer cases are due to molecular changes in somatic cells that occur during women's lifetimes rather than being present in the germ-line. These molecular

changes could arise from exposure to carcinogens in the environment, random mutations occurring in cell division during lifetime and too much exposure to stimuli within the body such as oestrogen. Inherited mutations can sometimes sensitize certain genes to mutation. For example, BRCA1 and BRCA2 can repair DNA damage and if they are mutated, the ability of cells to correct the genetic mistakes happening during cell division will be diminished. As a result, mutations accumulate faster than they would otherwise.

Past history of breast cancer

Women who have had breast cancer in one breast have an increased risk of developing cancers in the other breast. Women who were diagnosed with LCIS and/or DCIS have an increased risk of developing invasive breast cancers.

Current age

It is understandable that age is considered as a risk factor. The longer that women live, the greater the chance that harmful mutations will accumulate. In addition, generally speaking, younger women have more potent immune systems than the elderly, which means that the immune system in young women has stronger surveillance ability. The table below (table 3) adapted from a published report written by the American Cancer Society in 2003 *'Breast cancer facts and Figures 2003-2004'* demonstrates the age-specific probability of developing breast cancer.

Table 3 Age-specific probability of developing breast cancer*

If current age is	*Then the probability of developing breast cancer in the next 10 years is:*	**or 1 in:**
20	0.05%	2,152
30	0.40%	251
40	1.45%	69
50	2.78%	36
60	3.81%	26
70	4.31%	23

*Among those free of cancer at the beginning of age interval. Based on the cases diagnosed between 1988 and 2000. Percentages and '1 in' may not be numerically equivalent due to rounding.

Radiation exposure

It is understandable that excessive exposure to radiation will cause genetic mutations in essential genes some of which correlate with the development of breast cancer such as in the BRCA1 and BRCA2 genes mentioned above.

Breast density

Younger women have denser breasts than the elderly. With aging, gland tissues will be replaced by fat tissues and connective tissues. Denser breasts have more dark areas which interfere with the interpretation of mammograms. Several studies have demonstrated that breast cancer risk increases with rising breast density (54, 55).

Family history

Women in families where the first-degree relatives have had breast cancer have an increased risk of developing the disease (56). The risk is even higher if the first-degree relative developed breast cancer before age 40 or if they have had cancers in both breasts (57). The effect of family history on breast cancer risk may be due to both the inherited mutations mentioned above and the similar life styles including environmental factors (58).

Age at first birth and breast feeding

The breasts before giving birth to babies are not completely developed, which means that some cells (mammary gland cells) are not well differentiated before first pregnancy (59-61) and have a higher potential to proliferate. The breasts will develop completely during pregnancy and after years of breast feeding when mammary gland cells divide and differentiate to be able to produce milk. Under the stimulation of circulating oestrogen, non-differentiated cells have an increased risk of uncontrolled growth and may become malignant. Women of an older age at their first birth have a higher risk themselves. Women who have never been pregnant have an even higher risk for developing breast cancer. Studies demonstrate those women who have their first full-term pregnancies at age before 25 have a lower risk than those nulliparous women or women who have their first pregnancies at the age of 30 or above. Extra pregnancies can also reduce the risk to an even lower level (62). It has also been

shown that long-term breastfeeding can decrease risk (63). The longer the period of the breastfeeding, the lower the risk of developing breast cancers.

Early menarche and late menopause

During menopause the circulating levels of hormones such as oestrogen and progesterone produced by the ovaries reduces dramatically. Late menopause (after age 55) as well as early menarche (before age 12) means a longer exposure of the breast tissues to hormones, which increases the risk of breast cancer.

Hormone replacement therapy

Hormone replacement therapy (HRT) is a type of medical treatment applied to surgically premenopausal, menopausal and postmenopausal women who feel uncomfortable when the circulating hormones such as oestrogen and progesterone diminish. It involves the administration of oestrogen alone or with progesterone to boost hormone levels. The longer HRT is taken, the higher the risk of developing breast cancer (64).

Alcohol intake

It has been reported in multiple studies that alcohol consumption is associated with an increased risk of developing breast cancer (65-69). Ellison and Zhang et al (67) in their meta-analysis of epidemiologic studies carried out through 1999 demonstrated a dose-dependent monotonic increase of the relative risk for breast cancer regardless of the menopausal status and beverage types. The study conducted by Singletary and Gapstur (70) investigated the potential mechanisms of the association of alcohol intake with the increased risks. They found that the increased levels of oestrogen and androgen in women who consume alcohol were likely to be one of the mechanisms underlying the association. The other plausible mechanism was that the alcohol consumption may increase the susceptibility of the breasts to carcinogens. Controversially, others showed an inverse relation between red wine consumption along with other types of beverage and risks (71-73) which may be due to the effects of resveratrol and other substances in red wine causing a reduction of breast cancer risk (74-76).

Other risk factors

Apart from the risk factors mentioned above, other factors such as race/ethnic groups, unhealthy living habits, physical activity and obesity have been associated with the risk of developing breast cancer. In the USA, white women are diagnosed with breast cancer more often than African American/black, Hispanic/Latina, Asian Pacific Islander, or American Indian/Alaska Native women (77). Women with poor physical activity (unhealthy living habits often result in poor physical activity) or who are overweight have an increased risk of developing breast cancer.

From the above description it is likely that each individual factor interacts with others. Although many risk factors have been identified, it is impossible to determine which women will develop breast cancer and who will not as well as when and how individual women will develop breast cancer. Many women never develop breast cancer even though they bear some of risks mentioned above.

1.8 Treatments for breast cancer

There are multiple treatments for breast cancer in clinical use, including local therapy and systemic therapy. The local therapies include surgery and radiotherapy. The systemic therapy can be sub-grouped as chemotherapy, endocrine therapy and biological therapy.

Surgery

This treatment refers to the medical removal of the cancer from the breast and the lymphatic nodes. Basically there are two types of surgery including partial and entire breast removal known as lumpectomy and mastectomy respectively. In lumpectomy, which is often followed by adjuvant radiation for a couple of weeks, only the cancerous tissues as well as a rim of normal tissues are removed to conserve the breasts. Women who choose lumpectomy with adjuvant radiation will have the same expected lifetime survival as those who undergo mastectomy (78). There are a variety of mastectomy techniques in clinical use including simple mastectomy, modified radical mastectomy, radical mastectomy, skin sparing mastectomy and nipple sparing mastectomy. Which mastectomy approach is used will depend on

many factors such as breast size, the location of the lesion, whether the surgery is for prophylaxis or treatment and whether the patient intends to undergo reconstruction surgery. In simple mastectomy, one or both breasts are completely removed but the lymphatic nodes under the arm are not included. In the modified radical mastectomy procedure, the breasts and the axillary contents are removed but the pectoral muscles are retained while in radical mastectomy pectoral major and minor muscles are removed as well. Radical mastectomy is now used less frequently as the other forms of surgery are more effective and less disfiguring (79). In skin sparing mastectomy, breast tissues are removed through conservative incision around the areola to preserve the skin for breast reconstruction surgery. This surgery is not applied to cancers that involve the skin such as inflammatory breast cancer. In nipple sparing mastectomy breast tissues are removed but the nipple-areola complex is preserved. In both lumpectomy and mastectomy regional lymph nodes are sometimes removed to test whether the breast cancer cells have spread beyond the breast tissues. The presence of breast cancer cells in lymph nodes will determine which subsequent therapies will be applied. Unfortunately, surgery on the axillary lymph nodes may cause serious swelling of the arm. There is an option called Sentinel lymph node biopsy in which two or three key lymph nodes are removed for the test before the others are removed to lower the need for full axillary lymph nodes excision (80). Sentinel lymph nodes are the first axillary lymph nodes into which the metastatic breast cancer cells are believed to drain.

Radiotherapy

Radiotherapy is used to kill residual cancer cells remaining in the breast tissues, chest wall or the area under the arm after surgery or to shrink the tumour size before surgery through use of ionizing radiation (81). Radiotherapy is often applied to ‘local’ cancers but is not effective for metastatic cancers since it is not feasible to irradiate the whole body. It not only destroys cancer cells but also normal tissue cells so more specific target radiation would reduce the side effects dramatically.

Systemic therapies

Systemic therapies are used alongside surgery and radiotherapy to kill the undetectable cancer cells or those cancer cells metastasizing to other places within

the body. They are also used in the neoadjuvant setting to reduce tumour size before surgery or radiotherapy to make the main treatment easier or more likely to succeed.

Chemotherapy

Chemotherapy of breast cancer involves administrating cytotoxic drugs such as alkylating agents, anti-metabolites, taxanes, plant alkaloids and terpenoids, vinca alkaloids, podophyllotoxin, and topoisomerase inhibitors to kill the cancer cells. It often results in side effects including hair loss, fatigue, compromise of immune system, nausea & vomiting and tendency to bleed easily (82). Since cancer cells are generally more proliferative than normal cells, cytotoxic drugs damage the replicating DNA in cancer cells more easily than in normal cells and DNA damage kills the cancer cells.

Endocrine therapy

Approximately 60% of breast cancers diagnosed in premenopausal women and 80% of those diagnosed in postmenopausal women are hormone receptor positive, which means that growth of these cancer cells can be driven by oestrogen and/or progesterone (83). Tamoxifen as a selective oestrogen receptor modulator (SERM) has been used to treat breast cancer for many years. Tamoxifen is an antagonist of ER. It competitively binds the ER and blocks the access of oestrogen to ER. Aromatase inhibitors block the synthesis of oestrogen from the precursor in ovaries and in other tissues. These drugs include letrozole and anastrozole and are highly effective in breast cancers that are dependent on the growth effects of oestrogen.

Biological therapy

HER-2 over-expression accounts for 20-25% of invasive breast cancers (38). Trastuzumab (Herceptin®) is a monoclonal antibody drug targeting HER-2 and is used against metastatic HER-2-overexpressing breast cancers in the clinic (84). Another monoclonal antibody drug pertuzumab also targets HER-2 but binds a different domain (dimerisation arm) from trastuzumab (85). Its anti-tumour activity is through the blocking of the cellular signalling mediated by HER-2. The detailed information of both drugs including mechanism of action, function and drug resistance will be presented in the following section.

In summary, these differing therapies are generally used in combination. Most patients will undergo surgery and this will generally be followed by radiotherapy. Similarly, most patients will receive either endocrine therapy or chemotherapy with those breast cancers expressing high HER-2 also receiving trastuzumab.

1.9 Cell signalling pathways in breast cancer

De-regulation of receptor tyrosine kinase mediated pathways is frequently involved in the occurrence and development of breast cancer and drug resistance. For example, acquired resistance to tamoxifen in ER-positive tumours is often linked to the over-activated human epidermal growth factor receptor (HER)-mediated pathways (86, 87). These pathways are being intensively studied at present in this disease. This study will focus on HER-2.

1.9.1 HER receptor tyrosine kinase family and therapy of breast cancer

The HER family receptors are key signalling regulators in breast cancer cells and act by transducing extracellular stimuli into intracellular signals (88-90). The ensuing intracellular signalling cascades modulate gene expression patterns and allow cells to make decisions regarding proliferation, differentiation, cell cycle control, survival, apoptosis suppression and resistance to therapies (88, 91-95). There are four members in this family (Figure 5): HER-1 (EGFR, ErbB1), the founding member of this family, HER-2 (ErbB2, neu), HER-3 (ErbB3) and HER-4 (ErbB4). HER receptors have four major domains: an extracellular ligand binding domain which is glycosylated, a transmembrane helix, a cytoplasmic kinase domain and a C-terminal tail. Exclusively, HER-3 has no intrinsic kinase activity due to substitutions in crucial residues in kinase domain (90, 96, 97). The extracellular domain is divided into 4 sub-domains: I, II, III, and IV. A variety of EGF-like ligands activate these receptors: EGF, TGFα, amphiregulin and epiregulin bind HER-1; betacellulin, epiregulin and heparin-binding EGF bind both HER-1 and HER-4; neuregulin-1, neuregulin-2, and glial growth factor bind both HER-3 and HER-4; neuregulin-3 and -4 only bind HER-4 (Figure 6) (90). The binding of ligands causes the receptors to undergo a conformational change, homo- and/or hetero-dimerisation,

phosphorylation in specific tyrosine residues within the kinase domain and recruitment of signalling molecules which activate such signalling pathways as the Raf/MEK1&2/ERK1&2 and PI3K/Akt pathways (90). Deregulation of these signalling pathways is associated with malignant transformation and cancer progression (98-100).

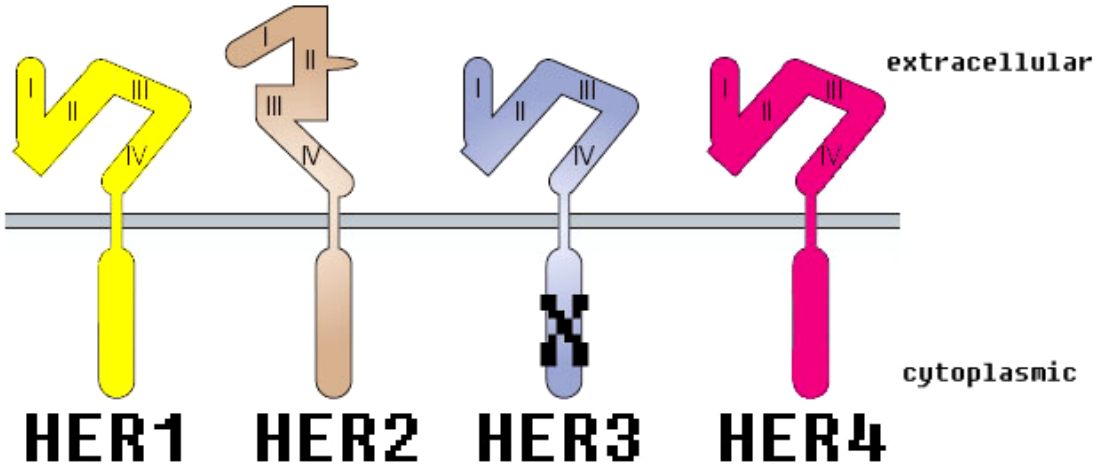

Figure 5 Four members of the HER family. HER-1 is the founding member of this family. HER-2 is an 'orphan' receptor and HER-3 has no intrinsic kinase activity.

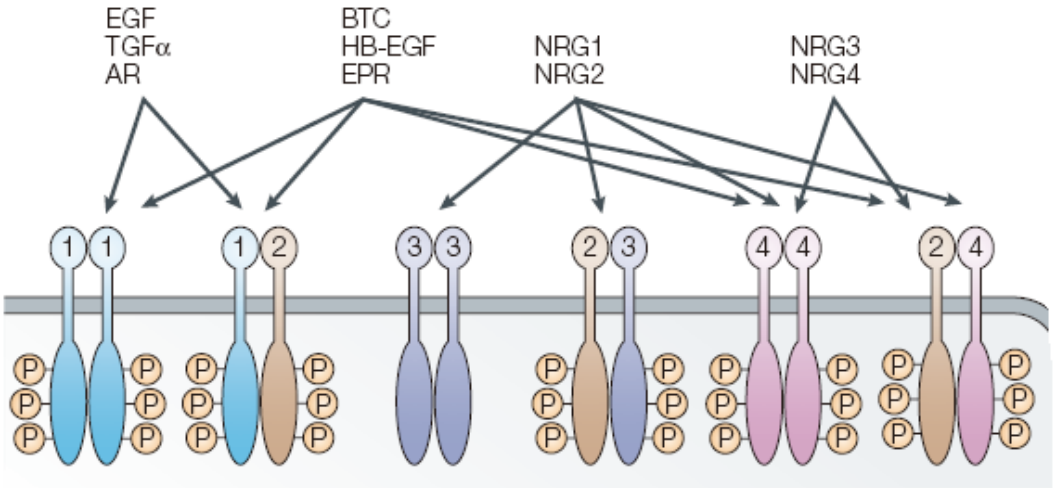

Figure 6 HER receptors and their cognate ligands (reproduced from ref (90)). EGF (epidermal growth factor), TGFα (transforming growth factor α), AR (amphiregulin), BTC (betacellulin), HB-EGF (heparin-binding EGF), EPR (epiregulin) and NRG (neuregulin).

Distinct from the other HER receptors, HER-2 has no known ligands and is constitutively activated for homo- (when HER-2 is over-expressing) or hetero-dimerisation with other HER family members (38, 90) . It has a conformation similar to other ligand-bound HER receptors, which explains why HER-2 is the preferred dimerisation partner (101, 102). In HER-2 over-expressing cells, it spontaneously forms homo-dimers and activates the downstream signalling cascades in the absence of ligands.

HER-2 has been intensively studied as a therapeutic target due to several features.

1) The over-expression of HER-2 protein is an adverse prognostic marker for breast cancer (103-106).
2) HER-2 over-expression is found not only in metastatic cancers but also in primary tumours (107), meaning that the therapies targeting HER-2 are effective in different stages and sites.
3) Normal adult tissues usually have much lower HER-2 expression than breast cancers, so therapies targeting HER-2 have high specificity.

As stated previously, HER-2 prefers to undergo hetero-dimerisation with other ligand-activated HER receptors. It is also known that distinct ligands govern different cell fate decisions (91, 108). This suggests that therapeutics based on blockade of HER-2's action may inhibit the effects of diverse ligands on cell fate. Hetero-dimerisation with HER-2 can enhance ligand binding affinity (109) and also ligand induced tyrosine phosphorylation (110). HER-2 over-expression is associated with approximately 20-25% of invasive breast cancers (38) and it has been shown to be associated with poor rates of disease free survival and increase the resistance to chemotherapeutic drugs (103, 111). Therefore, HER-2 is an attractive therapeutic target in breast cancer treatment (112).

One of the recombinant humanised anti-HER-2 monoclonal antibody drugs, trastuzumab (Herceptin®) developed by Genentech has been approved for clinical use to treat HER-2 over-expressing metastatic breast cancers since 1998 by the US Food and Drug Administration (113). It was humanised by replacing the antigen

binding region of human IgG with the hyper-variable antigen binding region of the potent murine anti-HER-2 monoclonal antibody (114). Trastuzumab is generally used as the first-line treatment of HER-2 over-expressing metastatic breast cancer patients (84). However, its exact mechanism of action *in vivo* remains unclear. Studies have shown that, to inhibit tumour progression, trastuzumab binds HER-2 on the cell surface and then triggers the internalization and degradation of receptors (115, 116), which block downstream signalling pathways (117, 118), such as Raf/ MEK 1&2/ERK 1&2 and PI3K/Akt pathways. Trastuzumab can inhibit the shedding of HER-2 by blocking the metalloproteinase activity (119). When over-expressed, HER-2 undergoes proteolytic cleavage by metalloproteinase. This cleavage causes the release of extracellular domain (ECD) of HER-2 and a truncated membrane-bound fragment (p95) (120). The shedding of HER-2's ECD was detected in conditioned media of HER-2 over-expressing cell lines (121-124) and could also be found in serum of cancer patients (125-127). High serum levels of ECD correlate with poor prognosis and lowered sensitivity to endocrine therapy and chemotherapy (128-130). Investigators found that trastuzumab could inhibit the shedding of ECD by inhibiting metalloproteinase activity (119). Clinical studies demonstrated that the decrease of serum levels of ECD during trastuzumab treatment improved progression-free overall survival, supporting indirectly the hypothesis that trastuzumab may act through inhibiting ECD of HER-2 shedding (131, 132). It also induces cell cycle arrest in the G1 phase through down-regulation of the proteins involving the sequestration of cyclin E/CDK2 complex inhibitor $p27^{Kip1}$, increased association of p27 with CDK2 and CDK2 inactivation (133, 134). Trastuzumab is not only cytostatic but also cytotoxic. It recruits immune effector cells onto the tumour cells which are then killed by immune cells through antibody dependent cellular cytotoxicity (ADCC) (135-138). It may also act through an anti-angiogenic effect (139). In adjuvant settings, trastuzumab sensitised the HER-2 over-expressing cells to apoptosis when treated by standard chemotherapy such as taxol or etoposide (140, 141) and also induced apoptosis in primary breast cancers in neoadjuvant settings (107). Although it has some side effects including flu-like symptoms, low white or red blood cell counts, diarrhoea, heart attacks, lung dysfunction, etc,

trastuzumab is widely used with great efficacy in women patients with HER-2 over-expression and increases overall survival.

Although trastuzumab is considered as one of the most effective treatments for HER-2 over-expressing metastatic breast cancers at present (38) , it is very common that some patients may have no response or some patients who initially respond to this drug may acquire drug resistance within one year (142), which will cause the treatment to fail. Understanding resistance mechanisms is crucial for developing more effective therapeutic strategies and multiple mechanisms have already been identified. Three possible mechanisms are described as follows: oncogenic mutations of the catalytic domain of the PI3 Kinase (PIK3CA), constitutively active Akt and the activity loss of PTEN (143-145). The low level of $p27^{kip1}$ which is a cyclin-dependent kinase inhibitor is also a reported possibility (146). As aforementioned, a truncated p95 HER-2, which is the intracellular part of HER-2 and has the kinase activity but doesn't possess the trastuzumab binding site, is a possible factor which could confer resistance. Hyper-activation of the metalloproteinase which catalyses the release of HER-2's ECD would make tumours resistant to trastuzumab since binding for trastuzumab site is removed (139). It is also possible that the steric inaccessibility or masking of the trastuzumab binding site on HER-2 explains the resistance (147, 148).

Nagy et al (147) demonstrated that in JIMT-1, a HER-2 over-expressing breast carcinoma cell line with primary trastuzumab resistance, the expression of MUC4 was higher than in trastuzumab-sensitive cell lines. MUC4 is a membrane associated mucin that was reported to play a role in masking the membrane protein and the expression level of MUC4 was inversely correlated with the binding capacity of trastuzumab with HER-2. Additionally, the ligands of other HER members, such as TGF-α and HB-EGF which trigger the homo-dimerisation of HER-1 and hetero-dimerisation with HER-2, possibly bypasses inhibition produced by trastuzumab (149, 150).

Activation of alternative pathways has also been observed in tumours resistance to trastuzumab and the insulin like growth factor-I (IGF-I) receptor mediated pathways have been investigated as causes of resistance (151). Lu et al (151) demonstrated that trastuzumab inhibited the proliferative growth of MCF-7/HER2-18 cells which over-expresses HER-2 and expresses IGF-I receptor when the IGF-I receptor mediated signalling was minimised, but when cells were grown in 10% FBS or under the stimulation of IGF-I, the growth inhibition by trastuzumab was blocked. In contrast to MCF-7/HER2-18 cells, trastuzumab inhibited the proliferation of SKBR3 cells which over-express HER-2 and have low IGF-I receptor expression, regardless of the addition of IGF-I. When SKBR3 cells were genetically altered to over-express IGF-I receptor and cultured with IGF-I, trastuzumab had no effects on proliferation. However, when IGF binding protein-3 was added to the media, the trastuzumab induced growth inhibition was restored (151). The involvement of IGF-I receptor in the development of resistance may be due to the interaction of IGF-I receptor with HER family members, which enhances the activation of downstream signalling pathways (152). Huang, Gao et al (152) demonstrated recently that interaction between IGF-I receptor and HER-2 or HER-3 exclusively occurred in trastuzumab resistant cell lines, where enhanced interaction of HER-2 and HER-3 was also observed. What's more, the heterotrimer of HER-2, HER-3 and IGF-I receptor was also observed in resistant cells. The knockdown of HER-3 or IGF-I receptor resensitised the cells to trastuzumab in this study. Finally, the decreased immune function of patients caused by the disease and the medical therapies, such as radio- and chemotherapy may also result in non-responsiveness to trastuzumab (153).

In contrast to trastuzumab which is only effective clinically in HER-2 over-expressed breast cancer, another humanized monoclonal antibody drug pertuzumab (Omnitarg, rhuMAb 2C4) developed by Genentech is known to inhibit HER-2 dimerisation by targeting the dimerisation arm (sub-domain II) in HER-2 expressing breast cancer cells (Figure 7) (85).

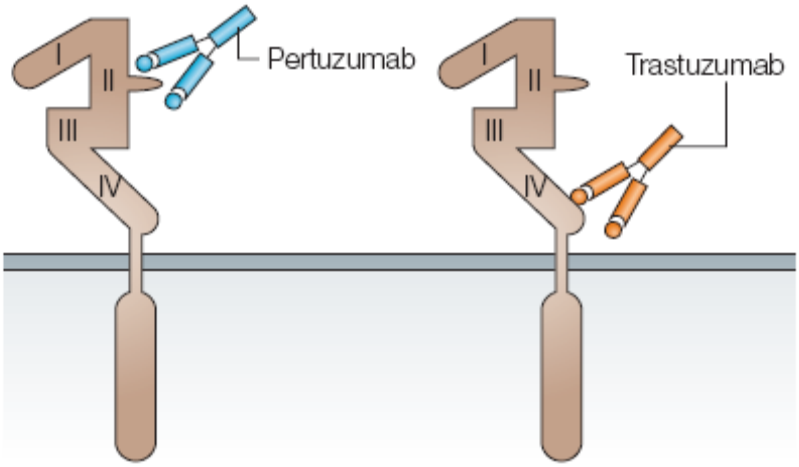

Figure 7 : Pertuzumab and trastuzumab bind different domain of HER-2 (reproduced from ref(90)).

Pertuzumab is the first in a new class of targeted anti-tumour therapies known as HER-2 dimerisation inhibitors and is now undergoing clinical trials (154, 155). Dimerisation is essential for the HER family to activate the intracellular signalling cascades governing proliferation, survival and differentiation. As previously mentioned, HER-2 is the preferred dimerising partner for all other members in the family (101). Therefore, inhibition of HER-2 dimer pairing may prevent the activation of several signalling pathways. In the laboratory setting, pertuzumab had shown excellent anti-tumour activity *in vitro* and *in vivo* against HER-2-positive breast and prostate cancers (156). Scheuer et al (157) showed that the combination of pertuzumab and trastuzumab or the addition of pertuzumab after the progression on trastuzumab in breast cancer xenografts synergistically increased the inhibition of the tumour growth compared with single drugs. They also observed that the metastasis of breast cancer cells to the lung was dramatically decreased by the combination of pertuzumab and trastuzumab compared with single drugs. These results suggested that pertuzumab and trastuzumab may have complementary mechanisms of action. These researchers confirmed by near-IR fluorescence imaging in their study that pertuzumab as well as trastuzumab could activate ADCC. A recent phase II clinical trial demonstrated that the combination of pertuzumab and trastuzumab was active and well tolerated in patients with HER-2 positive metastatic breast cancer who experienced progression during prior trastuzumab-based therapy (154). Therefore,

pertuzumab is a promising anti-HER-2 based drug in the clinic and further clinical development is likely.

In addition to the antibody agents, small molecule tyrosine kinase inhibitors (TKIs) are also attractive drugs in cancers (90, 158). These small molecules can enter the cytoplasm and inhibit receptors' auto-phosphorylation activity by impeding the binding of GTP with tyrosine kinase domain. For example, lapatinib is an oral dual TKI against HER-1/HER-2. Studies have shown that the addition of lapatinib to capecitabine improves the progression-free survival and increases the overall survival in patients with metastatic HER-2 over-expressing breast cancers which are resistant to trastuzumab (159). Its combined use with letrozole improves the progression-free survival compared to letrozole alone in patients with ER and HER-2 positive metastatic breast cancers (159).

To gain more effective treatments, it is reasonable to develop combined targeted therapies. It was shown that the combined treatment of trastuzumab, pertuzumab and gefitinib (a TKI against HER-1) in inhibiting the tumour growth of HER-2 over-expressing xenografts is statistically significantly better than single agent and dual combination therapies (160). The clinical trials combining trastuzumab and lapatinib have also investigated the new treatment approach beyond the progression on trastuzumab. O'Shaughnessy et al (161) demonstrated in their clinical study improved clinical outcomes with the combination of lapatinib and trastuzumab *vs* lapatinib alone in patients who progressed on prior trastuzumab-contained treatment regimes, but no significant changes in side effect profiles. The combination of trastuzumab and chemotherapy had an overall response rate ranging from 50% to 80% (162), while trastuzumab as a single agent had a response rate of only 15% to 30% (163). As mentioned above, the combination of pertuzumab and trastuzumab can bypass trastuzumab resistance.

It has been reported that one mechanism of endocrine resistance in ER^+ breast cancer is HER-1/HER-2 over-expression or hyper-activation of HER-1/HER-2 mediated signalling which results in ERα activation in an oestrogen independent manner (164).

Combined treatments targeting ERα and HER-1/HER-2 have shown high efficacy in preclinical models and clinical trials (165). Massarweh et al (87) demonstrated that gefitinib improved tamoxifen response and delayed acquired resistance in MCF-7 xenografts. Chu et al (166) demonstrated that combined use of tamoxifen and lapatinib effectively inhibited the growth of tamoxifen-resistant, HER-2 over-expressing MCF-7 xenografts. The phase III clinical trial led by Johnston et al (167, 168) demonstrated that compared with letrozole alone the combined targeted therapy of letrozole and lapatinib significantly enhanced progress free survival, objective response rate and clinical benefit rate in patients with metastatic breast cancer that co-expresses ER and HER-2. Some clinical trials have investigated the efficacy of the combination of trastzumab and endocrine therapy on HER-2^+-ER^+ metastatic breast cancer patients (169, 170). In TAnDEM (170) which was the first randomized phase III trial to study the combination of anastrozole and trastuzumab vs anastrozole as a treatment of HER-2^+-ER^+ metastatic breast cancers, investigators observed improved outcomes of patients treated with the combination compared with anatrozole alone. All the above studies suggested that the combined therapies may be more effective than single target therapies.

1.9.2 Raf/ MEK 1&2/ERK 1&2 and PI3K/Akt pathways and feedback loops in breast cancers

The Raf/ MEK1&2/ERK1&2 and PI3K/Akt pathways are the two primary signalling cascades mediated by HER receptors (38). Once activated, both pathways relay the extracellular signals to the nucleus through tiered phosphorylation cascades to induce nuclear gene expression. These pathways play pivotal roles in cell proliferation, anti-apoptosis, differentiation, growth arrest and drug resistance (38). Apart from the core phosphorylation cascades, complex feedback regulation is also induced. So even within the same core pathways different cell responses can be induced, depending on the external stimuli types, timing, duration and strength of signal and cell types (93). The aberrant activation of these pathways is associated with the development and progression of cancers (90). For example, loss of PTEN and oncogenic mutation of PIK3CA are often found in breast cancers which are resistant to trastuzumab therapy

(171). Both pathways are key therapeutic targets for cancer treatment (172, 173). A schematic overview is presented in Figure 8.

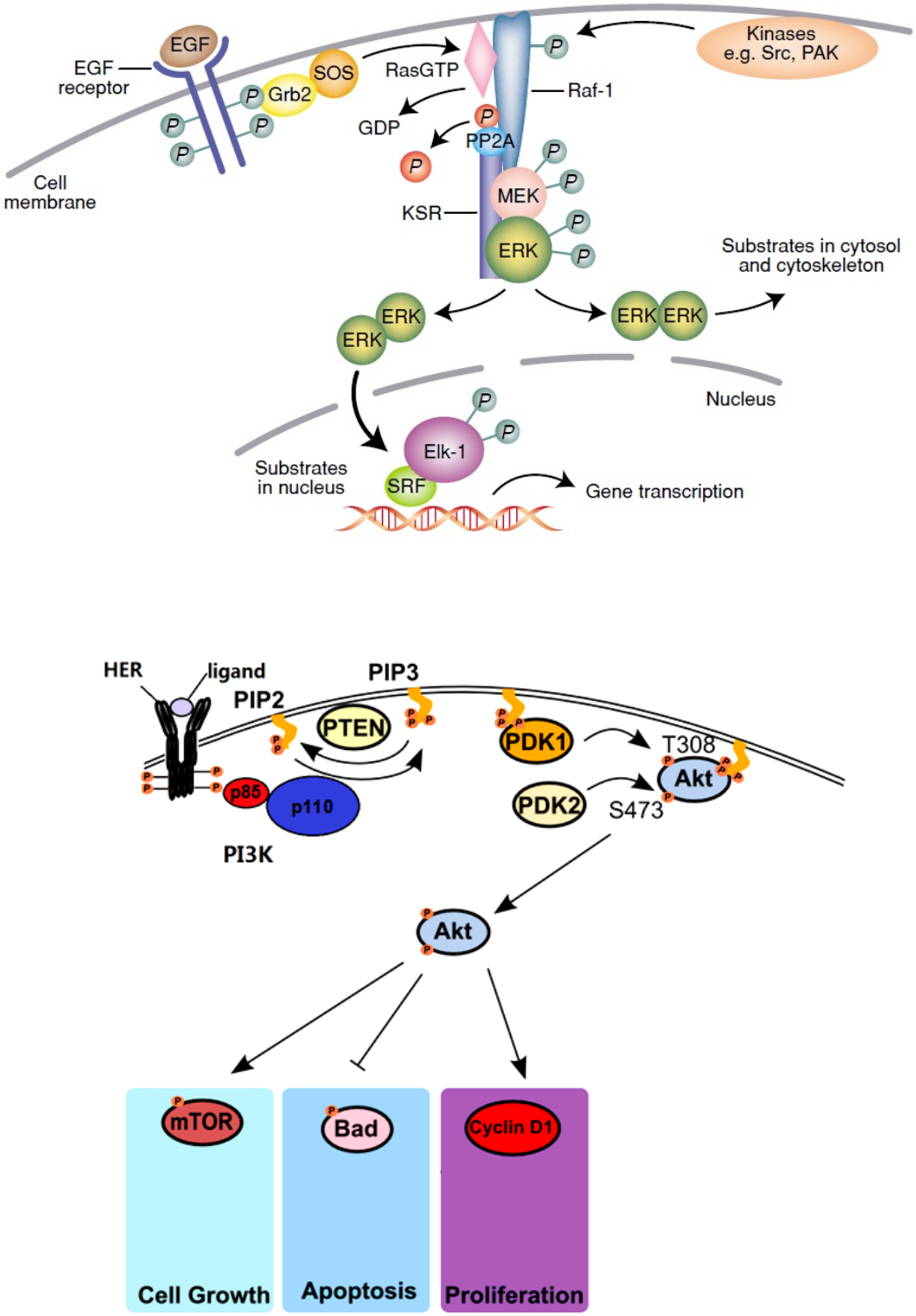

Figure 8 Schematic overview of Raf/MEK1&2/ERK1&2 (174) and PI3K/Akt pathways. The scheme of the PI3K/Akt pathway is produced through modifying the online image (http://knol.google.com/k/protein-kinase-b#).

In the response of mitogenic stimuli, receptor tyrosine kinases are auto-phosphorylated. The phosphorylated residues become the docking sites for adaptor proteins (Grb2). Grb2 recruits the guanine exchange protein SOS to the cell membrane, where SOS activates Ras from the GDP-bound inactive state to the GTP-bound active state. This exchange of Ras state elicits a conformational change in Ras, enabling it to bind to Raf-1 and recruit it from the cytosol to the cell membrane, where Raf-1 activation takes place. Raf-1 activation is a multi-step process that involves the dephosphorylation of inhibitory sites by protein phosphatase 2A (PP2A) as well as the phosphorylation of activating sites by PAK ($p21^{rac/cdc42}$-activated kinase), Src-family and yet unknown kinases (174). Raf is considered the first kinase in the cascade leading to activation of the MAPKs (ERK1 and ERK2). The best characterized substrates of ERK1/2 are ternary complex factors (TCFs) (175-177) such as Elk-1 and SAP-1 which are transcription factors and activate the expression of multiple mitogen inducible immediate early genes responsible for cell proliferation.

PI3K is a lipid kinase and consists of two subunits: catalytic subunit p110 and regulatory subunit p85. p85 binds and inhibits p110 when PI3K is inactivated. PI3K is activated through binding of the regulatory subunit p85 with the phosphorylated tyrosine residues on receptors. Meanwhile, p110 is dissociated from p85 and recruited to the membrane to catalyse the conversion of PIP2 to PIP3, which is bound to the cell membrane. Once Akt binds PIP3 correctly through the PH (Pleckstrin Homology) domain, it is activated by phosphoinositide dependent kinase 1 (PDK1 at T^{308}) and PDK2 (at S^{473}) (178). Then, activated Akt stimulates the activation or inactivation of their target molecules. PI3K can also be activated in a p85-independent manner. Ras interacts with p110 on the Ras binding domain (RBD) and tethers it to the membrane for activation (179, 180).

The Ras/Raf/MEK/ERK pathway plays a critical role in breast cancer tumourigenesis and cancer progression. This pathway is often involved in the regulation of oestrogen receptor α (ERα)-positive breast cancers. In oestrogen-dependent breast cancer cells, oestrogen can regulate in a non-genomic way the ERK1/2 pathway through binding

to the extracellular domain of the cell membrane-bound ERα and initiating a cascade involving Shc, Grb2 and SOS to activate ERK1/2 which in turn enhances the transcriptional activity of nuclear ERα (181). In this way, ERK1/2 is rapidly activated by the stimulation of oestrogen. In a genomic manner, oestrogen can also increase the expression level of some growth factors and their receptors such as IGF-I and IGF-I receptor which in turn activate the ERK1/2 pathway and play important roles in growth and differentiation (182). Reddy et al (183) demonstrated the expression of transforming growth factor-α (TGF-α) which was a specific ligand of HER-1 induced by oestrogen and the enhancement of proliferation. Hyper-activation of Raf/MEK/ERK pathway is often involved in drug resistance in breast cancers (184). Oestrogen-dependent breast cancers which initially respond to tamoxifen treatment frequently become resistant. This responsiveness alteration was suggested to be due to the shift from ERK1/2-independence to ERK1/2-dependent cell growth (185). Tamoxifen resistance can be produced by the hyper-activation of ERK1/2 through over-expression of HER-2 (87, 186). It was shown that the proliferation of ERα-positive breast cancer cells could be induced by oestrogen through the activation of ERα (187). The antiestrogen drug tamoxifen has been used extensively for decades in ER-positive patients. Tamoxifen blocks oestrogen's proliferation action through competing for the binding of oestrogen with ERα and then suppressing ERα's transcriptional activity (188). ERα activation could also be induced through the hormone-independent phosphorylation of S^{118} in the hormone-independent transcription activation function-1 (AF-1) domain by ERK1/2 and the phosphorylation of this site enhanced the transcriptional activity of ERα (189-191). Therefore, the hormone-independent activation of ERα by ERK1/2 may contribute to tamoxifen resistance. The study by Thomas et al (192) indicated that phosphorylation of another two residues S^{104} and S^{106} by ERK1/2 were also required for ER α activity. Glaros et al (86) showed that phosphorylation of S^{167} in the AF-1 domain of ERα in MCF-7 cells by over-expressed HER-1 enhanced the interaction of ERα with its co-activator in the presence of tamoxifen and led to resistance to tamoxifen. In addition, resistance to tamoxifen is also enhanced by the increased expression of ERα co-activator AIB1, which can be activated by HER-2 signalling (184, 193). Jaime et al (194) showed that the transcriptional activity of AIB1 was enhanced by ERK1/2

phosphorylation. The hyper-activation of ERα by ERK1/2 in a hormone-independent manner may contribute to tamoxifen resistance in breast cancer patients.

Activation of the PI3K/Akt pathway is considered to play a crucial role in breast cancer cell growth (195) and the high proportion (72%) of aberrant activation of this pathway is associated with poor clinical outcomes and progressive tumour properties such as high histological grade, basal-like phenotype, ER/PR negative status and correlation with HER-2 over-expression (196-198). The best known aberrant genetic alterations within this pathway in breast cancers are the oncogenic mutation of PI3KCA, the loss of PTEN and the mutation of AKT1 (179, 198). The mutations in PI3KCA, the gene encoding p110α are somatic and often involve three 'hotspots' (180). The first two reside on exon 9. E 542 and E545 in the helical domain are mutated to lysine. These two mutations lower the inhibitory interaction of p85 with p110α. The third 'hotspot' is on exon 20. H1047 in the kinase domain is mutated to arginine, which increases the access of p110α to cell membrane. All three mutations increase catalytic activity and lead to growth factor independent activation of Akt (180). PTEN is a dual lipid/protein phosphatase. The loss of phosphatase activity in PTEN occurs in 28% of invasive breast cancers (198). It can be produced by gene deletion in chromosome 10 (199), somatic mutations which are rarely documented (200) and epigenetic silencing such as promoter hyper-methylation (201). The loss of activity results in accumulation of the amount of PIP3 and produces growth factor-independent proliferation of non-tumourigenic mammary cells in vitro but is insufficient to promote anchorage-independent growth (202). The correlation of loss of PTEN with prognosis is controversial. Some studies showed no prognostic value of PTEN loss (197, 203) but some showed a correlation with poor prognosis (204-206). AKT1 mutations have been reported in 1-8% of breast cancers (207). It has been shown that the hotspot mutation (E17K) in the PH domain of AKT1 conferred constitutive localization of Akt to the cell membrane regardless of the ligand stimulation, caused marked increased phosphorylation at both T^{308} and S^{473} and kinase activity, activated downstream signalling and transformed cells in culture (208). The PI3K/Akt pathway also plays a critical role in breast cancer treatment. The activation of PI3K/Akt pathway has been implicated in conferring resistance to

conventional chemotherapy. Knuefermann et al (209) demonstrated that the activation of PI3K/Akt pathway by HER-2 over-expression increased the resistance of MCF-7 cells to multiple chemotherapeutic drugs (paclitaxel, doxorubicin, 5-fluorouracil, etoposide, and camptothecin). Vitolo et al (202) showed the increased susceptibility of MCF-10A cells with deleted/reduced PTEN to chemotherapeutic drug doxorubicin. The hyper-activation of PI3K/Akt pathway also confers resistance to endocrine therapy (210, 211). As aforementioned, the aberrant activation of this pathway could confer resistance to trastuzumab-contained therapy as well.

The intracellular signalling that regulates cellular behaviour in 'normal' cells must be precisely controlled to avoid dangerous disorders. Signals produced at the wrong time or in the wrong place will lead to inappropriate cell fate or may cause tumourigenesis. Moreover, even produced at the correct time and places, signals must be robust enough to ensure cells receive them at high enough levels against background signal to respond. Signalling not only operates in different cell types with different environments but also functions with different spatial and kinetic properties. This is defined as versatility. Feedback loops play critical roles in maintaining the three signalling properties-- precise regulation, robustness and versatility. Both the Raf/MEK/ERK and the PI3K/Akt pathways are regulated tightly through the spatiotemporally coordinated action of positive and negative feedback loops at multiple levels of the cascades (212). Feedback loops are the processes that link output signals back to input signals. Positive feedback loops are those with which output signals can enhance input signals as opposed to negative feedback loops which attenuate input signals. Both types of loops are very common modulatory elements in cellular signalling processes. Many components in signalling pathways have multiple upstream effectors and downstream targets which would form a complex web of connectivity within and between pathways. The presence of feedback loops poses a challenge to understanding how the extracellular signals through receptors modulate cellular behaviour (213). Perhaps the most obvious function of negative feedback is to restrain signalling duration and amplitude. Negative feedback can produce stability even when systems confront environmental fluctuations (212, 214). In some cases, this homeostatic function of negative

feedback plays an important role in protecting cells from out of control growth and cancer development. Sprouty (Spry) proteins are ligand-inducible negative feedback modulators of HER-mediated ERK1/2 signalling pathways. Four mammalian isoforms are identified in this family: Spry1, Spry2, Spry3 and Spry4. When the Raf/MEK/ERK pathway is activated by activated HER receptors, the transcription of Spry proteins is induced (215). In turn, they specifically inhibit the Raf/MEK/ERK pathway, leaving the PI3K/Akt pathway and other MAPK pathways unaffected, but the action mode is unclear and the point at which Spry blocks the activation of Raf/MEK/ERK is controversial (216, 217). Spry proteins play important roles in breast cancers. Lo et al (218) showed that expression levels of Spry1 and Spry2 were down-regulated consistently in breast cancers. Real time PCR assay confirmed this demonstration and showed gene expression suppression of *Spry1* and *Spry2* in more than 90% of patient samples. They also showed in this study that the abrogation of endogenous Spry activity in MCF-7 cells enhanced proliferation and anchorage-independent growth *in vitro* and dramatically increased the tumourigenesis potential of the cells in nude mice *in vivo*. To date these results suggested Spry proteins as possible tumour suppressors in breast cancers.

Another family of ligand-inducible negative feedback regulators of ERK1/2 pathway is the dual specificity phosphatase (DUSP) family. Dual specificity refers to phospho-serine/threonine and phospho-tyrosine. DUSPs are induced by the activation of ERK1/2 pathway and act to attenuate the signalling by dephosphorylating activated ERK1/2. Noticeably, not all DUSPs are inducible. The following are identified as ERK1/2-activating inducible /immediate-early DUSPs: DUSP1, DUSP2, DUSP4 and DUSP5 and these phosphatases except DUSP1 modulate the kinetics of ERK1/2 in the nucleus (219-222). Among this family, DUSP1 is the most investigated in breast cancers. The preference substrate of DUSP1 is JNK or p38 MAPK over ERK1/2. The over-expression of DUSP1 was observed in a large percentage of breast cancers (223). Over-expression of this phosphatase is a mediator of chemotherapy resistance (224) and an independent prognosis predictor in breast cancers (225). This is because the chemotherapy drugs use proapoptotic signalling through JNK activity to exert their anticancer activities

(224). DUSP4 preferentially dephosphorylates ERK1/2 and JNK over p38 MAPK. Wang et al (223) observed a 3-fold increase of its expression in breast cancer samples against non-malignant samples. Additionally, they also observed the sharp increase of expression and activity of ERK1/2 and p38 MAPK. Although the over-expression of JNK was observed, the activity was reduced by 35%. The over-expression of DUSP4 may inhibit the proapoptotic signalling through JNK. DUSP2 has highly selective dual phosphatase activity towards ERK1/2 over p38 MAPK and JNK and it is a transcription target of the tumour suppressor protein p53 in signalling apoptosis and cell growth suppression (226, 227). Knockdown of DUSP2 inhibited p53-mediated apoptosis and over-expression increased the susceptibility to apoptosis and growth suppression (227). Wu et al (228) demonstrated the cell killing role of DUSP2 in E2F-1-mediated apoptosis in breast cancer cells following treatment with a chemotherapeutic agent N-4-hydroxyphenylretinamide and that the increased expression of DUSP2 inhibited the activation of ERK1/2 and mediated cell killing. DUSP5, whose specific substrate is ERK1/2, was demonstrated to have reduced gene expression in breast carcinomas (229). Hence, DUSP2 and DUSP5 the negative regulators of ERK1/2 signalling play key roles in controlling cellular growth and are favourable factors in preventing cancer development and progression. In addition to these *de novo* negative feedback regulators, activated ERK1/2 attenuates the signalling from itself by acting back to inhibit phosphorylation of SOS and this inhibitory phosphorylation leads to the dissociation of SOS from Grb2 resulting in Ras inactivation (230-233). This negative feedback loop was reported to play a critical role in oscillation of ERK1/2 (234, 235). In addition to ERK/SOS negative feedback, multiple site inhibitory phosphorylation of Raf-1 by ERK1/2 was reported (236). The hyper-phosphorylation at these sites of Raf-1 blocked the association between Ras and Raf-1 and desensitized Raf-1 to additional stimuli, which protected cells from aberrant growth. The third negative feedback loop resulted from the inhibitory phosphorylation of Grb2-associated-binding protein 1 (GAB1) by activated ERK1/2 (237-239). This phosphorylation blocked the interaction of GAB1 with Grb2-SOS complex and thereby led to Ras inactivation. Activated ERK1/2 could also attenuate the signalling through feedback to phosphorylate MEK1 at T^{292} (240). Phosphorylation at this site prevents the further enhancement (through

phosphorylation at S^{298} in MEK1 by PAK1 (p21-activated kinase 1)) of MEK1/2-ERK1/2 complex formation (241) and thereby reduces ERK1/2 activity.

The simplest use of positive feedback is to enhance and prolong signals and produce instability. An example of positive feedback loop regulating ERK1/2 activity is the phosphorylation of cytosolic DUSP6 (DUSP6 specifically deactivates ERK1/2 and is a non-inducible DUSP (219)) at $S^{159/197}$ by ERK1/2 and this phosphorylation sensitized DUSP6 to degradation in proteosome (242). Amplified positive feedback loops often result in tumour formation and progression. A good example of this in cancers occurs in the hyper-activation of HER receptors by autocrine or paracrine production of EGF family ligands (90). To date, there are very limited studies of positive feedback loops in HERs-mediated signalling pathways in breast cancers. In summary, the loss of negative feedback loops or amplification of positive feedback loops can be an adverse factor of controlled cell growth.

1.9.3 Oscillatory dynamics in Raf/MEK 1&2 /ERK 1&2 pathway

Oscillations occur in diverse areas of cellular biology, from mechanotransduction to circadian control. There has been a growing body of evidence showing oscillation in protein levels (243-246). Hilioti et al (243) demonstrated the oscillation of yeast p-Fus3 MAPK induced by pheromone regulated periodic mating-gene expression and periodic formation of mating projections. Each peak coincided with the formation of projections. Once the oscillation was severely dampened only the first projection formed. As well, they showed the requirement of negative regulator for the formation of oscillation. Fus3 is a MAPK in yeast mediating the mating signalling. It has more than 50% sequence identity as human ERK1/2. In their studies oscillations were observed to be correlated with periodic formation of projections, suggesting that oscillation may be a regulator of cycling cellular behaviours. Wee et al (244) demonstrated that the oscillation of tumour suppressor p53 expression level sensitized cells to apoptosis induced by ionic radiation. Compared to non-oscillatory p53, oscillatory p53 increased the target gene expression, thus influencing the cell fate decisions between cell cycle arrest/DNA repair and apoptosis. Nakayama et al

(234) also observed the FGF-induced oscillation of activated ERK1/2 in Hela and NIH 3T3 cells, but the significance was not elucidated by the authors.

Oscillation of active ERK1/2 levels in breast cancer cells was not demonstrated before the observations presented in this thesis. Their physiological, pathological, and therapeutic significance in breast cancer remains undetermined. The simplest way to produce an oscillation is by negative feedback with delay (247-249). However, many oscillators have positive feedback loops embedded as well, raising the question of what the advantages of the positive feedback loops are. Mathematical models show that it is generally difficult to modulate the frequencies of negative feedback oscillation without changing amplitude (249). The involvement of positive feedback loops generates the oscillator with tuneable frequency and robust amplitude. The tunability and robustness make the oscillator suitable for those biological rhythms which need constant output over a range of frequencies such as cell cycles and heart beats (249). Computational modelling studies pioneered by Kholodenko et al (235, 250-252) have described models of the oscillation dynamics in Raf/MEK/ERK pathways. In their models, they suggested that negative feedback, ultra-sensitivity, multi-site phosphorylation and competitive inhibition were able to cause oscillation dynamics. They hypothesized that MEK and MAPK were phosphorylated at two specific residues by two separate collisions, as presented (252) in Figure 9. Ultra-sensitivity refers to the signal amplification through kinase cascades which means a tiny change in a stimulus results in a large change in response. They predicted two types of oscillatory dynamics as well. The first example was called relaxation oscillation, assuming that the fully phosphorylated form of the kinases in the cycle represses the formation of the upstream phosphorylated kinases. The second example is ring oscillation in which a cascade of two cycles was considered. In this oscillator the fully phosphorylated kinases of the first layer activated the second layer and induced a feedback loop from the second layer. In this feedback loop, the fully active kinases of the second layer competitively bound and inhibited the kinases phosphorylating the first layer. They predicted that the periodicity could range from minutes to hours and the phosphorylation level could vary between base level to almost 100% of total protein (235). To date the

oscillation of p-ERK1/2 expression level in mammalian cells are intensively investigated theoretically through computational modelling with ordinary differential equations. Here in this thesis, the oscillations of p-ERK1/2 and p-Akt expression levels are observed experimentally in breast cancer cells. Raw data have been subjected to mathematical modelling (in collaboration with Dr. Alexey Goltsov, SIMBIOS Centre, University of Abertay), but the modelling is not included in this thesis. Oscillations in breast cancer cells presented in this thesis may be an adverse factor indicating malignancy.

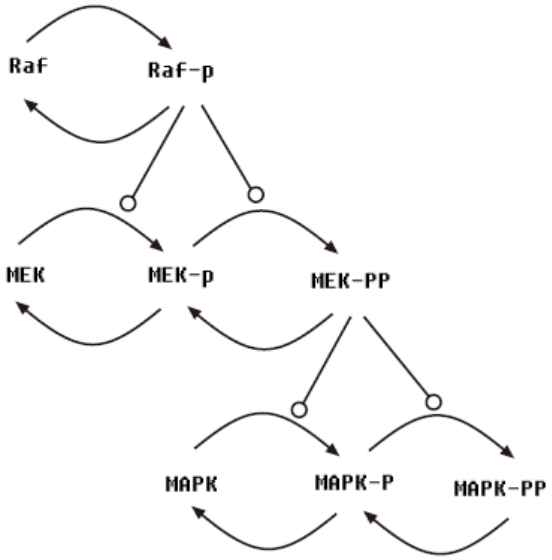

Figure 9 MAPK modules: hierarchical 3-tiered typical MAPK module. Raf is phosphorylated in a single site. MEK and MAPK are phosphorylated at double sites by two collisions. In each tier, forward reactions are catalyzed by kinases and reverse reactions by phosphatases (252).

1.10 Aims

The general aim of this thesis was to investigate how growth factor-induced dynamics of ERK1/2 and Akt pathways in breast cancer cells are regulated.

First of all, to achieve this goal, it was necessary to elucidate what type of dynamics would be induced by growth factors, so the following experiments were undertaken.

EGF and HRG were used to stimulate MCF-7 cells and expression levels of p-ERK1/2 and p-Akt within a 2h time course were analysed. Oscillatory dynamics of Raf/MEK/ERK and PI3K/Akt pathways were observed.

Secondly, to elucidate the characteristics of signalling oscillations including feedback and feedforward regulating factors, the following experiments were undertaken.

MCF-7 cells were stimulated with either EGF or HRG in the presence of cycloheximide (CHX, a protein synthesis inhibitor) and expression levels of p-ERK1/2 and p-Akt within a 2h time course were analysed to test whether transcriptional feedback loops can modulate oscillations.

HER-2 over-expressing MCF-7 cells were stimulated with HRG either in the presence or the absence of pertuzumab and expression levels of p-ERK1/2 and p-Akt within a 2h time course were analysed to test whether feedforward drive can regulate oscillations.

Thirdly, to find out whether signalling oscillations are influenced by serum deprivation and whether they are a cell line-dependent phenomenon, the following experiments were conducted.

MCF-7 cells were stimulated with HRG±CHX in serum deprivation or in the presence of 5% DCSS and expression levels of p-ERK1/2 and p-Akt within a 2h time course were analysed to elucidate whether oscillations were dependent upon serum.

BT474 cells were treated with HRG±CHX and the expression levels of p-Akt and p-ERK1/2 were assayed to find out whether oscillations were a general phenomenon across breast cancer cell lines.

Fourthly, to identify which molecules may act within the transcriptional feedback loops, the following experiments were conducted.

PTPN13 might be a possible oscillation candidate which could regulate oscillations based on the published studies and the effect of this phosphatase on signalling was investigated by knockdown with RNAi. The correlation of its expression levels with clinical parameters in a series of breast cancers was investigated as well.

To identify candidate molecules exerting transcriptional feedback in a high throughput manner, MCF-7 cells were treated with HRG for 5, 10, 20 and 40 min respectively and mRNA was extracted from each sample for gene expression array analysis.

Using these experimental data, an ordinary differential equation-based mathematical model has been established through collaboration with Dr. Alexey Goltsov from the SIMBIOS Centre, University of Abertay, Dundee to help predict the mechanisms of oscillation.

Finally, to elucidate which types of signalling dynamics can be generated by the intervention of trastuzumab and pertuzumab and how the signalling is regulated, the following experiments were undertaken.

Cell growth of MCF-7, MCF-7/HER2-18 and BT474 cells driven by either HRG or EGF in the presence or absence of trastuzumab, pertuzumab or their combination was investigated.

Time course profiles of p-ERK1/2 and p-Akt in the above three cell lines stimulated with HRG or EGF in the presence or absence of trastuzumab, pertuzumab or their combination was assessed.

The mechanism of action of trastuzumab on the alteration of signalling dynamics in Akt and ERK1/2 pathways in HRG-stimulated MCF-7 cells was studied through assessing whether the crosstalk between p38 MAPK and ERK1/2 exists and analysing the gene expression in MCF-7 cells treated with HRG, trastuzumab and HRG+trastuzumab for 5, 10, 20 and 40 min respectively.

Chapter Two: Materials and Methods

2 Materials and Methods

Chemicals and reagents were obtained from Sigma unless otherwise stated. Materials are listed according to the order in which the methods are described.

2.1 Materials

2.1.1 Tissue culture reagents and inhibitors

Reagents	Manufacturer or supplier/Catalogue No.
DMEM with phenol red	Invitrogen /31885
DMEM without phenol red	Invitrogen/11880
Foetal Calf Serum	Harlan Sera-Lab LTD/S-0001 AE
Penicillin/streptomycin	Invitrogen/15140-122
G418	Invitrogen/11811-023
PBS tablets	OXOID/BR0014G
Trypsin/EDTA	Invitrogen/25300
DMSO	BDH Laboratory supplies /282164K
HRG	R & D systems/396-HB/CF
LY294002	Calbiochem/440204
UO126	Calbiochem/662005
Trastuzumab	kindly donated by Roche Pharmaceuticals
Pertuzumab	kindly donated by Roche Pharmaceuticals

2.1.2 Reagents used for the preparation of double charcoal stripped serum

Reagents	Manufacturer or supplier/catalogue No.
Foetal Calf Serum	Harlan Sera-Lab LTD/S-0001 AE
Dextran T70	Pharmacia /17-0280-01

2.1.3 Reagents used in the Sulphorhodamine B (SRB) assay

Reagents	Manufacturer or supplier/catalogue No.
Acetic acid	BDH Laboratory supplies /10001CU

2.1.4 Reagents and other materials used in protein detection in cell lines

Reagents and other materials	Manufacturer or supplier/catalogue No.
Mini complete protease inhibitor cocktail tablets	Roche Applied Science/11836153001
Aprotinin	Sigma Aldrich/A6279
Phosphatase inhibitor cocktail 1	Sigma Aldrich/P2850
Phosphatase inhibitor cocktail 2	Sigma Aldrich/P5726
CNMCS Compartmental Protein Extraction Kit	Biochain Institute, Inc., CA, USA/K3013010
30% acrylamide/Bis acrylamide stock solution	Severn Biotech Ltd/20-2100-05
TEMED	BioRad/161-0801
2-Propanol	BDH Laboratory supplies /102246L
Methanol	BDH Laboratory supplies /261296H
Tween-20	BioRad/170-6531
Odyssey Blocking Buffer	LI-COR Biosciences/927-40000
Anti-rabbit IgG, HRP-linked Antibody	CST/7074
PVDF membrane	Millipore/IPVH304F0
BM Chemiluminescence Blotting Substrate (POD) kit	Roche Applied Science/11500708001
Fuji Super RX medical X-ray film	FUJI Photo Film Co., Ltd, Tokyo, Japan

Continued for 2.1.4

CSA Ⅱ A Biotin free Tyramide Signal Amplification System for use with mouse primary antibodies	Dakocytomation/K1497
CSA Ⅱ Rabbit Link	Dakocytomation/K1501
Normal goat serum	Invitrogen/16210-064
Black-wall, clear-bottom 96-well microplate	BD Biosciences/ 353948

2.1.5 Reagents and other materials used in protein detection in tumours

Reagents and other materials	**Manufacturer or supplier/catalogue No.**
DAKO Protein Block Serum Free	Dako/X0909
DAKO Antibody Diluent	Dako/S0809
Dako Envision+System-HRP labelled polymer Anti-rabbit	Dako/ K4003
Dako Envision+System-HRP labelled polymer Anti-mouse	Dako/ K4001
DAB chromogen	Dako/K5007
Mouse anti-cytokeratin (Pan) antibody	Invitrogen/18-0132
Goat anti-mouse Alexa555 antibody	Invitrogen/A21422
Aquantiplex™ assay kit	HistoRX/AQ-EMR1-0001
Prolong Gold anti-fade reagent with DAPI	Invitrogen/P36931

2.1.6 Primary Antibodies used in Western Blot

Antibody name	Working dilution	Host species	Manufacturer /Catalogue No.
Anti-p-ERK1/2 (T^{202}/Y^{204})	1:1000	rabbit	CST/9101
Anti-ERK1/2	1:1000	rabbit	CST/9102
Anti-p-Akt (S^{473})	1:2000	rabbit	CST/4060
Anti-Akt	1:1000	rabbit	CST/9272
Anti-GAPDH	1:2000	rabbit	CST/2118
Anti-p-MEK1/2 ($S^{217/221}$)	1:1000	rabbit	CST/9154
Anti-p-Raf-1 (S^{259})	1:1000	rabbit	CST/9421
Anti-p-HER-2 (Y^{877})	1:1000	rabbit	CST/2241
Anti-p-HER-3 (Y^{1289})	1:1000	rabbit	CST/4791
Anti-p-p38 MAPK (T^{180}/Y^{182})	1:1000	rabbit	CST/9215
Anti-PTPN13	1:800	rabbit	SCB/sc-15356
Anti-GAPDH	1:5000	mouse	Abcam/Ab8245
Anti-α-tubulin	1:6000	mouse	Abcam/ab7291

2.1.7 List of primary antibodies used in RPPA

Antibody name	Dilution	Host species	Manufacturer/Catalogue No.
Anti-p-ERK1/2 (T^{202}/Y^{204})	1:100	rabbit	CST/9101
Anti-ERK1/2	1:150	rabbit	CST/9102
Anti-p-Akt (S^{473})	1:50	rabbit	CST/4060
Anti-Akt	1:150	rabbit	CST/9272
Anti-GAPDH	1:100	rabbit	CST/2118

2.1.8 Near-infrared fluorophore conjugated secondary antibodies used in this study purchased from LI-COR Biosciences

Antibody name	Dilution (WB/RPPA)	Host Species	fluorophore	Catalogue No.
IRDye 800CW conjugated Goat anti-rabbit IgG	1:15,000/1:2000	rabbit	800nm	926-32211
IRDye 800CW conjugated Goat anti-mouse IgG	1:15,000/1:2000	mouse	800nm	926-32210
IRDye 680 conjugated Goat anti-rabbit IgG	1:15,000/1:2000	rabbit	680nm	926-32221
IRDye 680 conjugated Goat anti-mouse IgG	1:15,000/1:2000	mouse	680nm	926-32220

2.1.9 Kits used in the gene expression analysis

Kits	Manufacturer or supplier/catalogue No.
STRATAGENE Absolutely RNA® Miniprep Kit	Agilent Technologies/400800
Illumina® TotalPrep™ RNA Amplification Kit	AMBION INC/AMIL1791

2.1.10 Reagents and other materials used in the cell cycle analysis

Reagents and other materials	Manufacturer or supplier/catalogue No.
Trisodium citrate	BDH Laboratory supplies/301287F
DMSO	BDH Laboratory supplies/140214P
BD Falcon tube	BD Biosciences/352052

2.2 Methods

2.2.1 Cell Culture

All the cell lines were grown at 37ºC in a humidified atmosphere of 5% CO_2 for both routine maintenance and drug treatment.

2.2.1.1 Routine cell line culture

Breast carcinoma cell lines MCF-7 and BT474 cells were routinely maintained in Dulbecco's modified Eagle's medium (DMEM) containing phenol red supplemented with 10% FCS and 0.1 mg/ml penicillin/streptomycin. A HER-2 over-expressing cell line, MCF-7/HER2-18 which was routinely maintained in DMEM supplemented with 0.5 mg/ml G418 along with 10% FCS and 0.1 mg/ml penicillin/streptomycin was obtained from the Osborne/Schiff lab, Baylor College of Medicine, Houston, Texas, USA.

2.2.1.2 Cell line culture for drug treatment

All the experiments involving drug treatment of cell lines adopted this procedure unless otherwise stated.

Cells were grown in DMEM without phenol red supplemented with 5% DCSS, 0.1 mg/ml penicillin/streptomycin and 2 mM L-glutamine (for MCF-7/HER2-18 cells, 0.5 mg/ml G418 was contained in the media as well) for 48 h before drug or stimuli treatment. For those experiments involving the treatment of inhibitors, cells were pre-incubated with inhibitors for 20 min before EGF or HRG treatment.

2.2.1.3 Subculturing of cells

Cells were trypsinised when the cell number reached roughly 80% confluence for continuing growth. Medium was discarded before the wash with pre-warmed PBS and then cells were incubated with trypsin/EDTA for 5 min at 37 ºC in the incubator. The reaction was stopped by addition of serum-containing medium to the dish or flask when the cells had detached. Cell suspension was transferred to a sterile spin tube and centrifuged for 4 min at 1200 rpm. The medium containing trypsin/EDTA was discarded and the cell pellet was re-suspended with medium. Cells were seeded into a new dish or flask at an appropriate dilution.

2.2.1.4 Cryopreservation and recovery of cells from liquid nitrogen

Cells were harvested when cell number reached roughly 80% confluence in a 175cm^2 flask. After centrifugation, the cell pellets were re-suspended with 10ml freezing media (10% DMSO in FCS). The cell suspension (2 ml) was aliquoted into cryopreservation vials. These vials were then transferred to a liquid nitrogen storage tank for long-term storage. To recover cells from liquid nitrogen, these vials were taken out and defrosted as rapidly as possible in a 37ºC water bath. The cell suspension in the vials was transferred to 25ml warmed-up medium when completely defrosted. The DMSO was removed by centrifugation and the supernatant was discarded. Cell pellets were re-suspended in 25 ml of warmed-up medium and transferred into a 175-cm^2 flask for routine growth.

2.2.2 Double charcoal stripped serum preparation

To study the functionality of the cell lines, it was necessary to grow cells in phenol red free medium containing charcoal stripped FCS in order to remove endogenous stimuli that may influence the signalling. These endogenous steroids from FCS were stripped using dextran-coated charcoal and type Ⅳ sulphatase (EC 3.1.6.1).

After being thawed at room temperature, 1L FCS was heat inactivated at 56 ℃ for 30 min and was then incubated with 2000 U sulphatase for 2 h at 37℃. The pH of the serum was adjusted to pH 4.2 using 2 M HCl. Pre-prepared charcoal mix (for 1 L, charcoal mix consists of 5 g charcoal and 25 mg dextran T70 in 50 mL H_2O) was added prior to stirring overnight in a cold room. Charcoal was removed from the serum via centrifugation at 10,000 rpm, 30 min, at 4℃. The pH was re-adjusted to pH 4.2 as above. A second charcoal mix was added and stirred overnight in the cold room once more. Charcoal was removed by centrifugation as above. To remove residual charcoal, it was necessary to spin further. The pH was adjusted back to pH 7.2 using 2 M NaOH before 0.2 μm filter sterilising serum. The serum then was aliquoted and stored at -20℃.

2.2.3 SRB assay for growth studies

2.2.3.1 Cell preparation

When cell growth reached 80% confluence, cells were harvested and 2,500 MCF-7 cells per well (6,000 for MCF-7/HER2-18 cells) were seeded in 96-well flat bottom plates and incubated in 10% FCS DMEM for 48 h at humidified 5% CO_2, 37℃. The medium was replaced by 200 μl/well phenol red free DMEM containing 5% DCSS after one wash of each well using warmed up PBS. Cells were incubated for another 48 h before drug treatments for a variety of days.

2.2.3.2 Relative cell numbers determined by SRB assay

96-Well plates were taken out of the incubator and 50 μl of cold 25% trichloracetic acid (TCA) was added to each well to fix the cells for 60 min in the cold room. TCA was discarded and wells were washed 10 times under running tap water followed by

drying in a 50 ℃ oven. 50 µl 0.4% SRB dye solution was added into each well and plates were left at room temperature for 30 min. The SRB dye was discarded and wells were rinsed by 1% acetic acid for 4 times and dried in a 50℃ oven. Finally, 150 µl of 10 mM Tris solution, pH 7.5 was added to each well and plates were left on a shaker at room temperature for 60 min before reading at 540 nm with the microplate reader (BP800, BIOHIT).

2.2.4 Protein detection in cell lines

2.2.4.1 Knockdown of PTPN13 in MCF-7 with RNAi

Reverse transfection for MCF-7 cells was conducted in 6-well plates.
RNAi duplex-Lipofectamine™ RNAMax complexes were prepared for each well to be transfected as follows.

1) 30 pmol RNAi duplex was diluted by mixing gently in 500 µl Opti-MEM I Medium without serum in the well of the tissue culture plate.
2) Lipofectamine™ RNAMax was gently mixed before use and then 5 µl was added to each well containing the diluted RNAi molecules followed by mixing gently. The mixture was incubated for 20 min at room temperature.

During the incubation time, MCF-7 cells in complete growth media without antibiotics were diluted to 2.4×10^5 cells /2.5 ml so that cells the would reach 30-50% confluence 24 h after plating. To each well with RNAi duplex-Lipofectamine™ RNAMax complexes, 2.5 ml of the diluted cells was added and then mixed gently by rocking the plate back and forth. This gave a final volume of 3 ml and a final RNAi concentration of 10nM. The cells and the complexes were incubated for 48 h at 37ºC in full serum without antibiotics. Before HRG stimulation the cell monolayer was washed with warmed-up PBS twice and incubated in phenol red- and antibiotic-free DMEM supplemented with 5% DCSS.

2.2.4.2 Total protein extraction from tissue cultured cell lines

Cells treated with drugs were rinsed with ice cold PBS immediately after discarding the medium and lysed with ice cold lysis buffer (50 mM Tris, pH 7.5, 5 mM EGTA, 150 mM NaCl, 1 mini complete protease inhibitor cocktail tablet (Roche in 10 ml),

50 µl/10ml aprotinin, 100 µl/10 ml Sigma phosphatase cocktail 1 and 100 µl/10 ml Sigma phosphatase cocktail 2). Cells were scraped and left on ice for 20 min. Cell debris was removed by spinning down at 13,000 rpm, at 4℃ for 6 min and supernatant was collected. Protein concentration was determined by BCA assay.

2.2.4.3 Compartmental protein extraction

The compartmental protein extraction was implemented using the *CNMCS Compartmental Protein Extraction Kits* as per the manufacturer's instruction. This kit was used to extract cytoplasmic (C), nuclear (N), membrane (M) and cytoskeleton (CS) proteins, but in this study CS proteins were not needed.

50×PI (protein inhibitor) was added to buffer C, N, M, and CS to working concentration (1 ×) before usage. Culture cells were pelleted using routine cell culture techniques. Ice cold buffer C was then added to cell pellets at 2.0 ml per 2×10^7 cells. Cells were mixed well with buffer C and the mixture was then rotated at 4˚C for 20 min. A syringe was prepared with a needle gauge between 26.5 and 30. The needle tip was removed by bending the needle several times and only the needle base was left on the syringe. The cell mixture was passed through needle base 50-90 times to disrupt the cell membrane and release the nuclei from the cells. The degree of cell membrane disruption and nucleus release was monitored by microscope. 90-95% of the nuclei should be released from the cells. The cell mixture was then spun at 15,000 g at 4˚C for 20 min. The cytoplasmic proteins were in the supernatant and were taken out and saved in another tube. The pellet was re-suspended with ice cold buffer W at 4.0 ml per 2×10^7 cells and rotated at 4˚C for 5 min. Mixture was spun at 15,000 g at 4˚C for 20 min and the supernatant was then drained. Ice cold buffer N was added at 1.0 ml per 2×10^7 cells to re-suspend pellet. The mixture was rotated at 4˚C for 20 min and then spun at 15,000 g at 4˚C for 20 min. The nuclear proteins were in the supernatant and were taken out and saved in another tube. Ice cold buffer M was added at 1.0 ml per 2×10^7 cells to re-suspend pellet from the above step. The mixture was rotated at 4˚C for 20 min and then spun at 15,000 g at 4˚C for 20 min. The membrane proteins were in the supernatant and were taken out and saved in another tube. Protein concentrations of the three fractions were measured. The three fractions were aliquoted and labelled and stored at -70˚C.

2.2.4.4 Measurement of protein concentration by BCA assay

Total protein concentration was determined with this method. A 1 mg/ml protein standard was used and an 8-point standard curve was set up as in the following table.

µg/ml	µl of 1 mg/ml protein standard	µl of distilled water
Tube 1 0	0	50
Tube 2 50	2.5	47.5
Tube 3 75	3.75	46.25
Tube 4 100	5	45
Tube 5 250	12.5	37.5
Tube 6 500	25	25
Tube 7 750	37.5	12.5
Tube 8 1000	50	0

Samples were diluted 10 fold with 5 µl samples in 45 µl distilled water. After dilution, assay reagent was prepared as 1 volume of copper (Ⅱ) sulphate solution (Sigma Aldrich, C2284) in 50 volumes of BCA solution (Sigma Aldrich, B9643). To each tube, 1ml of assay reagent was added and then incubated at 60℃ for 15 min. 200 µl of standards and samples in duplicate were transferred to a 96-well flat bottomed plate. The plate was read at 540 nm.

2.2.4.5 Western blot

Protein samples were resolved by SDS-PAGE and transferred to a PVDF membrane. The kit BM Chemiluminesecence Blotting Substrate (POD) from Roche was used for ECL detection of the endpoint. Membranes were blocked with the 1% Roche blocking reagent at room temperature for 60 min. After blocking, primary antibodies diluted in 0.5% Roche blocking reagent were incubated with membrane overnight at 4 ℃. Then, the membrane was rinsed 2 times with TBS/Tween-20 (0.1%) and washed 3 times for 5 min each. Before the HRP-linked secondary antibody incubation at room temperature for 60 min, the membrane was washed 2 times for 5 min each with 0.5% blocking reagent. ECL substrate solution A and solution B

(Roche) were taken out from the fridge to warm up to room temperature. The membrane was washed as above followed by another 3 washes (5 min each) with TBS. During the wash, the ECL substrate was prepared with 1 volume of solution A in 100 volumes of solution B. The membrane was incubated with ECL substrate at room temperature for 1 minute before development in the dark room with Fuji Super RX medical X-ray film. For the detection with the near-infrared imaging system (as shown in Figure 10), membranes were blocked with 50% Odyssey blocking buffer diluted in PBS at room temperature for 60 min. After blocking, primary antibodies were incubated in the diluted blocking buffer with membranes overnight at 4 ℃. Before the incubation with secondary antibodies in the dark for 45 min, the membrane was rinsed 2 times with TBS/Tween-20 (0.1%) and washed 3 times for 5 min each. After the wash, membranes were left in the dark to dry before scanning. Different secondary antibodies from those used in ECL detection were used for the infrared imaging system. In this study, the target proteins were detected with the primary antibodies raised in rabbit and the loading controls such as GAPDH and α-tubulin were detected with the primary antibodies raised in mouse. Therefore, near-infrared fluorophore conjugated goat anti-rabbit secondary antibodies were used for detecting target proteins and goat anti-mouse secondary antibodies were used for detecting loading controls. There are two near-infrared fluorophores commercially available: 680nm and 800nm. So, in this study, 680 and 800 nm conjugated goat anti-rabbit/mouse secondary antibodies were used. However, the same fluorophores weren't used for both targets and loading controls. For example, 680 nm was used for target and 800nm for loading controls and vice versa. In correspondence with the fluorophores of secondary antibodies there are two scanning channels in the scanner: 680 nm and 800 nm.

Figure 10 Odyssey Infrared Imaging System manufactured by LI-COR Biosciences.

2.2.4.6 Reverse phase protein array (RPPA)

RPPA is a high throughput protein quantitative detection technique that involves spotting small amount of hundreds of samples onto a single nitrocellulose membrane-coated glass slide and analyzing these samples simultaneously in a very short time with primary and secondary antibodies, usually over two days. Initially, I used a manual arrayer (Microcaster Microarray System, Whatman, Figure 11) to spot samples at the start of these studies and then later an automated microarrayer (as shown in Figure 12) was introduced.

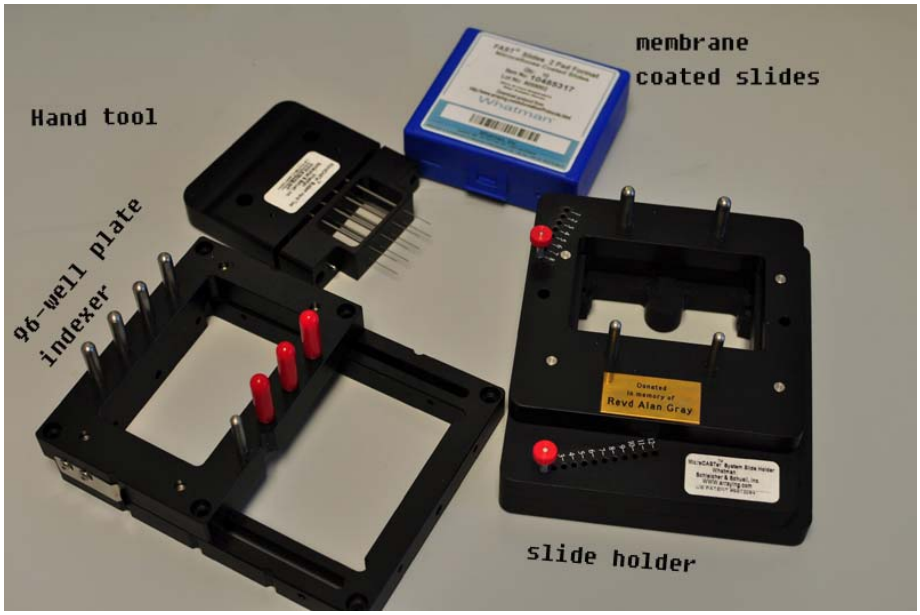

Figure 11 Whatman manual micro-arrayer (Microcaster 8-pin System) and the FAST nitrocellulose coated glass slides.

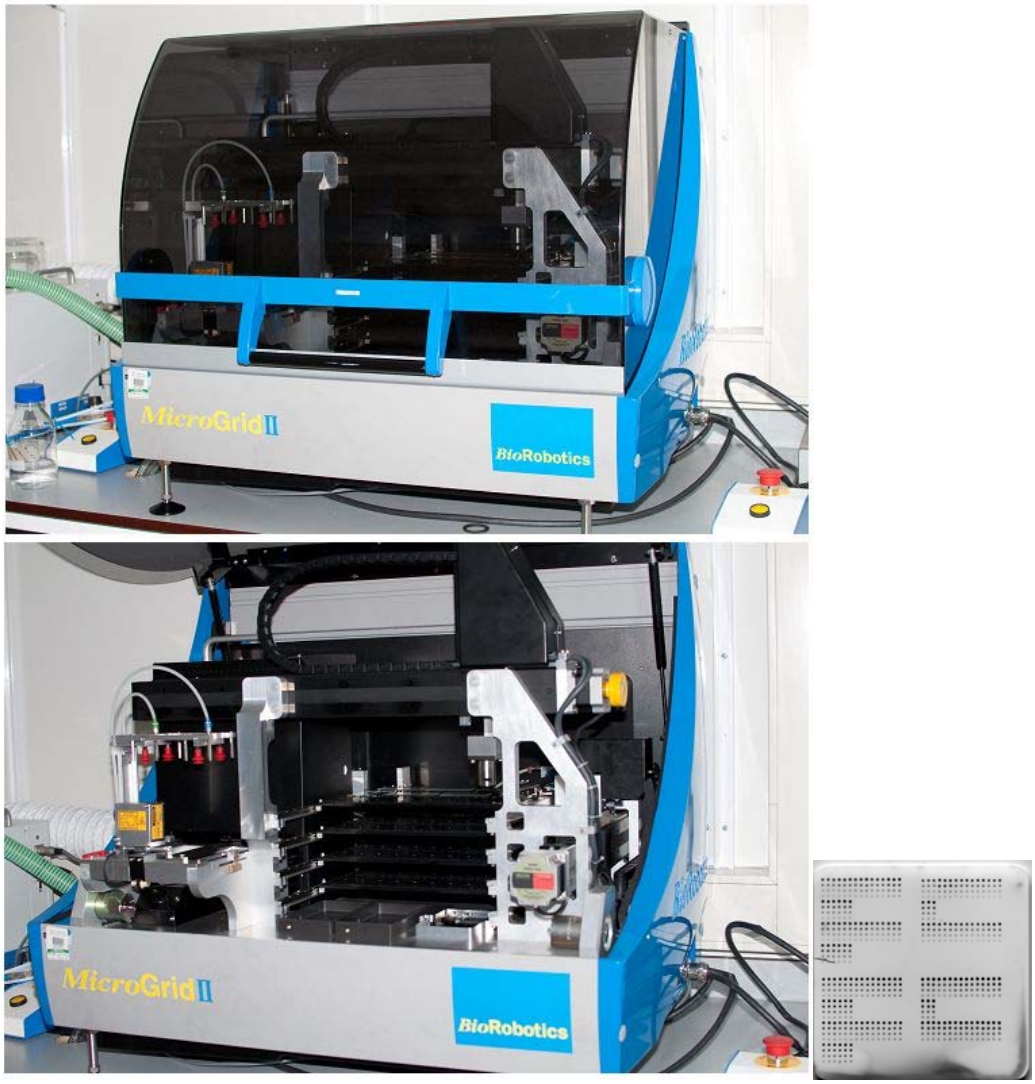

Figure 12 MicroGrid II automated microarrayer and the spotted slide.

Preparation of cell lysates and spotting. Cells were lysed as described above. The cell lysates were adjusted to 2 mg/ml with 4×SDS/2-ME sample buffer (35% glycerol, 8% SDS, 0.25 mol/L Tris-HCl, pH 6.8; with 10% β-mercaptoethanol added before use) and heated at 60^{o}C for 1 h. 2-fold serial dilutions were conducted in round bottom 96-well plates. Three replicates were spotted per sample in four two-fold dilutions.

Probing. In this study two probing methods and systems were compared. At the beginning of these studies, the DAKO signal amplification system and brown staining were used. Later on since the LI-COR Odyssey infrared imaging system was purchased and available, I used the near-infrared fluorophore conjugated secondary

antibodies to amplify signals. The two individual probing methods are described respectively as follows.

After printing, slides were hydrated in PBS for 5 min, 1% Roche Blocking reagent for 1 h, DAKO peroxidase Block (to deactivate endogenous peroxidase activity) for 10 min and then incubated with previously optimised primary antibodies in 0.5% Roche Blocking reagent overnight at 4^{o}C in a sealed box containing a damp paper towel. The following day, slides were washed in PBS/Tween-20 (0.1%) at room temperature for 5 min (X3) before signal amplification with DAKO CSA Ⅱ Biotin-free Tyramide Signal Amplification System. This commercially available kit catalyzed the deposition of tyramide-fluorescein and used 3, 3'-diaminobenzidine tetrachloride as the substrate to amplify the signal detected by the primary antibody. An HRP-conjugated second antibody was attached to the primary antibody and catalysed the *in situ* deposition of tyramide-fluorescein which was then bound by HRP conjugated anti-fluorescein antibody. The HRP cleaves 3, 3'-diaminobenzidine tetrachloride, giving a stable brown precipitation with excellent signal-to-noise ratio. Slides were dried and scanned as TIFF files for further analysis. The signal intensity was analysed with ImageQuant (GE Healthcare).

For the detection with the LI-COR Odyssey infrared imaging system, slides were blocked with 50% Odyssey Blocking buffer in PBS at room temperature for 1 h after printing. Slides then were incubated with previously optimised primary antibodies in 50% Odyssey Blocking buffer overnight at 4 ^{o}C in a sealed box containing a damp paper towel. The following day, slides were washed in PBS/Tween-20 (0.1%) at room temperature for 5 min (X3) before incubation in the dark with near infrared fluorophore conjugated secondary antibodies in 50% Odyssey Blocking buffer diluted in PBS/Tween-20 (0.1%) for 45 min at room temperature. In this study secondary antibodies were diluted 1:2000. After incubation with secondary antibodies, slides were protected from light and dried at room temperature before subjecting to the scan with the Odyssey imaging system.

RPPA analysis was performed using MicroVigene RPPA analysis module (VigeneTech, Carlisle, MA, USA). Spots were quantified by accurate single segmentation, with actual spot signal boundaries determined by the image analysis algorithm. Each spot intensity was quantified by measuring the total pixel intensity of the area of each spot (volume of spot signal pixels), with background subtraction of 2 pixels around each individual spot. The mean of the replicates was used for normalisation and curve fitting. Curve fitting was performed using four parameter logistical non-linear regression using a joint estimation approach ('supercurve method'), with quantification y0 (intensity of curve) of sample dilution curves used in subsequent analysis.

2.2.4.7 In-cell Western analysis

Preparation of solutions: 10X PBS was prepared by dissolution of ten PBS tablets in 100 ml ddH_2O. Methanol was cooled at -20°C for at least for 1 h before use. 4% Formaldehyde was made up in PBS before use. Blocking Buffer was prepared (25 mL) by adding 2.5 mL 10X PBS, 1.25 mL normal serum from the same species as the secondary antibody (eg. normal goat serum in this study) to 21.25 mL dH_2O and was mixed well. While stirring, 75 µL Triton X-100 was added. For the preparation of the antibody dilution buffer (40 ml), 4 ml 10×PBS was added to 36 ml dH_2O and mixed. 0.4 g BSA was added and mixed well. While stirring, 120 µl Triton X-100 was added.

Specimen Preparation: Cells were grown in black-walled, clear-bottom 96-well microplates for the drug treatment. Media were discarded immediately once the treatment was completed and was followed by fixing cells with 100 µl of 4% formaldehyde in each well for 15 min at room temperature. Fixed cells were rinsed three times in 200 µl/well of PBS for 5 min each after the fixative was aspirated. Cells were permeabilised with 100 µl of ice cold 100% methanol for 10 min in -20°C freezer followed by three washes in 200 µl/well of PBS for 5 min each.

Immunostaining: All subsequent incubations were carried out at room temperature, unless otherwise noted, in a humid light-tight box or covered dish/plate to prevent

drying and fluorochrome fading. Specimens were blocked in 40 µl/well of Blocking Buffer for 60 min. After blocking, diluted primary antibodies were applied with 40µl/well. For double-labelling, a cocktail of the primary antibodies was applied at their appropriate dilution in Antibody Dilution Buffer. Specimens were incubated with primary antibodies overnight at 4°C in a sealed wet box followed by three washes in PBS for 5 min each. Specimens were then incubated with 40 µl/well of the cocktail of 1:800 of IRdye680 anti-mouse IgG (for the normaliser) and 1:800 of IRdye800CW anti-rabbit IgG (for the target) diluted in Antibody dilution buffer for 1 h at room temperature in dark. Specimens were washed three times for 5 min each before scanning with Odyssey Infrared Imaging System (dry samples generate stronger signals than wet ones).

2.2.5 Protein detection in tumours

2.2.5.1 Immunohistochemistry of the paraffin embedded tissue for the optimization of antibody dilution

The paraffin embedded sections were dewaxed in xylene twice for 5 min each and rehydrated for 2 min respectively in 99%, 99%, 80% and 50% alcohol and for another 2 min in tap water. After rehydration, antigen retrieval was performed on slides by treating them with either boiled 0.1M sodium Citrate/0.1M Citric Acid pH6.0 or Tris/EDTA buffer pH9.0 (1.21g Tris, 0.37g EDTA, pH9.0, 0.5ml Tween-20 in 1L) for 5 min in a microwavable pressure cooker in a microwave. Thereafter slides were put aside to cool for 20 min. Slides were then washed in PBS/Tween-20 (0.05%) twice for 5 min each before treatment in 1% H_2O_2 for 10 min in the coplin jar. The same wash as above was repeated once the treatment finished. Sections were then loaded to Sequenza (a slide staining rack) for non-specific blocking with DAKO Protein Block Serum Free for 10 min followed by the primary antibody incubation in DAKO Antibody Diluent for either 1 h at room temperature or overnight at 4°C. Slides were washed again as the above before the incubation with Dako Envision+System-HRP labelled polymer Anti-rabbit or Anti-mouse for 30 min at room temperature. Washes were performed again before and after visualization with DAB for 10 min. Sections were counterstained in haematoxylin for 2 min followed

by Scot's tap water for 2 min. Before mounting, sections were dehydrated for 2 minutes respectively in 50%, 80%, 99%, and 99% alcohol sequentially.

2.2.5.2 Immunofluorescence

Immunofluorescence shares the same methods of de-waxing and rehydration, antigen retrieval, blocking and primary antibody incubation with imunohistochemistry as described above, but the primary antibody cocktail of anti-cytokeratin antibody (murine) as tumour mask and anti-target protein antibody (rabbit) replaced the single antibody incubation. After the primary antibody incubation, the goat anti-mouse Alexa555 antibody diluted at 1:25 in ready-to-use Dako Envision+System-HRP labelled polymer Anti-rabbit was incubated with sections for 1 h at room temperature. After incubation, 3 washes for 5 min each in PBS/Tween-20 (0.05%) were performed. The target visualisation was implemented with the Aquantiplex™ assay kit. Sections were incubated with Cy5-tyramide diluted in signal amplification diluent at 1:50 in the dark at room temperature for 10 min and then washed 3 times for 5 min each. Sections were dehydrated in 80% ethanol for 1 min and air dried in the dark. For the counterstaining, 45 µl of Prolong Gold anti-fade reagent with DAPI was applied to the tissue sections. Images were acquired with AQUA imaging system (as shown in Figure 13) after drying. Data were analyzed with ***AQUAnalysis***™ Software (HistoRX**,** Connecticut, USA).

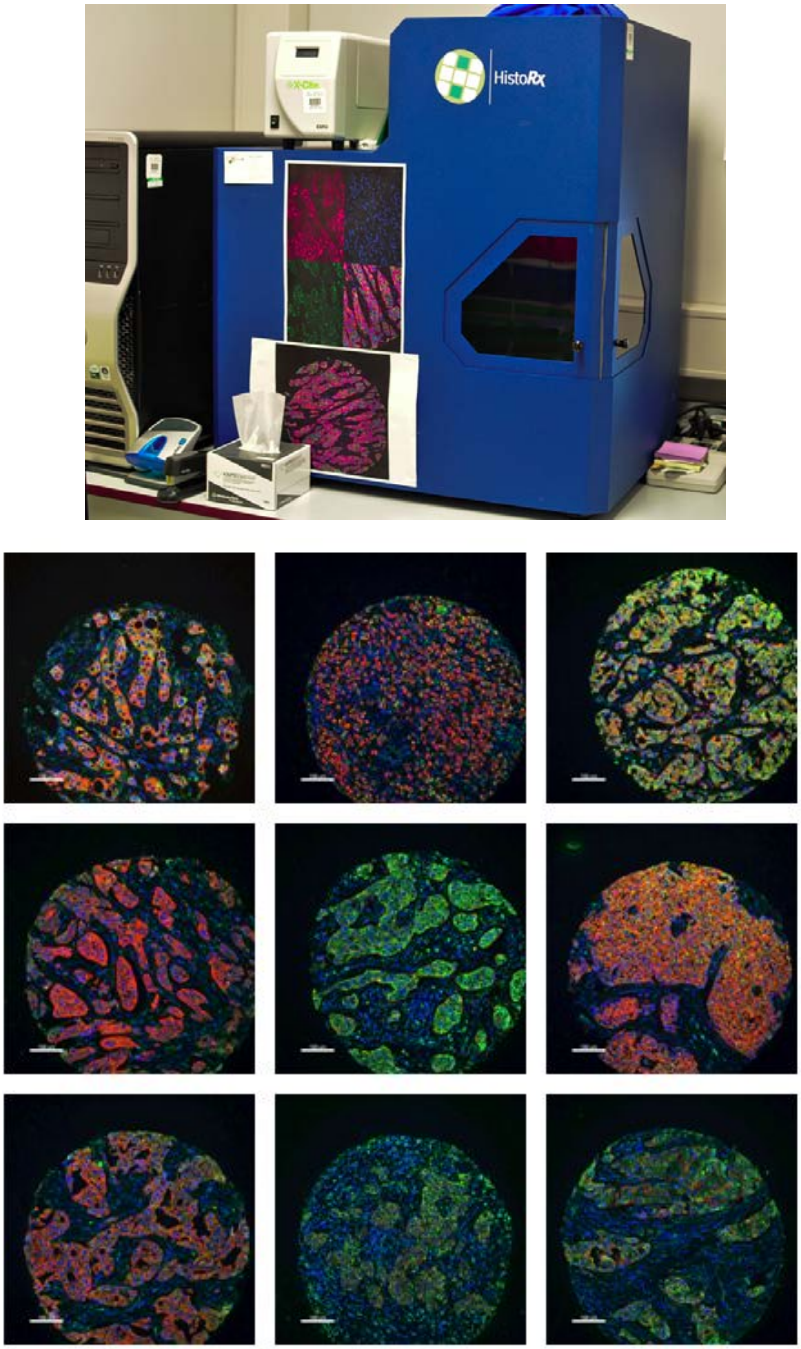

Figure 13 HistoRX AQUA imaging system and examples of acquired images. These images are acquired from Tumour Microarray (TMA) cores with the imaging system. Blue indicates DAPI staining of nucleus. Green indicates cytokeratin staining as tumour mask of tumour epithelial cells. Red indicates target staining.

2.2.6 Gene expression analysis

2.2.6.1 Total RNA extraction

The RNA extraction was implemented with *STRATAGENE Absolutely RNA® Miniprep Kit* from Agilent Technologies as per the manufacturer's instruction.

Briefly, after drug treatment, MCF-7 cells grown in 92-mm petri dishes were lysed by incubating with 600 µl lysis buffer. Cell lysates were transferred to 1.5 ml microcentrifuge tubes and vortexed to decrease the viscosity. Up to 700 µl of homogenate was transferred to a seated Prefilter Spin Cup and spun at maximum speed for 5 min. The spin cup was discarded and the filtrate was retained for further processing. To the filtrate an equal volume of 70% ethanol was added and mixed thoroughly by vortexing the tube for 5 s. Up to 700 µl of the mixture was transferred to a seated RNA Binding Spin Cup and spun at the maximum speed for 60 s. The Spin Cup was retained.

The Spin Cup was washed by adding 600 µl 1×Low-Salt Wash Buffer and spinning in a microcentrifuge tube at the maximum speed for 60 s. The filtrate was discarded and the Spin Cup was retained for a further spin at the maximum speed for 2 min to dry the matrix. 50 µl reconstituted RNase-Free DNase I was added directly onto the matrix and incubated at 37°C for 15 min. After the incubation, 600 µl of 1×High-Salt Wash Buffer was added to the Spin Cup and spun in a microcentrifuge tube at the maximum speed for 60 s. The Spin Cup was retained for the addition of 600 µl 1×Low-Salt Wash Buffer and spun in a microcentrifuge tube at the maximum speed for 60 s. A further 300 µl of 1×Low-Salt Wash Buffer was applied to the Spin Cup and spun for 2 min to dry the matrix. Finally, 80 µl of Elution Buffer was added directly onto the matrix of the Spin cup which was seated in a 1.5-ml microcentrifuge tube and incubated for 2 min at room temperature before spinning down for 60 s to collect the RNA solution. The concentration of the RNA solution was then measured using a spectrophotometer Nanodrop 2000c, Thermo Scientific.

2.2.6.2 RNA amplification

The RNA amplification was implemented with *Illumina® TotalPrep™ RNA Amplification Kit* as per the manufacturer's instruction. The working flow is shown in the following figure, which is adapted from the manual.

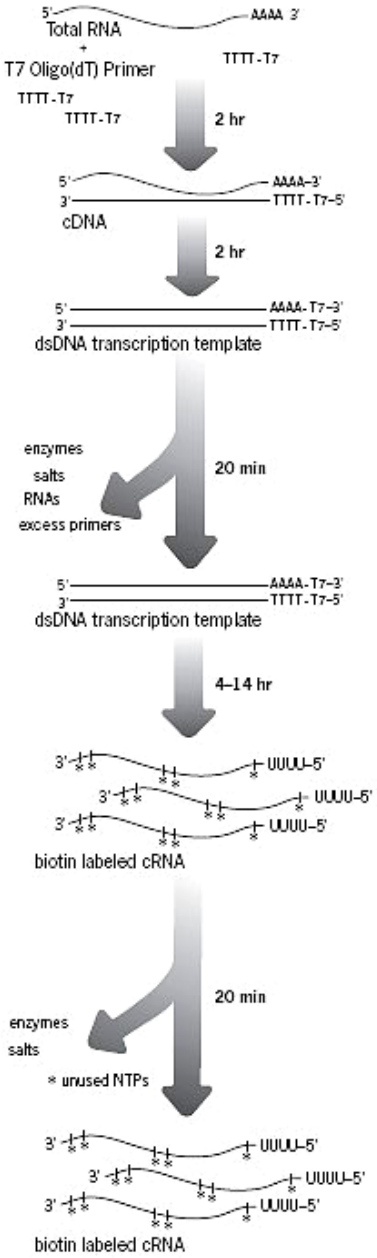

II.C. Reverse Transcription to Synthesize First Strand cDNA

1. Bring RNA samples to 11 µL with Nuclease-free Water
2. Add 9 µL of Reverse Transcription Master Mix and place at 42°C
3. Incubate for 2 hr at 42°C

II.D. Second Strand cDNA Synthesis

1. Add 80 µL Second Strand Master Mix to each sample
2. Incubate for 2 hr at 16°C

Potential stopping point

II.E. cDNA Purification

Preheat Nuclease-free Water to 55°C

1. Add 250 µL cDNA Binding Buffer to each sample
2. Pass the mixture through a cDNA Filter Cartridge
3. Wash with 500 µL Wash Buffer
4. Elute cDNA with 20 µL of 55°C Nuclease-free Water

Potential stopping point

II.F. In Vitro Transcription to Synthesize cRNA

1. Add 7.5 µL of IVT Master Mix to each cDNA sample, and mix
2. Incubate for 4–14 hr at 37°C
3. Add 75 µL Nuclease-free Water to each sample

Potential stopping point

II.G. cRNA Purification

Before you begin: preheat Nuclease-free Water and assemble filter cartridges and tubes

1. Add 350 µL cRNA Binding Buffer to each sample
2. Add 250 µL 100% ethanol and pipet 3 times to mix
3. Pass samples through a cRNA Filter Cartridge(s)
4. Wash with 650 µL Wash Buffer
5. Elute cRNA with 200 µL 55°C Nuclease-free Water

Potential stopping point

2.2.6.3 Gene expression analysis

The measured cRNA was subjected to gene expression array analysis based on HumanHT-12 Expression Beadchips purchased from Illumina®, which was carried out by Welcome Trust Clinical Research Facility, Western General Hospital in Edinburgh. Data processing was conducted with the assistance of the bioinformatician, Dr. Andrew H. Sims in Breakthrough Breast Cancer Research Unit, the University of Edinburgh. Gene expression analysis was performed using the open source statistical programming language, R (253), and associated Bioconductor package (254). Data was quantile normalised using the Lumi packages (255). Differentially expressed genes were identified with the siggenes package which implements Significance analysis of Microarrays (SAM) (256) and Rank Products (257). A minor batch effect was eliminated using empirical Bayes batch-correction methods (ComBat) (258) as described previously (259, 260). The Cluster and TreeView programs (261) were used to generate heatmaps.

2.2.7 Flow cytometric analysis for cell cycle

The preparation of solutions

Citrate Buffer was prepared by dissolution of 85.5 g Sucrose and 11.76 g Trisodium Citrate in 800 mL distilled water. 50 mL DMSO was added and the pH was adjusted to 7.6. Finally, the solution was made up to 1000 mL with distilled water and was stored at 4ºC. This is stable for up to 2 years.

Stock solution was prepared by dissolution of 2000 mg trisodium citrate, 121 mg Tris base, 1044 mg spermine tetrahydrochloride and 2 mL Nonidet NP40 in 1800 mL distilled water. The pH of the solution was adjusted to 7.6 and the solution was made up to 2000 mL with distilled water.

Solution A was prepared by dissolution of 15 mg trypsin type IX-S in 500 mL stock solution pH7.6. The solution was dispensed into 25 x 20mL aliquots which were labelled and frozen at -20ºC.

Solution B was prepared by dissolution of 250 mg trypsin inhibitor and 50 mg RNAse A in 500 mL stock solution pH7.6. The solution was dispensed into 25 x 20 mL aliquots which were labelled and frozen at -20ºC.

Solution C was prepared by dissolution of 208 mg propidium iodide and 500 mg spermine tetrahydrochloride in 500 mL stock solution pH7.6. The solution was dispensed into 25 x 20mL aliquots which were labelled and frozen at -20ºC.

Cells were trypsinised as described above and transferred to 5mL (12 x 75mm) 'BD Falcon' tubes. Cells were collected by centrifugation at 1600 rpm for 5min and tubes were inverted to allow excess moisture to be absorbed onto a paper towel. Cells were re-suspended in citrate buffer (100 µl) and tubes were covered with Parafilm and stored at -20ºC prior to analysis. For the analysis, solutions A, B and C were defrosted (keeping solution C on ice after thawing) and were kept at room temperature. 450 µL of solution A was added to the sample tubes, whirl mixed and incubated at room temperature for 2 min (mixing throughout the incubation). Then, 375 µL of solution B was added, briefly whirlimixed and incubated at room temperature for a further 10 min. Finally, 250µL of solution C was added, briefly whirlimixed and incubated on ice in the dark for a further 10 min. Samples were kept on ice and in the dark prior to analysis. Samples were run using the Flow Cytometer according to the appropriate settings, templates, etc. Cell cycle analysis was performed using FlowJo7 software.

2.2.8 Statistics

One-way ANOVA followed by Tukey HSD post HOC test was used to conduct multiple comparisons of groups with equal variance. The homogeneity of variances was tested with the Levene's test run by SPSS17.0. The ANOVA and Tukey HSD post HOC test are based on normal distribution and equal variances.

For the multiple comparisons of groups with unequal variance, the Brown-Forsythe test followed by Games-Howell post HOC test was conducted. Brown-Forsythe test is an equivalent to ANOVA based on unequal variances. The Games-Howell post

HOC test designed for unequal variances is an equivalent to Tukey HSD post HOC test.

For experiments, in which there were only two groups, the Student's t-test was used.

For the gene expression analysis, the Student's t-test was used to find out whether individual genes were significantly induced by HRG treatment for 20 min or 40 min compared with control.

For correlation analyses between Roche and DAKO blocking buffers and spotting reproducibility between slides in the RPPA technique, a 2-tailed Pearson correlation test was used.

For correlation analysis between biomarkers, a 2-tailed Spearman correlation test was used. For analysis of PTPN13 expression in the wild-type versus mutated PI3KCA groups, a Mann-Whitney U-test was used to compare groups.

Chapter Three: Methodology Development

3 Methodology development

3.1 RPPA development

Reverse phase protein array (RPPA) is so termed in contrast to traditional FPPA (Forward Phase Protein Array). The working principles are shown in Figure 14.

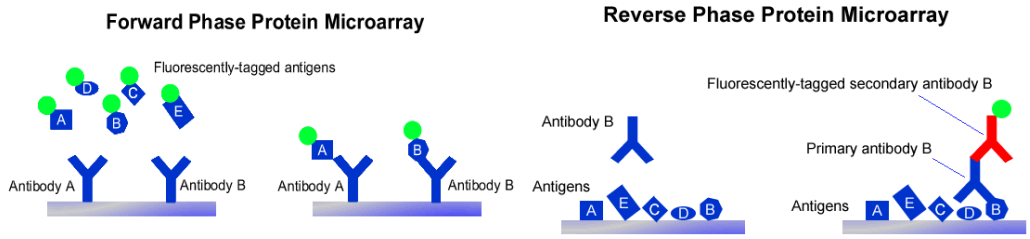

Figure 14 the schematic representation of forward phase protein array and reverse phase protein array (reproduced from http://www.microarray.prostatecentre.com/Services_Proteins.htm).

In FPPA, a variety of antibodies are immobilised on slides and incubated with fluorescein-tagged protein samples such as cell lysates and for higher specificity, fluorescein-tagged secondary antibodies are often applied to form a sandwich. Antibody array and ELISA are the most common versions of FPPA. The advantage of FPPA is that depending on the number of antibodies immobilised, hundreds or thousands of proteins in one protein sample can be analysed simultaneously on one chip. In contrast in RPPA, hundreds or thousands of protein samples are immobilised on membrane-coated slides and then incubated with one primary antibody to analyse the difference of one target under a variety of treatments. FPPA is often used in the screening of therapeutic targets from hundreds of proteins. RPPA is used to detect the changes of a known protein under different conditions. For example, in this study RPPA is used to profile signalling components in PI3K/Akt and Raf/MEK/ERK pathways under the stimulation of HRG or EGF with or without inhibitors. One major concern of RPPA is the specificity of primary antibodies which are required to be validated by Western Blot. Hundreds of antibodies by which only specific bands are recognised have been validated but the antibodies listed in section 2.1.7 were used for this study. Another major concern is the level of sensitivity as it is necessary to amplify the signal intensity to a detectable level. At the very beginning

of the development of RPPA in our laboratory, the entry-level manual arrayer (as shown in Figure 11) was used to optimise various conditions before the application of automated robotics. The manual arrayer is competent to deal with small number of samples. Apart from the validation of primary antibodies and sensitivity, there are other different conditions requiring optimisation including sample preparation, application of automated robotic microarrayer, blocking buffer application and ending point detection.

3.1.1 Sample preparation

In this section, native *vs* reduced denatured samples were compared for the end point detection. To optimise the sample preparation procedure, cells were lysed with the lysis buffer mentioned in section 2.2.4.2. Cell lysates were then measured and adjusted to the same concentration with either lysis buffer (for native samples) or SDS/2-ME sample buffer (for reduced denatured samples, it is very similar to the loading buffer of SDS-PAGE). Only samples adjusted with SDS/2-ME sample buffer were heated at 60 ºC for 1 h (the same heating procedure as used for western blotting). The procedures for RPPA are exactly the same for both sample preparation methods. The largest difference between lysis buffer and SDS/2-ME sample buffer is that the reducing reagent β-mercaptoethanol and glycerol are supplemented in the latter one. Additionally, the commercial antibodies for western blot are generally developed for reduced denatured samples. The reduced denaturation makes linear epitopes more exposed to antibodies. So the reduced denatured samples in RPPA make the RPPA approach comparable with western blot. It was observed in Figure 15 that reduced samples generated stronger signals than non-reduced ones. It was evident that reduced samples had better circular shape and inter-spot separation than non-reduced ones. Since glycerol was included in the reduced sample buffer, reduced sample spots were less spreadable than non-reduced samples. The spread would cause sample contamination between dilutions and interfere with the inter-dilution signal. In conclusion, denaturing the samples in a reduced sample buffer by heating 60 ºC for 1 h appeared useful for RPPA. The reduced preparation method was adopted for the entire study.

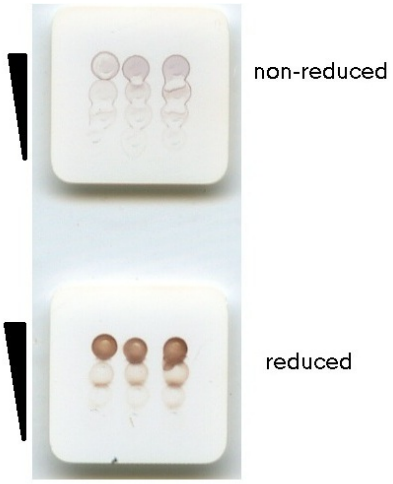

Figure 15 Effects of sample preparation procedures on the signal intensity of GAPDH and spot shapes. Non-reduced (native) samples were not heated in lysis buffer (2-ME and glycerol free) and reduced samples were heated in a reduced sample buffer (2-ME and glycerol positive) at 60 ºC for 1 h followed by exactly the same procedures for both sample preparation methods. Samples were diluted in a 2-fold serial dilution for 3 times from the top row to the bottom on the manual arrayer spotting slide. The reversed triangles indicate the dilution direction. Signals were amplified with DAKO CSA Ⅱ Biotin-free Tyramide Signal Amplification System and scanned as TIFF files.

3.1.2 Application of automated robotic microarrayer

Although a manual arrayer is very useful and convenient for entry-level use, it is not competent for high throughput application which is one of the strengths of RPPA. Automated robotics was introduced into the laboratory as shown in Figure 12. Compared with robotics, the primary weaknesses of the manual arrayer include the following.

1) A limited number of samples can be arrayed by manual arrayer due to the large pin size of 0.457 mm diameter and the fixed pin configuration. In contrast, the diameter of the robotic pin is 0.2mm. The pin configuration of the robotic arrayer is flexible. Pins of manual arrayer are fixed into the hand tool which means pins are undetachable and irreplaceable. This also restricts the number of spots which are able to be printed on slides. While pins of robotics are separate from the pin head, investigators can put a couple of types of pins including solid pins and split pins in the head with

different pin layouts. So, different layouts of spots are available for robotics rather than for manual arrayer. The spot layout is also a key factor influencing the number of samples spotted on slides. Therefore, thousands of samples can be spotted onto a single slide by the robotic arrayer while only hundreds are feasible for the manual arrayer.

2) It is hard to control the dwelling time of the pins on the membrane by hand. The dwelling time determines the amount of samples absorbed by the membrane. So, the inter-slide reproducibility is poor.
3) The spot shape is not a regular circle, which causes problems for the analysis software to quantify precisely.
4) It is time consuming for large number of samples and not suitable for high throughput array.

The robotic arrayer was used for the following optimisation.

3.1.3 Application of different blocking buffers

After spotting samples onto the slides with the robotic arrayer, slides were blocked for non-specific binding sites on the membrane with blocking buffer. Two blocking buffers were compared in this study. One is the DAKO Protein Block Serum Free (Copenhagen, Denmark, CAT No K1497) which comes with the DAKO CSA Ⅱ Biotin-free Tyramide Signal Amplification System and the other is the Roche Blocking reagent (Roche Applied Science, Mannheim, Germany, CAT No 11500708001). The expression level of p-ERK1/2 (T^{202}/Y^{204}) was analysed. The anti-p-ERK1/2 (T^{202}/Y^{204}) primary antibody was validated for application in RPPA with no non-specific bands in Western Blot in which the membrane was blocked with Roche Blocking Reagent. It was observed in Figure 16 that most of the individual values were above the $y=x$ line and the trend line had a slope of 2.0387 (R^2=0.9186), which meant the intensities of spots blocked by the Roche blocking reagent were nearly 2-fold higher than those blocked by DAKO blocking buffer (Pearson correlation coefficient is 0.963, p value is 0.000). So the Roche Blocking

Reagent resulted in a one-more-dilution higher sensitivity. Therefore, Roche Blocking Reagent was accepted to use in RPPA with DAKO CSA Ⅱ Biotin-free Tyramide Signal Amplification System.

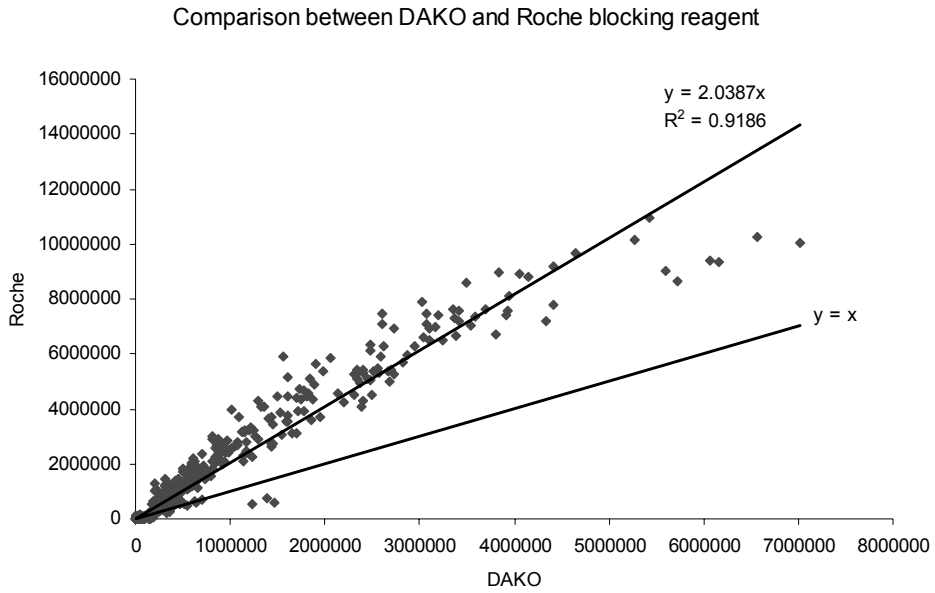

Correlation analysis

Pearson correlation coefficient	P value (2-tailed)
0.963	0.000

Figure 16 Effects of Roche and DAKO blocking buffers on the spots' intensities. These spots were probed with anti-p-ERK1/2 (T^{202}/Y^{204}) primary antibody and the signals were amplified with the DAKO CSA Ⅱ Biotin-free Tyramide Signal Amplification System. The spots' intensities were measured with the array module of **ImageQuant TL** from GE Healthcare using 'average spot edge' background method. The anti-p-ERK1/2 (T^{202}/Y^{204}) primary antibody was validated for application in RPPA with no non-specific bands in Western Blot in which the membrane was blocked with Roche Blocking Reagent.

3.1.4 The application of LI-COR imaging system in RPPA

The application of the LI-COR imaging system requires the use of the near infrared flurophore for end point detection. Since the LI-COR imaging system can perform simultaneously a two-channel scan, 680nm and 800nm, it becomes possible to normalize the target protein expression against the normaliser such as tubulin, GAPDH and actin in a single slide. This would be more accurate than normalization against the normaliser on another slide. Meanwhile, compared with chromogen-based colourimetry, the application of LI-COR imaging system saves half the number of slides. The application of LI-COR imaging system requires fewer steps than chromogen-based colourimetry, which would reduce the chances of introducing errors. In theory, the near infrared fluorescence has a broader dynamic range than chromogen-based colourimetry (communication with LI-COR® Biosciences). Additionally the near infrared red region in the spectrum has low noise response to both the membrane and the printed samples which have visual auto-fluorescence. If protected from light properly, the fluorescence on slides can be maintained for a couple of months without signal fading. Therefore, it was judged reasonable to use the LI-COR imaging system in the RPPA analysis. In this system, 50% Odyssey Blocking buffer in PBS is used as the blocking reagent as well as the antibody diluent. The protocols are described in *'2.2.4.6 Reverse Phase Protein Array (RPPA)'*.

3.2 In-cell Western development

The In-cell Western is a technique based on detecting immunofluorescence in fixed cell lines and the availability of the LI-COR imaging system. It detects the protein expression level directly in formaldehyde-fixed cells in 96-well microplates. The In-cell Western doesn't require the lysate preparation, SDS-PAGE and membrane transfer which are required in the regular western blot procedure. The In-cell Western technique saves time and can more easily allow analysis of large numbers of replicates than standard Western blotting. This technique uses the same principle as

immunofluorescence. However, four differences from immunofluorescence should be noted.

1) All the procedures are performed in 96-well plates rather than on cover slides.
2) It is more quantitative in a higher throughput manner.
3) The final signal is captured by the LI-COR imaging system which acquires fluorescence rather than by microscope.
4) Secondary antibodies linked to near-infrared fluorophore rather than visible wave-length fluorophore are applied.

For this technique clear bottom and black wall 96-well plates are required to remove the noise from autofluorescence at 680 nm which is present in the commonly used clear 96-well plates. The immunofluorescence protocol was followed in the In-cell Western. As shown in Figure 17, both ERK1/2 and Akt were activated by 1nM EGF at a very early time and the signals then gradually decreased to the base line. This observation was consistent with previous reports (91). Since in this experiment the 'normal' tissue culture 96-well plate was applied, autofluorescence in 680 nm was detected from the wall of each well not from the bottom. However, when black wall/clear bottom plates were used, the autofluorescence disappeared (Figure 18). In this example, MCF-7 cells were stimulated by 1nM HRG in the presence of 10 μM CHX. It was observed that ERK1/2 was activated and the level of p-ERK1/2 reached a maximum at the10-min point and was then sustained during the rest of the whole time course, which supported the previous findings (91). Albeit more quantitative, In-cell Western is not as sensitive as 'normal' western blot, since oscillation was less easily observed by In-cell Western in MCF-7 cells treated with HRG+CHX. As presented later in this thesis, the oscillation was observed and confirmed by both western blot and RPPA.

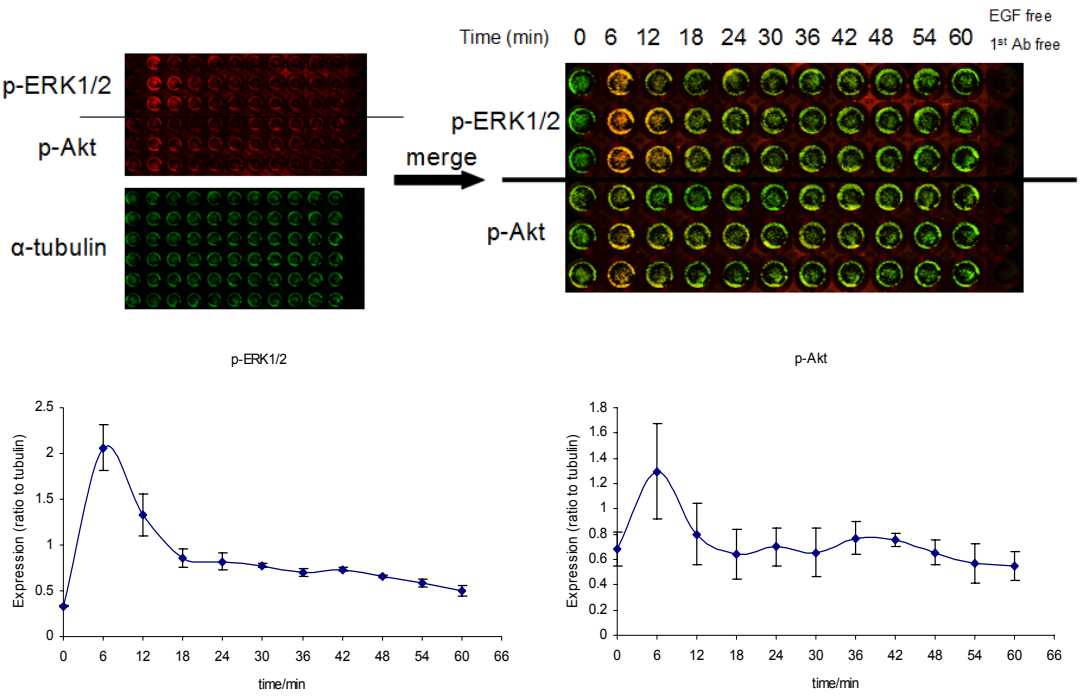

Figure 17 In-cell Western analysis of the stimulation of MCF-7 by 1nM EGF. MCF-7 cells were grown in DMEM supplemented with 10% FCS in 96-well plates for 48 h and then in phenol red free DMEM supplemented with 5% DCSS for another 48 h. Cells were stimulated with 1nM EGF for the time indicated. The treatment was stopped by adding 4% formaldehyde to the wells. After being fixed in 4% formaldehyde for 15 min at RT, cells were permeabilised in methanol for 10 min at -20°C before blocking at RT for 1 h. Primary antibodies were incubated overnight with cells at the optimal dilution at 4°C before the incubation with secondary antibodies at RT for 1 h. Images were acquired with LI-COR imaging system when plates were dry. The 680nm channel (**red**) was for p-ERK1/2 and p-Akt and the 800nm channel (**green**) was for α-tubulin. The OD was measured by In-cell Western module of the analysis software supplied along with the imaging system. The ratio of OD of p-ERK1/2 or p-Akt against that of α-tubulin at each time point was applied to compare the signal intensity. The results are presented as the average of the ratio ±SD.

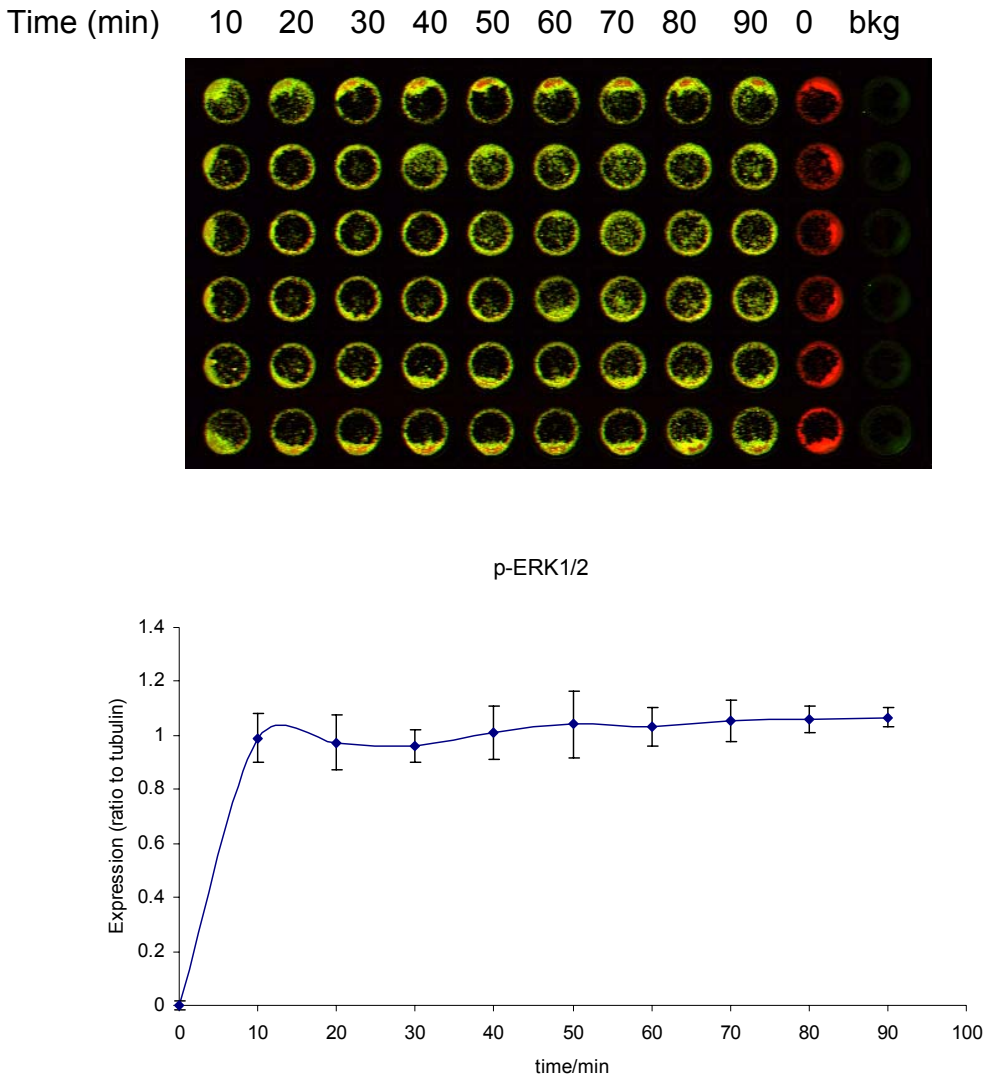

Figure 18 In-cell Western analysis of the stimulation of MCF-7 by 1nM HRG in the presence of 10 µM CHX. MCF-7 cells were grown in DMEM supplemented with 10% FCS in 96-well plates for 48 h and then in phenol red free DMEM supplemented with 5% DCSS for another 48 h. Cells were stimulated with 1nM HRG in the presence of 10 µM CHX for the time indicated. The treatment was stopped by adding 4% formaldehyde to wells. After being fixed in 4% formaldehyde for 15 min at RT, cells were permeabilized in methanol for 10 min at -20°C before blocking at RT for 1 h. Primary antibodies were incubated overnight with cells at the optimal dilution at 4°C before the incubation with secondary antibodies at RT for 1 h. Images were acquired with LI-COR imaging system when plates were dry. The 680nm channel (**red**) was for α-tubulin and the 800nm channel (**green**) was for p-ERK1/2. The OD was measured by In-cell Western module of the analysis software supplied along with the imaging system. The ratio of OD of p-ERK1/2 against that of α-tubulin at each time point was applied to compare the signal intensity. The results are presented as the average of the ratio ±SD. 'bkg' denotes background, in which HRG stimulation and primary antibody were absent.

Chapter Four: Results

4 Results

The behaviour of cells is reflected by the complex dynamics of molecular signalling spatiotemporally. In this study I explored the effects of different interventions on signalling through the application of inhibitors after stimulation with HRG and EGF over a time course and linking the dynamics with outcome.

4.1 The oscillatory dynamics of phospho-ERK1/2(T^{202}/Y^{204}) and phospho-Akt (S^{473})

4.1.1 Characteristics of the cell line models used

Before starting the oscillation studies, it was necessary to characterize the MCF-7 and MCF-7/HER2-18 cell lines to confirm that their responsiveness was consistent with the published data.

All the cell lines used were breast carcinoma cell lines. The MCF-7 cell line was originally isolated from the pleural effusion of a 69-year-old woman in 1970 and is a luminal epithelial cell line (262). The name of this cell line refers to the acronym of *Michigan Cancer Foundation-7*. This cell line is ER positive, and has a proliferative response to 17β-estradiol (Figure 19) (262). As one of the Selective oestrogen receptor modulators (SERMs), tamoxifen blocked the effect of 17β-estradiol in this cell line as reported (263). MCF-7 cells were also growth stimulated by HRG and EGF (Figure 19). Trastuzumab inhibited the growth of MCF-7 cells stimulated by 1nM EGF (EGF+trastuzumab *vs* EGF 84.0%) but did not inhibit the growth stimulated by 1nM HRG. Pertuzumab inhibited the growth stimulated by both growth factors (HRG+pertuzumab *vs* HRG 79.3%, EGF+pertuzumab *vs* EGF 62.3%). The combination of trastuzumab and pertuzumab produced a further inhibition of the growth stimulated by HRG than either single agent (HRG+trastuzumab+pertuzumab *vs* HRG 43.5%). The combination also inhibited the growth stimulated by EGF (EGF+trastuzumab+pertuzumab *vs* EGF 67.2%) and had a stronger inhibitory effect than trastuzumab alone, but the inhibitory effect of the combination was not

statistically different compared with that of pertuzumab alone under the stimulation of EGF.

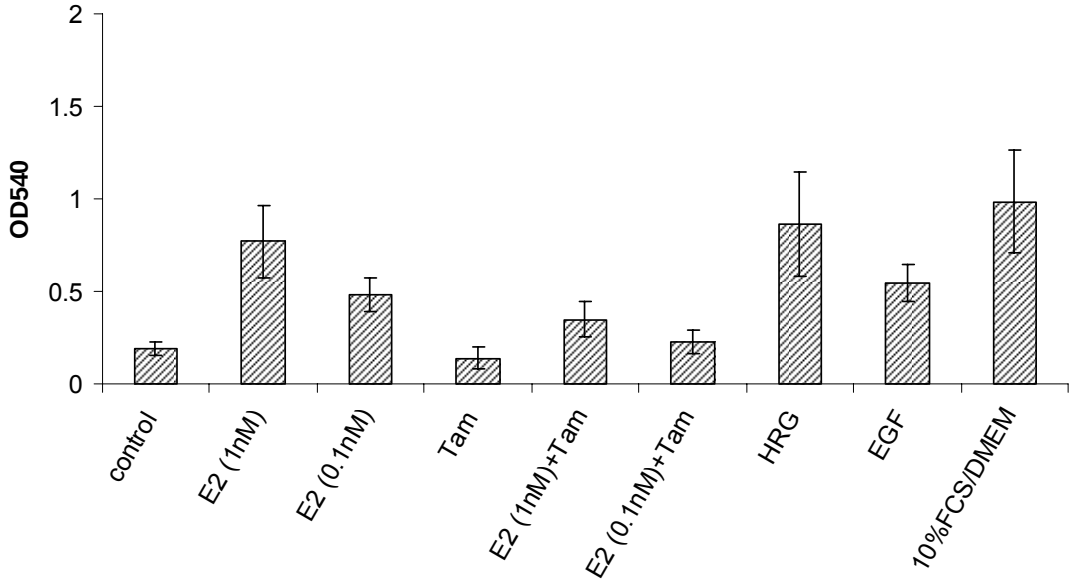

Brown-Forsythe test for all-group comparison (N=6, unequal variances), p=0.000

Games-Howell Post Hoc test run by SPSS 17.0

P value	control	E2 (1nM)	E2 (0.1nM)	Tam	E2 (1nM)+Tam	E2 (0.1nM)+Tam	HRG	EGF	10%FCS/DMEM
control	--	0.008	0.004	0.667	0.094	0.948	0.021	0.002	0.010
E2 (1nM)	0.008	--	0.145	0.004	0.027	0.008	0.998	0.356	0.820
E2 (0.1nM)	0.004	0.145	--	0.001	0.355	0.006	0.184	0.929	0.064
Tam	0.667	0.004	0.001	--	0.026	0.392	0.014	0.000	0.007
E2 (1nM)+Tam	0.094	0.027	0.355	0.026	--	0.322	0.059	0.079	0.022
E2 (0.1nM)+Tam	0.948	0.008	0.006	0.392	0.322	--	0.024	0.002	0.011
HRG	0.021	0.998	0.184	0.014	0.059	0.024	--	0.335	0.996
EGF	0.002	0.356	0.929	0.000	0.079	0.002	0.335	--	0.115
10%FCS/DMEM	0.010	0.820	0.064	0.007	0.022	0.011	0.996	0.115	--

Continued for Figure 19

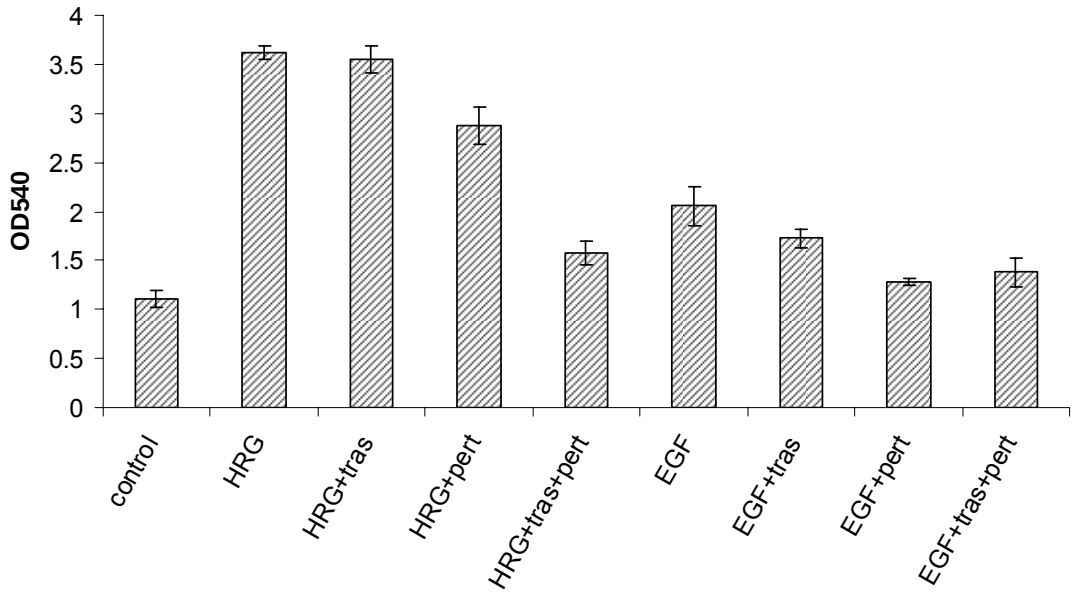

One-way ANOVA for all-group comparison (N=6, equal variances), p=0.000

Tukey HSD Post Hoc test run by SPSS 17.0

P value	control	HRG	HRG+tras	HRG+pert	HRG+tras+pert	EGF	EGF+tras	EGF+pert	EGF+tras+pert
control	--	0.000	0.000	0.000	0.000	0.000	0.000	0.352	0.016
HRG	0.000	--	0.988	0.000	0.000	0.000	0.000	0.000	0.000
HRG+tras	0.000	0.988	--	0.000	0.000	0.000	0.000	0.000	0.000
HRG+pert	0.000	0.000	0.000	--	0.000	0.000	0.000	0.000	0.000
HRG+tras+pert	0.000	0.000	0.000	0.000	--	0.000	0.554	0.007	0.203
EGF	0.000	0.000	0.000	0.000	0.000	--	0.002	0.000	0.000
EGF+tras	0.000	0.000	0.000	0.000	0.554	0.002	--	0.000	0.001
EGF+pert	0.352	0.000	0.000	0.000	0.007	0.000	0.000	--	0.905
EGF+tras+pert	0.016	0.000	0.000	0.000	0.203	0.000	0.001	0.905	--

Figure 19 Growth responses of MCF-7 cells to 17β-estradiol (E2, 1 nM & 0.1 nM), tamoxifen (Tam, 10 μM), HRG (1 nM), EGF (1 nM), 10% serum/90% medium, trastuzumab (tras, 100 nM), pertuzumab (pert, 100 nM) and their combinations. 2500 cells/well in 96-well microplates were grown in phenol-red positive DMEM supplemented with 10% FCS for 48 h followed by 48 h in phenol-red negative DMEM supplemented with 5% DCSS before incubation with the above agents for 3 days. After the treatment, cells were fixed with TCA for the SRB assay. The Optical Density (OD) was acquired at the wavelength of 540 nm. The results are shown as the average ±SD.

MCF-7/HER2-18 cell line is a HER-2 stably transfected MCF-7 cell line which over-expresses HER-2. It had the same response as MCF-7 to estrogen and tamoxifen (Figure 20). Tamoxifen also blocked the proliferative effect of 17β-estradiol. In a similar manner to MCF-7 cells, the growth of MCF-7/HER2-18 cells was stimulated by both HRG and EGF. Trastuzumab blocked the growth stimulation of EGF (EGF+trastuzumab *vs* EGF 72.0%) but not that of HRG. Pertuzumab blocked the growth effects of both EGF and HRG (HRG+pertuzumab *vs* HRG 82.5%, EGF+pertuzumab *vs* EGF 44.9%). Under the stimulation of HRG, the combination of trastuzumab and pertuzumab had a stronger inhibitory effect than pertuzumab alone (HRG+trastuzumab+pertuzumab *vs* HRG 63.7%). Under the stimulation of EGF, the combination of trastuzumab and pertuzumab had a stronger inhibitory effect than trastuzumab alone althogh not statistically significant ($p>0.05$), but a weaker effect than pertuzumab alone (EGF+trastuzumab+pertuzumab *vs* EGF 61.2%). The above results suggested that it would be interesting to study the dynamics of HER-mediated pathways under the treatment of the above growth factors.

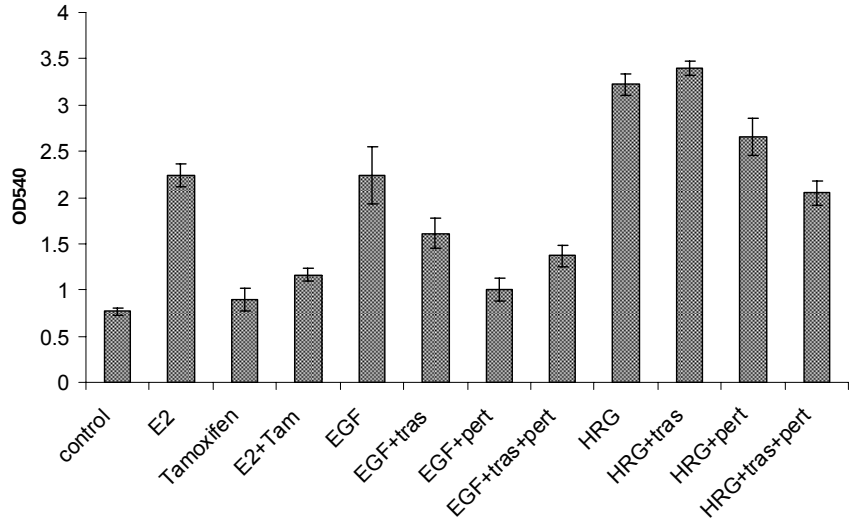

Brown-Forsythe test for all-group comparison (N=6, unequal variances), p=0.000

Games-Howell Post Hoc test run by SPSS 17.0

P value	control	E2	Tamoxifen	E2+Tam	EGF	EGF+tras	EGF+pert	EGF+tras+pert	HRG	HRG+tras	HRG+pert	HRG+tras+pert
control	--	0.000	0.475	0.000	0.001	0.001	0.077	0.000	0.000	0.000	0.000	0.000
E2	0.000	--	0.000	0.000	1.000	0.001	0.000	0.000	0.000	0.000	0.049	0.362
Tamoxifen	0.475	0.000	--	0.028	0.001	0.000	0.884	0.001	0.000	0.000	0.000	0.000
E2+Tam	0.000	0.000	0.028	--	0.005	0.009	0.371	0.117	0.000	0.000	0.000	0.000
EGF	0.001	1.000	0.001	0.005	--	0.057	0.001	0.011	0.006	0.003	0.329	0.943
EGF+tras	0.001	0.001	0.000	0.009	0.057	--	0.001	0.245	0.000	0.000	0.000	0.012
EGF+pert	0.077	0.000	0.884	0.371	0.001	0.001	--	0.012	0.000	0.000	0.000	0.000
EGF+tras+pert	0.000	0.000	0.001	0.117	0.011	0.245	0.012	--	0.000	0.000	0.000	0.000
HRG	0.000	0.000	0.000	0.000	0.006	0.000	0.000	0.000	--	0.268	0.008	0.000
HRG+tras	0.000	0.000	0.000	0.000	0.003	0.000	0.000	0.000	0.268	--	0.002	0.000
HRG+pert	0.000	0.049	0.000	0.000	0.329	0.000	0.000	0.000	0.008	0.002	--	0.005
HRG+tras+pert	0.000	0.362	0.000	0.000	0.943	0.012	0.000	0.000	0.000	0.000	0.005	--

Figure 20 Growth responses of MCF-7/HER2-18 cells to 17β-estradiol (E2, 1nM), tamoxifen (Tam, 1μM), HRG (1nM), EGF (1nM), trastuzumab (tras, 100nM), pertuzumab (pert, 100nM) and their combinations. 6000 cells/well in 96-well microplates were grown in phenol-red positive DMEM supplemented with 10% FCS for 48 h followed by 48 h in phenol-red negative DMEM supplemented with 5% DCSS before incubation with the above agents for 5 days. After the treatment, cells were fixed with TCA for the SRB assay. The Optical Density (OD) was acquired at the wavelength of 540 nm. The results are shown as the average ±SD.

4.1.2 Observation of signalling oscillation and experimental confirmation

Signalling oscillation is a very common phenomenon in biological systems occurring in a wide spectrum of organisms from bacteria to humans (264). It is often observed in relation to the biological clock, e.g. circadian rhythm, somite segmentation (265) and cell division (243). However, experimentally induced oscillation with minutes of periodicity in the components of HER-mediated signalling pathways has not been demonstrated prior to the start of these studies.

In initial studies, I observed oscillations of the expression levels of both p-Akt (S^{473}) and p-ERK1/2(T^{202}/Y^{204}) in MCF-7 cells stimulated by either HRG or EGF. Oscillation of p-ERK1/2 level across time was previously predicted by computational modelling (235, 250, 252). Treatment of MCF-7 cells with 1nM HRG or 1nM EGF produced oscillation of both p-Akt and p-ERK1/2 expression over a 2h time course (Figure 21). Cycling periodicity was around 20 min for p-ERK1/2 and 30 min for p-Akt. These results were confirmed in 5 further repeat experiments with cell lysates from independent experiments by Western Blotting. To attempt to minimise the possibility of artefactual differences, samples were randomised on the Western blots. The oscillation of both p-Akt and p-ERK1/2 was also observed in MCF-7/HER2-18 cells stimulated by 1nM HRG (Figure 22). However, the oscillation wasn't observed in BT474 cells stimulated by 1nM HRG which is also a HER-2 amplified and over-expressing cell line (Figure 23).

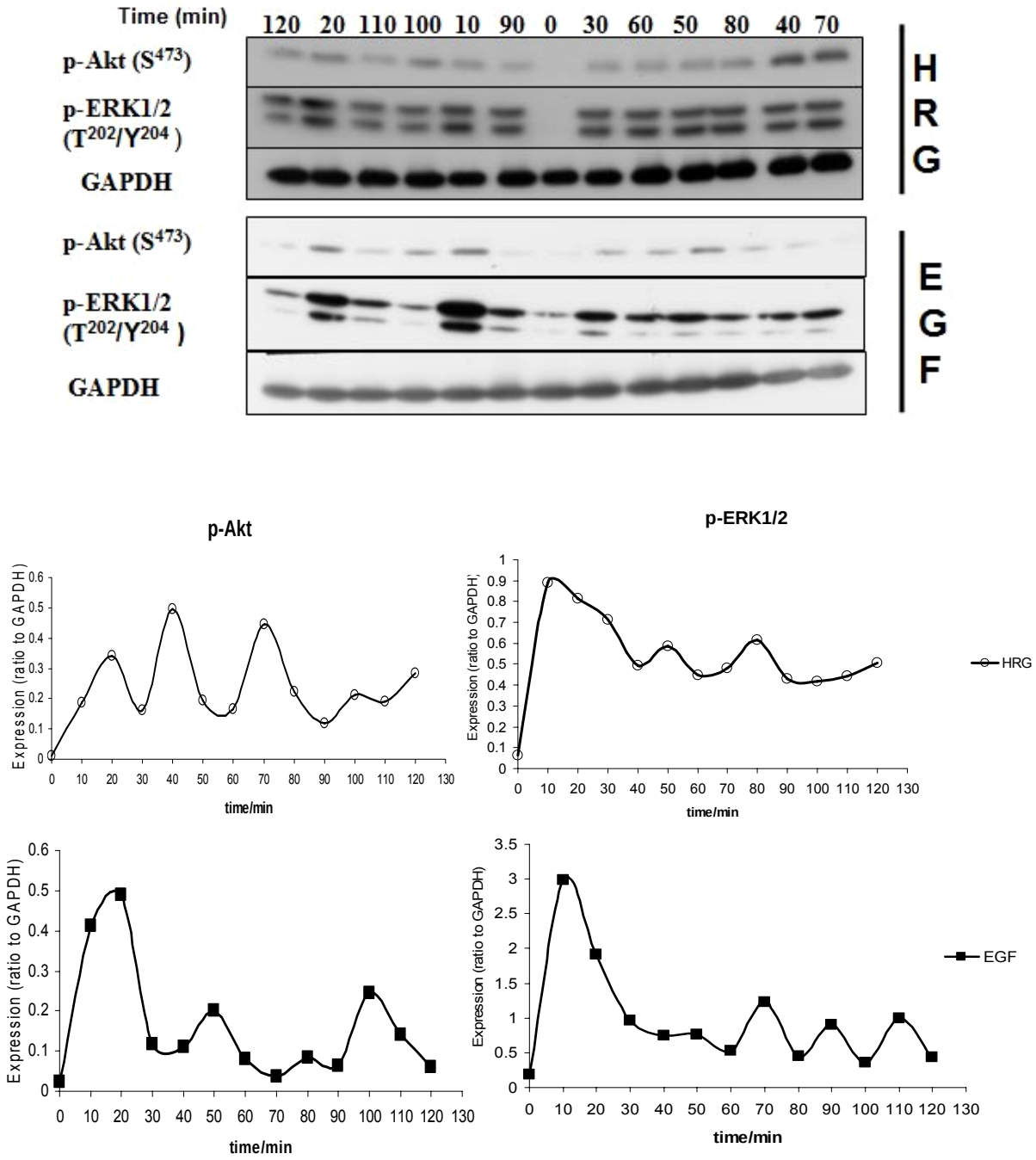

Figure 21 Oscillation across the time course indicated in the expression levels of p-Akt (S^{473}) and p-ERK1/2 (T^{202}/Y^{204}) induced by the stimulation of either HRG (1nM) or EGF (1nM) in MCF-7 cells. In the Western blot, samples were loaded in a random sequence when resolved by SDS-PAGE in order to remove potential artefactual edge effects. The targets were detected with ECL in a dark room. Results are indicated as the ratio of the optical density (OD) of phospho-targets to that of GAPDH.

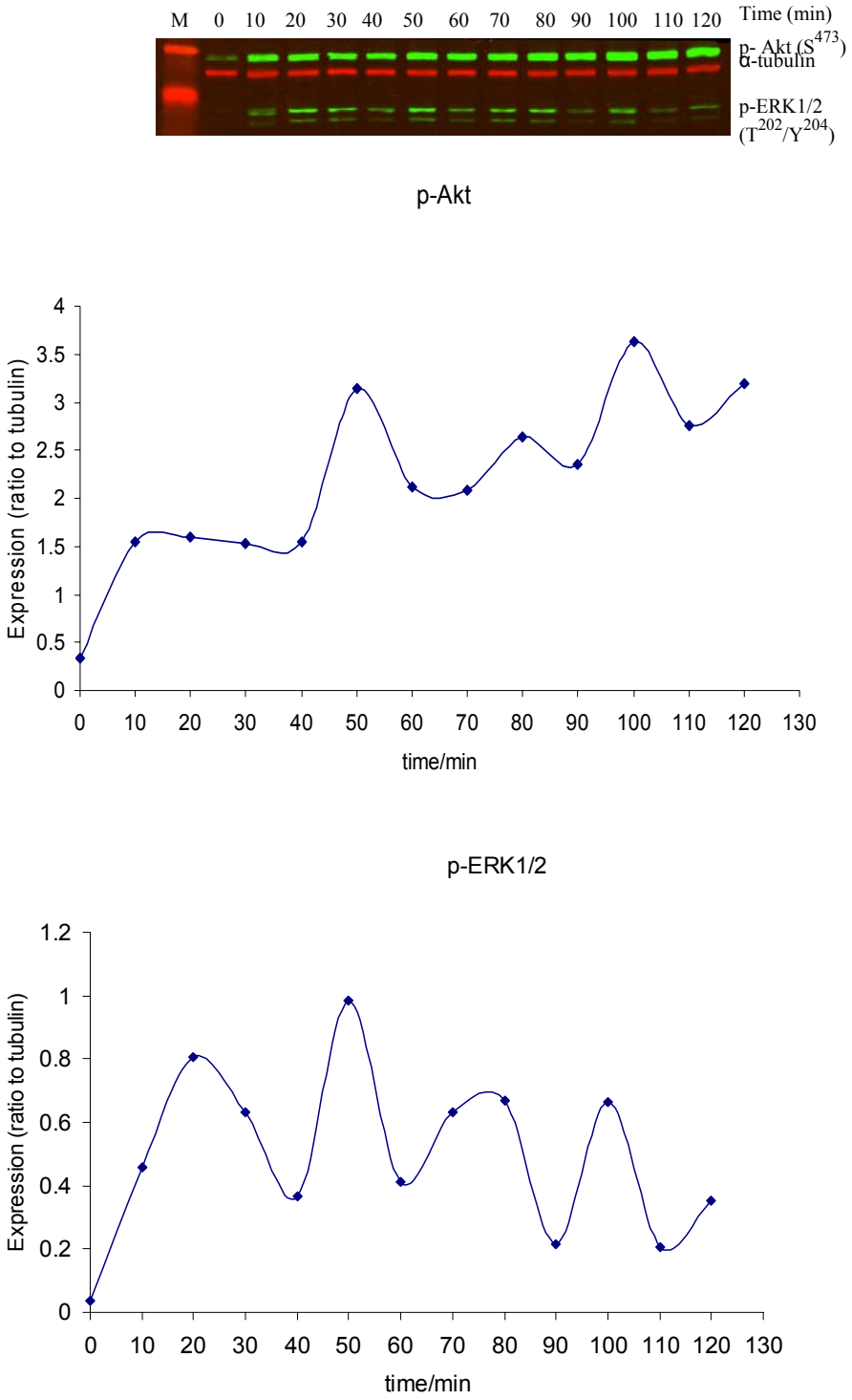

Figure 22 Effects of HER-2 over-expression on the oscillation of p-Akt and p-ERK1/2 expression. Time-course oscillatory profiles of p-Akt (S^{473}) and p-ERK1/2 (T^{202}/Y^{204}) in MCF-7/HER2-18 cells stimulated by HRG (1nM) for the time period as indicated. The targets were detected with the LI-COR infrared imaging system. 'M' denotes protein marker. Results are indicated as the ratio of the OD of phospho-targets to that of α-tubulin.

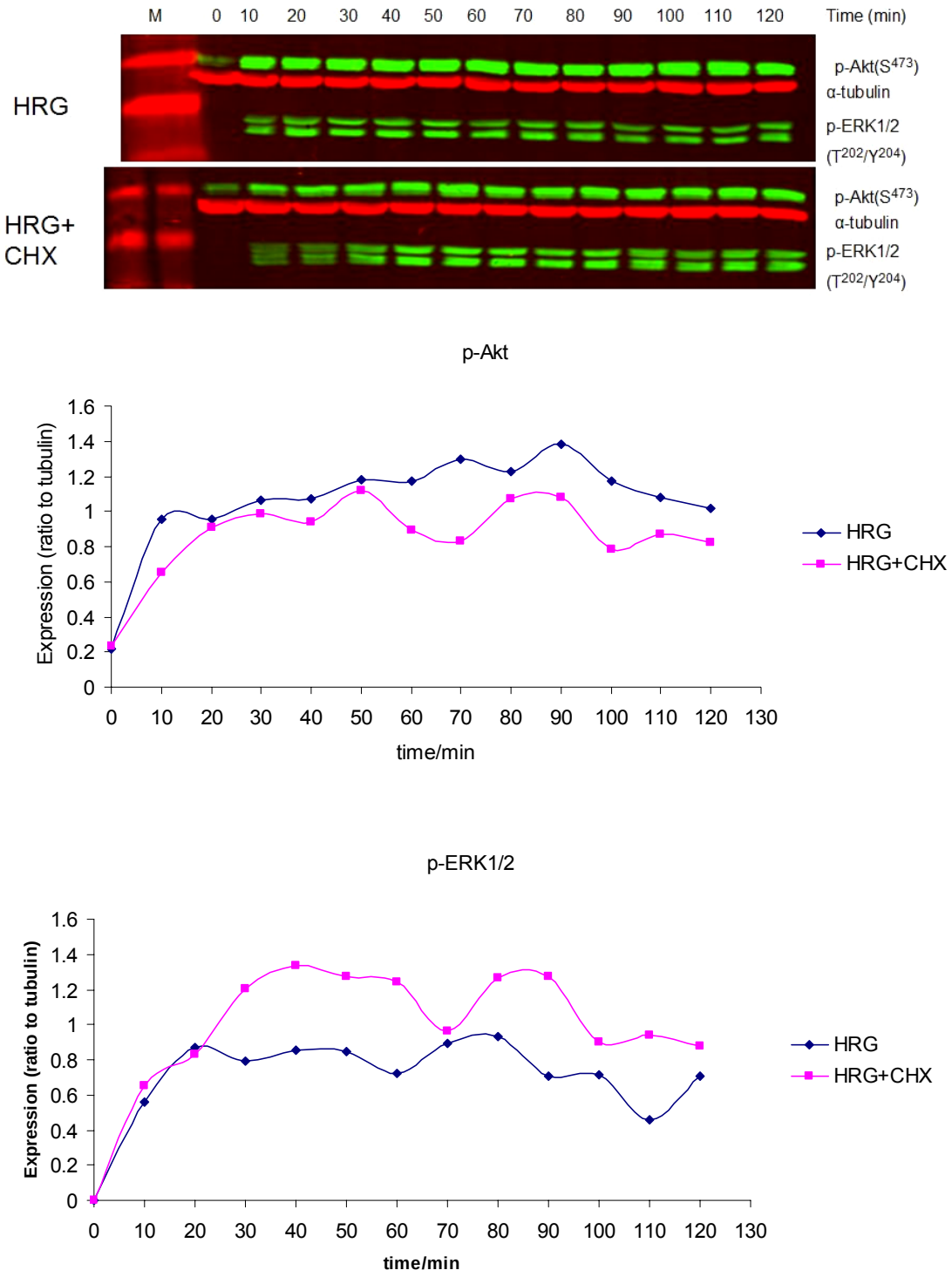

Figure 23 Time course profile of p-Akt (S^{473}) and p-ERK1/2 (T^{202}/Y^{204}) induced by the stimulation of HRG (1nM) with or without cycloheximide (CHX, 10μM) in BT474 cells. The targets were detected with LI-COR infrared imaging system. 'M' denotes protein marker. Results are indicated as the ratio of the OD of phospho-targets to that of α-tubulin.

4.1.3 Transcriptional feedback further modulated the oscillation

In MCF-7 cells stimulated by either 1 nM EGF or 1 nM HRG, the levels of both p-Akt and p-ERK1/2 demonstrated cycling. In the presence of the protein synthesis inhibitor 10 μM cycloheximide (CHX), the higher level of p-Akt and p-ERK1/2 initially produced oscillation with greater *y*-axial distance between peaks and troughs with sustained periodicity (Figure 24). These results were further confirmed by the use of the RPPA high throughput quantification method (Figure 25). The observation of p-Akt oscillation is novel since there is no computational model prediction yet or published experimental observation for the p-Akt oscillation prior to these results. The oscillation elicited by EGF dampened across this 2h time course while sustained by HRG. The clear peaks and troughs of oscillation caused by CHX suggested a contribution of transcriptional feedback in the modulation of oscillation. The expression level of p-Akt was increased by CHX initially at an early (10-20 min) time point. The increase of the expression level of p-ERK1/2 produced by CHX commenced between the 20- and 30-min points. This suggested that the transcriptional feedback modulated the oscillation at a very early time. However, there was minimal oscillation observed in BT474 cells regardless of CHX (Figure 23).

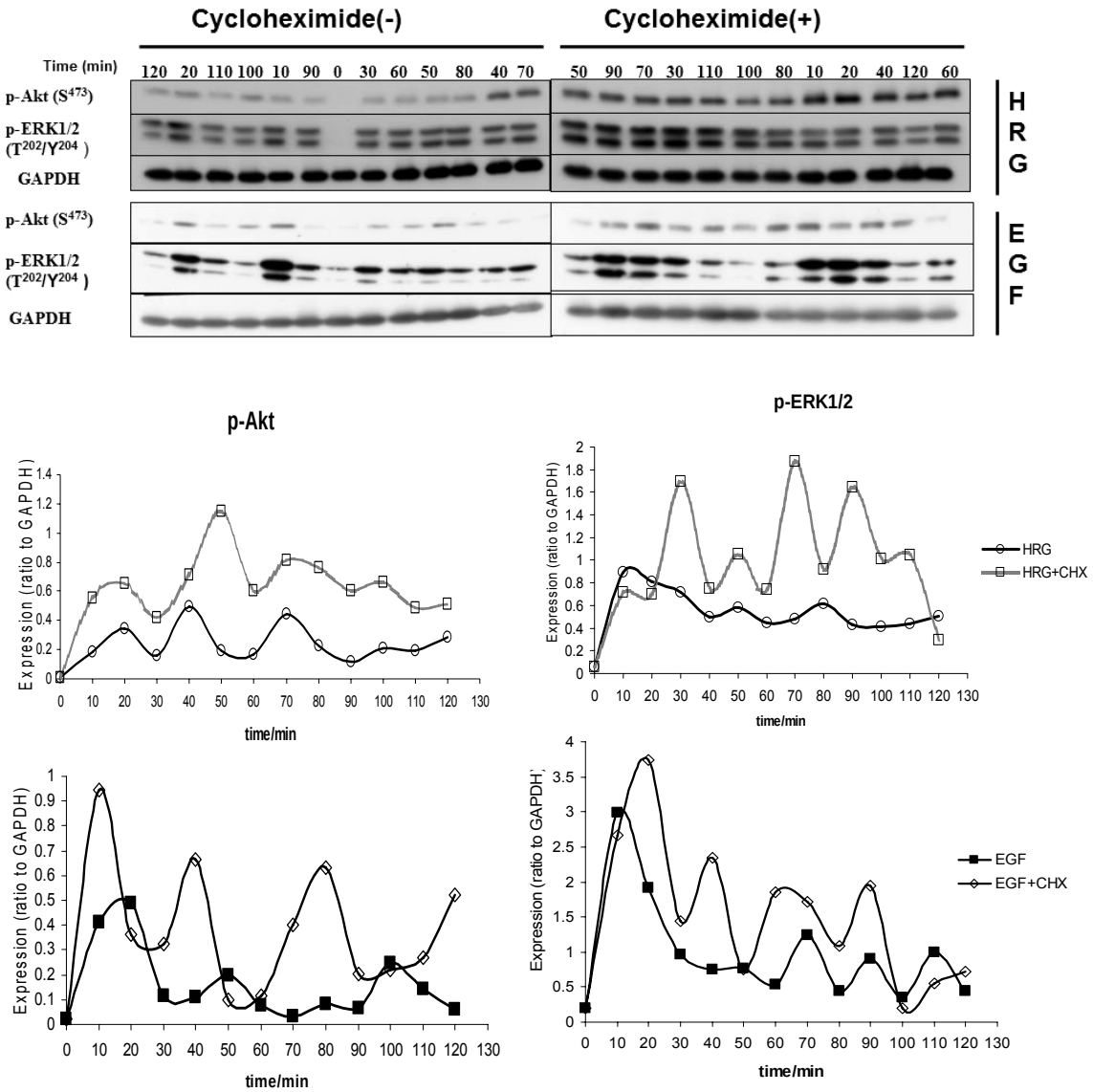

Figure 24 Oscillation in the levels of p-Akt (S^{473}) and p-ERK1/2 (T^{202}/Y^{204}) induced by the stimulation of either HRG (1nM) or EGF (1nM) with or without CHX (10μM) in MCF-7 cells. In the Western blot, samples were loaded randomly when resolved by SDS-PAGE in order to remove the edge effects. The targets were detected with ECL in a dark room. Results are indicated by the ratio of the OD of phospho-targets to that of GAPDH.

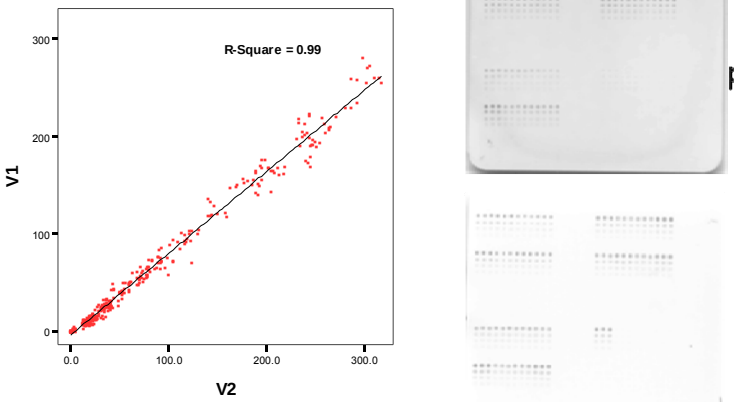

Correlations

		V1	V2
V1	Pearson Correlation	1	.994**
	Sig. (2-tailed)		.000
	N	335	335
V2	Pearson Correlation	.994**	1
	Sig. (2-tailed)	.000	
	N	335	335

**. Correlation is significant at the 0.01 level

A. High reproducibility between slides

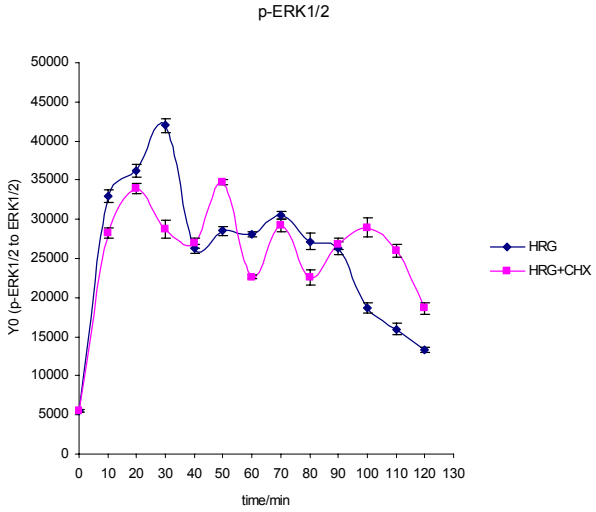

B. Normalized p-ERK1/2 time course profile

Figure 25 Oscillatory level of p-ERK1/2 (T^{202}/Y^{204}) was also observed by RPPA. MCF-7 cells were stimulated with HRG (1nM) with or without CHX (10μM) for the time course indicated. **A**, high reproducibility was observed between two slides printed at the same time with the robotics. This allows the level of p-ERK1/2 observed from one slide to be normalised against the level of ERK1/2 observed from another slide. **B**, Normalised p-ERK1/2 time course profile. Data were analyzed with Microvigene RPPA modules. The dilution curve intensity (Y0) of p-ERK1/2 was normalized to that of total ERK1/2. Results were shown as the normalized Y0. Error bars show the 95% confidence interval.

Interestingly, the phosphorylation profile of MEK1/2 (the upstream activator of ERK1/2) over the whole time course differed from that of ERK1/2 (Figure 26). There were three appreciable cycles with a periodicity of between 20-30 min within the whole time course under the stimulation of 1nM HRG alone. The addition of CHX caused the periodicity to double and two minimal cycles were observed within the whole time course. After the level of p-MEK1/2 reached the second peak (the 70-min point), the level of p-MEK1/2 commenced decreasing until the 90-min point when the level increased again. The level of p-MEK1/2 was sustained after treatment for 110 min with HRG plus CHX within this time course. The addition of CHX caused a longer duration of p-MEK1/2 signalling.

It was interesting that 1nM HRG induced the oscillation of p-HER-3 (Y^{1289}) in MCF-7 cells with 2 cycles within 2 h (Figure 27). The phosphorylation of HER-3 at Y^{1289} was induced by HRG and the level of p-HER-3 (Y^{1289}) was increased to the first peak at the 30-min point. After treatment with HRG for 30 min, the level of p-HER-3 (Y^{1289}) kept decreasing for 30 min. The first complete cycle was observed up to this time point. Subsequently, the phosphorylation level increased to a second peak after treatment with HRG for 80 min. After the 80-min point the level of p-HER-3 (Y^{1289}) was decreased with two different rates till the end of the time course. The first rate is higher (until the 90-min point) than the second one (from the 90-min point to the end). The level of p-HER-3 (Y^{1289}) expression during the whole time course was reduced by the addition of CHX. In the presence of CHX, it reached a peak when cells were stimulated by HRG for 10 min.

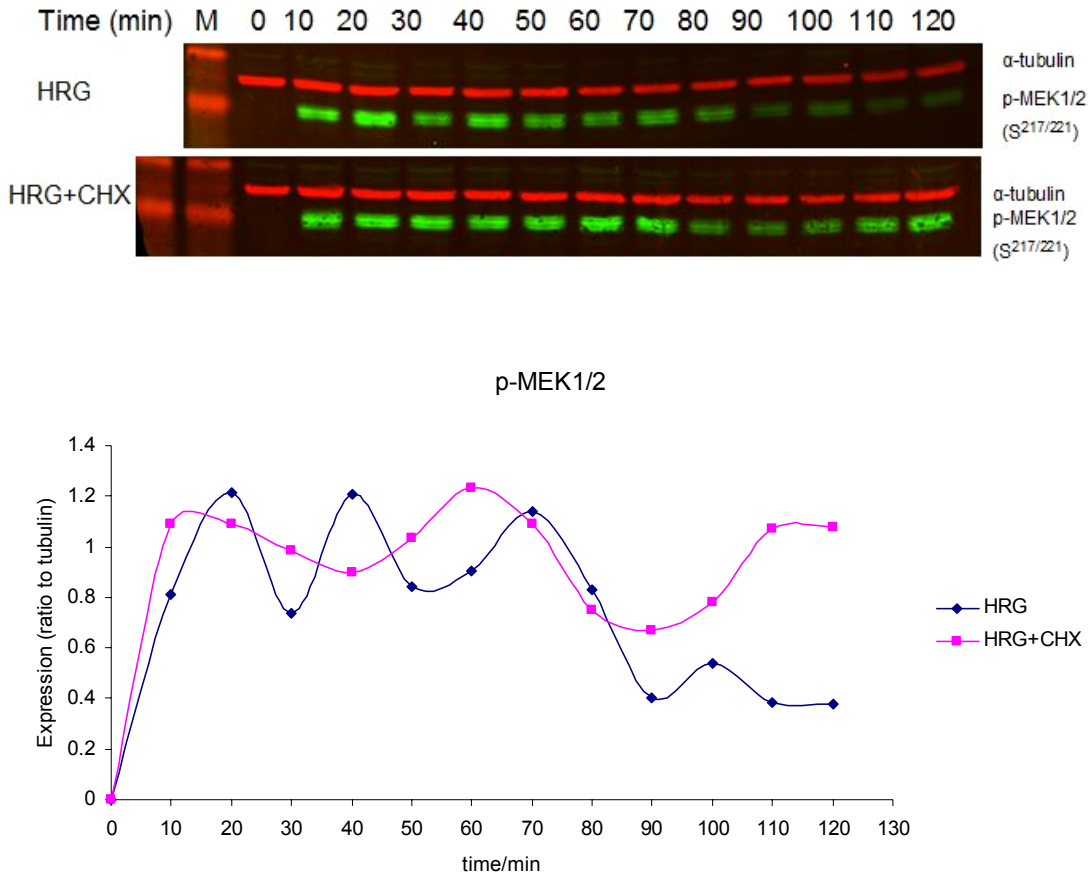

Figure 26 Expression profile of p-MEK1/2 ($S^{217/221}$) within the whole time course in MCF-7 cells stimulated by 1nM HRG plus/minus CHX. MCF-7 cells were incubated with 10 μM CHX for 20 min prior to the treatment of 1nM HRG for the time course indicated. Lysates were resolved with SDS-PAGE and analysed with Western Blotting. 'M' denotes protein marker. Results are demonstrated as the ratio of OD of p-MEK1/2 ($S^{217/221}$) to that of α-tubulin.

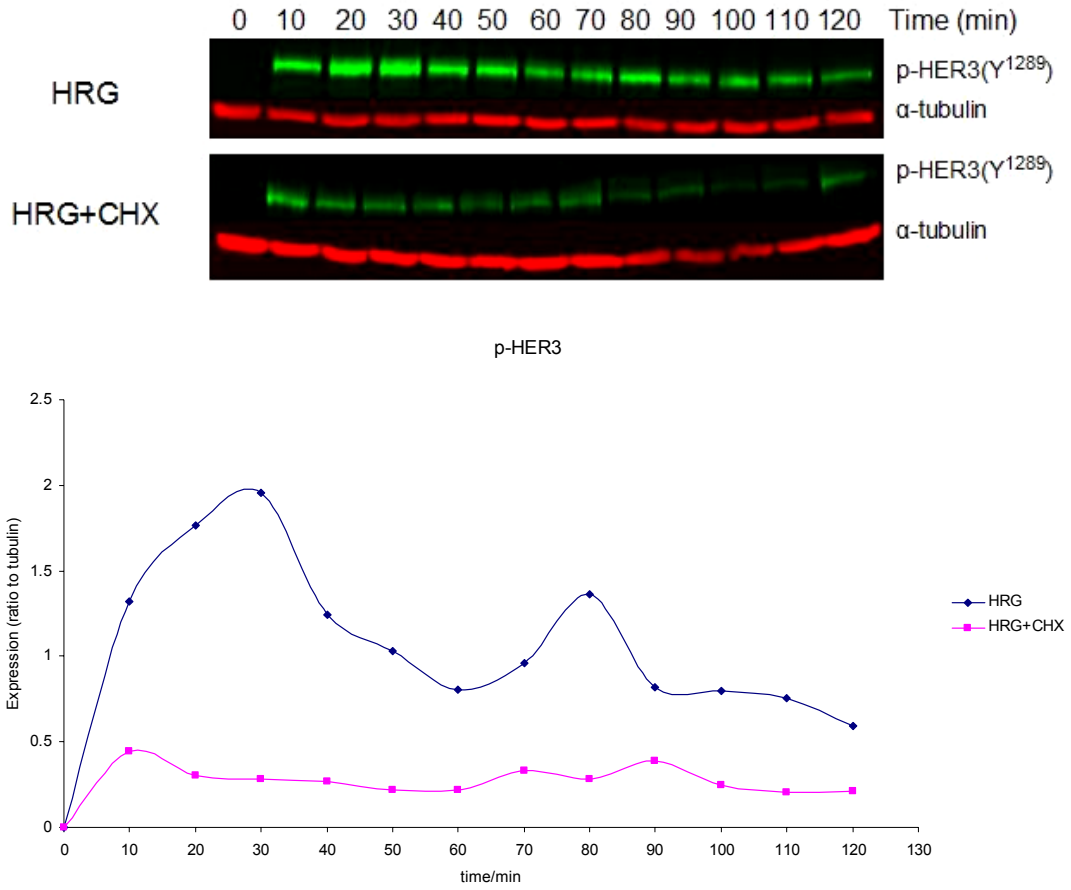

Figure 27 Expression profile of p-HER-3 (Y^{1289}) within the 2h time course in MCF-7 cells stimulated by 1nM of HRG plus/minus CHX. MCF-7 cells were incubated with 10μM CHX for 20 min prior to the treatment of 1nM HRG for the time course indicated. Lysates were resolved by SDS-PAGE and analysed by Western Blot. Results are demonstrated as the ratio of OD of p-HER-3 (Y^{1289}) to that of α-tubulin.

Since the generation of oscillation requires the involvement of negative feedback in ERK1/2 cascades and a simple negative feedback loop of interactive genes or proteins has the potential to generate a sustained oscillation (235, 247, 249, 266), the transcriptional feedback could result from dual specificity phosphatases (DUSPs) which inactivate MAPKs through dephosphorylating phospho-threonine, phospho-serine or phospho-tyrosine residues. In order to identify possible candidates that may modulate oscillation, gene expression analysis was conducted. Gene candidates were selected from the top 100 genes whose expression was induced significantly ($p<0.05$) after treatment for 20 min with HRG (Table S1 in the Supplement). Those 100 genes were selected according to the following criteria. The whole gene list of the array was sorted by fold-change (highest to lowest, 20'HRG *vs* control). The top 100 genes with p value less than 0.05 were selected. These 100 genes were put into DAVID Bioinformatics Resources 6.7 (267, 268) for functional annotation clustering; 9 genes were found to be involved in MAPK signalling pathway within the KEGG_PATHWAY database. These genes are: DDIT3, DUSP1, DUSP2, DUSP4, DUSP5, JUN, SRF, FOS and MYC. Since the DUSP family can dephosphorylate p-ERK1/2, this family was selected as candidate genes which might regulate oscillation of p-ERK1/2. DDIT3, JUN, SRF, FOS and MYC act as early transcription factors, which might regulate the production of feedback loops.

Takeshi Nagashima et al in 2007 (91) published a list of early transcription products (Table S2 in the Supplement) which might modulate the HER signalling pathways through positive and negative feedback loops. Nineteen out of 100 genes in the gene candidate pool (Table S1 in the Supplement) overlapped with the gene list proposed by Takeshi Nagashima et al (Table S2 in the Supplement). These genes are identified in blue in tables S1 and S2. Among the 19 genes, DUSP1, DUSP2, DUSP4, DUSP5, JUN, SRF, FOS and MYC identified above to be involved in MAPK signalling are also included. In addition to the 19 overlapping genes, 6 other genes proposed by Nagashima were also modulated significantly by HRG in this study (Table S3 in the Supplement). Among the 6 genes, AKAP9 and PPP1R3C were down regulated, which was consistent with Nagashima's report. AKAP9 and PPP1R3C as well as PPP1R15A encode regulatory subunits of serine/threonine protein phosphatase

1(PP1) which promotes the dephosphorylation of HER activated Akt (269). AKAP9 is also called CG-NAP (centrosome and Golgi localized PKN-associated protein) and encodes the protein that can interact with and promote PP1 activity (270). PPP1R3C is also called PPP1R5 (protein phosphatase 1 regulatory subunit 5) or PTG (protein targeting to glycogen) and encodes the glycogen-targeting subunit of PP1, which can increase PP1 activity (271). PPP1R15A, also called GADD34 (growth arrest and DNA-damage-inducible 34), can also promote PP1 activity (272). PPP1R15A was up-regulated by HRG in this study. So, the phosphatase activity of PP1 may be regulated by HRG negatively through down regulation of AKAP9 and PPP1R3C and positively through up-regulation of PPP1R15A. The expression levels of p-Akt were regulated indirectly by AKAP9, PPP1R3C and PPP1R15A.

HRG also induced genes of several autocrine growth factors (AREG, HB-EGF and VEGFA). AREG codes for the protein called amphiregulin which is a specific ligand of HER-1 and HB-EGF codes for heparin-binding EGF-like growth factor which is a specific ligand for HER-1 or HER-4 (Introduction section 1.7.1). VEGFA codes for vascular endothelial growth factor A. Guo et al (273) observed that VEGF could promote tyrosine phosphorylation of SH2 domain containing signalling mediators such as PI3K and Ras GTPase activating protein (GAP). The product of SPRED2 has been shown to inhibit ERK1/2 signalling through negatively regulating Raf activity (274). In addition to the genes mentioned above, CYR61, CTGF and RASD1 were also investigated due to their dramatic induction compared to other genes in the 100-gene pool (above 10-fold change, 20'HRG *vs* control). Gene products of CYR61 and CTGF can modulate the ERK1/2 and Akt pathways through binding of alphav-beta3 integrin (275-277) which is reported to be involved in the activation of the HER-mediated pathway (278, 279). So CYR61 and CTGF were selected as candidates.

Those genes (29 in total) whose products might regulate the dynamics of HER-mediated signalling are listed in Table 4. Time course profiles of individual genes are shown in Figure S1 in the Supplement. Among the 29 candidate genes, only AKAP9 and PPP1R3C were down regulated and all the other genes were induced significantly by HRG. These genes might regulate HER-mediated signalling at three

primary levels. The first level is the activation of HER receptors by autocrine growth factors. The second level is the regulation of signalling molecules such as Raf, ERK1/2 and Akt. The third level is transcriptional regulation.

Table 4 Twenty nine gene candidates which might regulate HER-mediated signalling dynamics ($p<0.05$, 20'HRG *vs* control, Student's t-test)

Genes	Description	Change fold	Functions
AKAP9	A kinase (PRKA) anchor protein (yotiao) 9	-1.10302	PP1 regulatory subunits to promote dephosphorylation of p-Akt
PPP1R3C	protein phosphatase 1, regulatory subunit 3C	-1.23493	
PPP1R15A	protein phosphatase 1, regulatory subunit 15A	2.07285	
AREG	amphiregulin	1.16968	Autocrine growth factors or stimulators to activate HER-mediated signalling
CTGF	connective tissue growth factor	19.8639	
CYR61	cysteine-rich, angiogenic inducer, 61	11.0838	
HBEGF	heparin-binding EGF-like growth factor	1.15978	
VEGFA	vascular endothelial growth factor A	1.11145	
DUSP1	dual specificity phosphatase 1	3.45639	ERK1/2 pathway regulators
DUSP2	dual specificity phosphatase 2	1.96664	
DUSP4	dual specificity phosphatase 4	1.29122	
DUSP5	dual specificity phosphatase 5	2.00690	
SPRED2	sprouty-related, EVH1 domain containing 2	1.16878	
ATF3	activating transcription factor 3	1.84061	Transcription regulation induced by HER-mediated signalling
BHLHB2	basic helix-loop-helix domain containing, class B, 2	1.31653	
DDIT3	DNA-damage-inducible transcript 3	1.56236	
EGR1	Early growth response 1	7.80240	
EGR2	Early growth response 2	12.66171	
EGR3	Early growth response 3	2.26183	
EGR4	Early growth response 4	2.81039	
FOS	v-fos FBJ murine osteosarcoma viral oncogene homolog	18.0963	
JUN	jun oncogene	6.62094	
KLF10	Kruppel-like factor 10	1.31216	
KLF2	Kruppel-like factor 2	5.90560	
KLF6	Kruppel-like factor 6	2.21098	
MYC	v-myc myelocytomatosis viral oncogene homolog (avian)	1.48810	
NR4A2	nuclear receptor subfamily 4, group A, member 2	1.27107	
NR4A3	nuclear receptor subfamily 4, group A, member 3	3.73471	
SRF	serum response factor (c-fos serum response element-binding transcription factor)	1.72515	

Since protein synthesis inhibitors and transcriptional inhibitors can both block the *de novo* protein production, I expected CHX and actinomycin D (a transcriptional inhibitor) would have the same effects on the oscillation, but it was not true (Figure 28). Actinomycin D decreased the signal amplitude of p-Akt and p-ERK1/2 induced by HRG rather than increased as CHX did. However, it made the level of both p-Akt and p-ERK1/2 more sustained than HRG alone did. Clear cycles of the level of p-ERK1/2 across the time course were generated in the presence of actinomycin D with longer-than-20-min periodicity. It may be that CHX and actinomycin D affect the signalling pathways with different mechanisms apart from the protein synthesis inhibition.

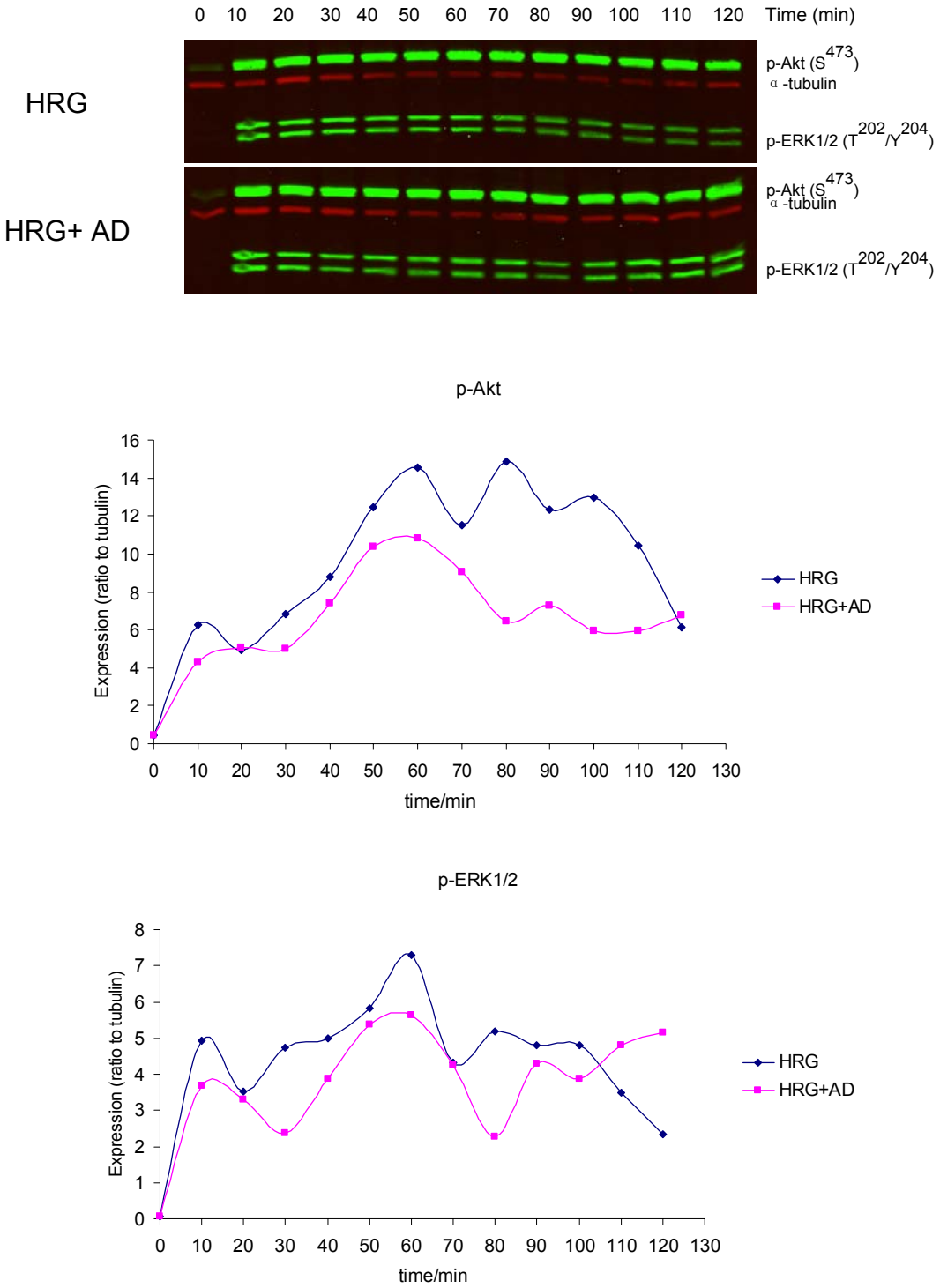

Figure 28 Effects of actinomycin D on the time course profile of p-Akt (S^{473}) and p-ERK/12 (T^{202}/Y^{204}) in MCF-7 cells. MCF-7 cells were incubated with 2 μg/ml of Actinomycin D for 20 min prior to the treatment of 1nM HRG for the time course indicated. Lysates were resolved by SDS-PAGE and analysed by Western Blot. Results are demonstrated as the ratio of OD of phospho-targets to that of α-tubulin.

4.1.4 HER-2 over-expression induces oscillation in a cell line dependent manner

It was observed that positive feedforward signalling also played a role in the modulation of oscillation. Similar to observations in MCF-7 cells in the presence of CHX, levels of both p-Akt and p-ERK1/2 expression oscillated with a periodicity of roughly 20 min in HER-2-overexpressing MCF-7/HER2-18 cells stimulated by HRG alone (Figure 22). It was interesting that 1nM HRG alone induced an oscillation of p-ERK1/2 expression level with clearer peaks and troughs than it did in MCF-7, suggesting that the over-expression of HER-2 played a key role in the modulation of oscillation in MCF-7/HER2-18.

However, no detectable oscillation was observed in BT474 cells stimulated by HRG either in the presence or absence of CHX (Figure 23). The p-Akt level was reduced by CHX rather than increased. These results suggest that oscillation is cell line or intrinsically cellular signalling network dependent. Since BT474 is a HER-2 amplified and over-expressing cell line, HER-2's effects on the oscillation as aforementioned on MCF-7/HER2-18 cells were cell line dependent.

4.1.5 Role of crosstalk with the PI3K/Akt pathway in the modulation of oscillation of p-ERK1/2

In addition to transcriptional feedback and HER-2 over-expression, the crosstalk between the PI3K/Akt and Raf/MEK1/2/ERK1/2 pathways also influenced the oscillation. It has been demonstrated that p-Akt inhibits the Raf/MEK1/2/ERK1/2 pathway through phosphorylation of c-Raf at S^{259} (280, 281). In this study, I confirmed not only that this crosstalk was present but also observed its role in oscillation. When MCF-7 cells were treated with 5μM LY294002, an inhibitor of Akt phosphorylation, for 20 min prior to HRG stimulation, the oscillation of p-ERK1/2 came to have clear peaks as well as troughs and the amplitude became higher than that caused by 1nM HRG alone (Figure 29), which demonstrated the effect of pathway crosstalk on oscillation. However, the oscillation pattern caused by LY294002 which caused a decaying periodicity was different from that produced by

CHX (Figure 24). Distinct from the one caused by HRG or HRG+CHX which had a constant periodicity of 20 min, the oscillation of p-ERK1/2 produced by HRG plus LY294002 had two different lengths of periodicity: the first cycle was 80 min and the second one was 20 min.

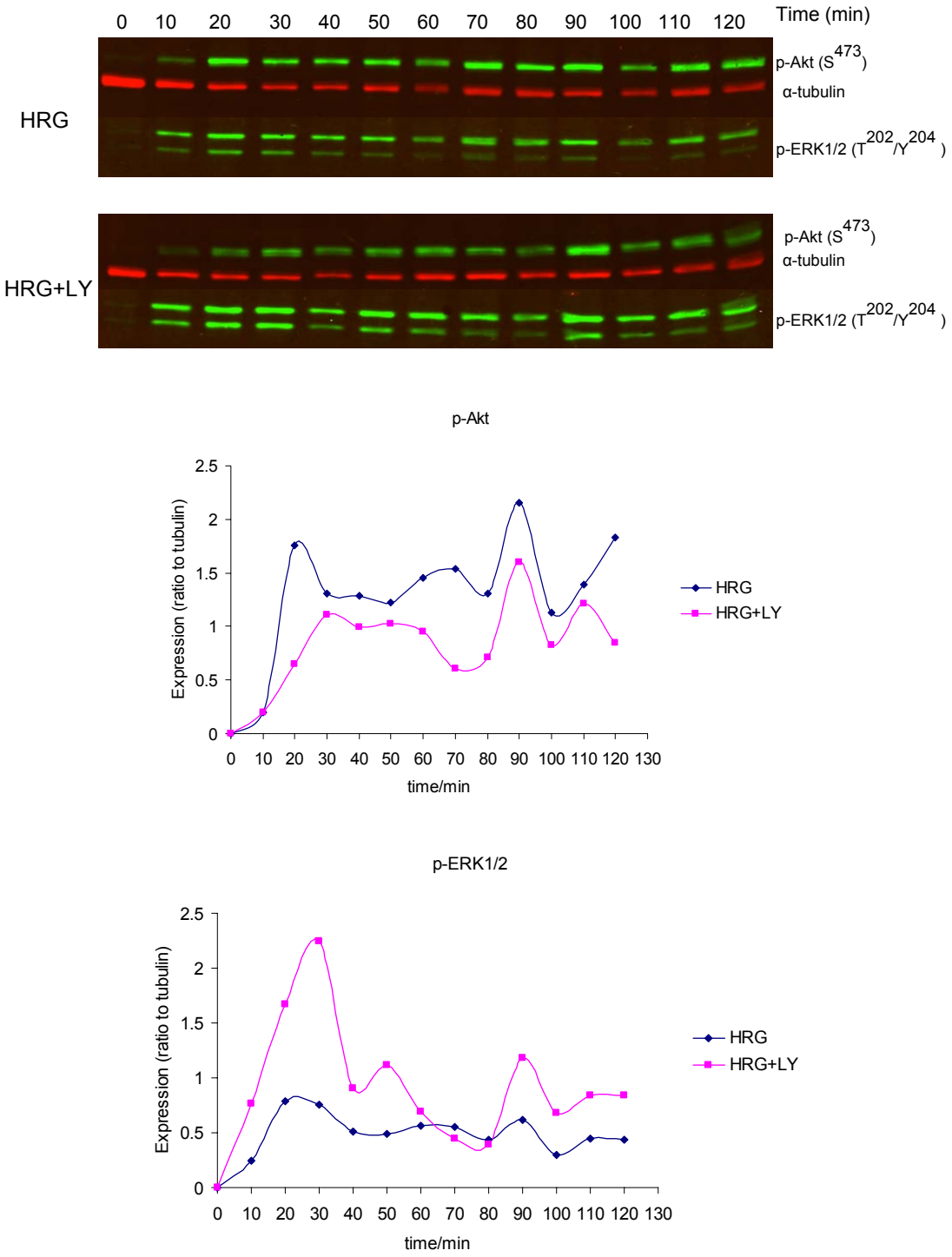

Figure 29 Effects of crosstalk with PI3K/Akt pathway on oscillation of the level of p-ERK1/2 (T^{202}/Y^{204}) in MCF-7 cells. MCF-7 cells were stimulated with HRG (1nM) for the time indicated in either the presence or absence of LY294002 (5μM). The targets were detected with the LI-COR infrared imaging system. Results are indicated as the ratio of the OD of phospho-targets to that α-tubulin.

4.1.6 Effects of EGF concentration on the oscillation

To assess how the oscillation was regulated by the concentration of the stimulus, MCF-7 cells were treated for the time course indicated in Figure 30 with 0.1, 1 and 10 nM EGF respectively in the presence of 10 μM CHX. p-Akt expression level oscillated throughout the 90-min time course with 2 cycles in a similar pattern after stimulation with any of the three concentrations. 0.1 nM EGF induced the highest first peak at the 10-min point, but the highest peak of the second cycle was produced by 10 nM EGF. It was very interesting that 1 nM EGF induced the lowest level of p-Akt expression across the whole time course. Moreover, the second cycle had a much longer cycling time than the first. The first cycle was roughly 20 min and the second one roughly 60 min.

The level of p-ERK1/2 expression had a clear oscillation after stimulation with 1 nM EGF and cycled four times across the whole time course with a periodicity of approximately 20 min. The oscillation of p-ERK1/2 expression induced by 10 nM EGF was much weaker. However, there was no oscillation observed through the whole time course stimulated by 0.1 nM EGF and the signal was delayed to around the 60-min point where there was a single peak. Thereafter, the signal of p-ERK1/2 came down to the base line. These results demonstrated that the oscillation was regulated by the concentration of EGF through variation in amplitude, the signal timing and the cycling periodicity.

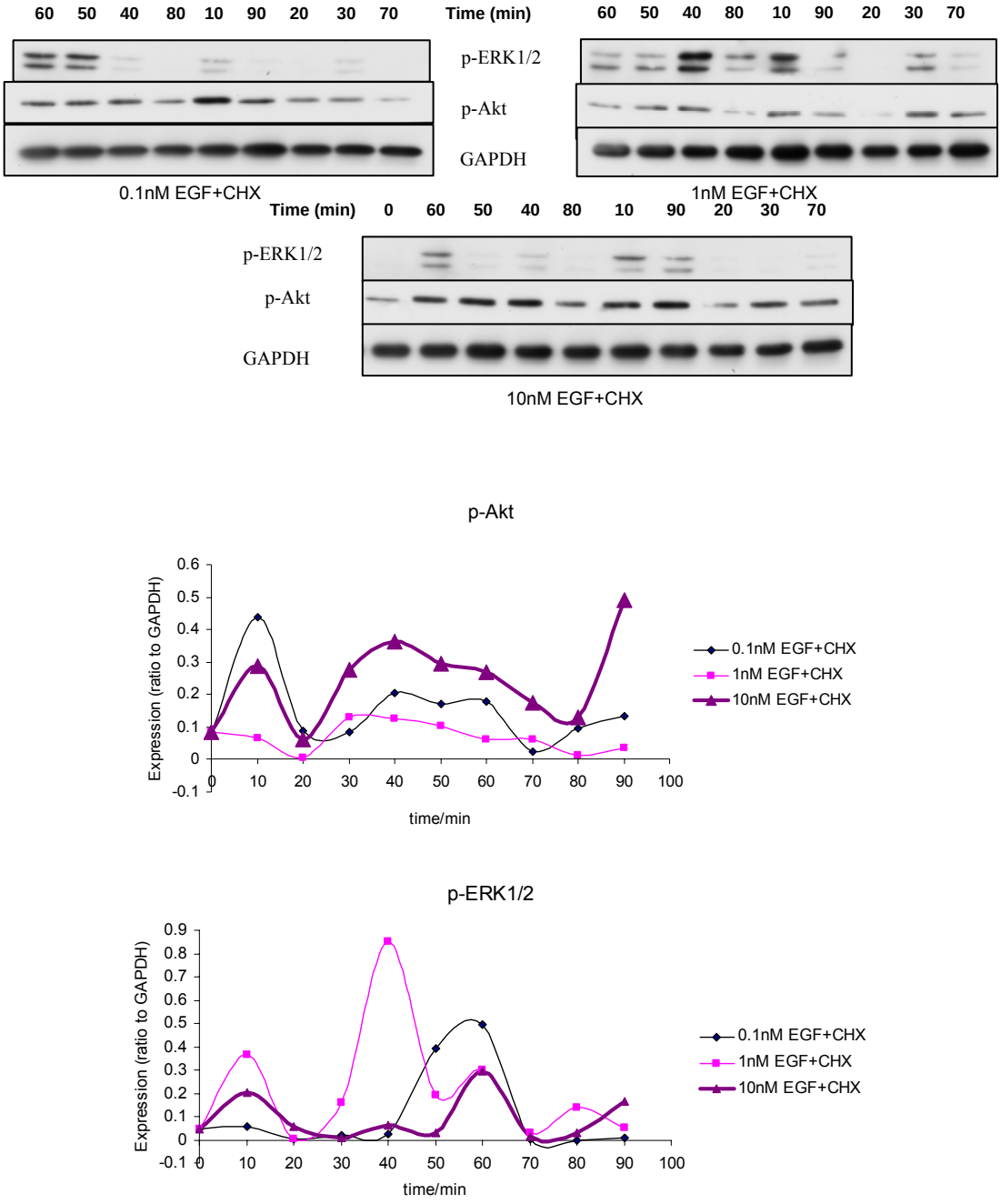

Figure 30 Effects of EGF concentration in the presence of CHX on the oscillatory level of p-Akt (S^{473}) and p-ERK1/2 (T^{202}/Y^{204}) expression in MCF-7 cells. MCF-7 cells were incubated with 10 μM CHX for 20 min prior to the treatment of concentrations (0.1, 1 and 10 nM) of EGF for the time course indicated (90 min in total). Samples were collected at each time point and subjected to western blot. Samples were randomly loaded into the gel for the avoiding of edge effects and the x-ray films were developed in the dark room. The results are shown as the ratio of the OD of p-Akt or p-ERK1/2 to that of GAPDH, which was used as a loading control.

4.1.7 Serum deprivation affected the generation of oscillation

The oscillation mentioned above was observed in cells which were incubated in DMEM supplemented with 10% FCS for 48 h and then incubated in phenol red-free DMEM supplemented with 5% DCSS for another 48 h before drug treatment. When MCF-7 cells were grown in DMEM supplemented with 10% FCS for 48 h and starved in phenol red-free DMEM supplemented with no serum for 20 h, no significant oscillation was observed regardless of the addition of CHX (Figure 31). The level of p-Akt expression increased after stimulation with HRG alone to a peak at the 40-min point and then came down at the 70-min point. The level of p-Akt expression was sustained from the 70-min point until the end of the time course. The phosphorylation of ERK1/2 was stimulated by HRG alone. The level of p-ERK1/2 expression increased to a peak at the 40-min point and then was reduced until the 60-min point after which the level remained constant until the 100-min point. The level of p-ERK1/2 expression then kept decreasing until the end of the time course. In the presence of CHX, the level of p-Akt expression was increased to a high level at the 20-min point and then came down until the 30-min point. After 30 min the level of p-Akt expression was increased again to the highest level at the 40-min point. Afterwards, the expression level was decreased until the 60-min point and then sustained until the end of the time course. The phosphorylation of ERK1/2 was induced very quickly by HRG in the presence of CHX. It reached the highest level after 10 min of induction. The level of p-ERK1/2 expression then came down for 20 min until the 30-min point. After the 30-min point, the level went up again to the second highest level between the 40-min and 50-min points. Afterwards, the level of p-ERK1/2 expression dampened until the 70-min point and then remained constant until the end of the time course.

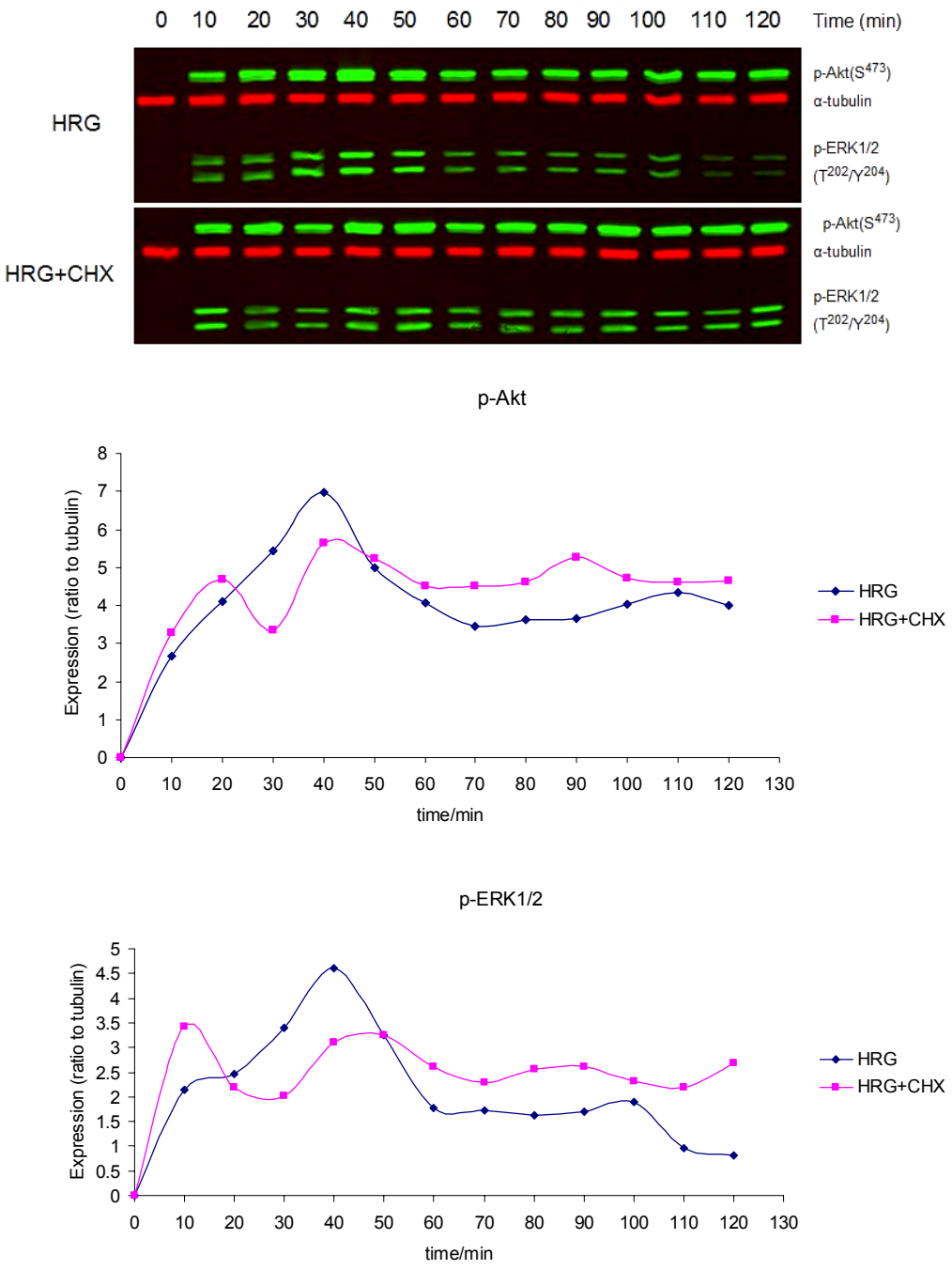

Figure 31 Effects of growth condition on the formation of oscillation. MCF-7 cells were grown in DMEM supplemented with 10% FCS for 48 h and then in DMEM supplemented with no serum for another 20 h before HRG plus/minus CHX treatment. CHX was incubated with cells for 20 min prior to HRG treatment. Cell lysates from each treatment were resolved in SDS-PAGE. p-Akt (S^{473}) and p-ERK1/2 (T^{202}/Y^{204}) were detected by Western Blotting. α-tubulin was a loading control. The images were acquired by scanning the membrane with LI-COR imaging system. The results are demonstrated as the ratio of the OD of p-Akt or pERK1/2 to that of corresponding α-tubulin.

4.1.8 Discussion on the oscillatory dynamics of p-Akt and p-ERK1/2

In this study, I have demonstrated the oscillatory dynamics of p-Akt and p-ERK1/2 under variable conditions in differing cell types, and evaluated the nature and concentration of ligands, and inhibitors that influence the oscillation. The oscillation is regulated by a variety of factors including transcriptional feedback loops, crosstalk with other pathways and over-expression of HER-2 as feedforward drive. The growth conditions also influenced the generation of oscillations.

According to the time course profile of p-HER-3 (Y^{1289}), the addition of CHX decreased the level of p-HER-3 within the whole time course, suggesting that the addition of CHX enhanced the negative feedback loop to HER-3. CHX is a protein synthesis inhibitor and I speculated that CHX enhanced the negative feedback loop through the loss of some protein synthesis. From the other angle, CHX could weaken positive feedback through the inhibition of protein synthesis. In Figure 27, under the stimulation of HRG alone, the level of p-HER-3 (Y^{1289}) oscillated, but the addition of CHX caused the oscillation to disappear. It implied that the inhibition of positive feedback caused the loss of oscillation. Results from another study support this conclusion. Nakakuki et al (282) found that the absence of a repressor caused the level of *c-fos* mRNA to oscillate when pulsed for the second time with EGF. The formation of oscillation is likely to involve either enhancement of positive feedback or loss of negative feedback, otherwise after the first decrease of the level of p-HER-3 (Y^{1289}) the level would not increase again. Therefore, there may be a transcriptional positive feedback to HER-3. This positive feedback could cause the oscillation of p-HER-3 (Y^{1289}). This conclusion was supported by Takeshi, Hidetoshi and colleague's study (91). In their study they proposed positive feedback to HER receptors through the *de novo* production of ligands. According to the gene expression analysis, HB-EGF which is a ligand for HER-1 and HER-4 and amphiregulin which is a specific ligand of HER-1 was induced significantly by HRG. HB-EGF and amphiregulin can activate HER-3 through triggering the dimerisation of HER-1-HER-3 or HER-4-HER-3. Moreover, genes of two molecules CTGF and CYR61 were also induced by

HRG. Both molecules can activate the Akt and ERK1/2 pathways through binding alphav-beta3 integrin (275-277). Integrin pathway and growth factor pathway can crosstalk and synergize to enhance Akt and ERK1/2 pathways (283) which in turn modulate HER-3. So HB-EGF, amphiregulin, CTGF and CYR61 may act in an autocrine manner to activate HER-3.

According to the hypothesis above, the oscillation of p-MEK1/2 ($S^{217/222}$) before 90 min under the treatment of HRG alone is explainable due to the positive feedback loop induced by HRG. Since CHX would block this positive feedback, the oscillation for HRG+CHX was weak. After 90 min, the level of p-MEK1/2 ($S^{217/222}$) was higher for HRG+CHX treatment than that for HRG treatment. It suggested that the addition of CHX inhibited the late negative feedback.

In contrast to the oscillations of p-HER-3 and p-MEK1/2 which were produced with the treatment of HRG without CHX, the oscillation of p-ERK1/2 was very appreciable under the treatment of HRG+CHX. As mentioned above, the enhancement of positive feedback or the loss of negative feedback can cause the formation of oscillation. Here, CHX will block the production of negative feedback molecules such as those from DUSP family. The expression of DUSPs was confirmed by gene expression analysis. In this study, the expression of DUSP1, DUSP2, DUSP4 and DUSP5 were significantly induced by HRG.

The involvement of signalling enhancer in the generation of oscillation was also supported by observations from MCF-7/HER2-18 cells. MCF-7/HER2-18 is a HER-2 over-expressing cell line. Oscillation of the level of p-ERK1/2 in MCF-7/HER2-18 cells treated with HRG alone was more appreciable than that in MCF-7 cells treated with HRG alone. It suggested that over-expression of HER-2 as a signalling enhancer was a modulator of oscillation.

Briefly, in terms of the above statements and the findings in Sections 4.1.2-4.1.7, I hypothesize that after the stimulation of HRG positive feedback loops to HER-3 were induced. Early positive and late (90 min) negative feedback loops to MEK1/2

were induced. Negative feedback loop to ERK1/2 was induced. The feedback loops are summarised in Figure 32.

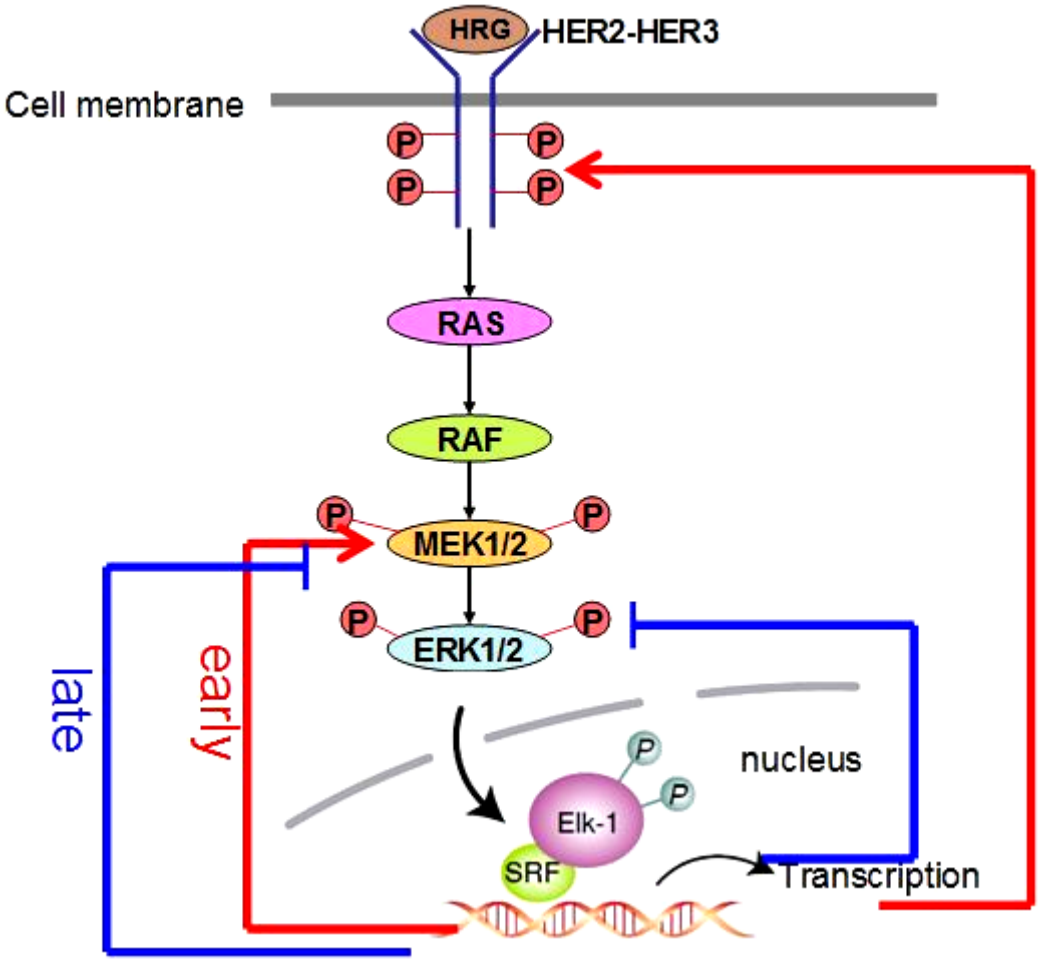

Figure 32 Scheme of the hypothesized HRG-induced transcriptional feedback loops. Blue lines denote the negative feedback loops and red lines denote the positive feedback loops.

It was interesting that the level of p-Akt and p-ERK1/2 was increased by CHX while the phosphorylation of HER-3 was attenuated. It suggested the involvement of feedback loops or crosstalk or that HRG activated ERK1/2 through other means such as the integrin-mediated pathways (278) besides HER-mediated pathways.

In a previous study, Nagashima et al (91) did not observe oscillation of p-ERK1/2 in MCF-7 cells treated with HRG with/without CHX. In their study, MCF-7 cells were serum-starved for 16-24 h before HRG treatment. In my study oscillation was observed in MCF-7 cells grown in medium with 5% DCSS. I hypothesized the

different observations about the oscillation was due to the different cell culture conditions. In my study, when MCF-7 cells were grown in phenol red-free DMEM without serum for 20 h before HRG treatment, oscillation of p-ERK1/2 (T^{202}/Y^{204}) was not observed regardless of CHX. This observation was consistent with the previous findings. The loss of oscillation may be due to the alteration of transcriptional negative feedback loops to ERK1/2 caused by serum-deprivation (220).

The oscillation of p-Akt expression has not been previously reported or predicted to the best of my knowledge. The oscillation was induced by both HRG and EGF in MCF-7 cells in either the presence or absence of CHX, while, the oscillation of p-ERK1/2 was appreciable only in the presence of CHX. The oscillation of p-Akt had a higher early response in the presence of CHX than that in the absence of CHX. This might be due to the oncogenic mutation of PI3K, which would amplify the signalling. It was demonstrated by Saal et al (284) that MCF-7 cells harboured an E545K mutation in PIK3CA. The MCF-7 cell line used in this study harbours an E545K mutation in PIK3CA which has been confirmed by my colleague (personal communication- Ms Charlene Kay, Breakthrough Breast cancer Unit, Edinburgh) using pyrosequencing. This mutation has been demonstrated to have oncogenic transforming activity and this transforming activity was related to the increased kinase activity (285) of PIK3CA. So this mutation is likely to be a signalling enhancer.

Additionally, negative feedback loops could be involved in the formation of oscillation as well. Kholodenko (235) predicted in his mathematical model that delayed negative feedback from p-ERK1/2 to the activation of Raf along with ultra-sensitivity could bring about sustained oscillation of p-ERK1/2. The sensitivity of the cellular targets to external stimuli increases multiplicatively with the number of cascade's tiers. So, a small change from external stimuli can result in a large change in the response. This is called ultrasensitivity. Nakayama et al (234) had observed the oscillation of Ras and ERK1/2 activity in FGF-stimulated NIH 3T3 cells. They demonstrated that the oscillation present there required the negative feedback

phosphorylation of SOS by active ERK1/2, which supported Kholodenko's hypothesis.

Since the transcriptional feedback loops could modulate the oscillation of p-Akt and p-ERK1/2, I undertook gene expression analysis to identify possible gene candidates which may be involved in the modulation. These candidates could all modulate the HER-mediated signalling dynamics through positive or negative feedback loops and were induced by HRG at an early time (at 20 min). DUSP1, DUSP2, DUSP4 and DUSP5 dephosphorylate p-ERK1/2. As mentioned above, CYR61 and CTGF can activate Akt and ERK1/2 through binding integrin. PPP1R15A could inhibit the dephosphorylation of p-Akt by protein phosphatase 1 (286). Further studies will be required to assess the role of these candidates in the modulation of oscillation.

In this study, the inhibitory crosstalk between the PI3K/Akt and Raf/MEK/ERK pathways was observed and this crosstalk can occur via inhibitory phosphorylation of Raf at S^{259} by activated Akt (281). It was reasonable that the inhibition of the phosphorylation of Akt by LY294002 could induce the more appreciable oscillation of p-ERK1/2 since the inhibitory crosstalk from Akt to Raf was blocked by LY294002, suggesting a loss of signalling attenuator. As mentioned above, the enhancement of positive signalling or the loss of signalling attenuator would cause oscillation.

Apart from the temporal regulation of the oscillation, Shankaran et al (287) reported that the oscillation was also modulated spatially. The authors demonstrated that p-ERK1/2-GFP oscillated with a periodicity of approximately 15 min between cytoplasm and nucleus after stimulation by EGF in individual human mammary epithelial cell line 184A1. This periodicity was very close to that observed in my study (roughly 20 min). The shift of p-ERK1/2 between different compartments may correlate with the oscillation of the total level of p-ERK1/2 (which was observed in my study) since the shifting could cause the concentration of p-ERK1/2 in the compartments to vary. I postulated that the varying concentrations might be a feedback to the input. If the concentration is higher than the cells' requirement, the

system would dephosphorylate p-ERK1/2. If the concentration is lower than that needed, the system would activate more ERK1/2 molecules. Hence, this process would cause the oscillation of total p-ERK1/2 in the whole cell across the time.

In this study, two different detection methods for western blot were used. One method uses HRP-conjugated secondary antibodies and ECL as substrate of HRP to generate chemiluminescent signals. Signals are captured with x-ray film in a dark room. The other method uses fluorophore-conjugated secondary antibodies. Fluorescent signals are captured by scanning western membranes with the LI-COR imaging system. The differences between these two methods are the involvement of biochemical reactions and signal characteristics. Although the latter method can save more time and detect total and phosphorylated cognates simultaneously, the inconsistency between the two methods introduces difficulties into interpreting results since secondary antibodies may have different affinities and the two detection methods may have different linear ranges of signal intensities against protein amount. This will make the results non-comparable. To resolve this problem, the two different systems of western blot can be run with serially diluted purified proteins. A standard curve of signal intensities (y axis) against protein amount (x axis) can be generated for each of these two systems and then a linear range can be determined for each system. Ideally, both linear curves should go through the point (0, 0) at the intersection of the axes. So based on the linear ranges, fitted linear curves which intersect at point (0, 0) as well as the curve functions can be generated. According to the fitted linear curves, ODs can be transformed to protein amount. Alternatively, the ratio of the fitted curve slopes can be used to normalise the band ODs of the target proteins (same as the standard proteins) between the two systems. The normalisation will make the results comparable. Additionally, two different internal controls (GAPDH and tubulin) were used in the western blots, which will also make the results non-comparable since the abundance of the two proteins in a cell may be not the same and the antibody affinities may be different as well. To resolve this problem, western blots can be run for serially diluted purified GAPDH and tubulin. Standard curves of band ODs (y axis) against protein molar amount (x axis) for each protein can be generated. Linear ranges and fitted linear curves (intersecting at (0, 0)) can be

determined as well. Ratio of the slopes between the two fitted linear curves can be used to normalise ODs of GAPDH and tubulin on the basis of the same molecule numbers. Therefore, the normalised ODs of GAPDH or tubulin can be used to normalise the ODs of target proteins. After the final normalisation, results from the experiments with different internal controls are comparable. For comparing the results from western blot and RPPA, standard curves for each method can be generated and ODs then can be transformed to concentration (μ g/ml).

In light of the investigations on the signalling oscillation as well as the regulating factors, the following conclusions can be made.

1) Signalling oscillations for p-Akt and p-ERK1/2 were observed experimentally for the first time in breast cancer cells.
2) Oscillations were cell line dependent and were observed in serum supplemented media instead of serum deprived media.
3) HER-2 over-expression could augment p-ERK1/2 oscillation and the HER-2 dimerisation inhibitor (pertuzumab) could block the oscillation of p-ERK1/2.
4) Transcriptional feedback loops could regulate the oscillations of both p-Akt and p-ERK1/2. Based on the results in this study, it was hypothesized that there was a transcriptional positive feedback to HER-3, an early positive and a late negative feedback loop to MEK1/2 and finally a negative feedback loop to ERK1/2. Based on gene expression analysis, twenty-nine genes were identified which might regulate the oscillations transcriptionally through positive or negative feedback loops.
5) Crosstalk between ERK1/2 and Akt pathway could also regulate oscillations.
6) In conclusion, oscillations were produced by interlinked positive feedback/feedforward and negative feedback loops. Functional consequences of changes in oscillations might have fundamental consequences in oncogenesis and therapy efficacy.

4.2 Effects of trastuzumab, pertuzumab and their combination in breast cancer cell lines

4.2.1 Growth inhibitory effects of trastuzumab, pertuzumab and their combination

Trastuzumab is an established therapy for patients with HER-2 over-expressing metastatic breast cancers. However, *in vitro,* this drug also inhibited the HER-2 low/medium expressing MCF-7 cell growth when stimulated by 1nM EGF in phenol red-free DMEM supplemented with 5% DCSS for 5 days. This contrasted with no growth inhibition of HRG-stimulated growth (Figure 33A&B). In order to test whether trastuzumab itself had any effect on HRG stimulation or whether the saturation of cell number masked trastuzumab's effects, I carried out a time course growth assay with different concentrations of HRG (1nM, 0.1nM and 0.01nM) and observed that cells treated with HRG plus trastuzumab grew at a slower rate than those treated with HRG alone but finally both groups of HRG alone and HRG plus trastuzumab reached the same cell numbers at the stationary phase (Figure 34). Therefore, under the stimulation of HRG, trastuzumab slowed down the growth rate but did not impact on final cell numbers. In contrast, MCF-7 cells treated with EGF plus trastuzumab grew at a slower rate through the whole time course indicated and achieved a lower cell density at the stationary phase than those treated with EGF alone (Figure 34). I concluded that trastuzumab slowed down the growth rate under the stimulation of HRG and inhibited the growth under the stimulation of EGF in MCF-7, but without stimulation trastuzumab alone did not have detectable effects on the growth of cells (compared to the control at Day 7 in Figure 34, student's t-test, $p>0.05$) of which 96.5%±0.0012 (average±SD, N=6) was synchronized to G0-G1 phase (data not shown).

Pertuzumab which is a HER-2 dimerisation inhibitor caused lower cell numbers after 3-day stimulation by both HRG and EGF (Figure 33B). Under the stimulation of 1nM HRG, the combination of trastuzumab and pertuzumab had more potent effects than each drug alone. Under the stimulation of 1nM EGF, the combination had a similar effect to that of pertuzumab on growth. The combination of pertuzumab and

trastuzumab had a more potent inhibition under the stimulation of HRG than under that of EGF. It was also observed that trastuzumab was working over a broad range of concentrations from at least 10 to 1000 nM (Figure 35) in MCF-7 cells. 10, 100 and 1000 nM trastuzumab respectively produced no significant differences in the growth inhibition under the stimulation of either HRG or EGF.

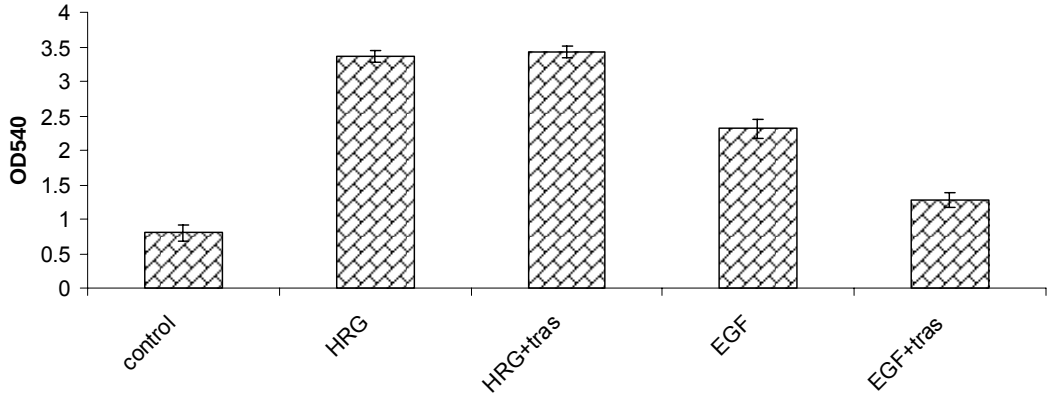

One-way ANOVA for all-group comparison (N=6, equal variances), p=0.000

Tukey HSD Post Hoc test run by SPSS 17.0

P value	control	HRG	HRG+tras	EGF	EGF+tras
control	--	0.000	0.000	0.000	0.000
HRG	0.000	--	0.764	0.000	0.000
HRG+tras	0.000	0.764	--	0.000	0.000
EGF	0.000	0.000	0.000	--	0.000
EGF+tras	0.000	0.000	0.000	0.000	--

A

Continued for Figure 33

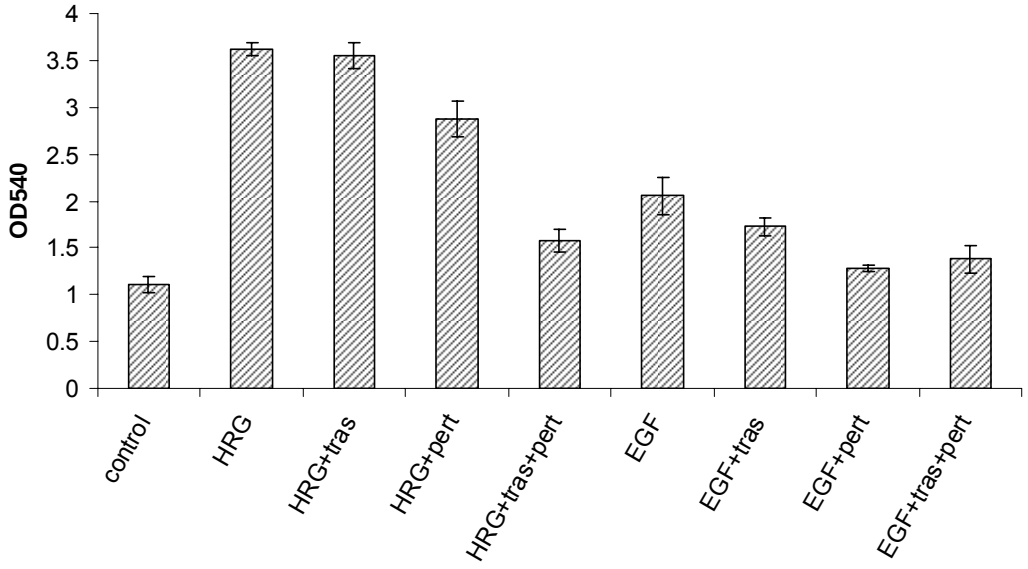

One-way ANOVA for all-group comparison (N=6, equal variances), p=0.000

Tukey HSD Post Hoc test run by SPSS 17.0

P value	control	HRG	HRG+tras	HRG+pert	HRG+tras+pert	EGF	EGF+tras	EGF+pert	EGF+tras+pert
control	--	0.000	0.000	0.000	0.000	0.000	0.000	0.352	0.016
HRG	0.000	--	0.988	0.000	0.000	0.000	0.000	0.000	0.000
HRG+tras	0.000	0.988	--	0.000	0.000	0.000	0.000	0.000	0.000
HRG+pert	0.000	0.000	0.000	--	0.000	0.000	0.000	0.000	0.000
HRG+tras+pert	0.000	0.000	0.000	0.000	--	0.000	0.554	0.007	0.203
EGF	0.000	0.000	0.000	0.000	0.000	--	0.002	0.000	0.000
EGF+tras	0.000	0.000	0.000	0.000	0.554	0.002	--	0.000	0.001
EGF+pert	0.352	0.000	0.000	0.000	0.007	0.000	0.000	--	0.905
EGF+tras+pert	0.016	0.000	0.000	0.000	0.203	0.000	0.001	0.905	--

B

Figure 33 Effects of trastuzumab (tras), pertuzumab (pert) and their combination on the growth of MCF-7 under the stimulation of EGF (1nM) or HRG (1nM). MCF-7 cells were grown in phenol red positive DMEM supplemented with 10% FCS in 96-well microplate for 48 h before being grown in phenol red free DMEM supplemented with 5% DCSS for another 48 h. Cells were then treated with EGF or HRG plus/minus the drugs indicated for 5 days (A) and 3 days (B). The working concentration of either trastuzumab or pertuzumab was 100 nM. The results are presented as the average of the OD540 value ±SD.

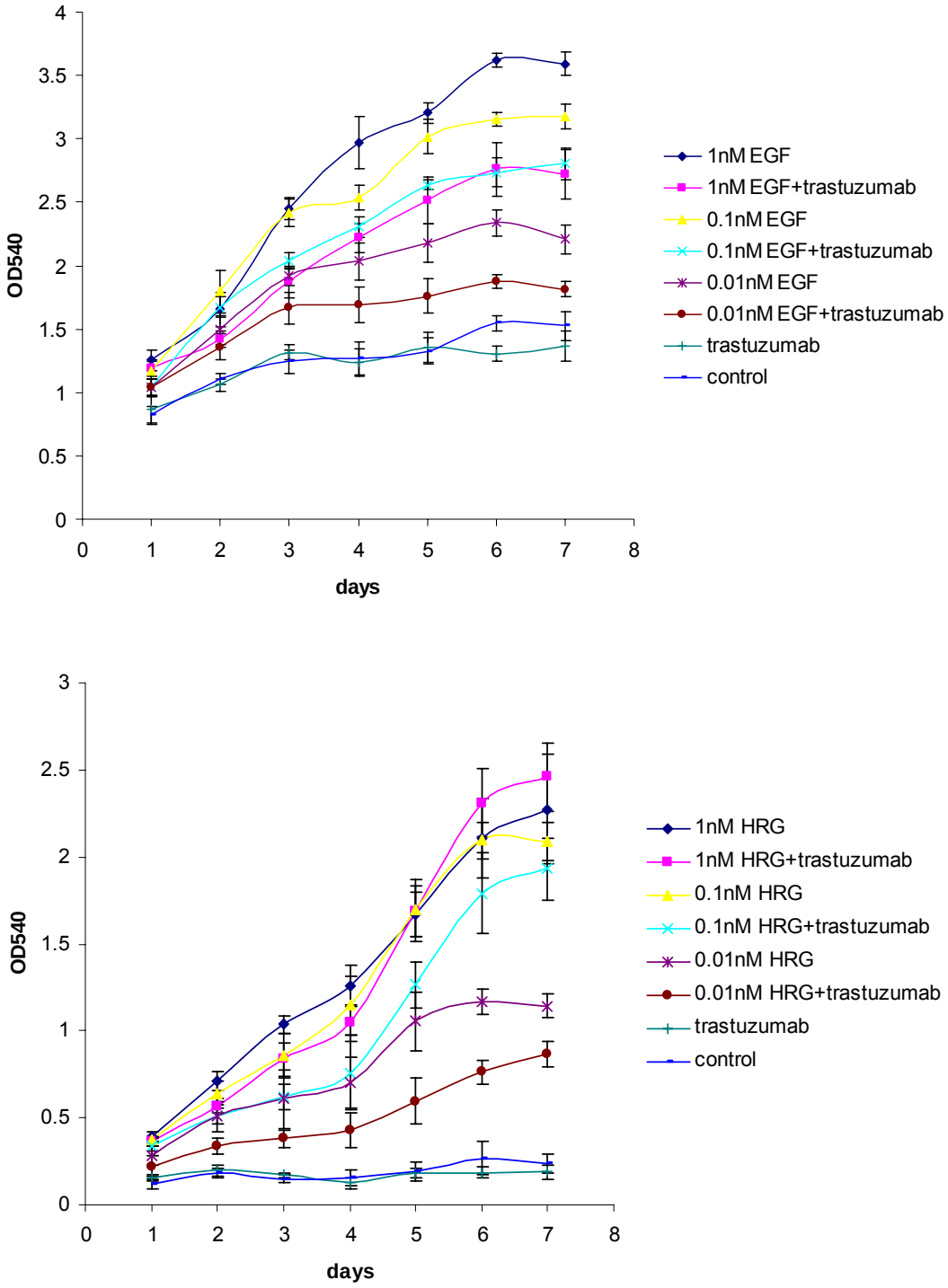

Figure 34 Dose effects of EGF or HRG on the growth inhibition of trastuzumab for MCF-7 cells. Cells were treated with 1nM, 0.1nM and 0.01nM HRG or EGF for a 7-day time course with the one-day interval under the intervention of 100nM of trastuzumab. The results are presented as the average of the OD540 value ±SD.

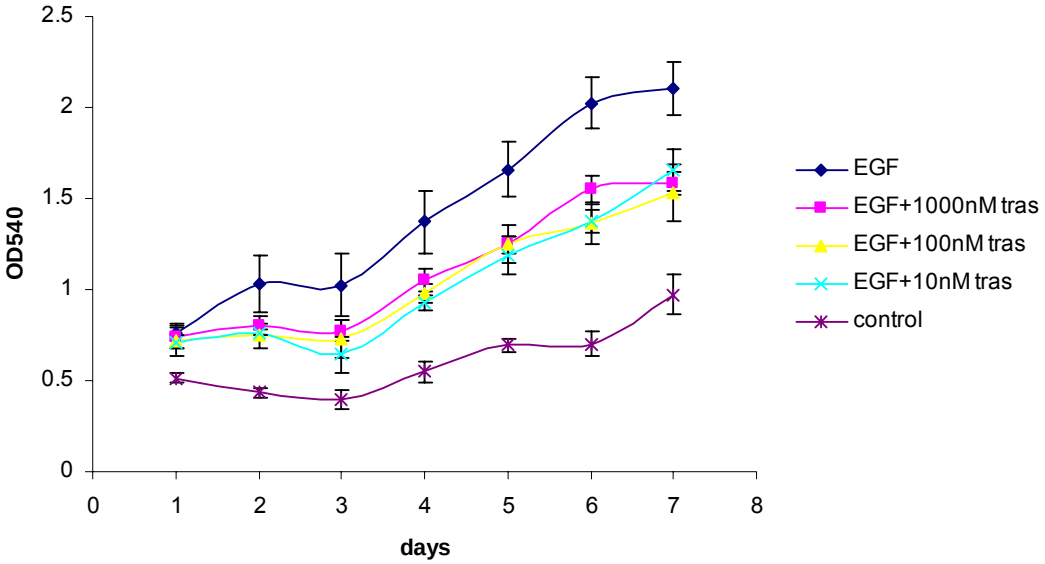

One-way ANOVA for all-group comparison (N=6, equal variances), p=0.000

Tukey HSD Post Hoc test run by SPSS 17.0

P value (at Day 7)	EGF	EGF+1000nM tras	EGF+100nM tras	EGF+10nM tras	control
EGF	--	0.000	0.000	0.000	0.000
EGF+1000nM tras	0.000	--	0.913	0.876	0.000
EGF+100nM tras	0.000	0.913	--	0.399	0.000
EGF+10nM tras	0.000	0.876	0.399	--	0.000
control	0.000	0.000	0.000	0.000	--

Continued for Figure 35

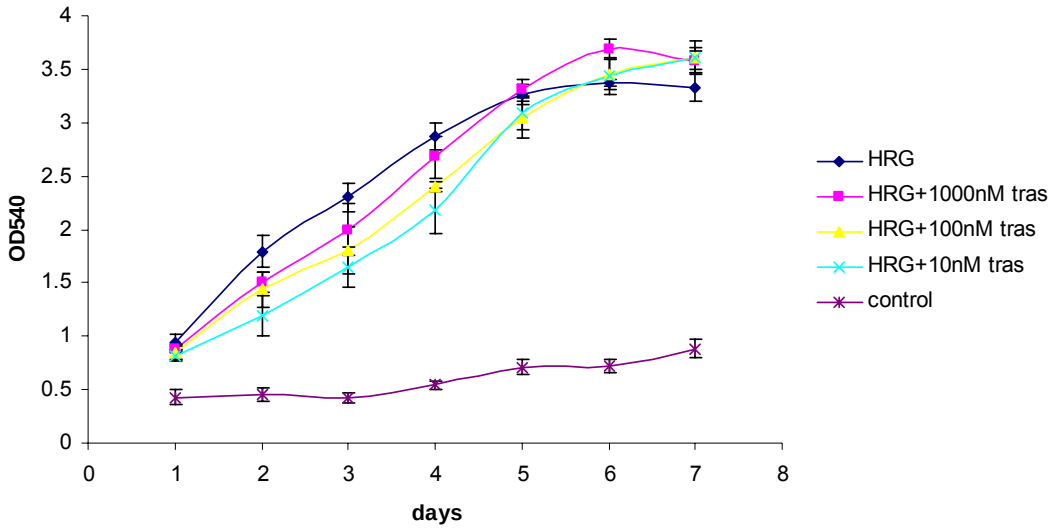

One-way ANOVA for all-group comparison (N=6, equal variances), p=0.000

Tukey HSD Post Hoc test run by SPSS 17.0

P value (at Day 7)	HRG	HRG+1000nM tras	HRG+100nM tras	HRG+10nM tras	control
HRG	--	0.011	0.004	0.002	0.000
HRG+1000nM tras	0.011	--	0.989	0.970	0.000
HRG+100nM tras	0.004	0.989	--	1.000	0.000
HRG+10nM tras	0.002	0.970	1.000	--	0.000
control	0.000	0.000	0.000	0.000	--

Figure 35 Growth inhibitory effects of different concentrations of trastuzumab in MCF-7 cells. Cells were stimulated with 0.1nM HRG or 0.1nM EGF plus the treatment of 10, 100 and 1000nM trastuzumab (tras) respectively for a 7-day time course with the one-day interval. The results are presented as the average of OD540 value ± SD. The p values for Day 7 were shown.

A similar growth time course profile for MCF-7/HER2-18 cells was also observed. The growth of MCF-7/HER2-18 induced by 1, 0.1 and 0.01nM EGF was inhibited by 100nM trastuzumab (Figure 36), but 100nM trastuzumab just slowed down the growth rate induced by 1 and 0.1nM HRG. Distinct from the effect of trastuzumab on the growth of MCF-7 stimulated by HRG, trastuzumab inhibited the growth of MCF-7/HER2-18 stimulated by 0.01nM HRG rather than slowing down the growth rate. Here, it was observed that trastuzumab seemed to inhibit the basal growth in

phenol red free DMEM supplemented with 5% DCSS. This inhibition would be confirmed in the following assay.

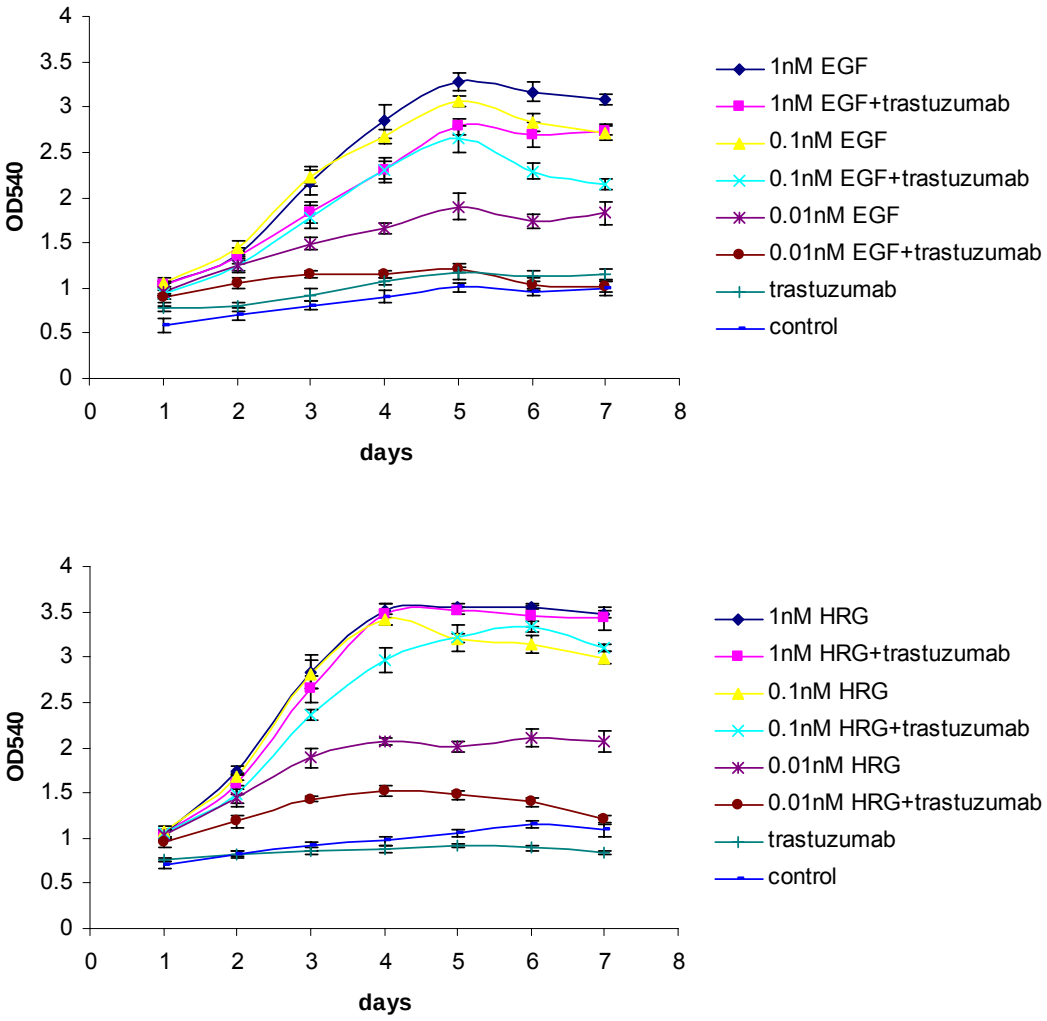

Figure 36 Dose effects of EGF or HRG on the growth inhibition of trastuzumab for MCF-7/HER2-18 cells. Cells were treated with 1nM, 0.1nM and 0.01nM HRG or EGF for a 7-day time course with the one-day interval under the intervention of 100nM trastuzumab. The results are presented as the average of the OD540 value ±SD.

Similar to the effects on MCF-7 and MCF-7/HER2-18 cells, trastuzumab inhibited the growth of BT474 cells stimulated by 1nM EGF but not HRG (Figure 37). Trastuzumab had no effects on the growth stimulated by HRG within the entire 7-day time course. Pertuzumab inhibited the growth of BT474 cells stimulated by both EGF and HRG, but it had more potent effects on the stimulation of EGF than on that of HRG. At Day 7, pertuzumab inhibited the growth driven by EGF by nearly 50%,

down to the control level but inhibited only about 18% of the growth driven by HRG. The combination of trastuzumab and pertuzumab had no statistically significant difference with pertuzumab alone on the growth driven by HRG but further inhibited the growth driven by EGF, compared with either trastuzumab or pertuzumab. It was interesting that the combination inhibited the growth driven by EGF below the control level, particularly at day 7 about 3.6-fold inhibition against control level. Across the time course, the cell numbers were reduced under the treatment of 'EGF+trastuzumab+pertuzumab', roughly 2-fold fewer at day 7 than at day 1, which may be in part due to the increased apoptosis (288).

It was mentioned above that trastuzumab alone had no detectable or ambiguous effects on growth, but there was a possibility that the cell number seeded for the time course growth assay in Figure 34 was not high enough to show the growth differences between trastuzumab-treated and the control group. Therefore, the cell numbers were increased to 10,000/well for MCF-7 and 16,000/well for MCF-7/HER2-18. In Figure 38, statistically significant differences were observed between trastuzumab treated and control groups in both MCF-7 and MCF-7/HER2-18 but the differences were small.

In summary, trastuzumab had growth inhibitory effects *in vitro* on MCF-7, MCF-7/HER2-18 and BT474 cell lines.

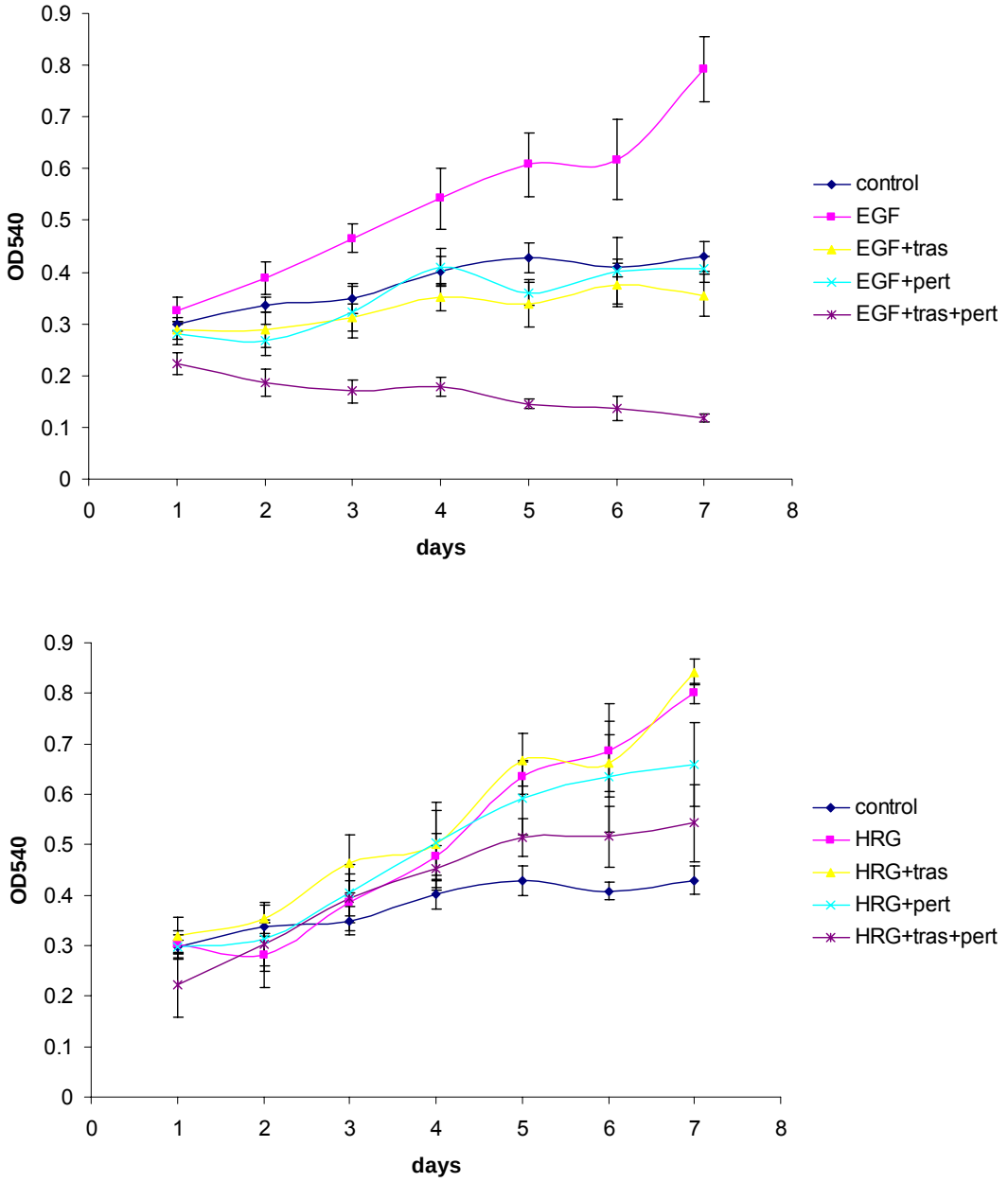

A

Continued for Figure 37

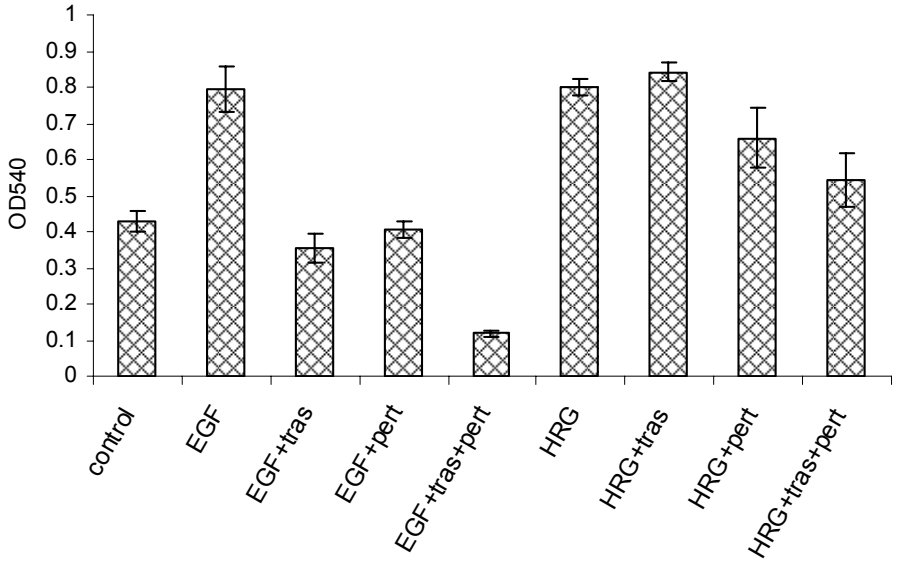

Brown-Forsythe test for all-group comparison (N=6, unequal variances), p=0.000

Games-Howell Post Hoc test run by SPSS 17.0

P value (Day 7)	control	EGF	EGF+tras	EGF+pert	EGF+tras+pert	HRG	HRG+tras	HRG+pert	HRG+tras+pert
control	--	0.000	0.071	0.817	0.000	0.000	0.000	0.008	0.143
EGF	0.000	--	0.000	0.000	0.000	1.000	0.675	0.145	0.002
EGF+tras	0.071	0.000	--	0.293	0.000	0.000	0.000	0.001	0.013
EGF+pert	0.817	0.000	0.293	--	0.000	0.000	0.000	0.005	0.068
EGF+tras+pert	0.000	0.000	0.000	0.000	--	0.000	0.000	0.000	0.000
HRG	0.000	1.000	0.000	0.000	0.000	--	0.126	0.083	0.004
HRG+tras	0.000	0.675	0.000	0.000	0.000	0.126	--	0.026	0.001
HRG+pert	0.008	0.145	0.001	0.005	0.000	0.083	0.026	--	0.318
HRG+tras+pert	0.143	0.002	0.013	0.068	0.000	0.004	0.001	0.318	--

B

Figure 37 Effects of trastuzumab (tras), pertuzumab (pert) and their combination on the growth of BT474 cells under the stimulation of EGF (1nM) or HRG (1nM). BT474 cells were grown in phenol red positive DMEM supplemented with 10% FCS in 96-well microplate for 48 h before being grown in phenol red free DMEM supplemented with 5% DCSS for another 48 h. Cells were then treated with EGF or HRG plus/minus the drugs indicated for a 7-day time course with the one-day interval (**A**). The working concentration of either trastuzumab or pertuzumab was 100nM. **B** represents the cell density of the last day (Day 7) treatment within the time course. The results are presented as the average of the OD540 value ±SD.

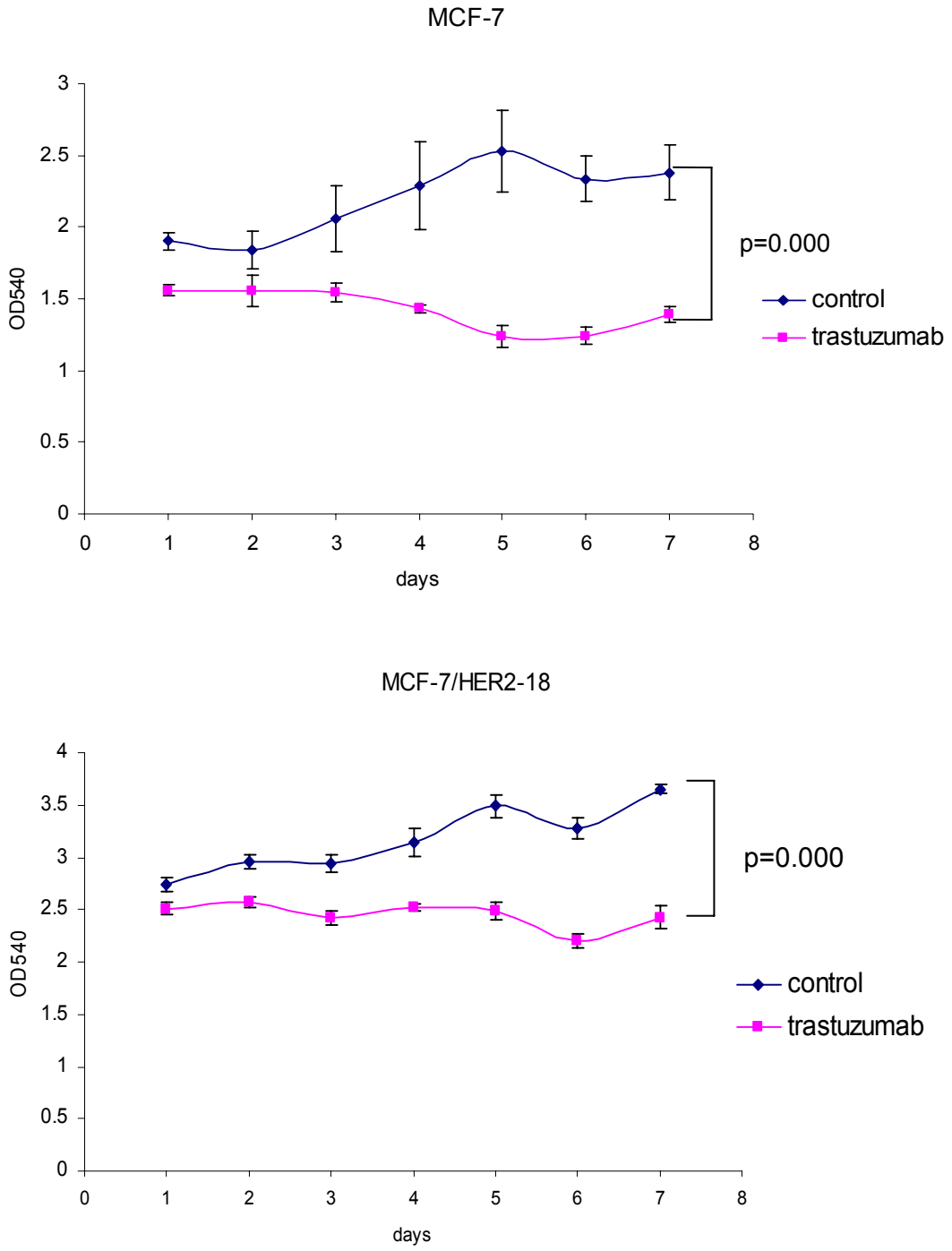

Figure 38 Inhibition of basal growth by 100 nM trastuzumab in MCF-7 and MCF-7/HER2-18 cells. MCF-7 and MCF-7/HER2-18 cells were seeded in 96-well microplate. The effects of trastuzumab on both MCF-7 and MCF-7/HER2-18 cells which were cultured in phenol red-free DMEM supplemented with 5% DCSS were analyzed with SRB assay. The results are presented as the average of the OD540 value±SD. The p values for Day 7 were shown. The student's t-test was applied to compare the significant differences.

4.2.2 Trastuzumab regulates gene expression

HRG induced expression of hundreds of genes in MCF-7 cells when cells were treated with HRG for 40 min and generally, HRG and HRG+trastuzumab induced similar gene expression patterns (Figure 39), but among the 300 significantly ($p<0.05$) induced genes by HRG (Table S4 in the Supplement), 29 genes were modulated by trastuzumab (Table 5). These 300 genes are selected according to the following criteria. The whole gene list of the array was sorted by fold-change (highest to lowest, 40'HRG *vs* control). The top 300 genes with p value less than 0.05 were selected.

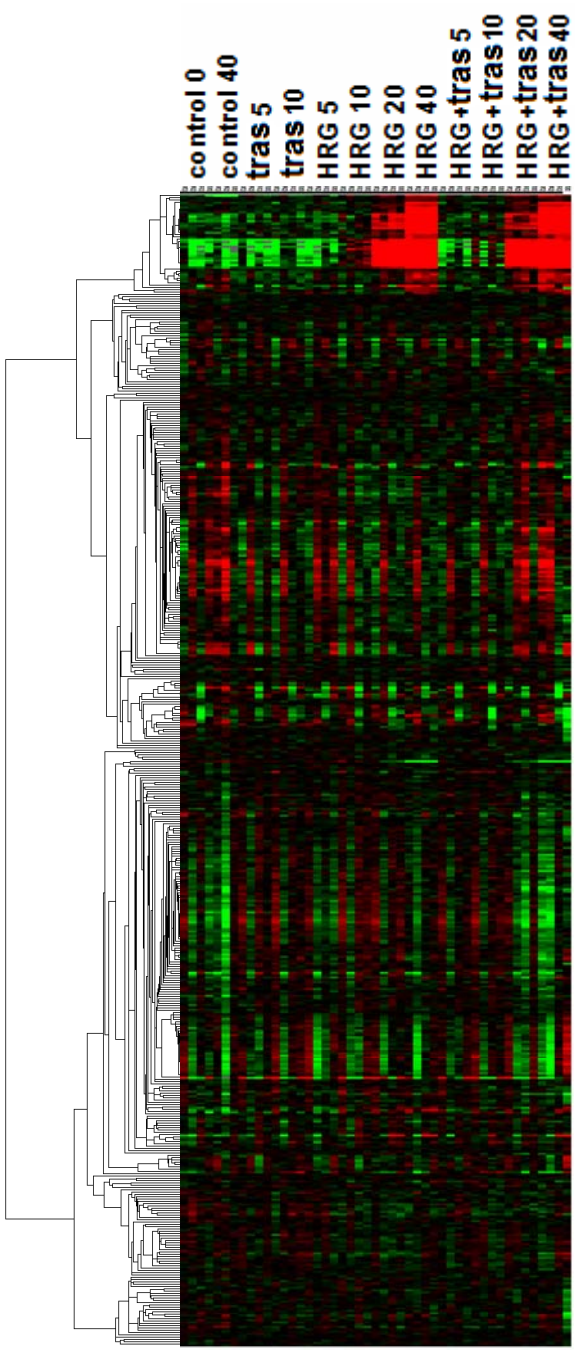

Figure 39 Gene expression patterns of MCF-7 cells treated with trastuzumab (tras), HRG or HRG plus trastuzumab for 5, 10, 20 and 40 min respectively and controls. HRG and trastuzumab were used at 1nM and 100nM respectively. Individual rows highlighted are a cluster of genes that were increased over the time course expression profile. There are four replicates for each treatment. Colours are relative expression across the samples the brightest red is for most highly expressed genes and green for reduced expression, relative to the mean (black).

Table 5 Twenty nine genes regulated significantly by trastuzumab ($p<0.05$, 40'HRG+trastuzumab *vs* HRG, student's t -test)

Gene	Description	Fold change
RCAN1	regulator of calcineurin 1	1.24096
MESDC1	mesoderm development candidate 1	1.21774
CNTD2	cyclin N-terminal domain containing 2	1.20362
PPP1R10	protein phosphatase 1, regulatory subunit 10	1.19679
PIM3	pim-3 oncogene	1.15688
FVT1	3-ketodihydrosphingosine reductase	1.13937
LOC201164	unknown	1.13512
INSIG1	insulin induced gene 1	1.11095
C11orf56	unknown	1.10295
C12orf44	unknown	1.08569
TRIM26	tripartite motif-containing 26	1.07298
NT5DC3	5'-nucleotidase domain containing 3	-1.09757
VGF	VGF nerve growth factor inducible	-1.10285
ZNF274	zinc finger protein 274	-1.10831
DUSP1	dual specificity phosphatase 1	-1.11174
ERRFI1	ERBB receptor feedback inhibitor 1	-1.11981
PHLDA1	pleckstrin homology-like domain, family A, member 1	-1.16008
C20orf111	unknown	-1.17105
JUN	jun oncogene	-1.17573
KLF2	Kruppel-like factor 2	-1.21052
KLF6	Kruppel-like factor 6	-1.23382
KLF10	Kruppel-like factor 10	-1.24995
FZD9	frizzled homolog 9 (Drosophila)	-1.25084
CCNL1	cyclin L1	-1.26052
LOC651621	unknown	-1.26450
MEF2D	myocyte enhancer factor 2D	-1.29517
LRRC8A	leucine rich repeat containing 8 family, member A	-1.39029
UBC	ubiquitin C	-1.40686
FOSB	FBJ murine osteosarcoma viral oncogene homolog B	-1.40732

Among the 29 genes, 11 genes were up-regulated and 18 genes were down regulated. The functions of the 3 genes (C11orf56, C12orf44 and LOC201164) among the 11 up-regulated genes and 2 genes (LOC651621 and C20orf111) among the 18 down-regulated genes have not been described. Among the 16 (LOC651621 and C20orf111 excluded) down-regulated genes, expression products of the following 10 genes FOSB, KLF10, KLF2, KLF6, CCNL1, JUN, MEF2D, PHLDA1, UBC and ZNF274 were clustered in the group of nuclear proteins. Among these 10 genes, 9 genes excluding PHLDA1 were clustered in regulation of transcription. Five genes (KLF10, DUSP1, JUN, PHLDA1 and UBC) were clustered as positive regulators of apoptosis using the functional annotation tool of DAVID Bioinformatics Resources 6.7 (267, 268). ERRFI1 which is also called RALT interacts with HER-2 directly and is a

transcriptionally controlled feedback inhibitor of HER receptor-mediated signalling (289) which can inhibit HER-2 mitogenic and transforming activity (290). According to the DAVID functional annotation tool, DUSP1, JUN and ERRFI1 are involved in HER-mediated signalling regulation and FZD9 is involved in activation of Wnt/β-catenin pathway. NT5DC3 is a novel gene. Little is known about this gene which may contribute to development/progression of human pancreatic cancer (291). Similarly, little is known about LRRC8A a novel gene which is required for B cell development (292). The 11 up-regulated genes could not be clustered in any functional category. The protein product of RCAN1 can inhibit calcineurin signalling and inhibit angiogenesis (293). Little is known about MESDC1 and CNTD2. PPP1R10 is a hypoxia inducible gene and its expression product is a nuclear targeting subunit of PP1. Over-expression of this protein markedly increases cell death to hypoxia through increasing the nuclear localization, phosphorylation and transcriptional activity of p53 as well as the ubiquitin-dependent proteosomal degradation of MDM2 (294). Aberrantly expressed serine/threonine kinase Pim-3 can cause autonomous proliferation or prevent apoptosis of human hepatoma cell lines (295). The protein product of PVT1 plays a role in the synthesis of sphingolipids which are essential membrane components of eukaryotic cells (296). The protein product of INSIG1 is a membrane bound protein of endoplasmic reticulum and plays a role in feedback control of lipid synthesis in cultured cells (297). The protein encoded by TRIM26 is a member of the tripartite motif (TRIM) family which contains one B box-type zinc finger, one B30.2/SPRY domain and one RING-type zinc finger, but its function is unknown (from NCBI gene database, gene ID: 7726). So, it is likely that growth rate reduction of HRG-stimulated MCF-7 cells by trastuzumab might be due to down-regulation of transcription.

4.2.3 Effects of trastuzumab, pertuzumab and their combination on signalling dynamics

To assess how these differential growth profiles were reflected in signalling, I analyzed the dynamics of p-Akt and p-ERK1/2 under the stimulation of 1nM EGF and 1nM HRG with the aforementioned drugs in MCF-7, MCF-7/HER2-18 and BT474 cell lines.

In MCF-7 cells, 1nM HRG alone induced a sustained p-ERK1/2 level throughout the time course indicated, but in the presence of 100nM trastuzumab, p-ERK1/2 level became transient (Figure 40). However, the p-ERK1/2 level was higher than that in HRG alone treatment within the first one hour and then decreased to a comparable level. Pertuzumab greatly inhibited the p-ERK1/2 expression level. The combination of trastuzumab and pertuzumab brought down p-ERK1/2 expression to a baseline value (Figure 40). The p-Akt expression level was reduced by trastuzumab, pertuzumab and their combination. Pertuzumab had a much stronger reduction effect than trastuzumab (Figure 41). Among the interventions the combination of trastuzumab and pertuzumab had the strongest reduction effect on the level of p-Akt as well as on that of p-ERK1/2 (Figure 41). It was interesting that the activity of MEK1/2 which is the molecule upstream of ERK1/2 was reduced by trastuzumab while the level of p-ERK1/2 was increased within the first hour (Figure 41 & 42). Both antibodies and their combination had no detectable effects on the level of p-ERK1/2 under EGF stimulation, but all reduced the level of p-Akt (Figure 43). Here, pertuzumab had a stronger inhibition than trastuzumab. The effects of the combination of both drugs on p-Akt were not simply the sum of individual drugs. Trastuzumab partially reversed the inhibitory effect of pertuzumab. The addition of pertuzumab facilitated trastuzumab's ability to inhibit p-Akt further within the first 20 min but thereafter had little added impact. It demonstrated that under the drive of EGF, growth inhibition by trastuzumab, pertuzumab and their combination was primarily through altering dynamics of the PI3K/Akt pathway and through that of both PI3K/Akt and Raf/MEK1&2/ERK1&2 pathways under the drive of HRG.

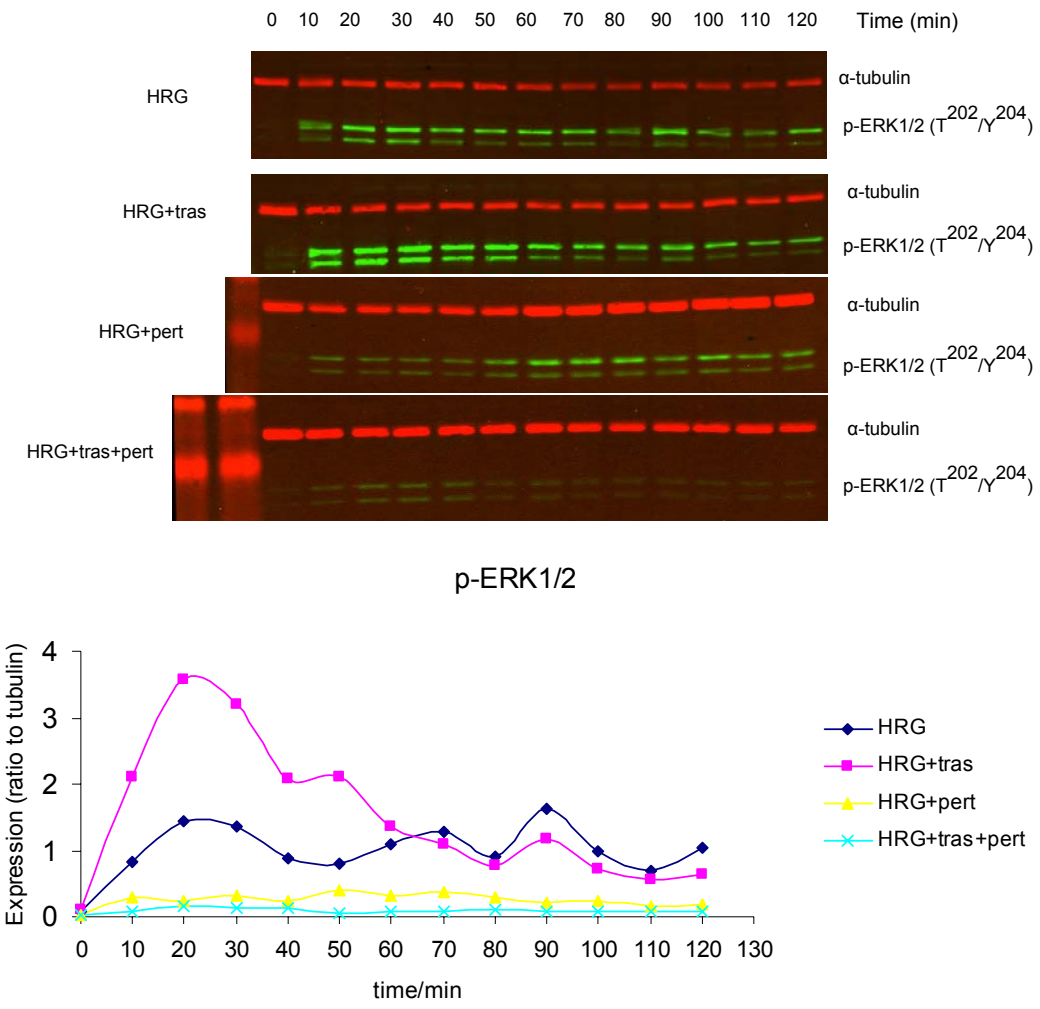

Figure 40 Time-course profile of p-ERK1/2(T^{202}/Y^{204}) in MCF-7 cells treated with 1nM HRG plus/minus trastuzumab (tras, 100nM), pertuzumab (pert, 100nM) and their combination. α-tubulin was used as the loading control. The results are presented as the ratio of OD of p-ERK1/2 to that α-tubulin.

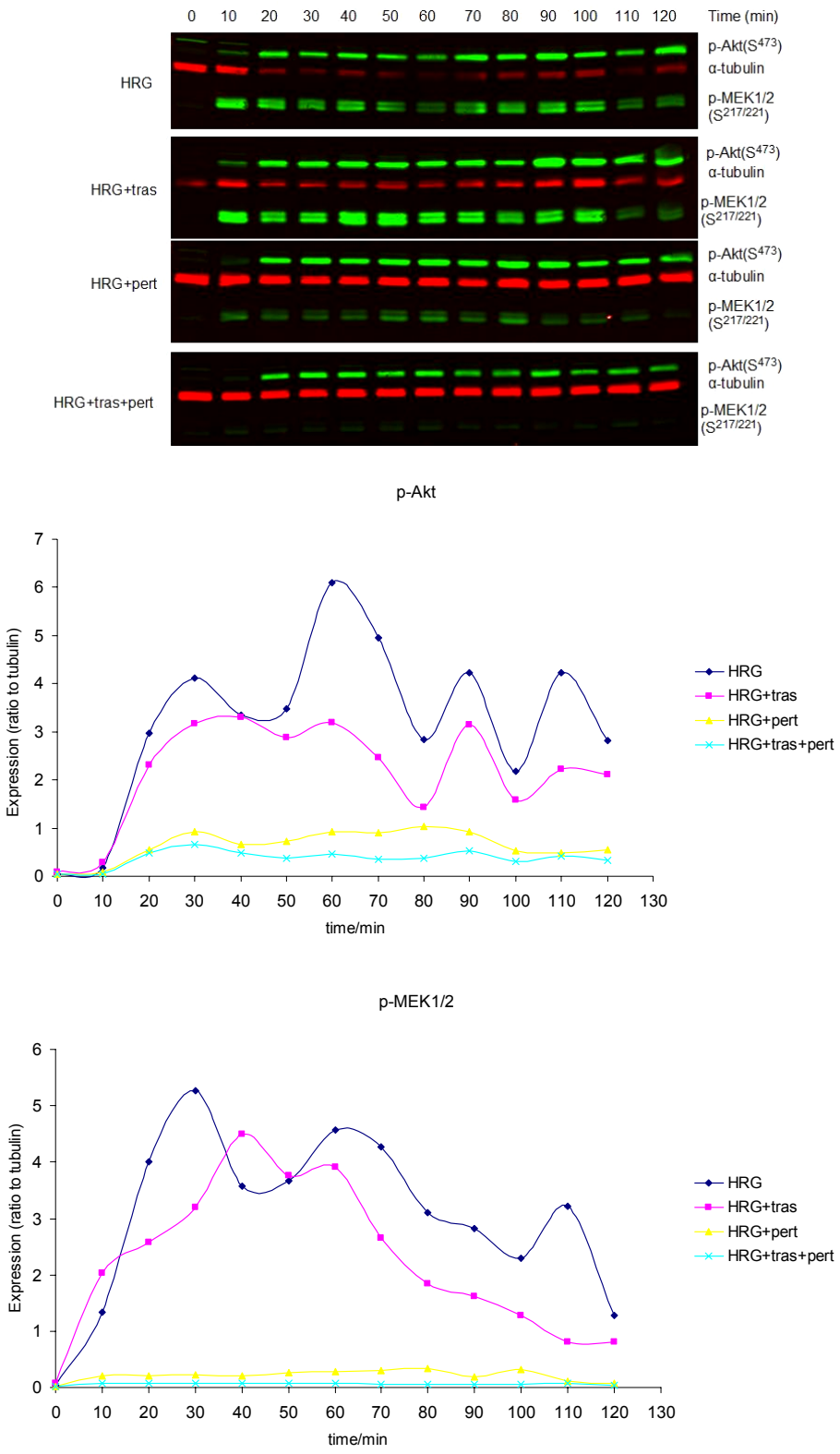

Figure 41 Time-course profile of p-Akt (S^{473}) and p-MEK1/2 ($S^{217/221}$) expression in MCF-7 cells treated with HRG (1nM) plus/minus trastuzumab (tras, 100nM), pertuzumab (pert, 100nM) and their combination. α-tubulin was used as the loading control. The results are presented as the ratio of OD of phospho-targets to that α-tubulin.

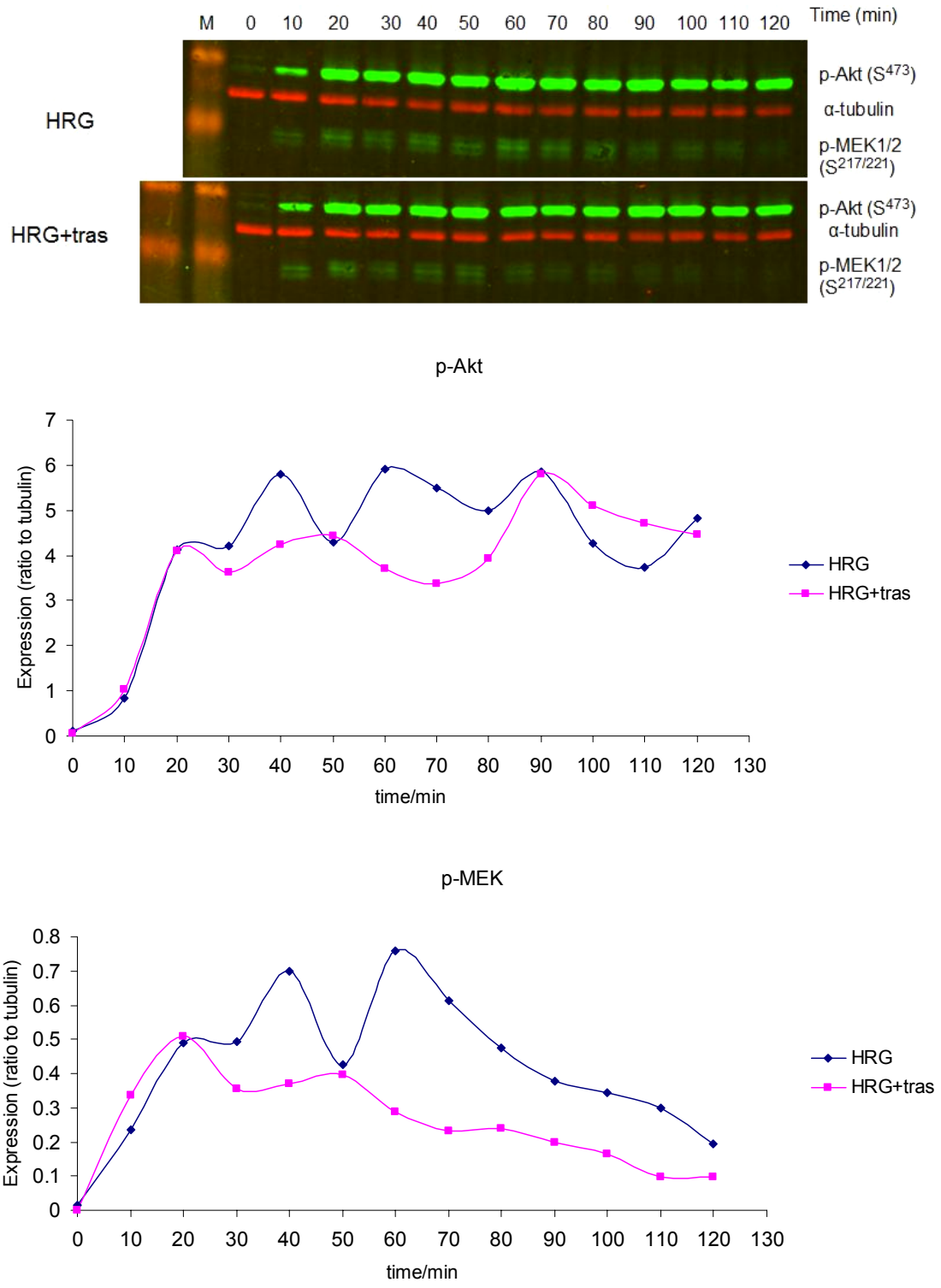

Figure 42 Repeat of the time-course profile of p-Akt (S^{473}) and p-MEK1/2 ($S^{217/221}$) in MCF-7 cells treated with HRG (1nM) plus/minus trastuzumab (tras, 100nM). 'M' denotes protein ladder. α-tubulin was used as the loading control. The results are presented as the ratio of OD of phospho-targets to that α-tubulin.

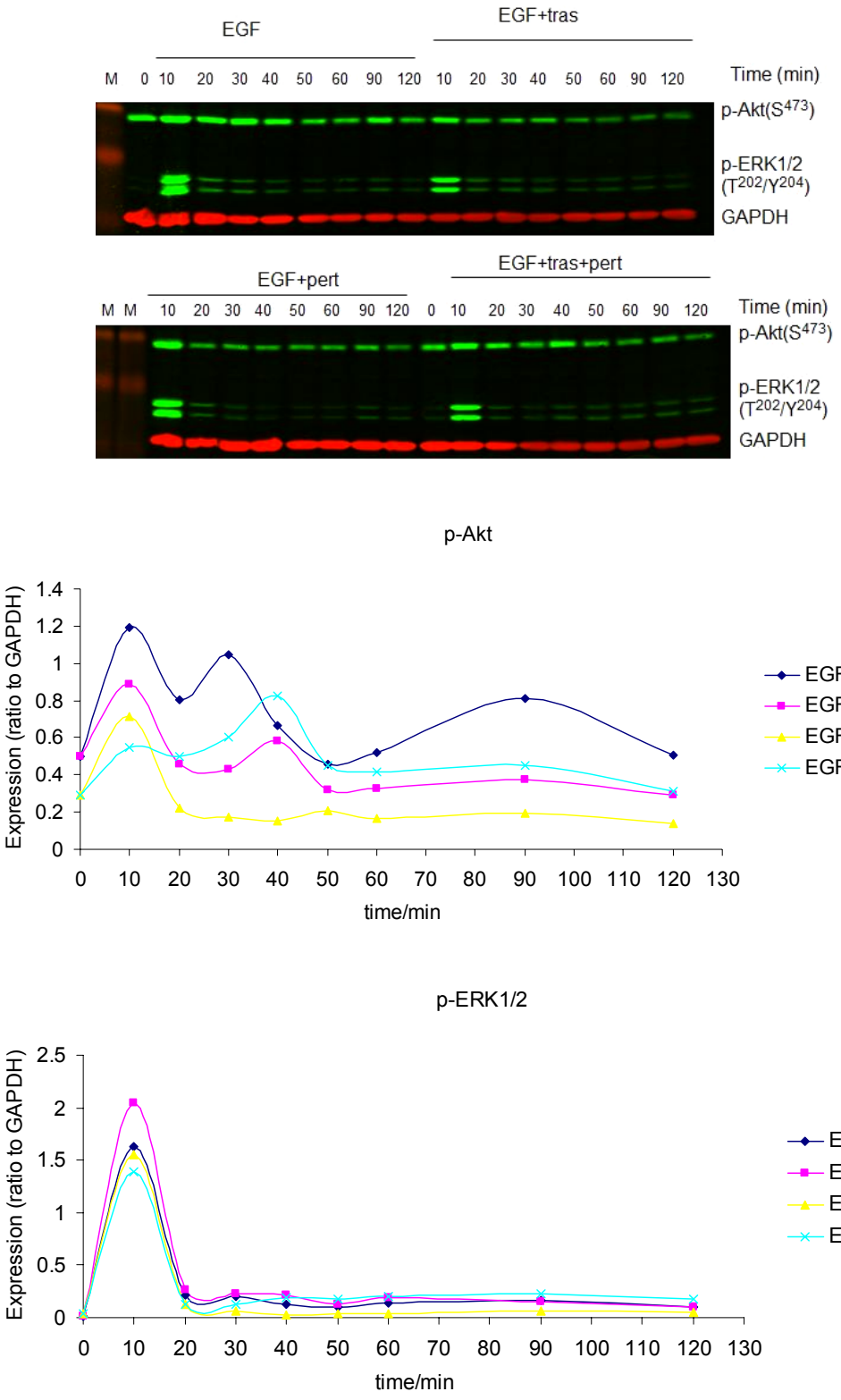

Figure 43 Time-course profile of p-Akt (S^{473}) and p-ERK1/2(T^{202}/Y^{204}) expression in MCF-7 cells treated with EGF (1nM) plus/minus trastuzumab (tras, 100nM), pertuzumab (pert, 100nM) and their combination. 'M' denotes protein ladder. GAPDH was used as the loading control. Results are presented as the raito of OD of phospho-targets to that GAPDH.

In MCF-7/HER2-18 cells, HRG alone elicited a sustained oscillatory activation of p-ERK1/2 during the whole time course for 2 h. Trastuzumab, pertuzumab and their combination reduced the level of p-ERK1/2 to different degrees (Figure 44). Trastuzumab triggered a shift of timing of the early activation peak from 20-min to 10-min point. Trastuzumab reduced not only the magnitude of the p-ERK1/2 signal but also the number of cycles from four to two. After trastuzumab treatment, only 2 cycles in the first hour were observed. Interestingly, there was only one cycle in the pertuzumab treatment group which was generated in the first 40 min. The magnitude of the first cycle was not reduced much. The combination of trastuzumab and pertuzumab brought down the level of p-ERK1/2 nearly to the basal line, which was consistent with the result from MCF-7 cells. For p-Akt, trastuzumab had no large effects on the magnitude before the 90-min point but reduced the level later. Noticeably, pertuzumab had a totally different effect on the level of p-Akt in MCF-7/HER2-18 cells compared to that in MCF-7 cells. In MCF-7 cells, pertuzumab reduced the level of p-Akt almost to background levels (Figure 41), while in MCF-7/HER2-18 cells it increased the level of p-Akt greatly in the first 40 min after which the level of p-Akt came down to a level comparable to that of the HRG alone treatment. The increasing effect of pertuzumab was reversed by trastuzumab since the level of p-Akt in the combination of trastuzumab and pertuzumab treatment group went back to a similar level to that of the HRG alone treatment group in the first 40 min and then to a lower level thereafter.

The phosphorylation of HER-2 at Y^{877} in MCF-7/HER2-18 cells was slightly induced by HRG (Figure 45). Addition of trastuzumab or pertuzumab drastically increased the phosphorylation. The combination of trastuzumab and pertuzumab had the most potent effects on the induction of phosphorylation of HER-2.

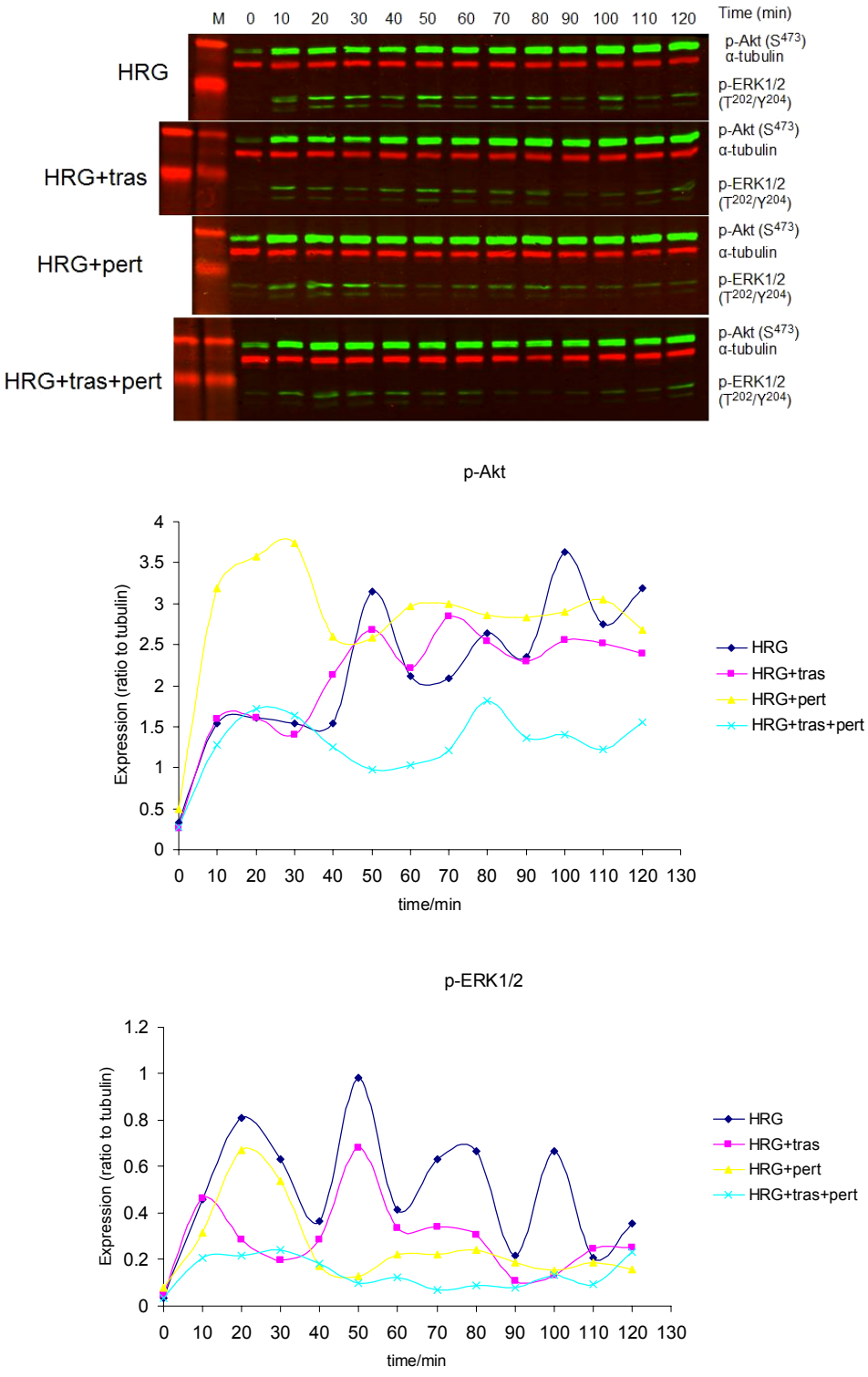

Figure 44 Effects of trastuzumab (tras, 100nM), pertuzumab (pert, 100nM) and their combination on the time course profiles of p-ERK1/2 and p-Akt expression in MCF-7/HER2-18 stimulated by 1nM HRG. 'M' denotes protein ladder. Results are indicated as the ratio of the OD of phospho-target to α-tubulin.

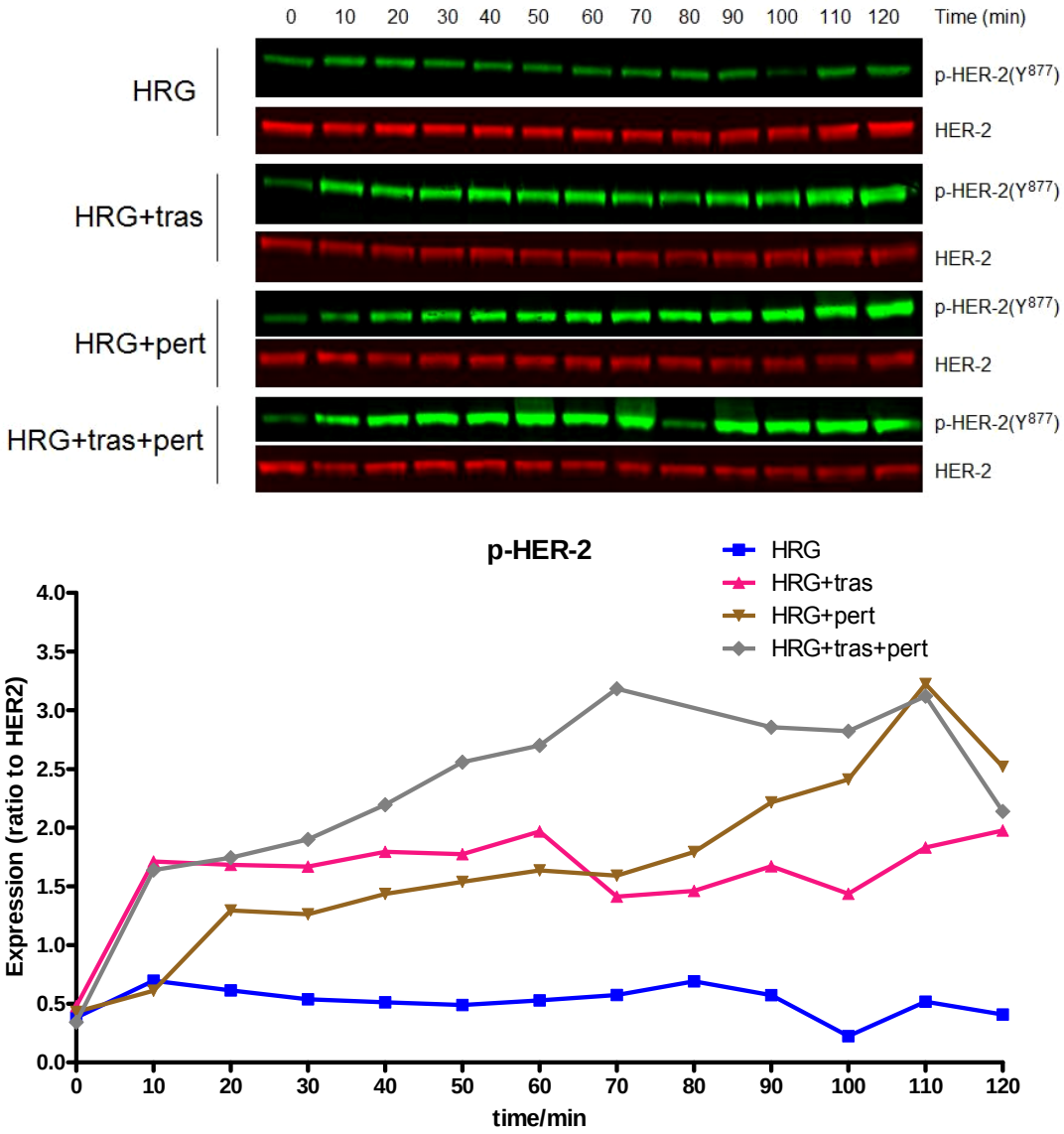

Figure 45 Effects of trastuzumab (tras, 100nM), pertuzumab (pert, 100nM) and their combination on the time course profile of p-HER-2 (Y^{877}) in MCF-7/HER2-18 cells stimulated by 1nM HRG. The targets were detected with LI-COR infrared imaging system. Results are indicated as the ratio of the OD of p-HER-2 to that of total HER-2. The ratio at 80min in HRG+pertuzumab+trastuzumab group was not plotted on the graph since the ratio was decreased sharply at 80min to the basal level in 10 min. This was considered as artefact.

The levels of p-Akt and p-ERK1/2 expression in BT474 cells stimulated by HRG were not affected by trastuzumab (Figure 46) within the 90-min time course, consistent with trastuzumab not affecting the growth stimulated by HRG in BT474 cells (Figure 37).

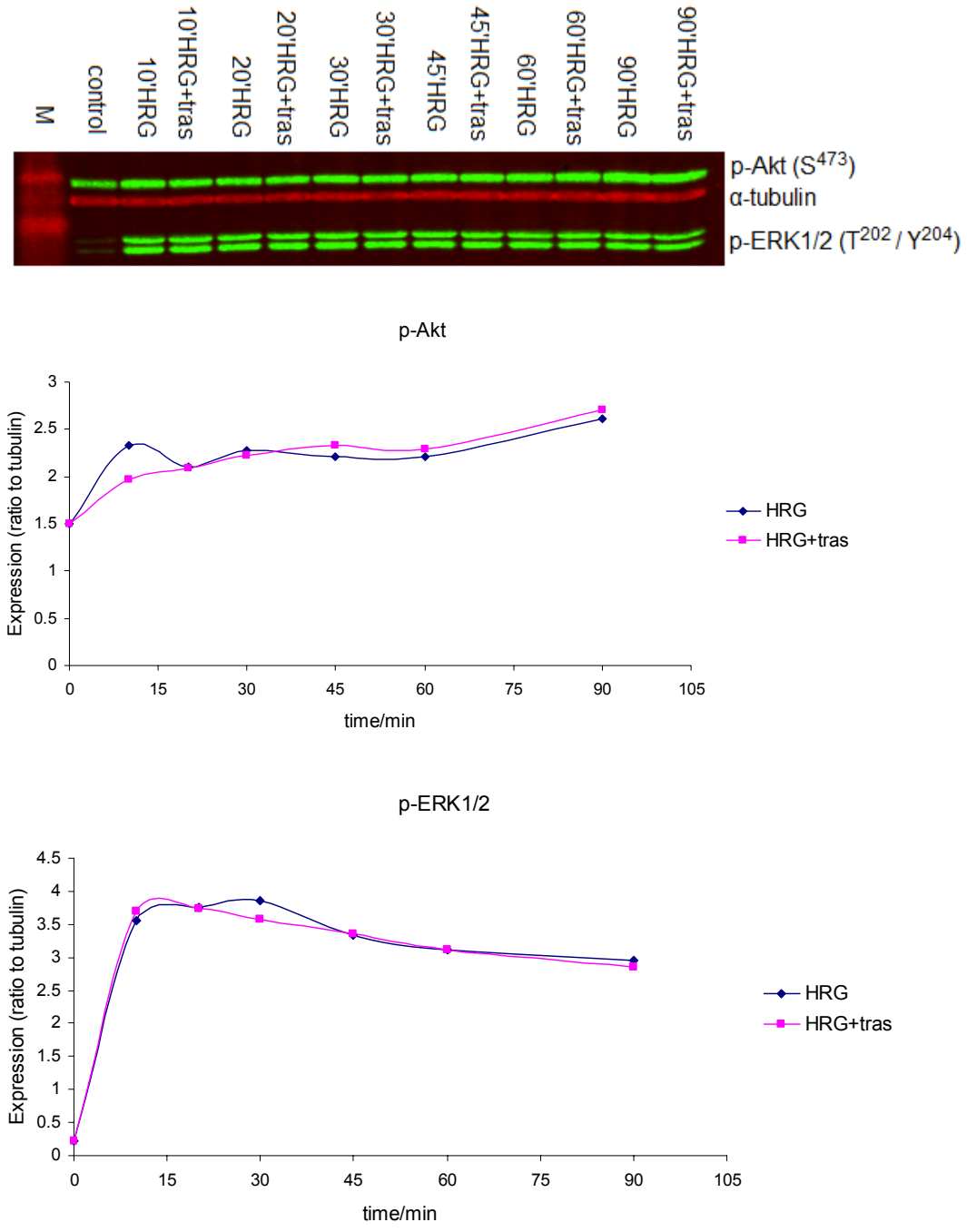

Figure 46 Time-course profiles of p-Akt (S^{473}) and p-ERK1/2(T^{202}/Y^{204}) in BT474 cells stimulated by 1nM HRG either with or without 100nM trastuzumab (tras). 'M' denotes protein ladder. Results were indicated as the ratio of the OD of phospho-targets to α-tubulin.

As previously described in this section, after stimulation of MCF-7 cells with HRG the level of p-ERK1/2 was enhanced by trastuzumab, while, the phosphorylation of the upstream molecule MEK1/2 was reduced. This contrary result was not due to the regulation of the interaction between HER-2 and HER-3 as mentioned above. It is possible that the transcriptional feedback plays a role in the regulation of the level of p-MEK1/2 and p-ERK1/2. If so, signalling alteration triggered by trastuzumab would be blocked by CHX, which blocks *de novo* protein synthesis. However, the reversal of the down-regulation of p-MEK1/2 was not observed (Figure 47). The regulation of p-ERK1/2 by trastuzumab was not mediated by transcriptional feedback either since the early enhancement of the level of p-ERK1/2 was still present in the presence of CHX (Figure 48). Another possibility is that crosstalk with another pathway regulates the Raf/MEK/ERK pathway at the node of MEK1/2. It was reported that p38 MAPK inhibited MEK1/2 through the activation of protein phosphatases (298). However, p-p38 MAPK was activated under the treatment of HRG plus trastuzumab at a very late time point (90 min) (Figure 49). It is inconsistent that this late activation of p38 MAPK would affect the early decrease of p-MEK1/2. Additionally, it was reported that ERK1/2 could exert negative feedback on MEK1 through the inhibitory phosphorylation of MEK1 at $T^{292/386}$, thereby facilitating the dephosphorylation of the activating residues of $S^{217/221}$ (240, 299). It is feasible that trastuzumab may cause the dissociation of MEK1 from the MEK1-MEK2 complex or enhance the inhibitory phosphorylation of MEK1 at T^{292}. A recently published study (300) showed that the knockout or dissociation of MEK1 from MEK1-MEK2 heterodimer could enhance the phosphorylation of MEK2 at $S^{222/226}$ and ERK1/2 at T^{202}/Y^{204} under the stimulation of growth factors. Compared to the wild type MEK1, mutant MEK1 with non-phosphorylatable T292A increased the level and duration of p-MEK1/2($S^{217/221}$) as well as p-ERK1/2(T^{202}/Y^{204}).

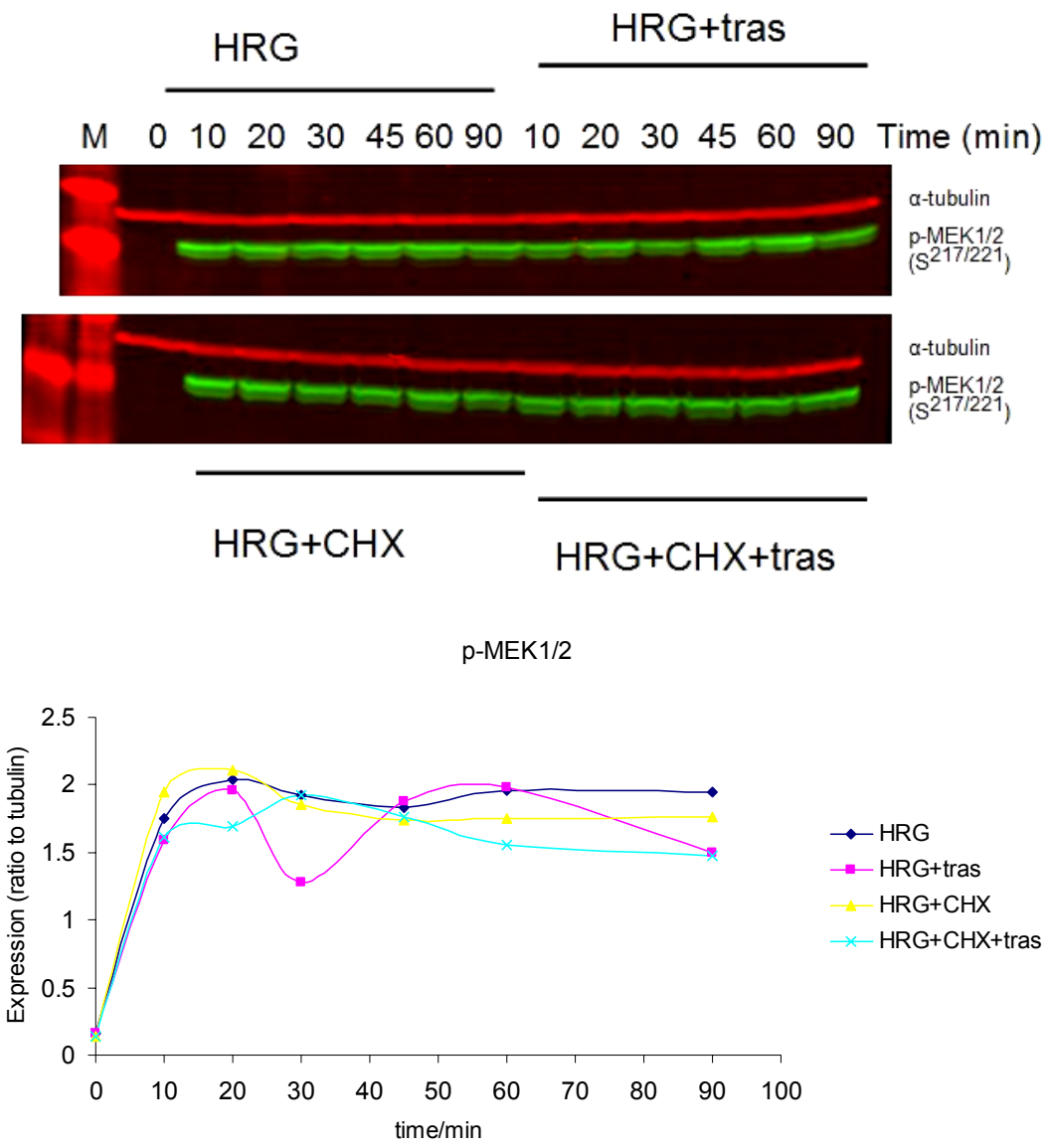

Figure 47 Time course profile of p-MEK1/2 ($S^{217/221}$) in MCF-7 cells treated with HRG plus trastuzumab or CHX or their combination. HRG, trastuzumab and CHX were used at 1nM, 100nM and 10μM respectively. 'M' denotes protein ladder. The results are presented as the ratio of OD of p-MEK1/2 to that α-tubulin.

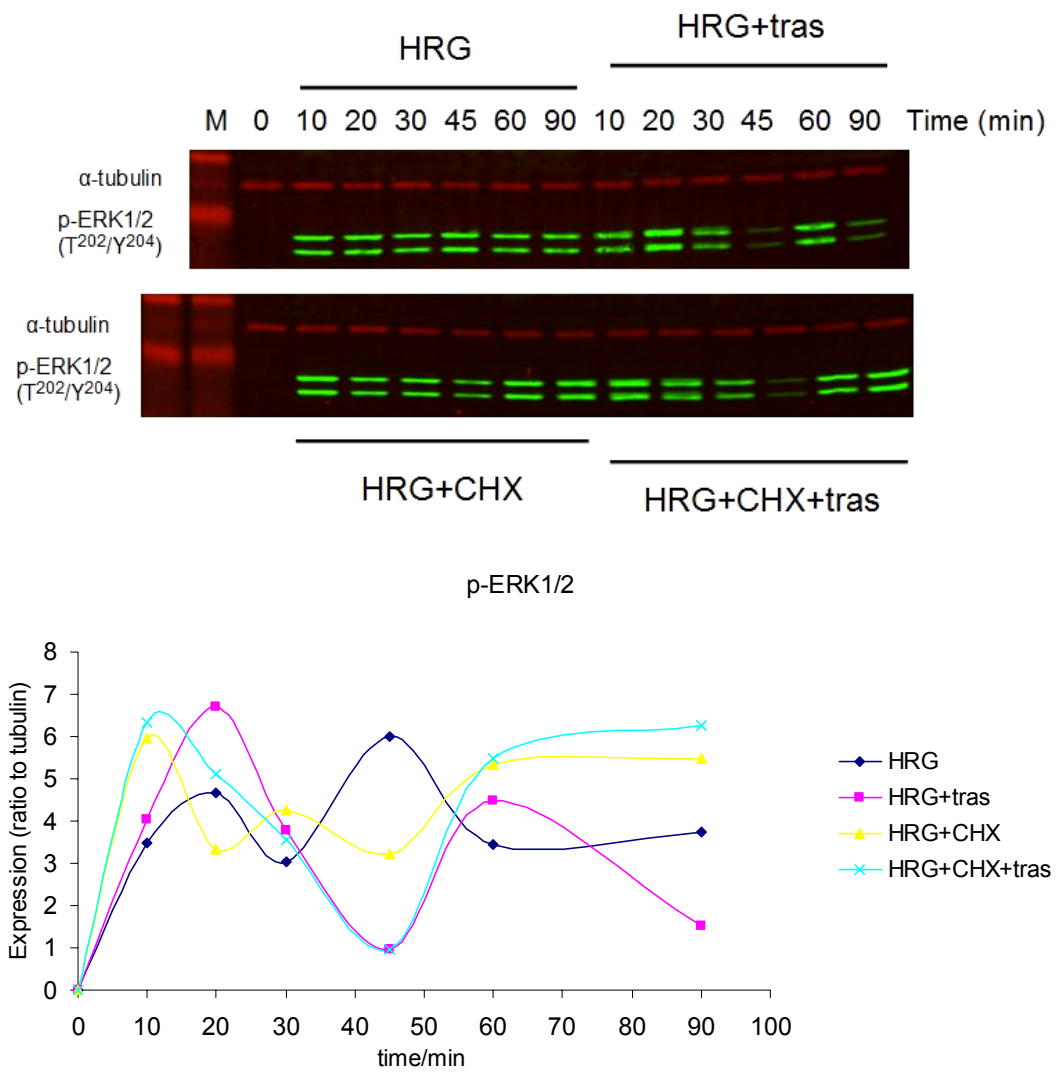

Figure 48 Time course profile of p-ERK1/2 (T^{202}/Y^{204}) in MCF-7 cells treated with HRG plus trastuzumab or CHX or their combination. HRG, Trastuzumab and CHX were used at 1nM, 100nM and 10μM respectively. 'M' denotes protein ladder. The results are presented as the ratio of OD of p-ERK1/2 to that α-tubulin.

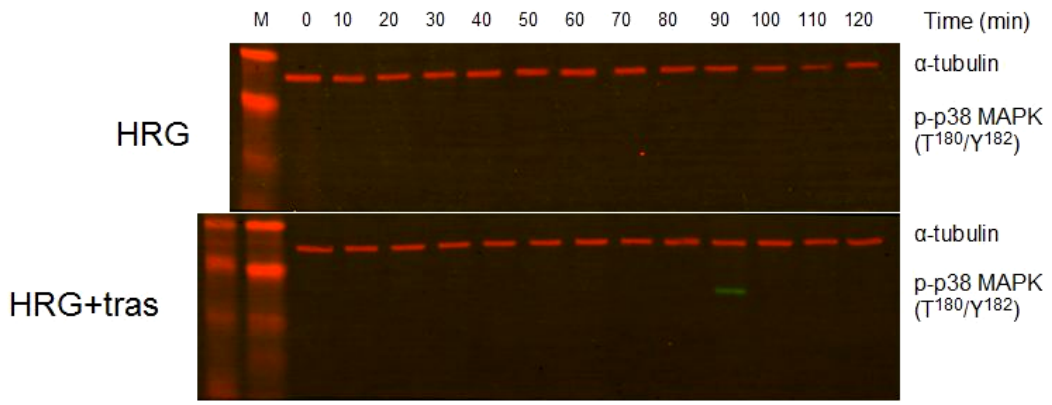

Figure 49 The activation of p38 MAPK in MCF-7 treated with HRG or HRG plus trastuzumab. p38 MAPK was activated when cells were treated with HRG plus trastuzumab for 90 min. HRG was used at 1nM. Trastuzumab was used at 100nM.

4.2.4 Discussion

Although several mechanisms of action of trastuzumab on breast cancers have been proposed (Introduction section 1.7.1), it has not been clearly elucidated why trastuzumab is only effective in HER-2 over-expressing metastatic breast cancers rather than in HER-2 low expressing breast cancers. Badache et al (301) in their review explained that trastuzumab could block the signalling mediated by HER-2 homodimers in HER-2 over-expressing cells but could not block the signalling mediated by heterodimers. In HER-2 over-expressing cells, the HER-2 homodimer could form spontaneously but could not in HER-2 low expressing cells. HER-2 over-expression is insufficient for the selection criteria of trastuzumab responding patients since only 30% of patients with HER-2 over-expression respond to trastuzumab monotherapy (302) and patients who were initially responsive to trastuzumab may develop resistance within one year (142). Yuste et al (303) and de Alava et al (304) demonstrated that trastuzumab inhibited the proliferation of HER-2 normally expressing MCF-7 cells which were transfected with membrane bound neuregulin *in vitro* and inhibited the growth of xenografts *in vivo*. In their studies, however, trastuzumab didn't affect the proliferation of wild type MCF-7 cells and HER-2 over-expressing MCF-7 cells, which was in line with my findings. In their studies, transmembrane neuregulin conferred sensitivity of MCF-7 cells to trastuzumab. In my study, trastuzumab only slowed down the proliferation rate of MCF-7 and MCF-

7/HER2-18 cells stimulated by 1nM of HRG, but trastuzumab had no effect on final cell numbers. However, trastuzumab inhibited the proliferation of both cell lines as well as BT474 cell line driven by 1nM EGF. It is therefore possible that trastuzumab inhibits tumour growth driven by EGF. These observations have clinical implications for where trastuzumab might be effective.

Since EGF binds HER-1 and HRG binds HER-3, trastuzumab's differential effects on growth could be explained by observations reported by Wehrman et al (115). They suggested that trastuzumab effectively inhibited the interaction of HER-2 and HER-1 but did not interfere with the interaction of HER-2 and HER-3. Treatment of cells expressing HER-1 and HER-2 with trastuzumab will induce more HER-1 homo-dimerisation and subsequently more internalization of HER-1. Diermeier et al (305) also showed that the growth inhibitory effect of trastuzumab was considerably modulated by HER-1 co-expression and subsequently the dimerisation of HER-1-HER-2 in HER-2 over-expressing cell lines. However, their study did not explain why trastuzumab just slowed down the growth rate under the stimulation of HRG.

Trastuzumab reduced the growth rate of both MCF-7 and MCF-7/HER2-18 cells stimulated by 1nM HRG, but the signalling induced by the intervention was different. The activation of ERK1/2 in MCF-7 cells was altered from the sustained to the transient by trastuzumab, while in MCF-7/HER2-18 cells trastuzumab did not change the duration but reduced the magnitude. Activation of Akt was reduced by trastuzumab in MCF-7 cells as well as in MCF-7/HER2-18 cells after treatment for 90 min. When comparing the time course profiles of p-ERK1/2 and p-Akt expression in MCF-7 cells induced by HRG+LY294002 (Figure 29) and HRG+trastuzumab (Figure 40 & 41), I observed a marked similarity of profiles caused by 5 μM LY294002 and 100 nM trastuzumab. Both drugs resulted in downstream inhibition of the activity of Akt over the whole time course and enhanced the activity of ERK1/2. LY294002 acts through inhibiting the kinase activity of PI3K, thereby inhibiting activation of Akt which inhibits the Raf/MEK1&2/ERK1&2 through phosphorylating Raf-1 at S^{259} as shown in Figure 50. It means that the inhibition of p-Akt by LY294002 can enhance the level of p-ERK1/2. Here, it is speculated that

trastuzumab may act on the signalling in MCF-7 cells in the same way as LY294002 does, suggesting that trastuzumab and LY294002 may have similar effects on cell growth. This hypothesis can be supported by the observation in the study of Zheng et al (306) that Akt inhibition by LY294002 could decrease cell growth rate of MCF-7 cells. These observations strongly argue that the inhibition of Akt plays a key role in trastuzumab's anti-proliferation effects. It is feasible that in MCF-7 cells, inhibition of EGF-triggering proliferation by trastuzumab is due to the inhibition of Akt and decreased HRG-triggering growth rate of MCF-7 and MCF-7/HER2-18 cells is also due to the inhibition of Akt. It was reported by other investigators (117) that the inhibition of Akt at least partly resulted in the changes of cell cycle and apoptosis regulatory molecules and the deactivation of PI3K and Akt was required for the anti-tumour effect of trastuzumab.

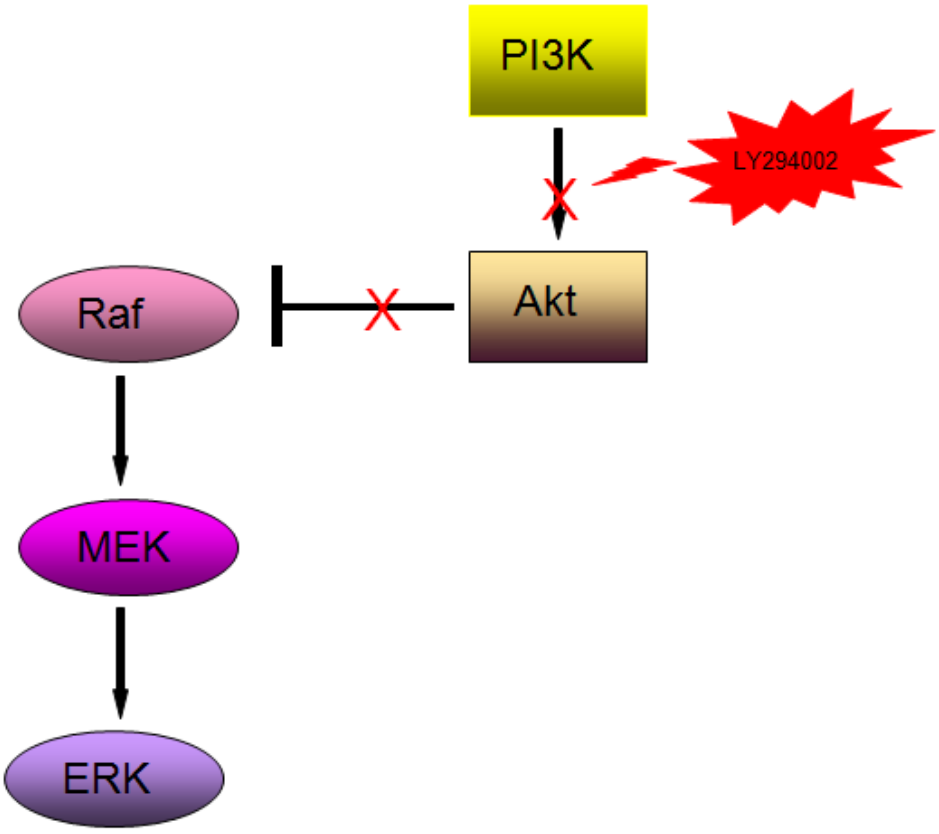

Figure 50 Schematic presentation of the crosstalk between PI3K/Akt and Raf/MEK/ERK pathways.

Studies presented in this thesis demonstrated that HER-2 phosphorylation alone is insufficient to drive cell growth. The slight phosphorylation induction of HER-2 by

HRG in MCF-7/HER2-18 cells was not due to the refractoriness of HER-2 to be phosphorylated, as was indicated by the dramatic induction by trastuzumab, pertuzumab and their combination. It demonstrated the high resting phosphorylation since over-expressed HER-2 was constitutively phosphorylated in breast cancer cells and tumours (307, 308), which may be induced by HER-2 homodimerisation. This observation supported the previous investigation reported by Yuste et al (303). In their study, the level of resting phospho-tyrosine at HER-2 in HER-2 over-expressing MCF-7 cells was very high and was not altered by the stimulation of neuregulin either. Although phosphorylation of HER-2 was slightly induced by HRG, the propagation of MCF-7/HER2-18 cells was increased 3.5 fold by the stimulation of 1nM HRG for 4 days. Moreover, the phosphorylation of HER-2 in MCF-7/HER2-18 cells was significantly up-regulated by trastuzumab (which was also observed by Yuste et al (303)), pertuzumab and their combination while cell growth was slowed down by trastuzumab and blocked by pertuzumab and their combination. Gijsen et al (309) demonstrated that the up-regulation of HER-2 phosphorylation by trastuzumab resulted from a feedback production of HER ligands which activated HER-1, HER-3 and HER-4 which in turn dimerised with HER-2. These observations suggested that the phosphorylation of HER-2 was not sufficient to drive cell growth. Since HRG is the specific ligand for HER-3, upon the stimulation of HRG, HER-3 would be phosphorylated and HER-2 required HER-3 to drive breast cancer cells to proliferate (310). Although the phosphorylation of HER-2 was not induced by HRG in HER-2 over-expressing MCF-7 cells, the phosphorylation of HER-3 was induced to a very high extent (303). The phosphorylation of HER-3 was inhibited by trastuzumab while the phosphorylation of HER-2 was increased (303). Activated HER-3 has six potential docking sites for SH2 domain of p85 subunit (the regulatory domain of PI3K) (89) and one proline-rich sequence forming consensus binding sites for the SH3 domain (311) and has potent activity mediating the PI3K/Akt pathway (312). In my study, although phosphorylation of HER-3 was not assayed, the activity of Akt in MCF-7/HER2-18 cells stimulated by HRG was slightly affected by trastuzumab before the 90-min point and then was reduced during the rest of the 2h time course.

Trastuzumab did not affect the level of p-Akt and p-ERK1/2 in BT474 cells stimulated by HRG, supporting the observation that trastuzumab does not affect the growth driven by HRG. Controversially, another reported study (305) demonstrated significant proliferation inhibition by trastuzumab in BT474 stimulated by HRG. However, consistent with the observation in MCF-7 cells, cell growth of BT474 cells driven by EGF was inhibited to the level comparable to that of control. It suggested again that trastuzumab may be more potent on the tumours driven by HER-1-binding ligands.

Since pertuzumab can block dimerisation with HER-2 and consequently inhibit signalling, the phosphorylation of Akt and/or ERK1/2 in MCF-7 was inhibited. Under the stimulation of HRG, both p-Akt and p-ERK1/2 in MCF-7 were reduced by pertuzumab to the basal line, suggesting that the association of HER-2 with HER-3 was vital for the induction for Akt and ERK1/2 pathways. Under the stimulation of EGF, only p-Akt was inhibited and p-ERK1/2 was not affected. Since HER-3 is deficient in kinase activity, pertuzumab is more potent in inhibiting HRG-mediated HER-3-HER-2 signalling than EGF-mediated HER-1-HER-2 signalling. The homodimerisation of HER-1 would increase when the HER-1-HER-2 complex was blocked by pertuzumab. These may explain why the levels of p-Akt and p-ERK1/2 stimulated by HRG in MCF-7 were inhibited to background level while the level of p-Akt was slightly reduced by pertuzumab and the level of p-ERK1/2 was not altered. Distinct from that in MCF-7 cells, the level of p-ERK1/2 was slightly reduced by pertuzumab for the first 50 min within the 2 h time course and then reduced to the background level over the duration of the time course in MCF-7/HER2-18 cells stimulated by HRG. It suggested that the signalling in MCF-7/HER2-18 cells was not blocked as effectively as in MCF-7 cells, which may be due to the over-expression of HER-2 and 100nM of pertuzumab was not sufficient to inhibit the signalling to the basal level. On the contrary, the level of p-Akt in MCF-7/HER2-18 cells stimulated by HRG was increased by pertuzumab for the first 50 min within the 2h time course and then went down to the similar level as that in HRG alone treatment group during the rest of the time course, suggesting that the interaction of HER-3-HER-2 was enhanced by pertuzumab since HER-3 was a potent mediator of PI3K/Akt pathway

as mentioned above. The enhancement of HER-3-HER-2 interaction was possibly due to the blockade of spontaneous homodimerisation of HER-2, which increased the chance of HER-3 to associate with free HER-2. The enhancement of HER-3-HER-2 interaction can also explain p-ERK1/2 profile.

When trastuzumab and pertuzumab were used in combination, trastuzumab and pertuzumab bind to the different epitopes at HER-2 and do not interfere with each other for binding when used together (157). The combination reduced the number of EGF-stimulated BT474 cells to fewer than the untreated group (control group). The combination led to continuous reduction of cell numbers during the 7-day time course, implying cell death. Nahta et al (288) demonstrated apoptosis induced by the combination in BT474 cells. They also observed that the inhibition of proliferation of BT474 cells either by trastuzumab or pertuzumab was mediated by cell arrest rather than by apoptosis. It was very interesting that the combined use of two cytostatic drugs had synergistic cytotoxic effects. However, the synergy was not observed in HRG-stimulated BT474 cells, suggesting the HERx-HER-2 complex dependent manner of the synergy in BT474 cells. The combined use of trastuzumab and pertuzumab conferred a promising example of effective multiplex targeted therapies. However, the molecular mechanism of synergy has not been elucidated. Although there are some preclinical and clinical studies about the anti-tumour activity of pertuzumab and the combined use with trastuzumab, there are very few published papers about the effects of pertuzumab and the combination on signalling in breast cancer cell lines. Further investigations of effects on signalling would uncover the biochemical mechanisms of action which in turn help researchers to develop therapeutic regimes to overcome drug resistance or effectively combine their use with other drugs or therapies.

In this study, variation was observed between two independent experiments measuring the same response of p-ERK1/2 and p-MEK1/2 to HRG stimulation in the presence or absence of trastuzumab. Variations may come from the technical replicates since in my study Western blotting on a different day measuring the same samples resulted in some degree of variation. Variations can be reduced if technical

replicates of one sample can be assigned on one blot and the results are shown as mean value with SD. Variation may also come from the biological replicates. Cells for the different experiments may have variations in viability so that the responses to HRG stimulation are different. Variation in cell viability can be due to over-digestion with trypsin/EDTA, over-confluence before sub-culturing and variable confluence at the time of HRG treatment. Although there are variations in terms of signalling response to trastuzumab between Figure 40 and 48, Figure 41 and 47, consistent early increase of p-ERK1/2 and some degree of inhibition of p-MEK1/2 by trastuzumab are observed in all individual experiments.

Generally, conclusions have been drawn from this study together with others' previous work.

1) Growth inhibitory effects of trastuzumab are ligand dependent, which means trastuzumab differentially interferes with differing HERx-HER-2 interactions.
2) Over-expression of HER-2 might be insufficient to be an indicator of the application of trastuzumab. The clinical use of trastuzumab might be expanded for example to EGF-driven low HER-2 expressing tumours.
3) Pertuzumab works effectively on low or high HER-2 expression cells line regardless of the types of ligands.
4) Trastuzumab and pertuzumab have synergistic anti-growth activity which is due to apoptosis in BT474 cells.
5) HER-3 and PI3K/Akt pathway plays a critical role in mediating cell growth and trastuzumab's anti-proliferation activity.

4.3 Tumour suppressor PTPN13 in breast cancer

4.3.1 PTPN13 as a candidate transcriptional regulator of the oscillation

PTPN13 (protein tyrosine phosphatase, non-receptor type 13) has been proposed as a tumour suppressor in breast cancers through the observation of epigenetic regulation by promoter hyper-methylation (313, 314). Expression levels of the protein are lower in breast cancers than in benign breast tumours (315) and this protein is a pro-apoptotic tyrosine phosphatase in breast cancers (316). PTPN13 inhibition drastically increased tumour growth in athymic mice and cell proliferation as well as cell invasion. It regulated breast cancer aggressiveness through being up-regulated by tamoxifen treatment and apoptosis was triggered by PTPN13 in breast cancer cells through inhibition of the PI3K/Akt pathway after treatment with tamoxifen (317). Tamoxifen-induced apoptosis was abrogated in stable antisense PTPN13 transfectants. The time-dependent expression of PTPN13 in MCF-7 cells specifically dephosphorylated IRS-1 (Insulin Receptor Substrate-1) and abolished the survival action of insulin-like growth factor through reducing the activity of the IRS-1/PI3K/Akt pathway (317, 318).

Initially, before screening candidate proteins which may transcriptionally modulate the oscillation in a gene expression assay, I found that PTPN13 was possibly involved in the modulation from a search of the literature. Zhu et al (319) demonstrated negative regulation of HER-2-mediated signalling pathways by PTPN13. They screened the phosphatases which may affect the phosphorylation of HER-2 with a phosphatase siRNA library. Among 193 phosphatases in the library, the knockdown of only 7 phosphatases increased dramatically the phosphorylation of HER-2 after growth factor stimulation. By over-expressing these 7 phosphatases in cells, they observed that over-expression of only PTPN13 and PTPN14 decreased the phosphorylation of HER-2. The phosphatase activity could only be detected in PTPN13. Moreover, increase of the phosphorylation of ERK1/2 and Akt by the knockdown of PTPN13 started immediately after stimulation for 5 min with EGF in HeLa cells. This observation was similar to the effect of HRG/EGF+CHX treatment

in MCF-7 cells in my study. The increase of phosphorylation of ERK1/2 and Akt by treatment of CHX started approximately 10 min after HRG or EGF stimulation. This similarity made me consider that PTPN13 might be a transcriptional feedback regulator of oscillation. Therefore, I knocked down PTPN13 with siRNA in MCF-7 cells within a time course experiment. The knockdown resulted in the death of a great number of cells with control siRNA. The number of cells adherent to the plate in the control siRNA group was much less than that in the PTPN13 siRNA group. The cell number in the PTPN13 siRNA group was less than in the non-transfection group. This suggested that the transfection reagent was toxic to MCF-7 cells. So, I incubated MCF-7 cells with transfection reagent with the RNAi tranfection protocol. No major difference in cell numbers adherent to the plate compared with the non-transfection group was observed. Since the confluence of the cells was dramatically different between PTPN13 siRNA group and control siRNA group, I did not carry on the time course experiment. However, an alternative way to find out whether PTPN13 was the transcriptional regulator of the oscillation was to seek whether this gene was modulated in the gene expression assay. PTPN13 mRNA expression was not induced by 1nM of HRG ($p>0.05$, 40'HRG *vs* control, student's t-test), suggesting PTPN13 was not a transcriptional feedback regulator of the oscillation (Figure 51).

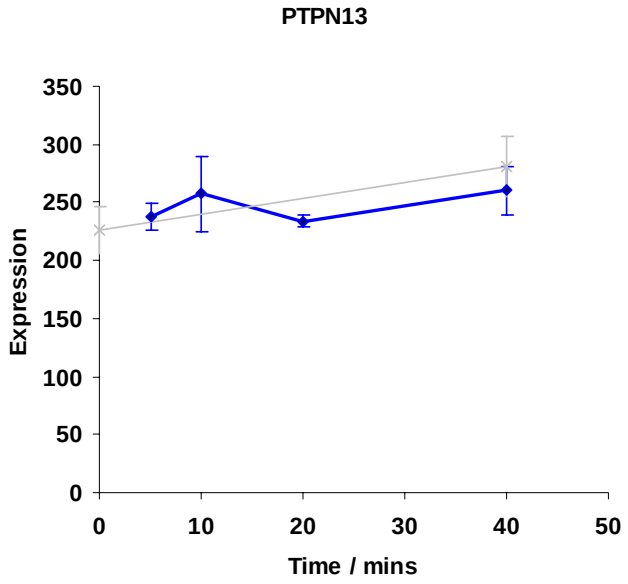

Figure 51 mRNA expression level of PTPN13 in MCF-7 stimulated by 1nM of HRG for 5, 10, 20 and 40 min. The grey line denotes the control and the blue line denotes the HRG stimulation group.

4.3.2 The expression level of PTPN13 was correlated with PIK3CA mutation

Bompard et al (317) demonstrated that PTPN13 was a tumour suppressor in breast cancer and could trigger apoptosis of breast cancer cells. In my study I observed that HER-2 over-expressing MCF-7 cells had a much lower expression of PTPN13 than parental MCF-7 (Figure 52). The expression level of PTPN13 was dramatically reduced by treatment with 0.01nM HRG, 100nM trastuzumab and HRG+trastuzumab for 3 days in MCF-7 cells. In contrast, the expression level in MCF-7/HER2-18 was not altered by HRG, but increased by trastuzumab and HRG+trastuzumab (Figure 52). The differential changes of the expression level of PTPN13 by the treatment of trastuzumab between MCF-7/HER2-18 were associated with differential growth. Trastuzumab slowed down the growth rate of MCF-7 stimulated by 0.01nM HRG and blocked the growth of MCF-7/HER2-18 stimulated by 0.01nM HRG (Figure 53). Additionally, in MCF-7/HER2-18 cells trastuzumab alone inhibited the growth compared to control, but in MCF-7 cells trastuzumab alone did not cause significant difference of the growth. These observations suggested that the increased level of PTPN13 was associated with the stronger growth inhibition. I hypothesized that the high level of PTPN13 in breast tumours was an indicator of favourable outcomes for breast cancer patients.

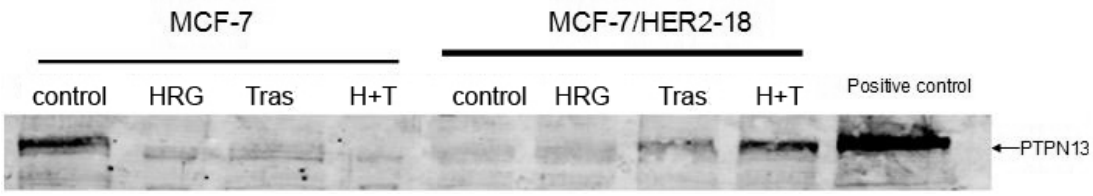

Figure 52 Differential expression level of PTPN13 in MCF-7 and MCF-7/HER2-18. Cells were treated with 0.01nM HRG, 100nM trastuzumab and their combination for 3 days before being subjected to Western Blot analysis. 'Tras' is a short form for trastuzumab. 'H+T' denotes the combination of 0.01nM HRG and 100nM trastuzumab. 'Positive control' was the whole HEK293 cell lysate and used as an indicator of PTPN13 molecular size.

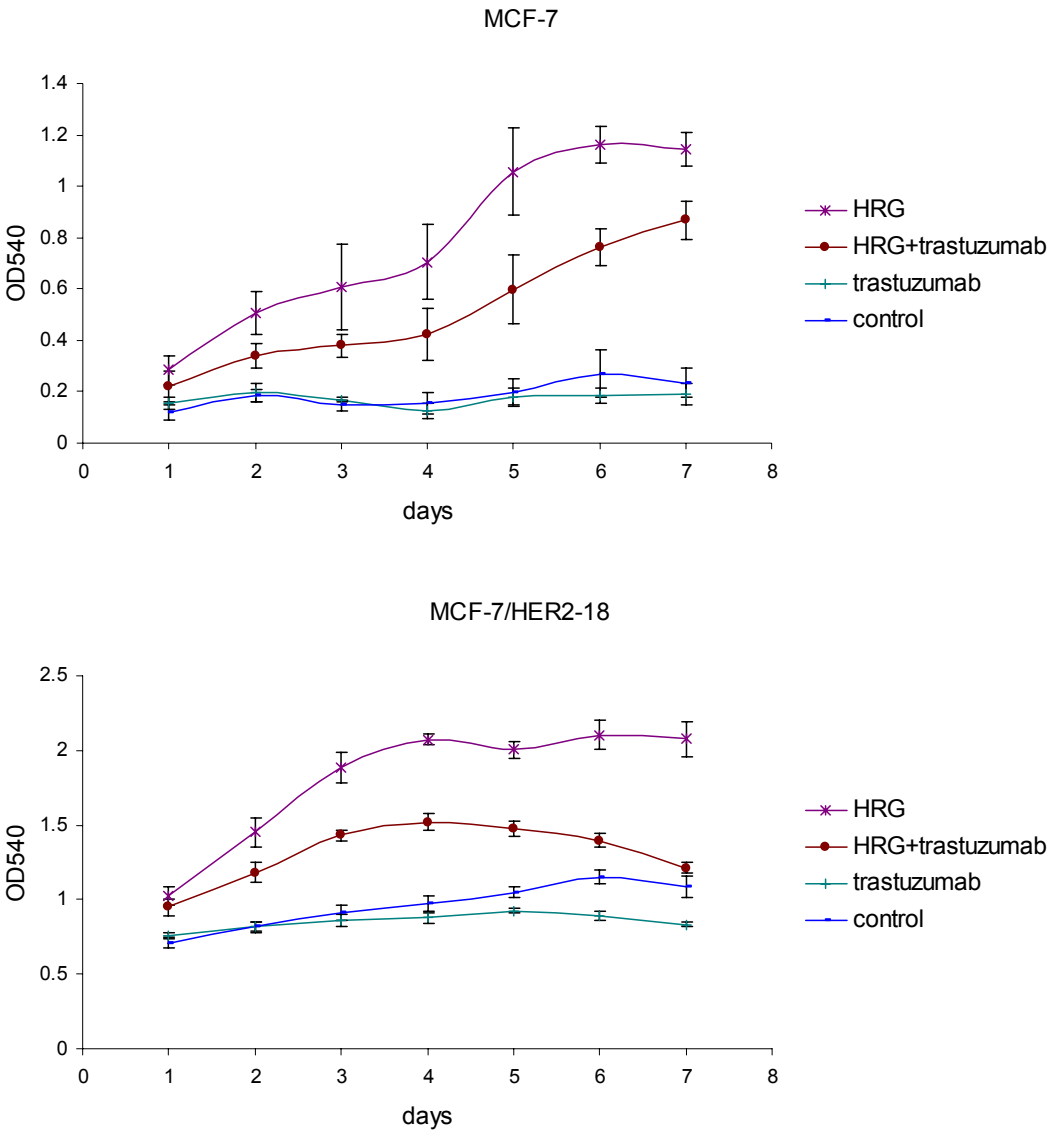

Figure 53 Time course growth assay of MCF-7 and MCF-7/HER2-18 cells. Cells were grown in 96-well plates and treated with 0.01nM HRG, 100nM trastuzumab and their combination for 1, 2, 3, 4, 5, 6 and 7 days respectively. SRB assay was applied to measure the relative cell numbers. The results are shown as the average of OD540 from 6 wells ±SD.

To test this possibility, I analyzed the expression level of PTPN13 by immunofluorescence in a cohort of 120 trastuzumab-treated tumours from metastatic breast cancer patients. Levels of PTPN13 expression did not associate directly with overall survival, HER-2 expression level or histological grade (Table 6). However I observed a correlation between the expression levels of PTPN13 and PIK3CA mutation (Spearman correlation coefficient -0.254, p value 0.005). The tumours harbouring oncogenic PIK3CA mutation had lower PTPN13 expression level compared to those without mutations ($p<0.01$, Mann-Whitney U test, Figure 54). Although the correlation of the protein level of PTPN13 with overall survival was not observed in this study, Revillion et al (320) suggested by analysing the mRNA levels from breast tumours that the expression of PTPN13 was an independent prognostic marker for overall survival in breast cancers. This controversy may result from the restricted subgroup of the tumours (trastuzumab-treated, metastatic, HER-2 over-expressing) in my study.

Table 6 Correlation analysis between PTPN13 expression level and other clinical parameters.

		PIK3CA Mutation (wild type or oncogenic mutation)	HER-2 expression (over-expression or normal expression)	Overall survival (months)	Grade
PTPN13 Expression	Correlation Coefficient	-0.254**	-0.012	0.007	0.057
	p value	0.005	0.899	0.936	0.539

2-tailed Spearman correlation test was used. The significant correlation is defined as p value less than 0.05. ** Correlation is significant.

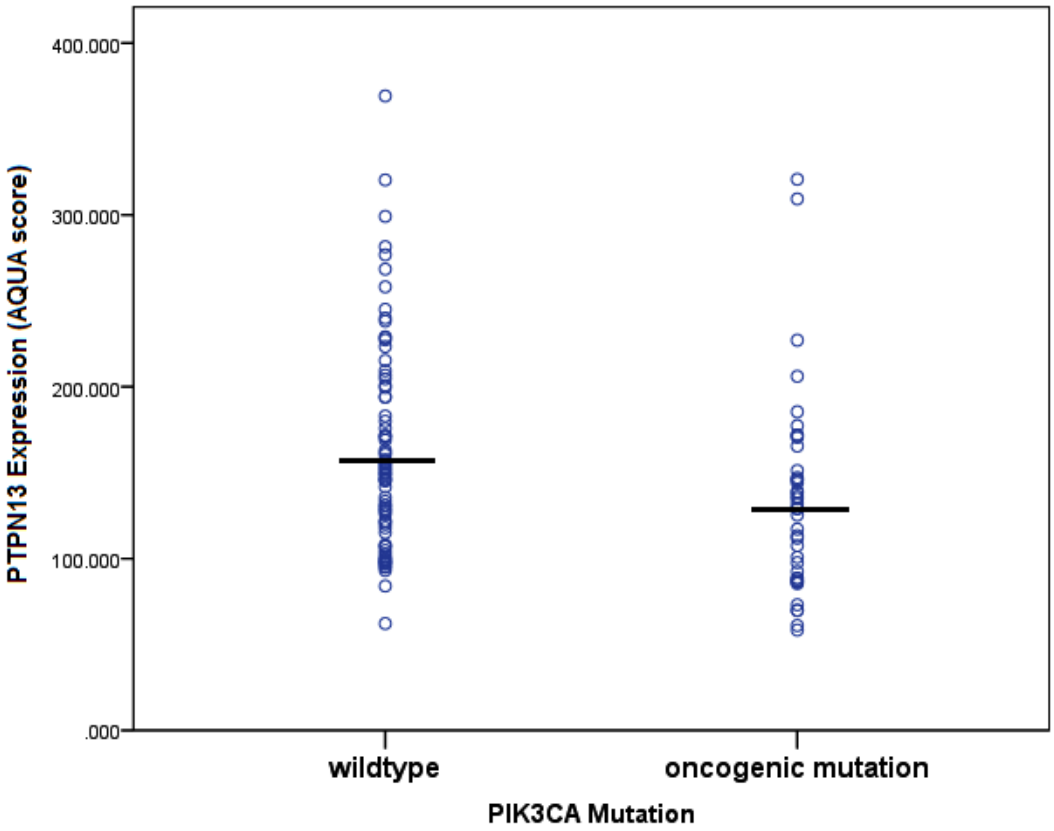

Figure 54 The correlation of PTPN13 expression level with PIK3CA mutation status in Trastuzumab-treated tumours from 120 metastatic breast cancer patients. Three sections from each tumour were analysed for the expression level of PTPN13 by immunofluorescence with AQUA imaging system. The y-axis value is the mean of the three AQUA scores from each tumour. The Black bars represent the individual medians from the two groups. Statistical significance was analyzed with Mann-Whitney U-test (p=0.006).

4.3.3 Discussion

The protein tyrosine phosphatase (PTP) super family functions co-ordinately with protein tyrosine kinases to regulate the amplification and duration of signalling pathways which are the basis for a wide range of fundamental physiological processes (313). In tumours this coordination is disrupted through for example the oncogenic mutation of kinases or suppression of phosphatases. Phosphatases often act as components of feedback loops in signalling pathways. For example, as mentioned previously DUSP family members were induced by growth factors and dephosphorylated p-ERK1/2 as part of a transcriptional negative feedback loop. Although PTPN13 was not observed to be involved in the transcriptional regulation

of the oscillation, it is possible that the existing PTPN13 protein in MCF-7 cells modulates the oscillation of p-ERK1/2 and p-Akt by dephosphorylating p-HER-2 and reducing the activity of PI3K/Akt pathway.

I observed in this study that the expression level of PTPN13 in trastuzumab-treated breast tumours was correlated with PIK3CA mutation status. The tumours harbouring the oncogenic mutation had lower PTPN13 expression, suggesting the high level of PTPN13 can protect cells from oncogenic PIK3CA mutation. The oncogenic PIK3CA mutations which caused the constitutive activation of PI3k/Akt pathway occurred in 18%-40% breast tumours (321). The study of Miron et al (322) suggested that the somatic PIK3CA mutation was an early event in breast cancer and played roles in cancer initiation rather than progression. Kataoka et al (145) demonstrated the association of the gain-of-function mutation of PIK3CA and the resistance to trastuzumab. Therefore, high level of PTPN13 may protect tissues from becoming malignant or be an indicator of trastuzumab responsiveness.

Conclusion

In this study, I have described the oscillation of both p-ERK1/2 and p-Akt expression after EGF and HRG activation in breast cancer cells. While oscillatory activation of p-ERK1/2 had been predicted by Kholodenko et al (235, 250-252), it required experimental validation, and I was able to demonstrate that not only could HRG as well as EGF produce p-ERK1/2 oscillation but another (Akt) pathway could also demonstrate this phenomenon. The presence of oscillation indicates the involvement of feedback signalling in ERK1/2 and Akt pathways (Figures 55 and 56). Based on the findings within this thesis, a scheme which demonstrates the oscillation-regulating transcriptional feedback loops, pathway interaction and impact of pertuzumab and trastuzumab on signalling is presented in Figure 55. Candidate feedback loops modulate dynamics of HER-mediated signalling primarily from three layers: enhancement of receptor activation by autocrine growth factors, positive or negative regulation of signalling molecules and regulation of transcription.

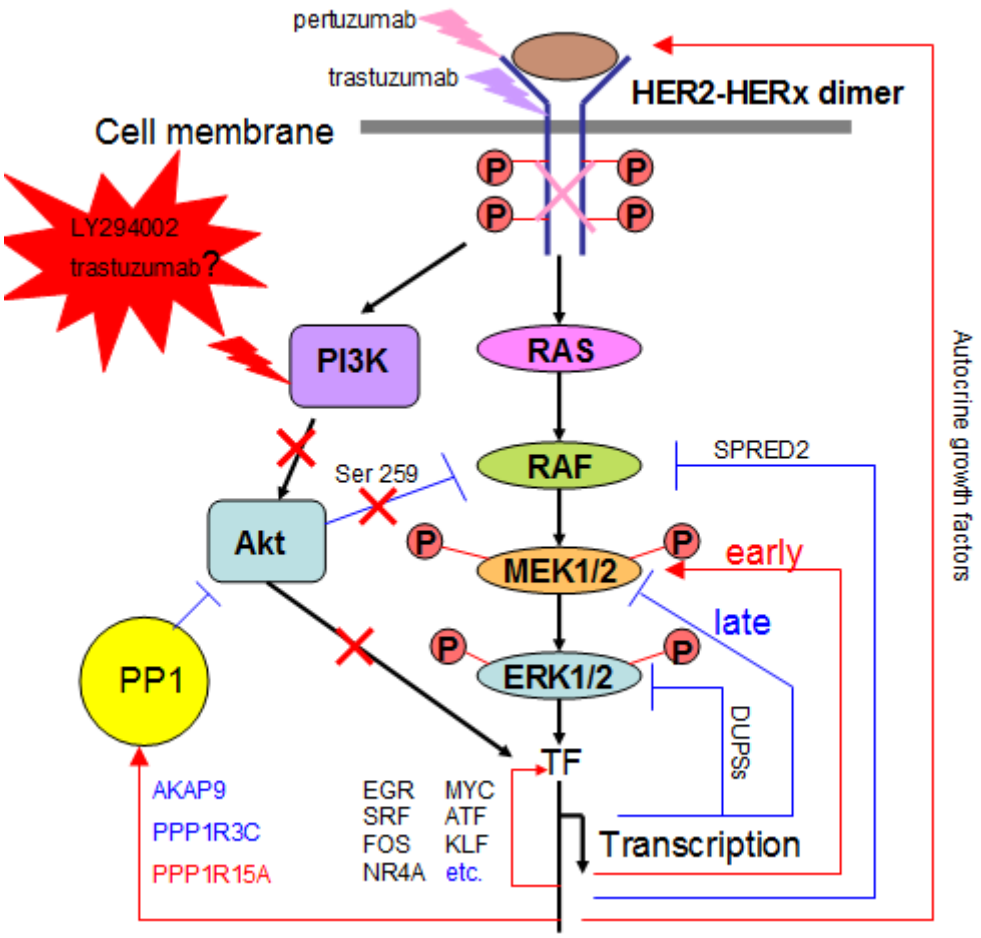

Figure 55 Scheme of HER-mediated signalling including crosstalk and transcriptional feedback loops based on the findings in this thesis. Ligand-bound HER receptors dimerise with HER-2 and activate the autophosphorylation of receptors. The phosphorylated residues on receptors provide docking sites for signalling molecules. Activated receptors mediate Ras/Raf/MEK/ERK and PI3K/Akt pathways. Effector molecules of the two pathways activate transcription factors (TF) that promote gene expression including genes functioning as feedback loops of the two pathways. Among the feedback loops, autocrine growth factors enhance the activation of HER receptors. DUSPs inhibit the phosphorylation of ERK1/2. Early positive and late negative feedback loops to MEK1/2 from unknown genes may be present. SPRED2 inhibits phosphorylation of Raf and inactivates Raf activity. PP1 can dephosphorylate Akt. AKAP9, PPP1R3C and PPP1R15A regulate the activity of PP1, so these three genes indirectly regulate Akt as negative transcriptional feedback loops. Gene expression of AKAP9 and PPP1R3C is down-regulated by HRG, but that of PPP11R15A is up-regulated. Ras/Raf/MEK/ERK and PI3K/Akt pathways interact through the inhibitory phosphorylation of Raf-1 at S^{259} from Akt. PI3K inhibitor LY294002 blocks (red cross) activation of Akt, therefore blocks (red cross) downstream gene expression and crosstalk with ERK1/2 pathway. The effects of LY294002 on signalling might be mimicked by trastuzumab. Pertuzumab binds the dimerisation arm of HER-2 and therefore blocks downstream signalling while trastuzumab binds the extracellular juxtamembrane domain of HER-2.

Referring to the experimental data presented in this thesis and published studies, an Ordinary Differential Equation (ODE)-based mathematical model established by Dr. Alexey Goltsov from SIMBIOS Centre, University of Abertay, Dundee in Scotland predicted that the negative feedback loop from p-ERK1/2 to SOS, negative feedback loops from DUSPs to p-ERK1/2, crosstalk with Akt pathway as well as the over-expression of HER-2 as a feedforward could modulate oscillations of p-ERK1/2. Simulations with HER-2 over-expression and DUSP expression generated by Dr. Goltsov fit the experimental data well (Figures 56 and 57). Negative feedback loops from Akt to casein kinase 2 (CK2)/glycogen synthase kinase 3 (GSK3) were also considered in this model. Further development of this model is underway at present.

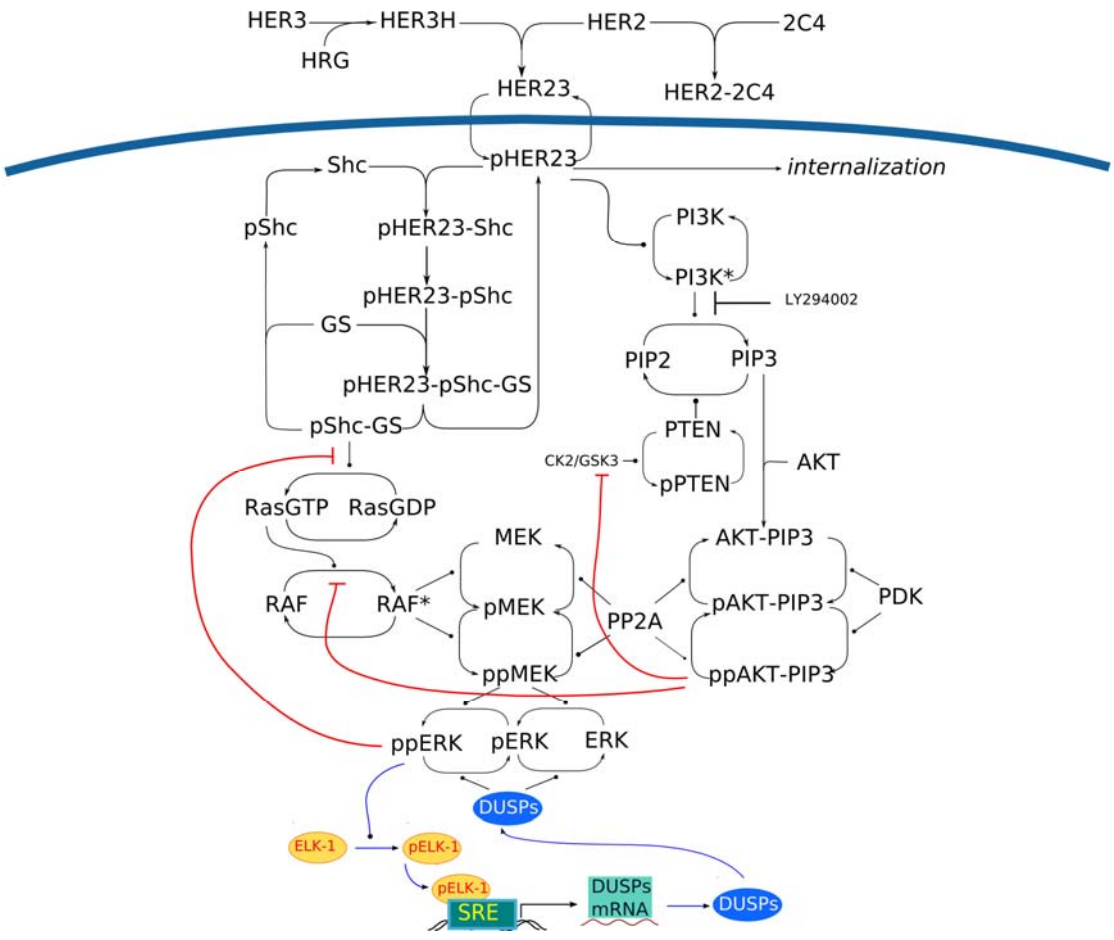

Figure 56 Scheme of mathematical model. Negative feedback loops from p-ERK1/2 to SOS, from DUSPs to p-ERK1/2 and crosstalk with Akt pathway as well HER-2 over-expression as feedforward were predicted to modulate oscillations of p-ERK1/2. Negative feedback loops from Akt to CK2/GSK3 were also considered in this model.

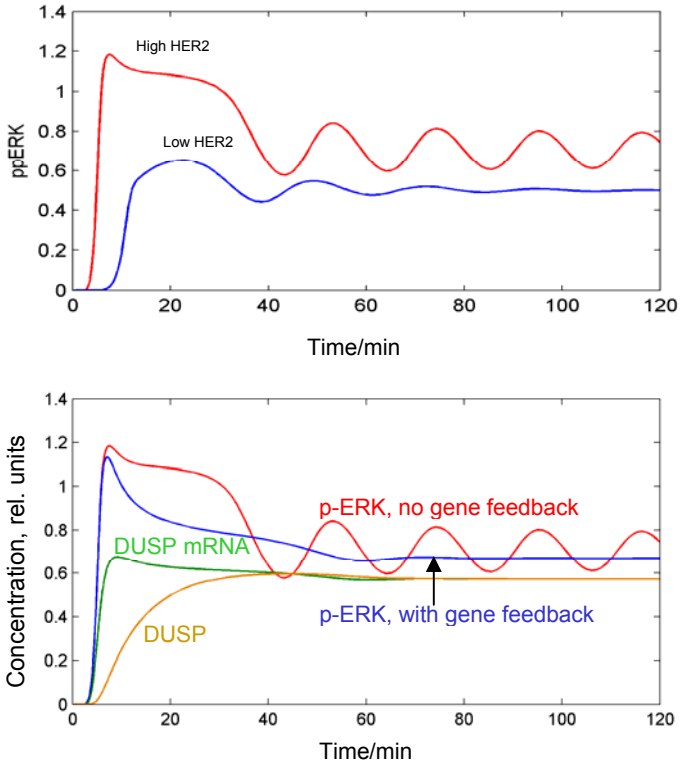

Figure 57 Simulations of the model. In the upper simulation figure, red curve is p-ERK1/2 time course profile with high HER-2 expression and blue curve is that with low HER-2 expression. In the lower simulation figure, red curve is p-ERK1/2 time course profile with no DUSP expression and blue curve is that with DUSP expression. Green curve is DUSP mRNA expression time course profile and orange curve is DUSP protein expression time course profile. Simulations of the model with/without HER-2 over-expression fitted well the experimental data that HER-2 over-expression could enhance oscillations. Simulations with/without DUSP gene expression also fitted well the experimental data, showing the modulation of p-ERK1/2 oscillations by DUSPs (kindly provided by Dr. Goltsov).

Significance of signalling oscillations

Oscillation is a particular form of dynamics and is a common biological phenomenon which has been shown to be significant in somite segmentation, cell cycle, and circadian control. Oscillations of p-ERK1/2 and p-Akt were observed in this study. The oscillation of p-Akt is a novel finding. In this study, oscillations were demonstrated as the outcome of the interaction of positive feedback/feedforward and negative feedback loops. Oscillations may reflect the defect of negative feedback loops in timing, strength and duration. In turn, this may indicate a defect in signalling control within breast cancer cells.

Components of the model / testing the model

The oscillation model established in collaboration with Dr. Alexey Goltsov is based on the previously published kinetic model of Raf/MEK/ERK and PI3K/PTEN/Akt signalling described by Faratian, Goltsov et al (323) which described the response kinetics of the signalling network to HRG-induced HER receptor activation and to pertuzumab on ERK1/2 and Akt activation in human carcinoma cell lines. Faratian and Goltsov's model took into account the following feedback loops and cross-talk in HER signalling: negative feedback through inhibition of Raf -1 activation by p-ERK1/2 phosphorylating SOS and cross-talk due to inhibition of Raf -1 activity by its phosphorylation by p-Akt at S^{259}. In addition to the above feedback loops and crosstalk, we also considered in the model gene regulation feedback due to p-ERK1/2-induced expression of DUSPs which in turn dephosphorylate p-ERK1/2. The model described phosphorylation of transcription factors (TF) by p-ERK1/2, binding of TF with DNA, transcription of DUSPs mRNA, and translation of DUSPs. The results of the modelling showed that modulation of these feedback loops by CHX, pertuzumab, and HER-2 expression levels significantly influenced the induction of p-ERK1/2 oscillation. Apart from DUSPs, possible genes that might regulate the oscillations such as regulatory subunits of PP1, SPRED2 and related transcription factors have been identified based on expression analysis and other published studies. Further work is needed to knockdown or over-expresses each gene and their combination to find out which genes modulate oscillations. Once oscillation-regulated genes are confirmed, it may be feasible to modulate oscillations transcriptionally through controlling gene product expression levels, timing or duration. The model-predicted feedback loops would also need further confirmation. For example, in order to test the existence of negative feedback loop from p-ERK1/2 to SOS, the four ERK1/2 phosphorylating sites in SOS (233) can be replaced with alanine residues. It will also be important to elucidate how oscillations are regulated spatially since timing together with location dynamics plays critical roles in determining cellular outcomes. Here, the developed RPPA method is an option to screen the feedback loops or molecules regulating oscillations in a high throughput manner. Large volumes of data on signalling molecule time course profiles can be

produced using this technique. Comparing the time course profiles under different treatments and through development of the mathematical model, it should be feasible to more completely define the pathways and mechanisms involved in the oscillation.

Impact of inhibitors and differential effects

Trastuzumab, pertuzumab and their combination altered the dynamics of either or both of the pathways and subsequently the cell growth in different cell lines. The oscillation pattern of p-ERK1/2 elicited by HRG in MCF-7 cells was altered from the sustained to the transient, but the amplitude was increased. Further experiments are required to elucidate how trastuzumab changed the oscillation pattern although I have suggested it is not through a transcriptional manner and trastuzumab may mimic the mechanism of action of LY294002. Pertuzumab inhibited signalling effectively in MCF-7 cells and pertuzumab and trastuzumab synergistically inhibited cellular growth driven by HRG. In the future the effectiveness of combined use of trastuzumab and pertuzumab can be tested in HRG-driven HER-2 'normally' expressing xenografts in mice. This work might expand the clinical use of trastuzumab not only in HER-2 over-expressing metastatic breast cancers but also in HER-2 'normally' expressing breast cancers and support the concept of multiplex therapy. As well, pertuzumab is a good option to bypass trastuzumab resistance. Further experiments are required to work out what resulted in the differential effects of pertuzumab on Akt signalling between MCF-7 cells and MCF-7/HER2-18 cells. As expected, pertuzumab inhibited ERK1/2 signalling in both cell lines stimulated by HRG. However, pertuzumab augmented Akt signalling in MCF-7/HER2-18 cells but inhibited signalling in MCF-7 cells. It is possible that this difference is caused by difference of HER-2/HER-3 molecule number ratio in the two cell lines and the concentration of pertuzumab used in this thesis primarily interferes with HER-2 homodimerization, so increases the chance of HER-3 interacting with HER-2 in MCF-7/HER2-18 cells but this concentration is high enough to block HER-2/HER-3 interaction in MCF-7 cells. In the future, increased concentrations of pertuzumab will be used in MCF-7/HER2-18 cells stimulated by HRG in order to block both HER-2 homodimerisation and HER-2/HER-3 interaction. HER-2 homo- and hetero-

interaction with HER-3 will be analysed. In addition, the expression levels of p-Akt will be analyzed under different concentrations of pertuzumab. It is expected that the higher concentrations would interfere with HER-2/HER-3 interaction and inhibit Akt signalling. The significance of this is that an optimal dose of pertuzumab might differ in breast cancers with varying HER-2/HER-3 ratio. RPPA and ICW both can be used to assay how the different concentrations of pertuzumab affect Akt signalling.

Ongoing and future modelling

The current model has considered a few factors that might modulate p-ERK1/2 oscillation. More work is needed to model p-Akt oscillation. As mentioned in Figure 55, besides the regulation of ERK1/2 by transcriptional feedback loops from DUSPs, MEK1/2 and Raf can also be regulated transcriptionally. Activation of HER receptors by growth factors can be enhanced by autocrine growth factors as positive feedback loops. Early transcription factors regulate the production of feedback loops that modulate HER-mediated signalling. Apart from the crosstalk with Raf/MEK/ERK pathway, PP1 might also regulate oscillation of p-Akt, so it is reasonable to consider in the model the gene expression of AKAP9, PPP1R3C and PPP1R15A which are the regulatory subunits of PP1. These factors should be taken into account in future modelling.

In summary, signalling oscillations demonstrate an interruption of tight feedback controls that are vital for cell growth. Oscillations may indicate the importance of feedback loops in controlling outgrowth of cancer cells. The impact of trastuzumab, pertuzumab and the combination on signalling and cell growth shows the promise of multiplex therapies and supports their value in more effective tumour control.

References

1. Ma L, *et al.* (2010) miR-9, a MYC/MYCN-activated microRNA, regulates E-cadherin and cancer metastasis. *Nat Cell Biol* 12(3):247-256.
2. Lu X & Kang Y (2007) Organotropism of breast cancer metastasis. (Translated from eng) *J Mammary Gland Biol Neoplasia* 12(2-3):153-162 (in eng).
3. Guise TA, Brufsky A, & Coleman RE (2010) Understanding and optimizing bone health in breast cancer. (Translated from eng) *Curr Med Res Opin* 26 Suppl 3:3-20 (in eng).
4. Talmadge JE (2007) Clonal selection of metastasis within the life history of a tumor. (Translated from eng) *Cancer Res* 67(24):11471-11475 (in eng).
5. Fidler IJ & Kripke ML (1977) Metastasis results from preexisting variant cells within a malignant tumor. (Translated from eng) *Science* 197(4306):893-895 (in eng).
6. Nowell PC (1976) The clonal evolution of tumor cell populations. (Translated from eng) *Science* 194(4260):23-28 (in eng).
7. Talmadge JE & Fidler IJ (1982) Cancer metastasis is selective or random depending on the parent tumour population. (Translated from eng) *Nature* 297(5867):593-594 (in eng).
8. Talmadge JE, Wolman SR, & Fidler IJ (1982) Evidence for the clonal origin of spontaneous metastases. (Translated from eng) *Science* 217(4557):361-363 (in eng).
9. Schmidt-Kittler O, *et al.* (2003) From latent disseminated cells to overt metastasis: genetic analysis of systemic breast cancer progression. (Translated from eng) *Proc Natl Acad Sci U S A* 100(13):7737-7742 (in eng).
10. Gray JW (2003) Evidence emerges for early metastasis and parallel evolution of primary and metastatic tumors. (Translated from eng) *Cancer Cell* 4(1):4-6 (in eng).
11. Hill RP, Chambers AF, Ling V, & Harris JF (1984) Dynamic heterogeneity: rapid generation of metastatic variants in mouse B16 melanoma cells. (Translated from eng) *Science* 224(4652):998-1001 (in eng).

12. Kalluri R & Weinberg RA (2009) The basics of epithelial-mesenchymal transition. (Translated from eng) *J Clin Invest* 119(6):1420-1428 (in eng).
13. Polyak K & Weinberg RA (2009) Transitions between epithelial and mesenchymal states: acquisition of malignant and stem cell traits. (Translated from eng) *Nat Rev Cancer* 9(4):265-273 (in eng).
14. Hay ED (2005) The mesenchymal cell, its role in the embryo, and the remarkable signaling mechanisms that create it. (Translated from eng) *Dev Dyn* 233(3):706-720 (in eng).
15. Yang J & Weinberg RA (2008) Epithelial-mesenchymal transition: at the crossroads of development and tumor metastasis. (Translated from eng) *Dev Cell* 14(6):818-829 (in eng).
16. Hugo H*, et al.* (2007) Epithelial--mesenchymal and mesenchymal--epithelial transitions in carcinoma progression. (Translated from eng) *J Cell Physiol* 213(2):374-383 (in eng).
17. Mani SA*, et al.* (2008) The epithelial-mesenchymal transition generates cells with properties of stem cells. (Translated from eng) *Cell* 133(4):704-715 (in eng).
18. Morel AP*, et al.* (2008) Generation of breast cancer stem cells through epithelial-mesenchymal transition. (Translated from eng) *PLoS ONE* 3(8):e2888 (in eng).
19. Bloom HJ & Richardson WW (1957) Histological grading and prognosis in breast cancer; a study of 1409 cases of which 359 have been followed for 15 years. (Translated from eng) *Br J Cancer* 11(3):359-377 (in eng).
20. American Joint Committee on Cancer (1997) *AJCC cancer staging manual* (Lippincott-Raven, Philadelphia: New York) 5th Ed.
21. American Cancer Society (2009) Breast cancer facts and figures 2009-2010. (Atlanta, Georgia: American Cancer Society).
22. Fisher B*, et al.* (1998) Tamoxifen for prevention of breast cancer: report of the National Surgical Adjuvant Breast and Bowel Project P-1 Study. *J Natl Cancer Inst* 90(18):1371-1388.

23. Virnig BA, Tuttle TM, Shamliyan T, & Kane RL (2010) Ductal carcinoma in situ of the breast: a systematic review of incidence, treatment, and outcomes. *J Natl Cancer Inst* 102(3):170-178.
24. Singletary SE, Patel-Parekh L, & Bland KI (2005) Treatment trends in early-stage invasive lobular carcinoma: a report from the National Cancer Data Base. *Ann Surg* 242(2):281-289.
25. Martinez V & Azzopardi JG (1979) Invasive lobular carcinoma of the breast: incidence and variants. *Histopathology* 3(6):467-488.
26. Borst MJ & Ingold JA (1993) Metastatic patterns of invasive lobular versus invasive ductal carcinoma of the breast. *Surgery* 114(4):637-641; discussion 641-632.
27. Li CI, *et al.* (2000) Changing incidence rate of invasive lobular breast carcinoma among older women. *Cancer* 88(11):2561-2569.
28. Moran MS, Yang Q, & Haffty BG (2009) The Yale University experience of early-stage invasive lobular carcinoma (ILC) and invasive ductal carcinoma (IDC) treated with breast conservation treatment (BCT): analysis of clinical-pathologic features, long-term outcomes, and molecular expression of COX-2, Bcl-2, and p53 as a function of histology. *Breast J* 15(6):571-578.
29. Reimer T (2008) Management of Rare Histological Types of Breast Tumours. *Breast Care (Basel)* 3(3):190-196.
30. Gunhan-Bilgen I & Oktay A (2007) Tubular carcinoma of the breast: mammographic, sonographic, clinical and pathologic findings. *Eur J Radiol* 61(1):158-162.
31. Diab SG, *et al.* (1999) Tumor characteristics and clinical outcome of tubular and mucinous breast carcinomas. *J Clin Oncol* 17(5):1442-1448.
32. Oakley GJ, 3rd, *et al.* (2006) HER-2 amplification in tubular carcinoma of the breast. *Am J Clin Pathol* 126(1):55-58.
33. Sinclair S & Swain SM (2010) Primary systemic chemotherapy for inflammatory breast cancer. *Cancer* 116(11 Suppl):2821-2828.
34. Caliskan M, *et al.* (2008) Paget's disease of the breast: the experience of the European Institute of Oncology and review of the literature. *Breast Cancer Res Treat* 112(3):513-521.

35. Marcus E (2004) The management of Paget's disease of the breast. *Curr Treat Options Oncol* 5(2):153-160.
36. Telli ML, Horst KC, Guardino AE, Dirbas FM, & Carlson RW (2007) Phyllodes tumors of the breast: natural history, diagnosis, and treatment. *J Natl Compr Canc Netw* 5(3):324-330.
37. Ma XJ, *et al.* (2004) A two-gene expression ratio predicts clinical outcome in breast cancer patients treated with tamoxifen. *Cancer Cell* 5(6):607-616.
38. Pohlmann PR, Mayer IA, & Mernaugh R (2009) Resistance to Trastuzumab in Breast Cancer. *Clin Cancer Res* 15(24):7479-7491.
39. Perou CM, *et al.* (2000) Molecular portraits of human breast tumours. *Nature* 406(6797):747-752.
40. Sorlie T, *et al.* (2001) Gene expression patterns of breast carcinomas distinguish tumor subclasses with clinical implications. *Proc Natl Acad Sci U S A* 98(19):10869-10874.
41. Sorlie T, *et al.* (2003) Repeated observation of breast tumor subtypes in independent gene expression data sets. *Proc Natl Acad Sci U S A* 100(14):8418-8423.
42. Sotiriou C, *et al.* (2003) Breast cancer classification and prognosis based on gene expression profiles from a population-based study. *Proc Natl Acad Sci U S A* 100(18):10393-10398.
43. Borresen-Dale AL (2003) TP53 and breast cancer. (Translated from eng) *Hum Mutat* 21(3):292-300 (in eng).
44. Rouzier R, *et al.* (2005) Breast cancer molecular subtypes respond differently to preoperative chemotherapy. *Clin Cancer Res* 11(16):5678-5685.
45. Brenton JD, Carey LA, Ahmed AA, & Caldas C (2005) Molecular classification and molecular forecasting of breast cancer: ready for clinical application? *J Clin Oncol* 23(29):7350-7360.
46. Carey L, Perou CM, & Dressler LG (2004) Race and the poor prognosis basal-like breast cancer (BBC) phenotype in the population-based Carolina Breast Cancer Study (Abstract 9510). *J Clin Oncol* 22.

47. Rouzier R, Anderson K, & Hess KR (2004) Basal and luminal types of breast cancer defined by gene expression patterns respond differently to neoadjuvant chemotherapy. *San Antonio Breast Cancer Symposium*.
48. Turner N, Tutt A, & Ashworth A (2004) Hallmarks of 'BRCAness' in sporadic cancers. *Nat Rev Cancer* 4(10):814-819.
49. Kennedy RD, Quinn JE, Mullan PB, Johnston PG, & Harkin DP (2004) The role of BRCA1 in the cellular response to chemotherapy. *J Natl Cancer Inst* 96(22):1659-1668.
50. Pusztai L, Mazouni C, Anderson K, Wu Y, & Symmans WF (2006) Molecular classification of breast cancer: limitations and potential. *Oncologist* 11(8):868-877.
51. Joy JE, Penhoet EE, & Petitti DB (2005) *Saving women's lives: strategies for improving breast cancer detection and diagnosis* (Natl Academy Pr).
52. Domchek SM*, et al.* (2003) Application of breast cancer risk prediction models in clinical practice. *J Clin Oncol* 21(4):593-601.
53. Ford D*, et al.* (1998) Genetic heterogeneity and penetrance analysis of the BRCA1 and BRCA2 genes in breast cancer families. *The American Journal of Human Genetics* 62(3):676-689.
54. Boyd NF*, et al.* (2002) Heritability of mammographic density, a risk factor for breast cancer. *N Engl J Med* 347(12):886-894.
55. Ursin G*, et al.* (2003) Mammographic density and breast cancer in three ethnic groups. *Cancer Epidemiol Biomarkers Prev* 12(4):332-338.
56. Loman N, Johannsson O, Kristoffersson U, Olsson H, & Borg A (2001) Family history of breast and ovarian cancers and BRCA1 and BRCA2 mutations in a population-based series of early-onset breast cancer. *J Natl Cancer Inst* 93(16):1215-1223.
57. Anonymous (2001) Familial breast cancer: collaborative reanalysis of individual data from 52 epidemiological studies including 58,209 women with breast cancer and 101,986 women without the disease. *Lancet* 358(9291):1389-1399.
58. Begg CB (2002) On the use of familial aggregation in population-based case probands for calculating penetrance. *J Natl Cancer Inst* 94(16):1221-1226.

59. Russo J, Tay LK, & Russo IH (1982) Differentiation of the mammary gland and susceptibility to carcinogenesis. *Breast Cancer Res Treat* 2(1):5-73.

60. Russo J, Rivera R, & Russo IH (1992) Influence of age and parity on the development of the human breast. *Breast Cancer Res Treat* 23(3):211-218.

61. Russo J & Russo IH (1999) Cellular basis of breast cancer susceptibility. *Oncol Res* 11(4):169-178.

62. Kelsey JL, Gammon MD, & John EM (1993) Reproductive factors and breast cancer. *Epidemiol Rev* 15(1):36-47.

63. Anonymous (2002) Breast cancer and breastfeeding: collaborative reanalysis of individual data from 47 epidemiological studies in 30 countries, including 50302 women with breast cancer and 96973 women without the disease. *Lancet* 360(9328):187-195.

64. Gompel A & Plu-Bureau G (2010) Is the decrease in breast cancer incidence related to a decrease in postmenopausal hormone therapy? (Translated from eng) *Ann N Y Acad Sci* 1205:268-276 (in eng).

65. Rohan TE & McMichael AJ (1988) Alcohol consumption and risk of breast cancer. *Int J Cancer* 41(5):695-699.

66. Fentiman IS (2001) Fixed and modifiable risk factors for breast cancer. *Int J Clin Pract* 55(8):527-530.

67. Ellison RC, Zhang Y, McLennan CE, & Rothman KJ (2001) Exploring the relation of alcohol consumption to risk of breast cancer. *Am J Epidemiol* 154(8):740-747.

68. Sneyd MJ, Paul C, Spears GF, & Skegg DC (1991) Alcohol consumption and risk of breast cancer. *Int J Cancer* 48(6):812-815.

69. Gapstur SM, Potter JD, Sellers TA, & Folsom AR (1992) Increased risk of breast cancer with alcohol consumption in postmenopausal women. *Am J Epidemiol* 136(10):1221-1231.

70. Singletary KW & Gapstur SM (2001) Alcohol and breast cancer: review of epidemiologic and experimental evidence and potential mechanisms. *Jama* 286(17):2143-2151.

71. Adami HO, Lund E, Bergstrom R, & Meirik O (1988) Cigarette smoking, alcohol consumption and risk of breast cancer in young women. *Br J Cancer* 58(6):832-837.
72. Rosenberg L, Palmer JR, Miller DR, Clarke EA, & Shapiro S (1990) A case-control study of alcoholic beverage consumption and breast cancer. *Am J Epidemiol* 131(1):6-14.
73. Freudenheim JL*, et al.* (1995) Lifetime alcohol consumption and risk of breast cancer. *Nutr Cancer* 23(1):1-11.
74. Jang M*, et al.* (1997) Cancer chemopreventive activity of resveratrol, a natural product derived from grapes. *Science* 275(5297):218-220.
75. Mgbonyebi OP, Russo J, & Russo IH (1998) Antiproliferative effect of synthetic resveratrol on human breast epithelial cells. *Int J Oncol* 12(4):865-869.
76. Subbaramaiah K*, et al.* (1998) Resveratrol inhibits cyclooxygenase-2 transcription and activity in phorbol ester-treated human mammary epithelial cells. *J Biol Chem* 273(34):21875-21882.
77. Society AC (2003) Breast cancer facts and figures 2003-2004. (Atlanta, Georgia: American Cancer Society).
78. Fisher B*, et al.* (2002) Twenty-year follow-up of a randomized trial comparing total mastectomy, lumpectomy, and lumpectomy plus irradiation for the treatment of invasive breast cancer. *N Engl J Med* 347(16):1233-1241.
79. Veronesi U*, et al.* (2002) Twenty-year follow-up of a randomized study comparing breast-conserving surgery with radical mastectomy for early breast cancer. *N Engl J Med* 347(16):1227-1232.
80. Cheng G, Kurita S, Torigian DA, & Alavi A (2010) Current status of sentinel lymph-node biopsy in patients with breast cancer. (Translated from Eng) *Eur J Nucl Med Mol Imaging* (in Eng).
81. Kirova YM (2010) Recent advances in breast cancer radiotherapy: Evolution or revolution, or how to decrease cardiac toxicity? (Translated from eng) *World J Radiol* 2(3):103-108 (in eng).

82. Selwood K (2009) Side effects of chemotherapy. *Cancer in Children and Young People: Acute Nursing Care*, (John Wiley & Sons, Ltd, Chichester, UK).
83. Clark GM, Osborne CK, & McGuire WL (1984) Correlations between estrogen receptor, progesterone receptor, and patient characteristics in human breast cancer. (Translated from eng) *J Clin Oncol* 2(10):1102-1109 (in eng).
84. Mannocci A*, et al.* (2010) Use of trastuzumab in HER2-positive metastatic breast cancer beyond disease progression: a systematic review of published studies. *Tumori* 96(3):385-391.
85. Langdon SP, Faratian D, Nagumo Y, Mullen P, & Harrison DJ (2010) Pertuzumab for the treatment of ovarian cancer. *Expert Opin Biol Ther* 10(7):1113-1120.
86. Glaros S, Atanaskova N, Zhao C, Skafar DF, & Reddy KB (2006) Activation function-1 domain of estrogen receptor regulates the agonistic and antagonistic actions of tamoxifen. *Mol Endocrinol* 20(5):996-1008.
87. Massarweh S*, et al.* (2008) Tamoxifen resistance in breast tumors is driven by growth factor receptor signaling with repression of classic estrogen receptor genomic function. (Translated from eng) *Cancer Res* 68(3):826-833 (in eng).
88. Yarden Y & Sliwkowski MX (2001) Untangling the ErbB signalling network. *Nat Rev Mol Cell Biol* 2(2):127-137.
89. Olayioye MA, Neve RM, Lane HA, & Hynes NE (2000) The ErbB signaling network: receptor heterodimerization in development and cancer. *Embo J* 19(13):3159-3167.
90. Lane NEHaHA (2005) ERBB receptors and cancer: the complexity of targeted inhibitors. *Nature Reviews Cancer* 5:341-354.
91. Takeshi Nagashima HS, Kaori Ide, Takashi Nakakuki, Yukitaka Tani, Kaoru Takahashi, Noriko Yumoto and Mariko Hatakeyama (2007) Quantitative Transcriptional Control of ErbB Receptor Signaling Undergoes Graded to Biphasic Response for Cell Differentiation. *J Biol Chem* 282(6):4045-4055.
92. von Kriegsheim A*, et al.* (2009) Cell fate decisions are specified by the dynamic ERK interactome. *Nat Cell Biol* 11(12):1458-1464.

93. Kholodenko BN (2006) Cell-signalling dynamics in time and space. *Nature Reviews Molecular Cell Biology* 7:165-176.
94. Baselga J & Swain SM (2009) Novel anticancer targets: revisiting ERBB2 and discovering ERBB3. *Nat Rev Cancer* 9(7):463-475.
95. Yarden ACaY (2006) EGF-ERBB signalling: towards the systems level. *Nature Reviews Molecular Cell Biology* 7:505-516.
96. Guy PM, Platko JV, Cantley LC, Cerione RA, & Carraway KL, 3rd (1994) Insect cell-expressed p180erbB3 possesses an impaired tyrosine kinase activity. *Proc Natl Acad Sci U S A* 91(17):8132-8136.
97. Citri A, Skaria KB, & Yarden Y (2003) The deaf and the dumb: the biology of ErbB-2 and ErbB-3. *Exp Cell Res* 284(1):54-65.
98. Lin NU & Winer EP (2004) New targets for therapy in breast cancer: small molecule tyrosine kinase inhibitors. *Breast Cancer Res* 6(5):204-210.
99. Mills GB*, et al.* (2001) The role of genetic abnormalities of PTEN and the phosphatidylinositol 3-kinase pathway in breast and ovarian tumorigenesis, prognosis, and therapy. *Semin Oncol* 28(5 Suppl 16):125-141.
100. Whyte J, Bergin O, Bianchi A, McNally S, & Martin F (2009) Key signalling nodes in mammary gland development and cancer. Mitogen-activated protein kinase signalling in experimental models of breast cancer progression and in mammary gland development. *Breast Cancer Res* 11(5):209.
101. Graus-Porta D, Beerli RR, Daly JM, & Hynes NE (1997) ErbB-2, the preferred heterodimerization partner of all ErbB receptors, is a mediator of lateral signaling. *Embo J* 16(7):1647-1655.
102. Tzahar E*, et al.* (1996) A hierarchical network of interreceptor interactions determines signal transduction by Neu differentiation factor/neuregulin and epidermal growth factor. *Mol Cell Biol* 16(10):5276-5287.
103. Slamon DJ*, et al.* (1987) Human breast cancer: correlation of relapse and survival with amplification of the HER-2/neu oncogene. *Science* 235(4785):177-182.
104. Hudziak RM, Schlessinger J, & Ullrich A (1987) Increased expression of the putative growth factor receptor p185HER2 causes transformation and tumorigenesis of NIH 3T3 cells. *Proc Natl Acad Sci U S A* 84(20):7159-7163.

105. Faltus T, *et al.* (2004) Silencing of the HER2/neu gene by siRNA inhibits proliferation and induces apoptosis in HER2/neu-overexpressing breast cancer cells. *Neoplasia* 6(6):786-795.
106. Choudhury A & Kiessling R (2004) Her-2/neu as a paradigm of a tumor-specific target for therapy. *Breast Dis* 20:25-31.
107. Mohsin SK, *et al.* (2005) Neoadjuvant trastuzumab induces apoptosis in primary breast cancers. *J Clin Oncol* 23(11):2460-2468.
108. Saeki Y, *et al.* (2009) Ligand-specific sequential regulation of transcription factors for differentiation of MCF-7 cells. *BMC Genomics* 10:545.
109. Karunagaran D, *et al.* (1996) ErbB-2 is a common auxiliary subunit of NDF and EGF receptors: implications for breast cancer. *Embo J* 15(2):254-264.
110. Beerli RR, *et al.* (1995) Neu differentiation factor activation of ErbB-3 and ErbB-4 is cell specific and displays a differential requirement for ErbB-2. *Mol Cell Biol* 15(12):6496-6505.
111. Slamon DJ, *et al.* (1989) Studies of the HER-2/neu proto-oncogene in human breast and ovarian cancer. *Science* 244(4905):707-712.
112. Roy V & Perez EA (2009) Beyond trastuzumab: small molecule tyrosine kinase inhibitors in HER-2-positive breast cancer. *Oncologist* 14(11):1061-1069.
113. Anonymous (2009) Herceptin® (trastuzumab) [full prescribing information]. *South San Francisco, CA: Genentech, Inc.* .
114. Albanell J & Baselga J (1999) Trastuzumab, a humanized anti-HER2 monoclonal antibody, for the treatment of breast cancer. *Drugs Today (Barc)* 35(12):931-946.
115. Wehrman TS, *et al.* (2006) A system for quantifying dynamic protein interactions defines a role for Herceptin in modulating ErbB2 interactions. *Proc Natl Acad Sci U S A* 103(50):19063-19068.
116. zum Buschenfelde CM, Hermann C, Schmidt B, Peschel C, & Bernhard H (2002) Antihuman epidermal growth factor receptor 2 (HER2) monoclonal antibody trastuzumab enhances cytolytic activity of class I-restricted HER2-specific T lymphocytes against HER2-overexpressing tumor cells. *Cancer Res* 62(8):2244-2247.

117. Yakes FM, *et al.* (2002) Herceptin-induced inhibition of phosphatidylinositol-3 kinase and Akt Is required for antibody-mediated effects on p27, cyclin D1, and antitumor action. *Cancer Res* 62(14):4132-4141.

118. Scotti ML, Langenheim JF, Tomblyn S, Springs AE, & Chen WY (2007) Additive effects of a prolactin receptor antagonist, G129R, and herceptin on inhibition of HER2-overexpressing breast cancer cells. *Breast Cancer Res Treat*.

119. Molina MA, *et al.* (2001) Trastuzumab (herceptin), a humanized anti-Her2 receptor monoclonal antibody, inhibits basal and activated Her2 ectodomain cleavage in breast cancer cells. *Cancer Res* 61(12):4744-4749.

120. Christianson TA, *et al.* (1998) NH2-terminally truncated HER-2/neu protein: relationship with shedding of the extracellular domain and with prognostic factors in breast cancer. *Cancer Res* 58(22):5123-5129.

121. Zabrecky JR, Lam T, McKenzie SJ, & Carney W (1991) The extracellular domain of p185/neu is released from the surface of human breast carcinoma cells, SK-BR-3. *J Biol Chem* 266(3):1716-1720.

122. Lin YZ & Clinton GM (1991) A soluble protein related to the HER-2 proto-oncogene product is released from human breast carcinoma cells. *Oncogene* 6(4):639-643.

123. Pupa SM, *et al.* (1993) The extracellular domain of the c-erbB-2 oncoprotein is released from tumor cells by proteolytic cleavage. *Oncogene* 8(11):2917-2923.

124. Brodowicz T, *et al.* (1997) Soluble HER-2/neu neutralizes biologic effects of anti-HER-2/neu antibody on breast cancer cells in vitro. *Int J Cancer* 73(6):875-879.

125. Leitzel K, *et al.* (1995) Elevated serum c-erbB-2 antigen levels and decreased response to hormone therapy of breast cancer. *J Clin Oncol* 13(5):1129-1135.

126. Yamauchi H, *et al.* (1997) Prediction of response to antiestrogen therapy in advanced breast cancer patients by pretreatment circulating levels of extracellular domain of the HER-2/c-neu protein. *J Clin Oncol* 15(7):2518-2525.

127. Codony-Servat J, Albanell J, Lopez-Talavera JC, Arribas J, & Baselga J (1999) Cleavage of the HER2 ectodomain is a pervanadate-activable process that is inhibited by the tissue inhibitor of metalloproteases-1 in breast cancer cells. *Cancer Res* 59(6):1196-1201.

128. Lipton A, *et al.* (2002) Elevated serum Her-2/neu level predicts decreased response to hormone therapy in metastatic breast cancer. *J Clin Oncol* 20(6):1467-1472.

129. Perez EA, *et al.* (2002) A randomized phase II study of sequential docetaxel and doxorubicin/cyclophosphamide in patients with metastatic breast cancer. *Ann Oncol* 13(8):1225-1235.

130. Colomer R, *et al.* (2004) Biweekly paclitaxel plus gemcitabine in advanced breast cancer: phase II trial and predictive value of HER2 extracellular domain. *Ann Oncol* 15(2):201-206.

131. Fornier MN, *et al.* (2005) Serum HER2 extracellular domain in metastatic breast cancer patients treated with weekly trastuzumab and paclitaxel: association with HER2 status by immunohistochemistry and fluorescence in situ hybridization and with response rate. *Ann Oncol* 16(2):234-239.

132. Kostler WJ, *et al.* (2004) Monitoring of serum Her-2/neu predicts response and progression-free survival to trastuzumab-based treatment in patients with metastatic breast cancer. *Clin Cancer Res* 10(5):1618-1624.

133. Baselga J, Albanell J, Molina MA, & Arribas J (2001) Mechanism of action of trastuzumab and scientific update. *Semin Oncol* 28(5 Suppl 16):4-11.

134. Lane HA, Motoyama AB, Beuvink I, & Hynes NE (2001) Modulation of p27/Cdk2 complex formation through 4D5-mediated inhibition of HER2 receptor signaling. *Ann Oncol* 12 Suppl 1:S21-22.

135. Barok M, *et al.* (2007) Trastuzumab causes antibody-dependent cellular cytotoxicity-mediated growth inhibition of submacroscopic JIMT-1 breast cancer xenografts despite intrinsic drug resistance. *Mol Cancer Ther* 6(7):2065-2072.

136. Kono K, *et al.* (2004) Trastuzumab (Herceptin) enhances class I-restricted antigen presentation recognized by HER-2/neu-specific T cytotoxic lymphocytes. *Clin Cancer Res* 10(7):2538-2544.

137. Baselga J, Norton L, Albanell J, Kim YM, & Mendelsohn J (1998) Recombinant humanized anti-HER2 antibody (Herceptin) enhances the antitumor activity of paclitaxel and doxorubicin against HER2/neu overexpressing human breast cancer xenografts. *Cancer Res* 58(13):2825-2831.

138. Mittendorf EA, Storrer CE, Shriver CD, Ponniah S, & Peoples GE (2006) Investigating the combination of trastuzumab and HER2/neu peptide vaccines for the treatment of breast cancer. *Ann Surg Oncol* 13(8):1085-1098.

139. Valabrega G, Montemurro F, & Aglietta M (2007) Trastuzumab: mechanism of action, resistance and future perspectives in HER2-overexpressing breast cancer. *Ann Oncol* 18(6):977-984.

140. Henson ES, Hu X, & Gibson SB (2006) Herceptin sensitizes ErbB2-overexpressing cells to apoptosis by reducing antiapoptotic Mcl-1 expression. *Clin Cancer Res* 12(3 Pt 1):845-853.

141. Lee S, *et al.* (2002) Enhanced sensitization to taxol-induced apoptosis by herceptin pretreatment in ErbB2-overexpressing breast cancer cells. *Cancer Res* 62(20):5703-5710.

142. Slamon DJ, *et al.* (2001) Use of chemotherapy plus a monoclonal antibody against HER2 for metastatic breast cancer that overexpresses HER2. *N Engl J Med* 344(11):783-792.

143. Berns K, *et al.* (2007) A functional genetic approach identifies the PI3K pathway as a major determinant of trastuzumab resistance in breast cancer. *Cancer Cell* 12(4):395-402.

144. Ben Ho park NED (2007) PI3 Kinase Activation and Response to Trastuzumab Therapy: What's neu with Herceptin Resistance? *Cancer Cell* 12:297-299.

145. Kataoka Y, *et al.* (2010) Association between gain-of-function mutations in PIK3CA and resistance to HER2-targeted agents in HER2-amplified breast cancer cell lines. *Ann Oncol* 21(2):255-262.

146. Nahta R, Takahashi T, Ueno NT, Hung MC, & Esteva FJ (2004) P27(kip1) down-regulation is associated with trastuzumab resistance in breast cancer cells. *Cancer Res* 64(11):3981-3986.

147. Nagy P, *et al.* (2005) Decreased accessibility and lack of activation of ErbB2 in JIMT-1, a herceptin-resistant, MUC4-expressing breast cancer cell line. *Cancer Res* 65(2):473-482.

148. Bussolati G, *et al.* (2005) A modified Trastuzumab antibody for the immunohistochemical detection of HER-2 overexpression in breast cancer. *Br J Cancer* 92(7):1261-1267.

149. Ritter CA, *et al.* (2007) Human breast cancer cells selected for resistance to trastuzumab in vivo overexpress epidermal growth factor receptor and ErbB ligands and remain dependent on the ErbB receptor network. *Clin Cancer Res* 13(16):4909-4919.

150. Motoyama AB, Hynes NE, & Lane HA (2002) The efficacy of ErbB receptor-targeted anticancer therapeutics is influenced by the availability of epidermal growth factor-related peptides. *Cancer Res* 62(11):3151-3158.

151. Lu Y, Zi X, Zhao Y, Mascarenhas D, & Pollak M (2001) Insulin-like growth factor-I receptor signaling and resistance to trastuzumab (Herceptin). *J Natl Cancer Inst* 93(24):1852-1857.

152. Huang X, *et al.* (2010) Heterotrimerization of the Growth Factor Receptors erbB2, erbB3, and Insulin-like Growth Factor-I Receptor in Breast Cancer Cells Resistant to Herceptin. *Cancer Res* 70(3):1204-1214.

153. Albanell J & Baselga J (2001) Unraveling resistance to trastuzumab (Herceptin): insulin-like growth factor-I receptor, a new suspect. *J Natl Cancer Inst* 93(24):1830-1832.

154. Baselga J, *et al.* (2010) Phase II Trial of Pertuzumab and Trastuzumab in Patients With Human Epidermal Growth Factor Receptor 2-Positive Metastatic Breast Cancer That Progressed During Prior Trastuzumab Therapy. *J Clin Oncol* 28(7):1138-1144.

155. Baselga J & Swain SM (2010) CLEOPATRA: A Phase III Evaluation of Pertuzumab and Trastuzumab for HER2-Positive Metastatic Breast Cancer. *Clin Breast Cancer* 10(6):489-491.

156. Agus DB, *et al.* (2002) Targeting ligand-activated ErbB2 signaling inhibits breast and prostate tumor growth. *Cancer Cell* 2(2):127-137.

157. Scheuer W, *et al.* (2009) Strongly enhanced antitumor activity of trastuzumab and pertuzumab combination treatment on HER2-positive human xenograft tumor models. *Cancer Res* 69(24):9330-9336.
158. Traxler P (2003) Tyrosine kinases as targets in cancer therapy - successes and failures. *Expert Opin Ther Targets* 7(2):215-234.
159. Macfarlane RJ & Gelmon KA (2011) Lapatinib for breast cancer: a review of the current literature. *Expert Opin Drug Saf* 10(1):109-121.
160. Arpino G, *et al.* (2007) Treatment of human epidermal growth factor receptor 2-overexpressing breast cancer xenografts with multiagent HER-targeted therapy. *J Natl Cancer Inst* 99(9):694-705.
161. O'Shaughnessy J, *et al.* (2008) A randomized study of lapatinib alone or in combination with trastuzumab in heavily pretreated HER2+ metastatic breast cancer progressing on trastuzumab therapy [abstract 1015]. *J Clin Oncol* 26(15 suppl):44s.
162. Montemurro F, Valabrega G, & Aglietta M (2004) Trastuzumab-based combination therapy for breast cancer. *Expert Opin Pharmacother* 5(1):81-96.
163. Montemurro F & Aglietta M (2005) Incorporating trastuzumab into the neoadjuvant treatment of HER2-overexpressing breast cancer. *Clin Breast Cancer* 6(1):77-80.
164. Osborne CK & Schiff R (2011) Mechanisms of endocrine resistance in breast cancer. (Translated from eng) *Annu Rev Med* 62:233-247 (in eng).
165. Arpino G, Wiechmann L, Osborne CK, & Schiff R (2008) Crosstalk between the estrogen receptor and the HER tyrosine kinase receptor family: molecular mechanism and clinical implications for endocrine therapy resistance. (Translated from eng) *Endocr Rev* 29(2):217-233 (in eng).
166. Chu I, Blackwell K, Chen S, & Slingerland J (2005) The dual ErbB1/ErbB2 inhibitor, lapatinib (GW572016), cooperates with tamoxifen to inhibit both cell proliferation- and estrogen-dependent gene expression in antiestrogen-resistant breast cancer. (Translated from eng) *Cancer Res* 65(1):18-25 (in eng).
167. Johnston S, *et al.* (2009) Lapatinib combined with letrozole versus letrozole and placebo as first-line therapy for postmenopausal hormone receptor-

positive metastatic breast cancer. (Translated from eng) *J Clin Oncol* 27(33):5538-5546 (in eng).

168. Schwartzberg LS, *et al.* (2010) Lapatinib plus letrozole as first-line therapy for HER-2+ hormone receptor-positive metastatic breast cancer. (Translated from eng) *Oncologist* 15(2):122-129 (in eng).
169. Marcom PK, *et al.* (2007) The combination of letrozole and trastuzumab as first or second-line biological therapy produces durable responses in a subset of HER2 positive and ER positive advanced breast cancers. *Breast Cancer Res Treat* 102(1):43-49.
170. Kaufman B, *et al.* (2009) Trastuzumab plus anastrozole versus anastrozole alone for the treatment of postmenopausal women with human epidermal growth factor receptor 2-positive, hormone receptor-positive metastatic breast cancer: results from the randomized phase III TAnDEM study. *J Clin Oncol* 27(33):5529-5537.
171. Mukohara T (2010) Mechanisms of resistance to anti-human epidermal growth factor receptor 2 agents in breast cancer. *Cancer Sci*:Epub ahead of print.
172. Andreas Gschwind OMFaAU (2004) The discovery of receptor tyrosine kinases: targets for cancer therapy. *Nature Reviews Cancer* 4:361-370.
173. McCubrey JA, *et al.* (2006) Roles of the RAF/MEK/ERK and PI3K/PTEN/AKT pathways in malignant transformation and drug resistance. *Adv Enzyme Regul* 46:249-279.
174. Kolch W, Kotwaliwale A, Vass K, & Janosch P (2002) The role of Raf kinases in malignant transformation. *Expert Rev Mol Med* 4(8):1-18.
175. Gille H, Sharrocks AD, & Shaw PE (1992) Phosphorylation of transcription factor p62TCF by MAP kinase stimulates ternary complex formation at c-fos promoter. *Nature* 358(6385):414-417.
176. Janknecht R, Ernst WH, Pingoud V, & Nordheim A (1993) Activation of ternary complex factor Elk-1 by MAP kinases. *Embo J* 12(13):5097-5104.
177. Marais R, Wynne J, & Treisman R (1993) The SRF accessory protein Elk-1 contains a growth factor-regulated transcriptional activation domain. *Cell* 73(2):381-393.

178. Meier F, *et al.* (2005) The RAS/RAF/MEK/ERK and PI3K/AKT signaling pathways present molecular targets for the effective treatment of advanced melanoma. *Front Biosci* 10:2986-3001.
179. Castaneda CA, Cortes-Funes H, Gomez HL, & Ciruelos EM (2010) The phosphatidyl inositol 3-kinase/AKT signaling pathway in breast cancer. *Cancer Metastasis Rev*.
180. Chalhoub N & Baker SJ (2009) PTEN and the PI3-kinase pathway in cancer. *Annu Rev Pathol* 4:127-150.
181. Santen RJ, *et al.* (2002) The role of mitogen-activated protein (MAP) kinase in breast cancer. *J Steroid Biochem Mol Biol* 80(2):239-256.
182. Maor S, *et al.* (2006) Estrogen receptor regulates insulin-like growth factor-I receptor gene expression in breast tumor cells: involvement of transcription factor Sp1. *J Endocrinol* 191(3):605-612.
183. Reddy KB, Yee D, Hilsenbeck SG, Coffey RJ, & Osborne CK (1994) Inhibition of estrogen-induced breast cancer cell proliferation by reduction in autocrine transforming growth factor alpha expression. *Cell Growth Differ* 5(12):1275-1282.
184. Shou J, *et al.* (2004) Mechanisms of tamoxifen resistance: increased estrogen receptor-HER2/neu cross-talk in ER/HER2-positive breast cancer. *J Natl Cancer Inst* 96(12):926-935.
185. Lange CA, Richer JK, Shen T, & Horwitz KB (1998) Convergence of progesterone and epidermal growth factor signaling in breast cancer. Potentiation of mitogen-activated protein kinase pathways. *J Biol Chem* 273(47):31308-31316.
186. Kurokawa H, *et al.* (2000) Inhibition of HER2/neu (erbB-2) and mitogen-activated protein kinases enhances tamoxifen action against HER2-overexpressing, tamoxifen-resistant breast cancer cells. *Cancer Res* 60(20):5887-5894.
187. Nilsson S, *et al.* (2001) Mechanisms of estrogen action. *Physiol Rev* 81(4):1535-1565.
188. Osborne CK (1998) Tamoxifen in the treatment of breast cancer. *N Engl J Med* 339(22):1609-1618.

189. Kato S, *et al.* (1995) Activation of the estrogen receptor through phosphorylation by mitogen-activated protein kinase. *Science* 270(5241):1491-1494.
190. Bunone G, Briand PA, Miksicek RJ, & Picard D (1996) Activation of the unliganded estrogen receptor by EGF involves the MAP kinase pathway and direct phosphorylation. *Embo J* 15(9):2174-2183.
191. Chen D, *et al.* (2002) Phosphorylation of human estrogen receptor alpha at serine 118 by two distinct signal transduction pathways revealed by phosphorylation-specific antisera. *Oncogene* 21(32):4921-4931.
192. Thomas RS, Sarwar N, Phoenix F, Coombes RC, & Ali S (2008) Phosphorylation at serines 104 and 106 by Erk1/2 MAPK is important for estrogen receptor-alpha activity. *J Mol Endocrinol* 40(4):173-184.
193. Osborne CK, *et al.* (2003) Role of the estrogen receptor coactivator AIB1 (SRC-3) and HER-2/neu in tamoxifen resistance in breast cancer. *J Natl Cancer Inst* 95(5):353-361.
194. Font de Mora J & Brown M (2000) AIB1 is a conduit for kinase-mediated growth factor signaling to the estrogen receptor. *Mol Cell Biol* 20(14):5041-5047.
195. Dillon RL, White DE, & Muller WJ (2007) The phosphatidyl inositol 3-kinase signaling network: implications for human breast cancer. *Oncogene* 26(9):1338-1345.
196. Aleskandarany MA, *et al.* (2010) PIK3CA expression in invasive breast cancer: a biomarker of poor prognosis. *Breast Cancer Res Treat* 122(1):45-53.
197. Noh WC, *et al.* (2008) Activation of the mTOR signaling pathway in breast cancer and its correlation with the clinicopathologic variables. *Breast Cancer Res Treat* 110(3):477-483.
198. Lopez-Knowles E, *et al.* (2010) PI3K pathway activation in breast cancer is associated with the basal-like phenotype and cancer-specific mortality. *Int J Cancer* 126(5):1121-1131.
199. Bose S, Wang SI, Terry MB, Hibshoosh H, & Parsons R (1998) Allelic loss of chromosome 10q23 is associated with tumor progression in breast carcinomas. *Oncogene* 17(1):123-127.

200. Rhei E, *et al.* (1997) Mutation analysis of the putative tumor suppressor gene PTEN/MMAC1 in primary breast carcinomas. *Cancer Res* 57(17):3657-3659.
201. Khan S, *et al.* (2004) PTEN promoter is methylated in a proportion of invasive breast cancers. *Int J Cancer* 112(3):407-410.
202. Vitolo MI, *et al.* (2009) Deletion of PTEN promotes tumorigenic signaling, resistance to anoikis, and altered response to chemotherapeutic agents in human mammary epithelial cells. *Cancer Res* 69(21):8275-8283.
203. Panigrahi AR, *et al.* (2004) The role of PTEN and its signalling pathways, including AKT, in breast cancer; an assessment of relationships with other prognostic factors and with outcome. *J Pathol* 204(1):93-100.
204. Depowski PL, Rosenthal SI, & Ross JS (2001) Loss of expression of the PTEN gene protein product is associated with poor outcome in breast cancer. *Mod Pathol* 14(7):672-676.
205. Tsutsui S, *et al.* (2005) Reduced expression of PTEN protein and its prognostic implications in invasive ductal carcinoma of the breast. *Oncology* 68(4-6):398-404.
206. Shoman N, *et al.* (2005) Reduced PTEN expression predicts relapse in patients with breast carcinoma treated by tamoxifen. *Mod Pathol* 18(2):250-259.
207. Dunlap J, *et al.* (2010) Phosphatidylinositol-3-kinase and AKT1 mutations occur early in breast carcinoma. *Breast Cancer Res Treat* 120(2):409-418.
208. Carpten JD, *et al.* (2007) A transforming mutation in the pleckstrin homology domain of AKT1 in cancer. *Nature* 448(7152):439-444.
209. Knuefermann C, *et al.* (2003) HER2/PI-3K/Akt activation leads to a multidrug resistance in human breast adenocarcinoma cells. *Oncogene* 22(21):3205-3212.
210. Miller TW, *et al.* (2010) Hyperactivation of phosphatidylinositol-3 kinase promotes escape from hormone dependence in estrogen receptor-positive human breast cancer. *J Clin Invest* 120(7):2406-2413.
211. Ghayad SE, *et al.* (2010) Endocrine resistance associated with activated ErbB system in breast cancer cells is reversed by inhibiting MAPK or PI3K/Akt signaling pathways. *Int J Cancer* 126(2):545-562.

212. Brandman O & Meyer T (2008) Feedback loops shape cellular signals in space and time. *Science* 322(5900):390-395.
213. Freeman M (2000) Feedback control of intercellular signalling in development. *Nature* 408(6810):313-319.
214. Bhalla US & Iyengar R (1999) Emergent properties of networks of biological signaling pathways. *Science* 283(5400):381-387.
215. Lo TL, *et al.* (2006) Sprouty and cancer: the first terms report. *Cancer Lett* 242(2):141-150.
216. Gross I, Bassit B, Benezra M, & Licht JD (2001) Mammalian sprouty proteins inhibit cell growth and differentiation by preventing ras activation. *J Biol Chem* 276(49):46460-46468.
217. Yusoff P, *et al.* (2002) Sprouty2 inhibits the Ras/MAP kinase pathway by inhibiting the activation of Raf. *J Biol Chem* 277(5):3195-3201.
218. Lo TL, *et al.* (2004) The ras/mitogen-activated protein kinase pathway inhibitor and likely tumor suppressor proteins, sprouty 1 and sprouty 2 are deregulated in breast cancer. *Cancer Res* 64(17):6127-6136.
219. Patterson KI, Brummer T, O'Brien PM, & Daly RJ (2009) Dual-specificity phosphatases: critical regulators with diverse cellular targets. *Biochem J* 418(3):475-489.
220. Amit I, *et al.* (2007) A module of negative feedback regulators defines growth factor signaling. *Nat Genet* 39(4):503-512.
221. Caunt CJ, Armstrong SP, Rivers CA, Norman MR, & McArdle CA (2008) Spatiotemporal regulation of ERK2 by dual specificity phosphatases. *J Biol Chem* 283(39):26612-26623.
222. Liu Y, Shepherd EG, & Nelin LD (2007) MAPK phosphatases--regulating the immune response. *Nat Rev Immunol* 7(3):202-212.
223. Wang HY, Cheng Z, & Malbon CC (2003) Overexpression of mitogen-activated protein kinase phosphatases MKP1, MKP2 in human breast cancer. *Cancer Lett* 191(2):229-237.
224. Small GW, Shi YY, Higgins LS, & Orlowski RZ (2007) Mitogen-activated protein kinase phosphatase-1 is a mediator of breast cancer chemoresistance. *Cancer Res* 67(9):4459-4466.

225. Rojo F, *et al.* (2009) Mitogen-activated protein kinase phosphatase-1 in human breast cancer independently predicts prognosis and is repressed by doxorubicin. *Clin Cancer Res* 15(10):3530-3539.
226. Zhang Q, *et al.* (2005) New insights into the catalytic activation of the MAPK phosphatase PAC-1 induced by its substrate MAPK ERK2 binding. *J Mol Biol* 354(4):777-788.
227. Yin Y, Liu YX, Jin YJ, Hall EJ, & Barrett JC (2003) PAC1 phosphatase is a transcription target of p53 in signalling apoptosis and growth suppression. *Nature* 422(6931):527-531.
228. Wu J, Jin YJ, Calaf GM, Huang WL, & Yin Y (2007) PAC1 is a direct transcription target of E2F-1 in apoptotic signaling. *Oncogene* 26(45):6526-6535.
229. Miller DV, *et al.* (2004) Utilizing Nottingham Prognostic Index in microarray gene expression profiling of breast carcinomas. *Mod Pathol* 17(7):756-764.
230. Langlois WJ, Sasaoka T, Saltiel AR, & Olefsky JM (1995) Negative feedback regulation and desensitization of insulin- and epidermal growth factor-stimulated p21ras activation. *J Biol Chem* 270(43):25320-25323.
231. Waters SB, *et al.* (1995) Desensitization of Ras activation by a feedback disassociation of the SOS-Grb2 complex. *J Biol Chem* 270(36):20883-20886.
232. Dong C, Waters SB, Holt KH, & Pessin JE (1996) SOS phosphorylation and disassociation of the Grb2-SOS complex by the ERK and JNK signaling pathways. *J Biol Chem* 271(11):6328-6332.
233. Corbalan-Garcia S, Yang SS, Degenhardt KR, & Bar-Sagi D (1996) Identification of the mitogen-activated protein kinase phosphorylation sites on human Sos1 that regulate interaction with Grb2. *Mol Cell Biol* 16(10):5674-5682.
234. Nakayama K, Satoh T, Igari A, Kageyama R, & Nishida E (2008) FGF induces oscillations of Hes1 expression and Ras/ERK activation. *Curr Biol* 18(8):R332-334.
235. Kholodenko BN (2000) Negative feedback and ultrasensitivity can bring about oscillations in the mitogen-activated protein kinase cascades. *Eur J Biochem* 267(6):1583-1588.

236. Dougherty MK, *et al.* (2005) Regulation of Raf-1 by direct feedback phosphorylation. *Mol Cell* 17(2):215-224.
237. Roshan B, *et al.* (1999) Activated ERK2 interacts with and phosphorylates the docking protein GAB1. *J Biol Chem* 274(51):36362-36368.
238. Yu CF, Liu ZX, & Cantley LG (2002) ERK negatively regulates the epidermal growth factor-mediated interaction of Gab1 and the phosphatidylinositol 3-kinase. *J Biol Chem* 277(22):19382-19388.
239. Lehr S, *et al.* (2004) Identification of major ERK-related phosphorylation sites in Gab1. *Biochemistry* 43(38):12133-12140.
240. Eblen ST, *et al.* (2004) Mitogen-activated protein kinase feedback phosphorylation regulates MEK1 complex formation and activation during cellular adhesion. *Mol Cell Biol* 24(6):2308-2317.
241. Slack-Davis JK, *et al.* (2003) PAK1 phosphorylation of MEK1 regulates fibronectin-stimulated MAPK activation. *J Cell Biol* 162(2):281-291.
242. Marchetti S, *et al.* (2005) Extracellular signal-regulated kinases phosphorylate mitogen-activated protein kinase phosphatase 3/DUSP6 at serines 159 and 197, two sites critical for its proteasomal degradation. (Translated from eng) *Mol Cell Biol* 25(2):854-864 (in eng).
243. Hilioti Z, *et al.* (2008) Oscillatory Phosphorylation of Yeast Fus3 MAP Kinase Controls Periodic Gene Expression and Morphogenesis. *Curr Biol*.
244. Wee KB, Surana U, & Aguda BD (2009) Oscillations of the p53-Akt network: implications on cell survival and death. *PLoS ONE* 4(2):e4407.
245. Shimojo H, Ohtsuka T, & Kageyama R (2008) Oscillations in notch signaling regulate maintenance of neural progenitors. *Neuron* 58(1):52-64.
246. Hirata H, *et al.* (2002) Oscillatory expression of the bHLH factor Hes1 regulated by a negative feedback loop. *Science* 298(5594):840-843.
247. Gore J & van Oudenaarden A (2009) Synthetic biology: The yin and yang of nature. *Nature* 457(7227):271-272.
248. Lev Bar-Or R, *et al.* (2000) Generation of oscillations by the p53-Mdm2 feedback loop: a theoretical and experimental study. *Proc Natl Acad Sci U S A* 97(21):11250-11255.

249. Tsai TY*, et al.* (2008) Robust, tunable biological oscillations from interlinked positive and negative feedback loops. *Science* 321(5885):126-129.
250. Wang X, Hao N, Dohlman HG, & Elston TC (2006) Bistability, stochasticity, and oscillations in the mitogen-activated protein kinase cascade. *Biophys J* 90(6):1961-1978.
251. Ortega F, Garces JL, Mas F, Kholodenko BN, & Cascante M (2006) Bistability from double phosphorylation in signal transduction. Kinetic and structural requirements. *Febs J* 273(17):3915-3926.
252. Chickarmane V, Kholodenko BN, & Sauro HM (2007) Oscillatory dynamics arising from competitive inhibition and multisite phosphorylation. *J Theor Biol* 244(1):68-76.
253. Ihaka R & Gentleman R (1996) R: a language for data analysis and graphics. *Journal of computational and graphical statistics* 5(3):299-314.
254. Gentleman RC*, et al.* (2004) Bioconductor: open software development for computational biology and bioinformatics. *Genome biology* 5(10):R80.
255. Du P, Kibbe WA, & Lin SM (2008) lumi: a pipeline for processing Illumina microarray. *Bioinformatics* 24(13):1547-1548.
256. Tusher VG, Tibshirani R, & Chu G (2001) Significance analysis of microarrays applied to the ionizing radiation response. *Proc Natl Acad Sci U S A* 98(9):5116-5121.
257. Breitling R, Armengaud P, Amtmann A, & Herzyk P (2004) Rank products: a simple, yet powerful, new method to detect differentially regulated genes in replicated microarray experiments. *FEBS Lett* 573(1-3):83-92.
258. Johnson W, Li C, & Rabinovic A (2007) Adjusting batch effects in microarray expression data using empirical Bayes methods. *Biostatistics* 8(1):118-127.
259. Sims AH*, et al.* (2008) The removal of multiplicative, systematic bias allows integration of breast cancer gene expression datasets - improving meta-analysis and prediction of prognosis. *BMC Med Genomics* 1:42.
260. Kitchen RR*, et al.* (2010) Correcting for intra-experiment variation in Illumina BeadChip data is necessary to generate robust gene-expression profiles. *BMC Genomics* 11:134.

261. Eisen MB, Spellman PT, Brown PO, & Botstein D (1998) Cluster analysis and display of genome-wide expression patterns. *Proc Natl Acad Sci U S A* 95(25):14863-14868.

262. Levenson AS & Jordan VC (1997) MCF-7: the first hormone-responsive breast cancer cell line. (Translated from eng) *Cancer Res* 57(15):3071-3078 (in eng).

263. Wakeling AE, Newboult E, & Peters SW (1989) Effects of antioestrogens on the proliferation of MCF-7 human breast cancer cells. (Translated from eng) *J Mol Endocrinol* 2(3):225-234 (in eng).

264. Young MW & Kay SA (2001) Time zones: a comparative genetics of circadian clocks. *Nat Rev Genet* 2(9):702-715.

265. Pourquie O (2003) The segmentation clock: converting embryonic time into spatial pattern. *Science* 301(5631):328-330.

266. Shin SY, *et al.* (2009) Positive- and negative-feedback regulations coordinate the dynamic behavior of the Ras-Raf-MEK-ERK signal transduction pathway. *J Cell Sci* 122(Pt 3):425-435.

267. Huang da W, Sherman BT, & Lempicki RA (2009) Systematic and integrative analysis of large gene lists using DAVID bioinformatics resources. (Translated from eng) *Nat Protoc* 4(1):44-57 (in eng).

268. Dennis G, Jr., *et al.* (2003) DAVID: Database for Annotation, Visualization, and Integrated Discovery. (Translated from eng) *Genome Biol* 4(5):P3 (in eng).

269. Xu W, *et al.* (2003) The heat shock protein 90 inhibitor geldanamycin and the ErbB inhibitor ZD1839 promote rapid PP1 phosphatase-dependent inactivation of AKT in ErbB2 overexpressing breast cancer cells. (Translated from eng) *Cancer Res* 63(22):7777-7784 (in eng).

270. Takahashi M, *et al.* (1999) Characterization of a novel giant scaffolding protein, CG-NAP, that anchors multiple signaling enzymes to centrosome and the golgi apparatus. (Translated from eng) *J Biol Chem* 274(24):17267-17274 (in eng).

271. Greenberg CC, Meredith KN, Yan L, & Brady MJ (2003) Protein targeting to glycogen overexpression results in the specific enhancement of glycogen

storage in 3T3-L1 adipocytes. (Translated from eng) *J Biol Chem* 278(33):30835-30842 (in eng).

272. Novoa I, Zeng H, Harding HP, & Ron D (2001) Feedback inhibition of the unfolded protein response by GADD34-mediated dephosphorylation of eIF2alpha. (Translated from eng) *J Cell Biol* 153(5):1011-1022 (in eng).
273. Guo D, Jia Q, Song HY, Warren RS, & Donner DB (1995) Vascular endothelial cell growth factor promotes tyrosine phosphorylation of mediators of signal transduction that contain SH2 domains. Association with endothelial cell proliferation. (Translated from eng) *J Biol Chem* 270(12):6729-6733 (in eng).
274. Wakioka T*, et al.* (2001) Spred is a Sprouty-related suppressor of Ras signalling. (Translated from eng) *Nature* 412(6847):647-651 (in eng).
275. Chen PS*, et al.* (2007) CTGF enhances the motility of breast cancer cells via an integrin-alphavbeta3-ERK1/2-dependent S100A4-upregulated pathway. *J Cell Sci* 120(Pt 12):2053-2065.
276. Menendez JA*, et al.* (2005) A novel CYR61-triggered 'CYR61-alphavbeta3 integrin loop' regulates breast cancer cell survival and chemosensitivity through activation of ERK1/ERK2 MAPK signaling pathway. *Oncogene* 24(5):761-779.
277. Crean JK*, et al.* (2006) Connective tissue growth factor/CCN2 stimulates actin disassembly through Akt/protein kinase B-mediated phosphorylation and cytoplasmic translocation of p27Kip-1. *The FASEB Journal* 20(10):E1037-E1048.
278. Ieguchi K*, et al.* (2010) Direct binding of the EGF-like domain of neuregulin-1 to integrins ({alpha}v{beta}3 and {alpha}6{beta}4) is involved in neuregulin-1/ErbB signaling. *J Biol Chem*:31388-31398.
279. Eliceiri BP (2001) Integrin and growth factor receptor crosstalk. (Translated from eng) *Circ Res* 89(12):1104-1110 (in eng).
280. Zimmermann S & Moelling K (1999) Phosphorylation and regulation of Raf by Akt (protein kinase B). *Science* 286(5445):1741-1744.
281. Moelling K, Schad K, Bosse M, Zimmermann S, & Schweneker M (2002) Regulation of Raf-Akt Cross-talk. *J Biol Chem* 277(34):31099-31106.

282. Nakakuki T, *et al.* (2010) Ligand-specific c-Fos expression emerges from the spatiotemporal control of ErbB network dynamics. *Cell* 141(5):884-896.
283. Kumar CC (1998) Signaling by integrin receptors. (Translated from eng) *Oncogene* 17(11 Reviews):1365-1373 (in eng).
284. Saal LH, *et al.* (2005) PIK3CA mutations correlate with hormone receptors, node metastasis, and ERBB2, and are mutually exclusive with PTEN loss in human breast carcinoma. *Cancer Res* 65(7):2554-2559.
285. Kang S, Bader AG, & Vogt PK (2005) Phosphatidylinositol 3-kinase mutations identified in human cancer are oncogenic. *Proc Natl Acad Sci U S A* 102(3):802-807.
286. Connor JH, Weiser DC, Li S, Hallenbeck JM, & Shenolikar S (2001) Growth arrest and DNA damage-inducible protein GADD34 assembles a novel signaling complex containing protein phosphatase 1 and inhibitor 1. *Mol Cell Biol* 21(20):6841-6850.
287. Shankaran H, *et al.* (2009) Rapid and sustained nuclear-cytoplasmic ERK oscillations induced by epidermal growth factor. *Mol Syst Biol* 5:332.
288. Nahta R, Hung MC, & Esteva FJ (2004) The HER-2-targeting antibodies trastuzumab and pertuzumab synergistically inhibit the survival of breast cancer cells. *Cancer Res* 64(7):2343-2346.
289. Anastasi S, *et al.* (2003) Feedback inhibition by RALT controls signal output by the ErbB network. (Translated from eng) *Oncogene* 22(27):4221-4234 (in eng).
290. Fiorentino L, *et al.* (2000) Inhibition of ErbB-2 mitogenic and transforming activity by RALT, a mitogen-induced signal transducer which binds to the ErbB-2 kinase domain. (Translated from eng) *Mol Cell Biol* 20(20):7735-7750 (in eng).
291. Yatsuoka T, Furukawa T, Sunamura M, Matsuno S, & Horii A (2004) TU12B1-TY, a novel gene in the region at 12q22-q23.1 frequently deleted in pancreatic cancer, shows reduced expression in pancreatic cancer cells. (Translated from eng) *Oncol Rep* 12(6):1263-1268 (in eng).

292. Sawada A*, et al.* (2003) A congenital mutation of the novel gene LRRC8 causes agammaglobulinemia in humans. (Translated from eng) *J Clin Invest* 112(11):1707-1713 (in eng).
293. Gollogly LK, Ryeom SW, & Yoon SS (2007) Down syndrome candidate region 1-like 1 (DSCR1-L1) mimics the inhibitory effects of DSCR1 on calcineurin signaling in endothelial cells and inhibits angiogenesis. (Translated from eng) *J Surg Res* 142(1):129-136 (in eng).
294. Lee SJ*, et al.* (2007) Protein phosphatase 1 nuclear targeting subunit is a hypoxia inducible gene: its role in post-translational modification of p53 and MDM2. (Translated from eng) *Cell Death Differ* 14(6):1106-1116 (in eng).
295. Fujii C*, et al.* (2005) Aberrant expression of serine/threonine kinase Pim-3 in hepatocellular carcinoma development and its role in the proliferation of human hepatoma cell lines. (Translated from eng) *Int J Cancer* 114(2):209-218 (in eng).
296. Kihara A & Igarashi Y (2004) FVT-1 is a mammalian 3-ketodihydrosphingosine reductase with an active site that faces the cytosolic side of the endoplasmic reticulum membrane. (Translated from eng) *J Biol Chem* 279(47):49243-49250 (in eng).
297. Sever N, Lee PC, Song BL, Rawson RB, & Debose-Boyd RA (2004) Isolation of mutant cells lacking Insig-1 through selection with SR-12813, an agent that stimulates degradation of 3-hydroxy-3-methylglutaryl-coenzyme A reductase. (Translated from eng) *J Biol Chem* 279(41):43136-43147 (in eng).
298. Wang Z*, et al.* (2006) Phosphatase-mediated crosstalk control of ERK and p38 MAPK signaling in corneal epithelial cells. *Invest Ophthalmol Vis Sci* 47(12):5267-5275.
299. Brunet A, Pages G, & Pouyssegur J (1994) Growth factor-stimulated MAP kinase induces rapid retrophosphorylation and inhibition of MAP kinase kinase (MEK1). *FEBS Lett* 346(2-3):299-303.
300. Catalanotti F*, et al.* (2009) A Mek1-Mek2 heterodimer determines the strength and duration of the Erk signal. *Nat Struct Mol Biol* 16(3):294-303.
301. Badache A & Hynes NE (2004) A new therapeutic antibody masks ErbB2 to its partners. *Cancer Cell* 5(4):299-301.

302. Vogel CL, *et al.* (2002) Efficacy and safety of trastuzumab as a single agent in first-line treatment of HER2-overexpressing metastatic breast cancer. *J Clin Oncol* 20(3):719-726.
303. Yuste L, Montero JC, Esparis-Ogando A, & Pandiella A (2005) Activation of ErbB2 by overexpression or by transmembrane neuregulin results in differential signaling and sensitivity to herceptin. *Cancer Res* 65(15):6801-6810.
304. de Alava E, *et al.* (2007) Neuregulin expression modulates clinical response to trastuzumab in patients with metastatic breast cancer. *J Clin Oncol* 25(19):2656-2663.
305. Diermeier S, *et al.* (2005) Epidermal growth factor receptor coexpression modulates susceptibility to Herceptin in HER2/neu overexpressing breast cancer cells via specific erbB-receptor interaction and activation. *Exp Cell Res* 304(2):604-619.
306. Zheng L, Ren JQ, Li H, Kong ZL, & Zhu HG (2004) Downregulation of wild-type p53 protein by HER-2/neu mediated PI3K pathway activation in human breast cancer cells: its effect on cell proliferation and implication for therapy. (Translated from eng) *Cell Res* 14(6):497-506 (in eng).
307. Alimandi M, *et al.* (1995) Cooperative signaling of ErbB3 and ErbB2 in neoplastic transformation and human mammary carcinomas. *Oncogene* 10(9):1813-1821.
308. DiGiovanna MP, *et al.* (2002) Active signaling by HER-2/neu in a subpopulation of HER-2/neu-overexpressing ductal carcinoma in situ: clinicopathological correlates. *Cancer Res* 62(22):6667-6673.
309. Gijsen M, *et al.* (2010) HER2 phosphorylation is maintained by a PKB negative feedback loop in response to anti-HER2 herceptin in breast cancer. (Translated from eng) *PLoS Biol* 8(12):e1000563 (in eng).
310. Holbro T, *et al.* (2003) The ErbB2/ErbB3 heterodimer functions as an oncogenic unit: ErbB2 requires ErbB3 to drive breast tumor cell proliferation. *Proc Natl Acad Sci U S A* 100(15):8933-8938.

311. Prigent SA & Gullick WJ (1994) Identification of c-erbB-3 binding sites for phosphatidylinositol 3'-kinase and SHC using an EGF receptor/c-erbB-3 chimera. *Embo J* 13(12):2831-2841.

312. Fedi P, Pierce JH, di Fiore PP, & Kraus MH (1994) Efficient coupling with phosphatidylinositol 3-kinase, but not phospholipase C gamma or GTPase-activating protein, distinguishes ErbB-3 signaling from that of other ErbB/EGFR family members. *Mol Cell Biol* 14(1):492-500.

313. Tonks NK (2006) Protein tyrosine phosphatases: from genes, to function, to disease. *Nat Rev Mol Cell Biol* 7(11):833-846.

314. Ostman A, Hellberg C, & Bohmer FD (2006) Protein-tyrosine phosphatases and cancer. *Nat Rev Cancer* 6(4):307-320.

315. Glondu-Lassis M, *et al.* (2010) PTPL1/PTPN13 regulates breast cancer cell aggressiveness through direct inactivation of Src kinase. *Cancer Res* 70(12):5116-5126.

316. Freiss G, Bompard G, & Vignon F (2004) [PTPL1, a proapoptotic protein tyrosine phosphatase in breast cancers]. *Bull Cancer* 91(4):325-332.

317. Bompard G, Puech C, Prebois C, Vignon F, & Freiss G (2002) Protein-tyrosine phosphatase PTPL1/FAP-1 triggers apoptosis in human breast cancer cells. *J Biol Chem* 277(49):47861-47869.

318. Dromard M, *et al.* (2007) The putative tumor suppressor gene PTPN13/PTPL1 induces apoptosis through insulin receptor substrate-1 dephosphorylation. *Cancer Res* 67(14):6806-6813.

319. Zhu JH, *et al.* (2008) Protein tyrosine phosphatase PTPN13 negatively regulates Her2/ErbB2 malignant signaling. *Oncogene* 27(18):2525-2531.

320. Revillion F, *et al.* (2009) Expression of the putative tumor suppressor gene PTPN13/PTPL1 is an independent prognostic marker for overall survival in breast cancer. *Int J Cancer* 124(3):638-643.

321. Karakas B, Bachman KE, & Park BH (2006) Mutation of the PIK3CA oncogene in human cancers. *Br J Cancer* 94(4):455-459.

322. Miron A, *et al.* (2010) PIK3CA mutations in in situ and invasive breast carcinomas. *Cancer Res* 70(14):5674-5678.

323. Faratian D*, et al.* (2009) Systems biology reveals new strategies for personalizing cancer medicine and confirms the role of PTEN in resistance to trastuzumab. *Cancer Res* 69(16):6713-6720.

Supplement

Table S1 100 most changed genes (20'HRG *vs* control, p<0.05, Student's t-test, fold changes of individual genes are listed below gene names)

ADM	ANKRD37	AP3S2	APOL2	ATF3	ATOX1	AXUD1	BAX	BHLHB2	C14orf138
1.349258	1.28936	1.27978	1.25813	1.84061	1.28881	2.03308	1.28735	1.31653	1.26545
C14orf28	CBX4	CCNL1	CKS2	CNTD2	CTGF	CXCR7	CYR61	DCDC5	DDIT3
1.62380	1.53946	1.35283	1.35714	1.27594	19.8639	1.25802	11.0838	1.38953	1.56236
DECR2	DNAJB1	DUSP1	DUSP2	DUSP4	DUSP5	EDN1	EGR1	EGR2	EGR3
1.26344	1.39141	3.45639	1.96664	1.29122	2.00690	2.23312	7.80240	12.66171	2.26183
EGR4	EIF1	FAM46B	FOS	FOSB	FOXC1	FRS3	GDF15	GLTSCR1	GTF2IRD2B
2.81039	1.32833	1.45368	18.0963	12.8431	1.81510	1.29067	1.46210	1.38040	1.25455
HIC2	HNRPDL	IER2	IER3	IRF2BP2	IRS2	IRX3	JUN	JUNB	KIAA17541.3
1.289293	1.34430	2.36808	1.81932	1.29629	1.31003	1.26798	6.62094	3.88905	3399
KLF10	KLF2	KLF6	LOC387763	LOC650826	LOC651380	LOC651816	MEPCE	MSX1	MYADM
1.31216	5.90560	2.21098	1.343778	1.27986	1.26706	1.29773	1.29976	1.39906	1.99979
MYC	NARF	NCOA7	NFKBIA	NFKBIZ	NOC4L	NPAS1	NR4A2	NR4A3	PHF15
1.48810	1.31994	1.81592	1.27235	1.29619	1.29041	1.25441	1.27107	4.17417	1.27841
PHLDA2	PPP1R15A	PSD4	PUF60	QPRT	RASD1	RND1	RPPH1	RPS4Y2	SERTAD11.9
1.29422	2.07285	1.29918	1.37693	1.29252	16.6704	1.50644	1.69254	1.25975	4420
SERTAD3	SLC25A25	SLCO4A1	SNF1LK	SRF	STBD1	TAGLN	TMEM93	TPM1	TRAF3IP21.2
1.49160	1.47573	1.33926	2.12870	1.72515	1.25243	2.35073	1.27196	1.55490	7699
TRIB1	TSKU	TSPYL2	UBXD5	YRDC	ZC3H12A	ZFP36	ZFP36L2	ZNF213	ZYX
1.25493	1.36154	1.32330	1.30895	1.30501	1.36066	4.47764	1.48141	1.25730	1.27489

Gene selection criteria: the whole gene list of the array was sorted by fold change (highest to lowest, 20'HRG vs control). The top 100 genes with p value less than 0.05 were selected.

After putting these 100 genes into DAVID Bioinformatics Resources 6.7 for functional annotation clustering, 9 genes were found to be involved in MAPK signalling pathway within KEGG_PATHWAY database.

Gene Name	Description
DDIT3	DNA-damage-inducible transcript 3
DUSP1	dual specificity phosphatase 1
DUSP2	dual specificity phosphatase 2
DUSP4	dual specificity phosphatase 4
DUSP5	dual specificity phosphatase 5
JUN	jun oncogene
SRF	serum response factor (c-fos serum response element-binding transcription factor)
FOS	v-fos FBJ murine osteosarcoma viral oncogene homolog
MYC	v-myc myelocytomatosis viral oncogene homolog (avian)

Table S2 Genes proposed by Takeshi Nagashima et al (91) which might regulate HER signalling dynamics through positive and negative feedback loops.

genes	description
AKAP9	A kinase (PRKA) anchor protein (yotiao) 9
AREG	amphiregulin
ATF3	activating transcription factor 3
BHLHB2	basic helix-loop-helix domain containing, class B, 2
DUSP1	dual specificity phosphatase 1
DUSP10	dual specificity phosphatase 10
DUSP2	dual specificity phosphatase 2
DUSP4	dual specificity phosphatase 4
DUSP5	dual specificity phosphatase 5
DUSP8	dual specificity phosphatase 8
EGR	Early growth response
family	
FOS	v-fos FBJ murine osteosarcoma viral oncogene homolog
FOXA1	forkhead box A1
HBEGF	heparin-binding EGF-like growth factor
JUN	jun oncogene
KLF family	Kruppel-like factor
MAP2K3	mitogen-activated protein kinase kinase 3
MAP3K14	mitogen-activated protein kinase kinase kinase 14
MAP3K3	mitogen-activated protein kinase kinase kinase 3
MYC	v-myc myelocytomatosis viral oncogene homolog (avian)
NFIL3	nuclear factor, interleukin 3 regulated
NR4A	nuclear receptor subfamily 4, group A
family	
PIP5K1A	phosphatidylinositol-4-phosphate 5-kinase, type I, alpha
PPP1R15A	protein phosphatase 1, regulatory subunit 15A
PPP1R3C	protein phosphatase 1, regulatory subunit 3C
PPP1R3D	protein phosphatase 1, regulatory subunit 3D
SOX2	SRY (sex determining region Y)-box 2
SPRED2	sprouty-related, EVH1 domain containing 2
TGFB2	transforming growth factor, beta 2
TOB2	transducer of ERBB2, 2
VEGF	vascular endothelial growth factor

Table S1 is overlapped with table S2 in Genes marked in blue ink. 19 out of 100 genes in table S1 are found in table S2, which means at least 19% of the genes in this gene candidate pool are involved in positive or negative feedback regulation of HER signalling dynamics.

Table S3 In addition to the overlapped genes, 6 other genes in table S2 which were induced significantly ($p<0.05$, 20'HRG *vs* control, Student's t-test) are observed. The remaining genes are not induced significantly by HRG.

Genes	**Change fold** (20'HRG vs control)
AKAP9	-1.10302
AREG	1.16968
HBEGF	1.15978
PPP1R3C	-1.23493
SPRED2	1.16878
VEGFA	1.11145

Figure S1 Time course profiles of individual candidate genes. MCF-7 cells were stimulated by 1 nM HRG for 5, 10, 20 and 40 min respectively. Controls for 0 and 40 min were included. Grey lines are controls. Blue lines are time course profiles of individual genes.

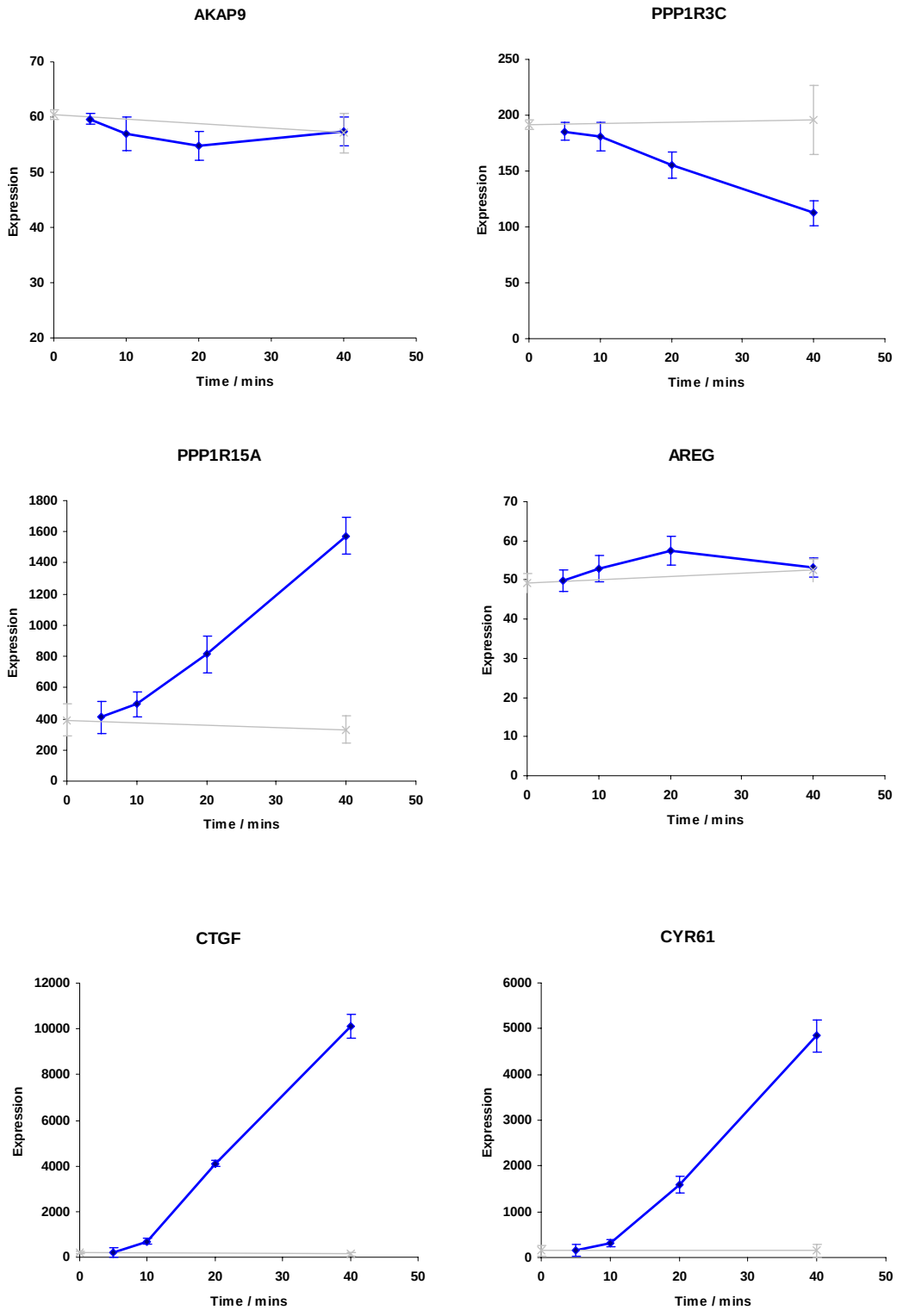

Figure S1 (continued)

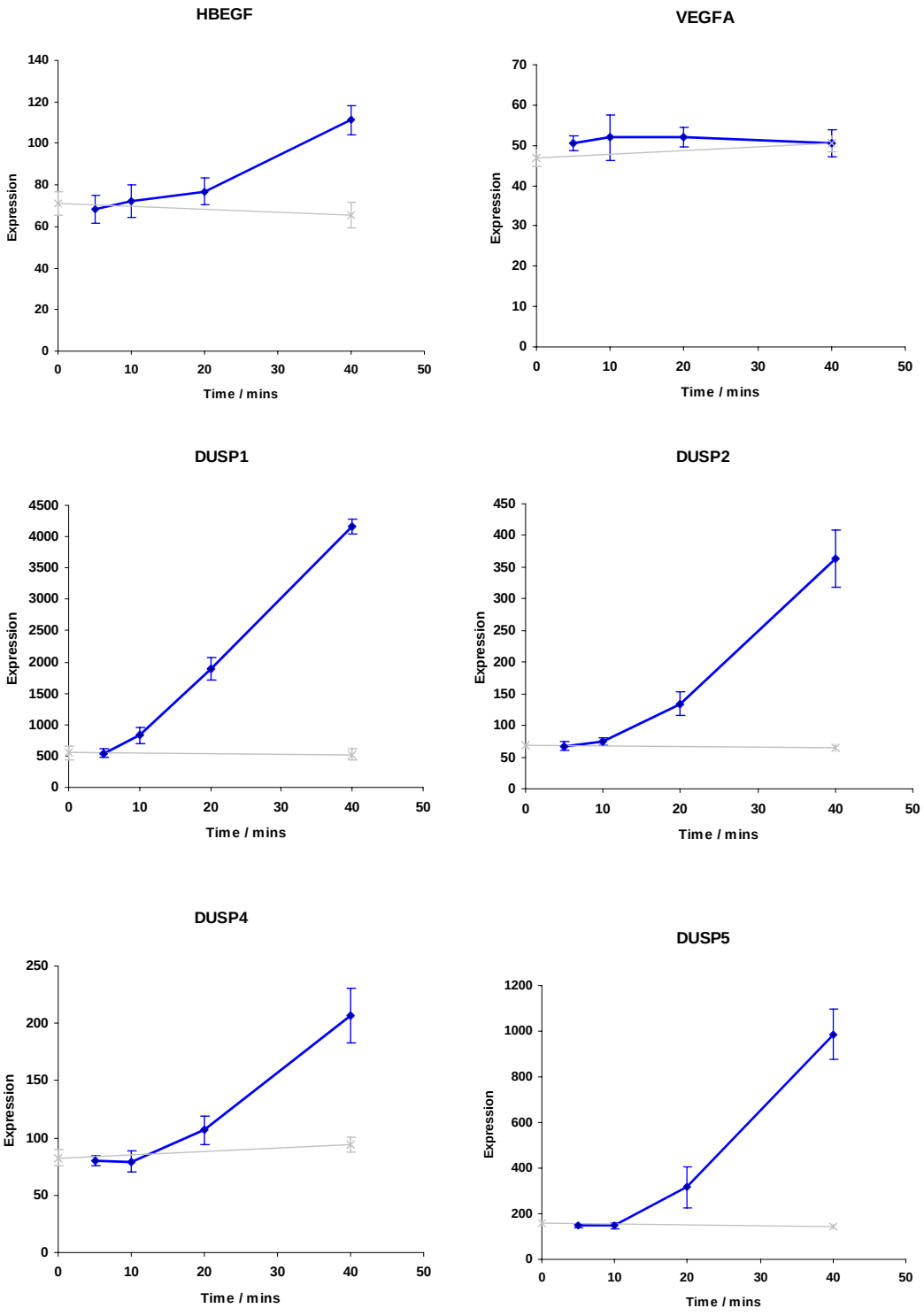

Figure S1 (continued)

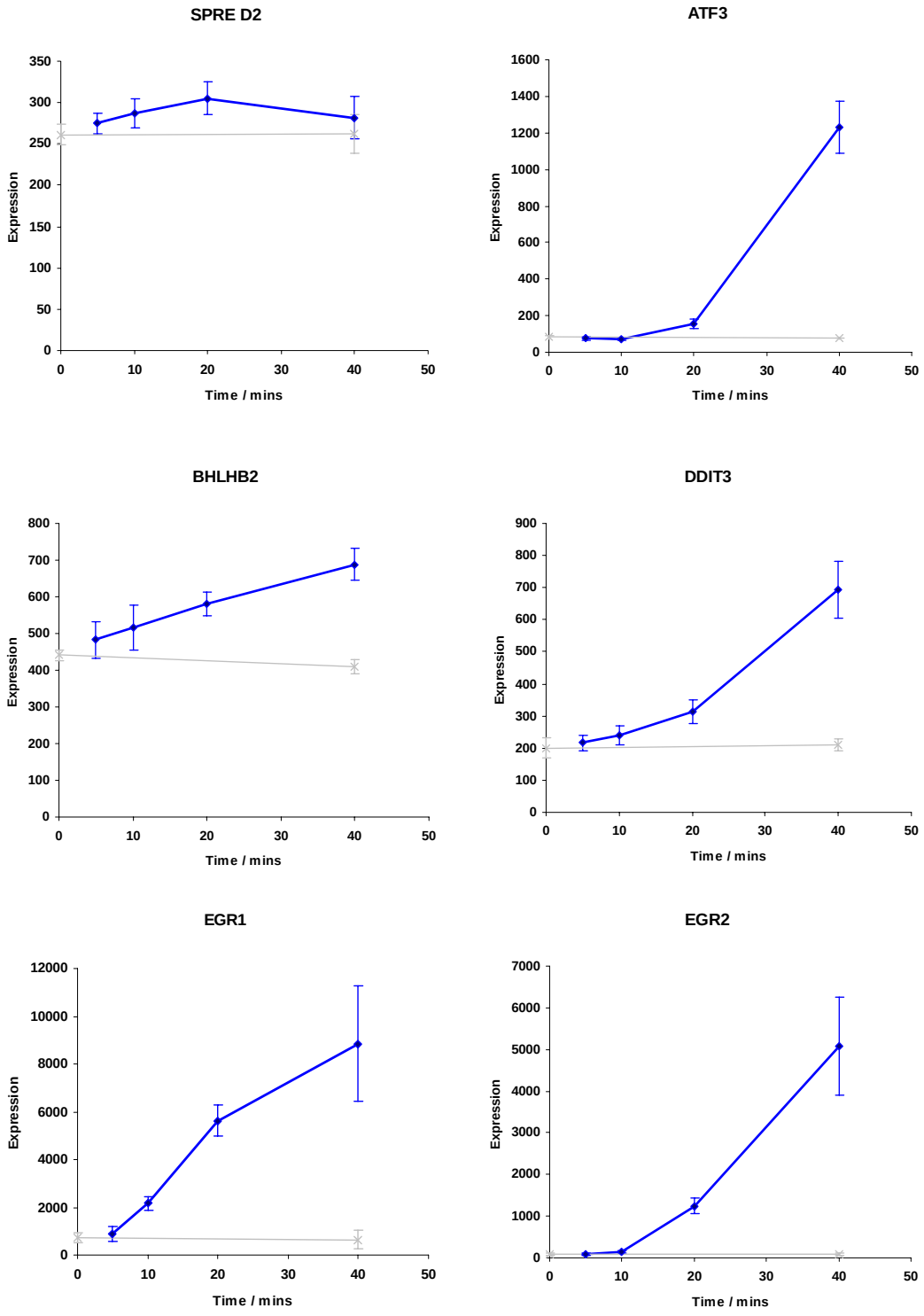

Figure S1 (continued)

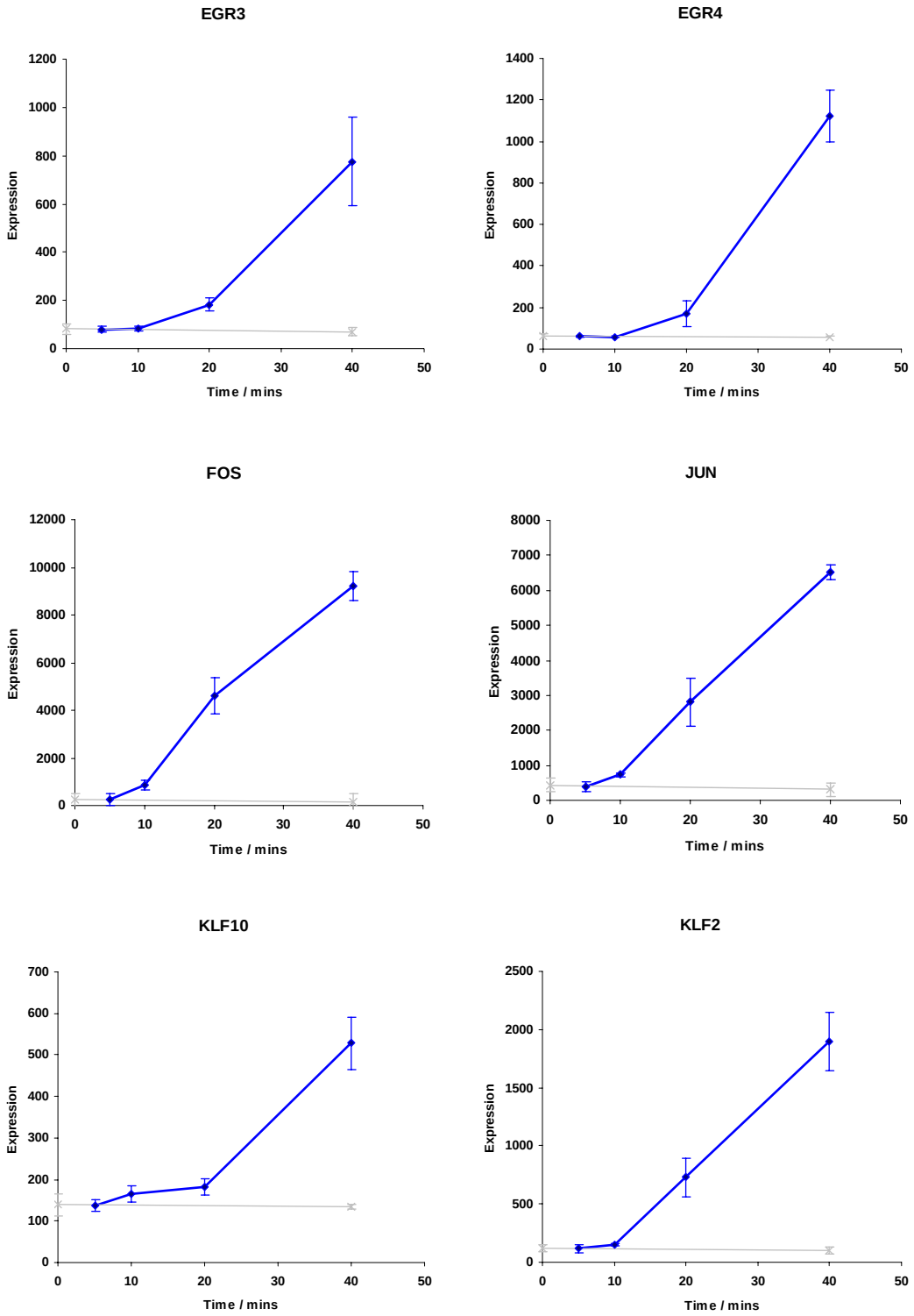

Figure S1 (continued)

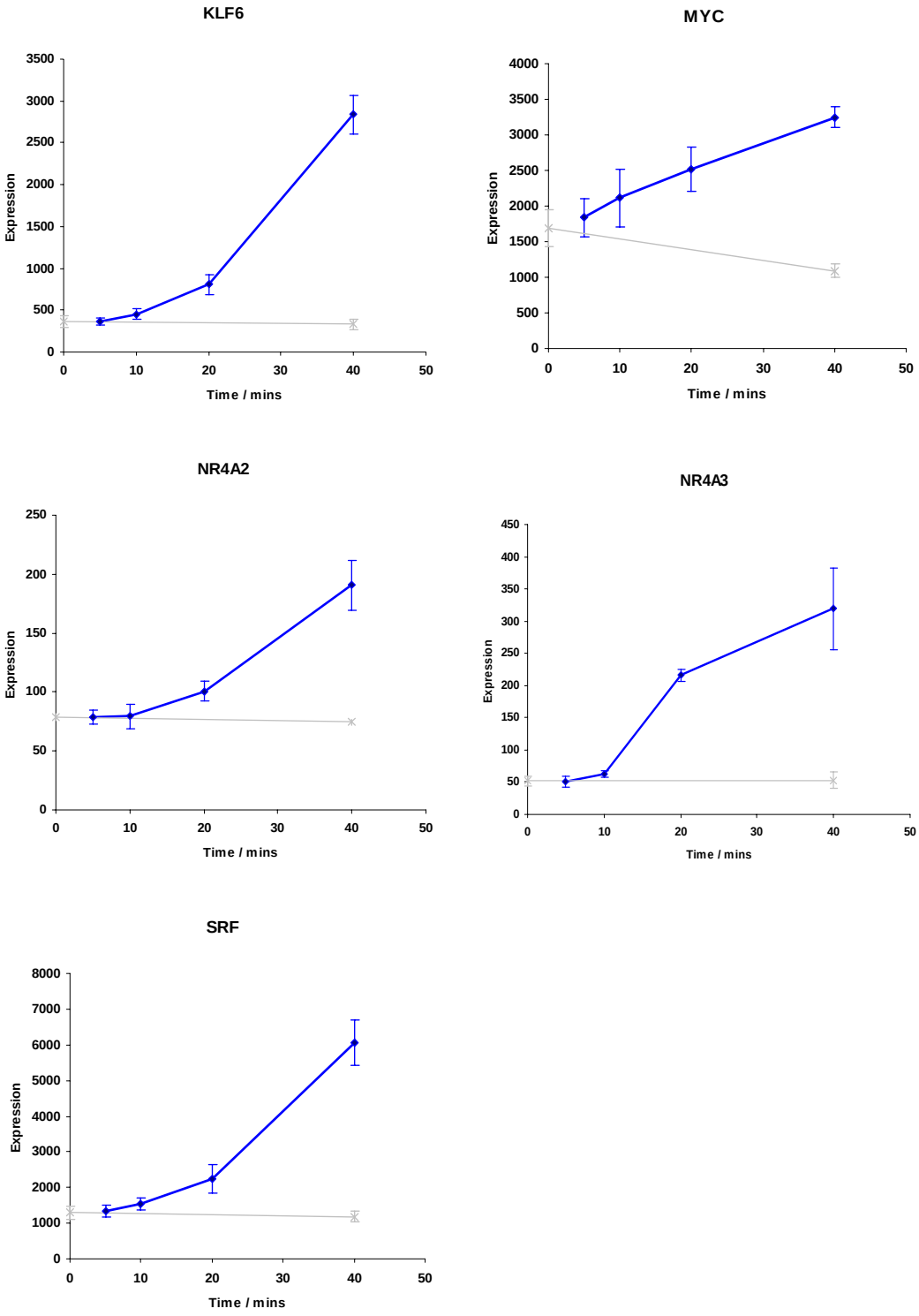

Table S4 300 most induced genes by HRG in MCF-7 cells ($p<0.05$, 40'HRG vs control, Student's t-test fold change ranging from 1.218 to 75.956).

Gene	Change fold	Gene	Change fold	Gene	Change fold	Gene	Change fold
ACTB	1.62669	C14orf4	1.38474	CNN2	1.73161	EIF1	1.72906
ACTG1	1.83804	C14orf43	1.49651	CNTD2	1.27937	EIF5	1.39554
ACTG2	4.58910	C17orf91	1.82824	COL1A1	1.24696	ELF3	1.21981
ADM	2.19308	C19orf6	1.54798	COQ10B	1.69496	EPC1	1.31558
AMY1A	1.38484	C1orf107	1.25691	CPEB3	1.23285	ERRFI1	2.37348
AMY1B	1.26357	C1orf108	1.48440	CTGF	49.31077	ETS2	2.07049
AMY1C	1.22017	C20orf111	1.69037	CXCR4	1.52925	FAM100A	1.98022
ANKRD37	1.82197	C20orf175	1.99327	CYCS	1.34182	FAM46B	2.27772
ANKRD57	1.95991	C5orf41	1.32870	CYCSL1	1.31683	FBXL12	1.34082
ARC	2.51931	C6orf66	1.21888	CYP26B1	1.58559	FBXO46	1.22011
ARF4	1.50702	C6orf85	1.22814	CYR61	33.65828	FERMT2	1.36869
ARG2	1.22830	C8orf4	1.32153	DCP1A	1.33534	FHL2	7.26980
ARL5B	1.43873	C9orf32	1.29058	DCUN1D3	2.60225	FILIP1L	1.21921
ATF3	14.73896	CACYBP	1.23473	DDIT3	3.46021	FLJ13236	1.23439
ATP2A2	1.35532	CBX4	2.79774	DDX43	1.22351	FOS	36.30673
AVPI1	1.52369	CCBL2	1.29739	DDX5	1.42818	FOSB	75.95573
AXUD1	5.62476	CCNL1	2.29506	DKK1	1.71896	FOSL1	2.56544
B3GNT2	1.48183	CD68	1.43461	DNAJB1	2.34937	FOXC1	3.31256
BARD1	1.35344	CDKN1A	1.68130	DUSP1	7.58109	FOXD4	1.31789
BCL10	1.60090	CDR2	1.42224	DUSP10	1.27175	FOXD4L1	1.29117
BCL2L12	1.21938	CEBPB	1.39998	DUSP2	5.32710	FOXQ1	1.35223
BCL7B	1.33776	CENTG3	1.22234	DUSP4	2.50582	FST	1.35207
BHLHB2	1.46824	CGGBP1	1.29393	DUSP5	6.25464	FVT1	1.29863
BIK	1.39729	CHIC2	1.25315	DUSP8	2.07186	FZD9	1.41816
C11orf56	1.22690	CISH	1.22228	EDN1	11.47651	GADD45A	1.49496
C12orf44	1.43087	CITED2	1.53932	EGR1	8.92255	GADD45B	1.27265
C12orf5	1.25434	CKS2	2.72874	EGR2	51.61896	GDF15	2.32124
C14orf138	1.24802	CLIC5	1.36216	EGR3	9.58592	GEM	1.55664
C14orf28	3.52274	CLK1	1.57975	EGR4	18.60352	HBEGF	1.56410

Table S4 (continued)

Gene	Change fold	Gene	Change fold	Gene	Change fold	Gene	Change fold
HERPUD1	1.67755	KCNF1	1.38426	LOC730820	1.23360	NT5DC3	1.23918
HIC2	1.31756	KCTD5	1.28848	LRRC8A	1.43109	OBFC2A	1.32572
HMGCR	1.36520	KIAA1754	3.50186	MAD2L1BP	1.42764	ODC1	1.31895
HNRNPAB	1.25618	KLF10	3.79783	MAFF	3.33847	OSGIN2	1.54713
HNRPDL	1.39168	KLF2	15.33393	MAFG	1.48002	P704P	1.33514
HSPC111	1.36865	KLF6	7.77205	MAP3K14	1.39146	PCF11	1.29996
ID3	1.51982	KLHL21	1.27807	MAT2A	1.75027	PDRG1	1.22870
IER2	3.13299	KLHL28	1.54178	MBD1	1.30854	PER2	1.43654
IER3	2.56416	KLK7	1.24449	MCL1	4.17160	PFKFB3	1.60087
IER5	1.67329	KRT17	2.28012	MED9	1.85101	PHC2	1.36963
IHPK2	1.32288	LAG3	1.88359	MEF2D	1.69797	PHF15	1.23802
IL8	4.92193	LDLR	2.46017	MESDC1	1.27075	PHF20L1	1.22219
ING1	1.36383	LMCD1	1.23056	METRNL	1.29323	PHLDA1	3.54013
ING3	1.41933	LOC199800	1.34867	MIDN	1.51456	PHLDA2	2.47347
INSIG1	1.23925	LOC201164	1.21848	MOAP1	1.81683	PIM3	1.47061
IRS2	2.64607	LOC387763	1.49174	MOBKL2C	1.80007	PLEKHO1	1.38972
IRX3	1.37716	LOC401238	1.45751	MRCL3	1.63551	PLEKHO2	1.47745
ISG20	1.33939	LOC402221	1.54847	MSX1	2.91829	PPP1R10	1.37753
ISG20L1	1.63042	LOC402617	1.50607	MYADM	4.65128	PPP1R15A	4.01235
ISG20L2	1.41785	LOC554206	1.38243	MYC	1.92173	PPRC1	1.42616
ISL1	1.51809	LOC642361	1.38485	NAB2	1.51991	PRO0628	1.88473
JMJD1A	1.43153	LOC646509	1.25847	NCOA7	5.35993	PTP4A1	1.37735
JMJD6	1.85434	LOC648526	2.47018	NEDD9	1.44814	PTRH2	1.59164
JUN	15.34621	LOC650369	1.22347	NFKBIZ	1.50377	RAB32	1.63393
JUNB	6.88658	LOC651621	1.31392	NOLA1	1.22817	RARA	1.32852
JUND	1.60029	LOC651816	1.40127	NR4A1	10.14752	RASD1	52.85122
KBTBD2	1.28119	LOC653158	1.84395	NR4A2	2.40912	RASSF1	1.33229
KBTBD8	1.27128	LOC654244	1.24214	NR4A3	5.31811	RBM15	1.85520

Table S4 (continued)

Gene	Change fold	Gene	Change fold	Gene	Change fold	Gene	Change fold
RCAN1	1.75154	SLC20A1	1.54543	TMEM55B	1.28005	UBC	1.72300
RCSD1	1.26873	SLC25A25	2.81230	TMEM88	1.49274	UBXD5	1.92992
REXO1	1.22645	SLC25A4	1.33224	TMEM93	1.25143	USP36	1.69171
RIPK1	1.23869	SLC3A2	1.62554	TNFAIP3	1.64358	VGF	1.40074
RND1	2.21130	SNF1LK	7.82245	TNFRSF12A	1.37110	WDR1	1.31833
RND3	1.47305	SNX16	1.26458	TOB1	1.51893	WDR47	1.29401
RNF103	1.22640	SOCS1	1.24618	TP53INP2	1.56635	WEE1	1.48444
RNF39	1.76369	SOS1	1.34167	TP53RK	1.24861	YRDC	2.00047
RPPH1	1.64545	SPRY4	1.26314	TPM1	4.63607	ZC3H12A	2.75004
RPS4Y2	2.20756	SRF	4.68190	TPM2	1.43071	ZFAND5	1.39870
RRM2	1.28802	STX12	1.30342	TRAFD1	1.40629	ZFP36	10.04192
SBDSP	1.56707	TAGLN	16.91685	TRIB1	5.25405	ZNF24	1.28397
SC5DL	1.30951	TFAP2C	1.26339	TRIM26	1.23237	ZNF274	1.32121
SEDLP	1.23294	THBS1	3.06056	TRK1	1.47276	ZNF446	1.26296
SERTAD1	5.70524	TIMP3	1.75374	TSC22D2	1.48793	ZNF593	1.28615
SLC10A3	1.30147	TIPARP	2.24564	TSKU	1.37215	ZNF787	1.26129
SLC16A6	1.30692	TMEM185B	1.30963	TSPYL2	1.61898	ZNF828	1.22182
SLC18A1	1.24372	TMEM49	1.60705	TUFT1	3.32892	ZYX	3.65502

Gene selection criteria: the whole gene list of the array was sorted by change fold (highest to lowest, 40'HRG vs control). The top 300 genes with p value less than 0.05 were selected.